

**Large scale experimental investigation of the relative drying capacity of  
building envelope panels of various configurations**

Arslan Z. M. Abed Alturkistani

A thesis in the Department  
of  
Building, Civil and Environmental Engineering

Presented in partial fulfillment of the requirements  
for the degree of Doctor of Philosophy  
at  
Concordia University  
Montréal, Québec, Canada

December 2007

© Arslan Z. M. Abed Alturkistani, 2007



Library and  
Archives Canada

Bibliothèque et  
Archives Canada

Published Heritage  
Branch

Direction du  
Patrimoine de l'édition

395 Wellington Street  
Ottawa ON K1A 0N4  
Canada

395, rue Wellington  
Ottawa ON K1A 0N4  
Canada

*Your file* *Votre référence*

*ISBN: 978-0-494-37739-0*

*Our file* *Notre référence*

*ISBN: 978-0-494-37739-0*

#### NOTICE:

The author has granted a non-exclusive license allowing Library and Archives Canada to reproduce, publish, archive, preserve, conserve, communicate to the public by telecommunication or on the Internet, loan, distribute and sell theses worldwide, for commercial or non-commercial purposes, in microform, paper, electronic and/or any other formats.

The author retains copyright ownership and moral rights in this thesis. Neither the thesis nor substantial extracts from it may be printed or otherwise reproduced without the author's permission.

#### AVIS:

L'auteur a accordé une licence non exclusive permettant à la Bibliothèque et Archives Canada de reproduire, publier, archiver, sauvegarder, conserver, transmettre au public par télécommunication ou par l'Internet, prêter, distribuer et vendre des thèses partout dans le monde, à des fins commerciales ou autres, sur support microforme, papier, électronique et/ou autres formats.

L'auteur conserve la propriété du droit d'auteur et des droits moraux qui protègent cette thèse. Ni la thèse ni des extraits substantiels de celle-ci ne doivent être imprimés ou autrement reproduits sans son autorisation.

---

In compliance with the Canadian Privacy Act some supporting forms may have been removed from this thesis.

Conformément à la loi canadienne sur la protection de la vie privée, quelques formulaires secondaires ont été enlevés de cette thèse.

While these forms may be included in the document page count, their removal does not represent any loss of content from the thesis.

Bien que ces formulaires aient inclus dans la pagination, il n'y aura aucun contenu manquant.

  
**Canada**

## ABSTRACT

Large scale experimental investigation of the relative drying capacity of building envelope panels of various configurations

Arslan Z. M. Abed Alturkistani, Ph.D.

Concordia University, 2007

Building envelope performance can be predicted through field investigation, laboratory investigation, modeling, or a combination of these. Large scale testing in the laboratory has been limited because of cost, but it is important in validating mathematical or empirical models since the impact of different variables on the envelope performance can be studied as other variables can be readily and reliably kept constant. In the context of a research project in collaboration with nine companies, three universities and the government, a two-story test hut, with overall dimensions of 16ft 8inches in length, 12ft 5inches in width, and 19ft 11¼inches in height to accommodate 31 instrumented wall assemblies 8ft high and 2½ft wide each, has been designed and erected within a large scale test chamber to investigate the drying capacity of 31 different envelope configurations. These wall configurations are reproduced in 31 assemblies that have been built and tested under pre-set loading conditions according to developed protocols: the specimens' protocol, the loading protocol for both moisture loading and climatic loads, and the monitoring protocol. These protocols are combined with the test methodology and data collection methods to yield a unique and state-of-the-art experiment.

The experimental investigation is based on the hypothesis "that the data generated from large scale tests on various wall configurations will yield recognizable patterns that would enable researchers to identify mechanisms relating measurable building envelope parameters to movement and accumulation of moisture in wood-based building envelope systems and that the knowledge gained would support a design process that would better predict the performance of envelope systems"<sup>1</sup>. This can be achieved by investigating the hygrothermal performance of different full-scale wall assemblies in relationship to envelope configurations under the same climatic and loading conditions by

---

<sup>1</sup> Unpublished internal report prepared by P., Fazio. CRD proposal. NSERC Collaborative Research & Development (CRD) grant, Concordia University, Montreal, Quebec.

performing comparative analytical studies to better characterize the relative performance of different wall configurations.

A new test method was introduced to provide identical and measurable moisture sources for evaporation in the stud cavity of wall assemblies. The moisture source consisted of a water tray on a load cell placed on the bottom plate to represent rain water penetrating the cavity and collecting at the bottom plate. This set up provides a uniform moisture source that submits the different wall configurations to wetting by evaporation and drying by moisture evacuation out of the stud cavity. The test method yielded consistent and repeatable correlations between parameters that can be used to perform comparative parametric analysis.

A new calculation by Mapping Method "MM" was adopted to calculate the moisture absorbed by components surrounding the stud cavity. The moisture evacuated from the cavity is taken as the difference of water evaporated from the tray and the water absorbed by the components surrounding the cavity. The ratio of the water evacuated divided by the water evaporated is defined as the drying capacity of a given configuration over a given period of time. This calculation by the mapping method provides a comparison tool between different wall systems.

The analysis of this drying or evacuation of the building envelope was taken one step further since the mapping method calculates the evacuation through the sheathing material only. A Calculation Evacuation Method (CEM) was introduced to calculate the evacuation through the outer layers of the building envelope including the sheathing, weather barrier, and cladding. CEM takes into account (i) the non-linear profile with height of the absorbed vapor mass which influences the permeability of the sheathing, (ii) and the non-linear profile along the height of the vapor pressure due to the moisture source located at the bottom of the wall cavity.

*In the name of God*

*To my parents*

Whatever I say won't be enough. I am the luckiest person for just being your son, and this is one of your dreams coming true.

*To Hadeel*

My beloved wife, I dedicate this to you and to my sons, Rayyan, Albaraa, and Faris. Your unconditional love, understanding, and patience were the burning candles along my long road.

## ACKNOWLEDGEMENTS

I would like to express my sincere gratitude to Dr. Paul Fazio for his supervision, guidance, and moral support throughout my graduate studies. His endless appetite for research made me a good taster of a well done piece of work. Working with Dr. Fazio had also greatly enriched my professional ability both as a researcher and a teacher. He also taught me how to keep in mind the bigger picture and how to look at things from distance above.

I wish to thank the Natural Sciences and Engineering Research Council (NSERC) of Canada and wood industry partners for funding this project. Thanks are also due to the committee members, Dr. Andreas Athienitis, Dr. Khaled Galal, and Dr. Amin Hammad for their comments and favorable interest in the research.

Being a part of a big experimental project such as the CRD gave me the opportunity to work among a big group of researchers, technicians, workers, and students. I value the help of each individual during the course of this research. Therefore, I would like to thank Dr. Jiwu Rao for his valuable comments during the analysis phase of my research and also for his endless help during the set-up of the experiment. Without his technical wisdom and expertise, this experiment would not have been a success. I also thank Guylaine Desmarais for her valuable help during the instrumentation and implementation of the wall assemblies. The technical support and advice given by Jaques Payer, Joe Hrib, Sylvain Bélanger, and Luc Demers is also greatly acknowledged.

I greatly thank Qian Mao, my friend and colleague, for being on this journey with me. Other colleagues helped a great deal during the instrumentation of the test. Therefore, I would like to thank Yang Wu, Xiangjin Yang, He Huasheng, Anik St-Hilaire, Gang Miao, Luis Candanedo, Sergio Vera, and Shan Huang. I also thank the undergrad students namely Jonathan St-Pierre, Nazmi Boran, and Jiejun Zhao who were a big help during the test hut instrumentation and during the data collection phase.

I am very grateful to all my friends that I met in Montreal for all their love and help. I would also like to express my appreciation to the wonderful atmosphere of the department of

Building, Civil, and Environmental Engineering. I deeply thank Olga Soares for her readiness to help in administrative manners. I also thank the rest of the staff of the department and namely, Kathy McAleese, Debbie Walker, Linda Swinden, and Betty Bondo.

Last but not least, I really thank my wife's parents Dr. Hani and Mrs. Thana for all the support they gave me. I also can never thank enough my sisters and brothers for their unconditional love, support, and constant encouragement. Iqbal, Shahnaz, Jalal, Kamal, Emtiyaz, and Jamal, I thank you all for being in my life.

# TABLE OF CONTENTS

List of Figures.....	xii
List of Tables .....	xvii
Nomenclature.....	xviii
Chapter 1 INTRODUCTION.....	1
1.1 Context of the research project .....	1
1.2 Moisture management characteristics.....	2
1.3 The water journey into the stud cavity.....	2
1.4 Literature on previous experimental studies .....	4
1.4.1 Methods of water insertion into the building envelope (Wetting) .....	5
1.5 In search of a common yardstick .....	11
1.6 Goal for the experimental study undertaken.....	13
1.7 Scope of the study .....	13
1.8 Objectives of the study.....	14
Chapter 2 DESIGN OF THE EXPERIMENT .....	15
2.1 Drying mechanism .....	16
2.2 Drying by Evaporation Index “DEI” and drying capacity .....	16
2.3 Loading conditions.....	17
2.3.1 Climatic loading.....	17
2.3.2 Moisture loading .....	18
2.4 Specimens' protocol .....	20
2.4.1 Different Wall Configurations .....	20
2.4.2 Wall assembly Frame Description and Dimensions .....	22
2.4.3 Construction Methods.....	22
2.5 Environmental chamber .....	24
2.6 Hut Design .....	26
2.7 Design of Wall assembly .....	27
2.8 Monitoring parameters of Instrumentation .....	28
2.8.1 Load Cell for measuring evaporation rate.....	29
2.8.2 Thermocouples in each wall assembly.....	30
2.8.3 Thermocouples for test hut .....	32



2.8.4	Relative Humidity probes inside the Wall assembly .....	33
2.8.5	Moisture content by metal pins .....	35
2.8.6	Moisture Content by gravimetric samples .....	37
2.9	Control of Test Conditions.....	39
2.9.1	HVAC equipment .....	39
2.9.2	Data Acquisition System.....	39
Chapter 3	IMPLEMENTATION .....	41
3.1	Test Hut Construction .....	41
3.2	Wall assemblies implementation .....	46
3.2.1	Wall assemblies Instrumentation and Installation.....	46
3.2.2	Wall frames .....	47
3.2.3	Installation of MC probes in the stud.....	47
3.2.4	Sheathing wiring and installation.....	48
3.2.5	Gravimetric samples preparation .....	49
3.2.6	Installation of wall assemblies into the hut.....	50
3.2.7	Cladding Installation.....	51
3.2.8	Connecting the wires to terminal blocks and DAS .....	55
3.2.9	RH sensors installation .....	56
3.2.10	Installation of load cell (LC) and net below insulation.....	57
3.2.11	Installation of fiberglass, vapor barrier and gypsum board.....	57
3.2.12	LC and water tray windows installation .....	60
3.2.13	Air tightness of the test hut .....	60
3.2.14	Organizing the wires beneath wall assemblies.....	61
3.2.15	HVAC System Inside the test hut for first and second floors .....	61
3.3	Locating wall assemblies inside the test hut .....	62
Chapter 4	TEST METHODOLOGY .....	64
4.1	Weather data conditions.....	64
4.2	Hygrothermal test – Montreal conditions .....	65
4.2.1	Pre-conditioning of the test hut.....	65
4.2.2	Establishment the base line .....	65
4.2.3	Test program .....	66
4.3	Gravimetric samples protocol .....	68

4.3.1 Initial moisture content of gravimetric samples.....	68
4.3.2 Collection Process of Gravimetric Samples.....	68
4.3.3 Samples enclosure during collection process.....	69
4.3.4 Evaporation rate of samples (during collection process).....	69
4.3.5 Gravimetric samples collection procedure.....	70
4.3.6 Gravimetric “Samples’ Travel Time”.....	72
4.3.7 Errors encountered with gravimetric samples.....	72
Chapter 5.....	75
RESULTS & COMPARATIVE ANALYSIS.....	75
5.1 Types of results.....	75
5.1.1 Accumulative evaporation.....	76
5.1.2 Relative humidity readings.....	77
5.1.3 Moisture content profiles by gravimetric samples.....	78
5.2 Comparative data analysis for test period 1.....	86
5.2.1 Evaporation rates for different wall configurations.....	86
5.2.2 Comparative parametric analysis.....	88
5.3 Data analysis for the stud cavity conditions in test period 2.....	93
5.3.1 Accumulative Evaporation values.....	94
5.3.2 Average relative humidity values in the stud cavities.....	94
5.3.3 Averaged temperature values in the stud cavities.....	95
5.3.4 Averaged vapor pressure values in the stud cavities.....	95
5.3.5 Convection inside the stud cavities.....	96
5.4 Moisture absorption vs. height analysis for test period 2.....	97
5.4.1 Moisture absorption percentage of total evaporation.....	99
5.4.2 Averaged moisture absorption percentages vs. Height.....	102
Chapter 6 DRYING CAPACITY.....	104
6.1 Introduction of DEI (Drying by Evaporation Index).....	104
6.1.1 Total evaporated moisture and drying capacity.....	104
6.1.2 DEI and drying capacity.....	105
6.2 Equilibrium Moisture Content EMC.....	105
6.2.1 Wetting and drying.....	105
6.2.2 Correlation between evaporated moisture and DEI.....	106

6.3 Absorption by the Mapping Method MM calculations.....	109
6.3.1 MM calculation assumptions .....	109
6.3.2 Calculation steps .....	110
6.4 Surfaces absorption.....	112
6.5 Drying capacities for different wall configurations .....	114
Chapter 7 MOISTURE EVACUATION FROM STUD CAVITIES OF BUILDING ENVELOPES ..	118
7.1 In-cavity profiles due to moisture loading .....	118
7.1.1 Vapor pressure profiles .....	118
7.1.2 Relative humidity profiles.....	121
7.1.3 Vapor pressure difference profiles.....	122
7.2 Vapor evacuation by the Calculated Evacuation Method "CEM" .....	123
7.2.1 Moisture content vs. height.....	123
7.2.2 Evacuation zones .....	125
7.2.3 Calculation steps .....	126
7.3 Results and evacuation profiles .....	129
7.4 Calculated Evacuation Method (CEM) vs. evacuation by Mapping Method (MM) .....	131
Chapter 8 CONCLUSION .....	134
8.1 Contributions .....	135
8.1.1 New methods .....	135
8.1.2 Experimental innovations .....	136
8.2 Limitations and future work.....	137
8.3 Related publications.....	139
References.....	140
Appendix A MEASURED HYGROTHERMAL PROPERTIES OF BUILDING MATERIALS.....	145
Appendix B TEST HUT DRAWINGS.....	174
Appendix C MONITORING PROTOCOL .....	179
Appendix D ACCUMULATED EVAPORATION.....	186
Appendix E MOISTURE CONTENT PROFILES .....	218

## List of Figures

Figure 2-1. Water tray and load cell (source: Fazio et al. 2006a)	19
Figure 2-2. Different configurations to be tested	20
Figure 2-3. Wall assembly frame dimensions	23
Figure 2-4. Schematic drawing of the environmental chamber (after Fazio et al. 1997)	25
Figure 2-5. The two story test hut inside the environmental chamber	25
Figure 2-6. Test hut layout for the first floor	26
Figure 2-7. Weighing system with load cells (source: Fazio et al. 2006a)	29
Figure 2-8. Thermocouple locations in the left stud and on sheathing of each wall assembly	31
Figure 2-9. First floor air temperature thermocouple locations	32
Figure 2-10. Second floor air temperature thermocouple locations	32
Figure 2-11. RH sensors positions in the wall assembly	34
Figure 2-12. Locations of Moisture Content pins in the wall assembly	36
Figure 2-13. Locations of gravimetric samples in the wall assembly	38
Figure 2-14. Diagram of DACs and data acquisition system	40
Figure 3-1. Environmental chamber before starting construction	41
Figure 3-2. Base studs and plywood footings for frame columns	41
Figure 3-3. Base studs and perimeter finished	41
Figure 3-4. Base insulation	41
Figure 3-5. First floor flooring	42
Figure 3-6. Engineered columns fixing	42
Figure 3-7. Joists installation supported by engineered composite beams	42
Figure 3-8. Cantilevered joists for second-floor walkway	42
Figure 3-9. Composition of column, beam and joists	42
Figure 3-10. Flooring for the walkway on the second floor	42
Figure 3-11. Composition of column, beam and joists with second floor flooring	43
Figure 3-12. Fiberglass insulation beneath the walkway	43
Figure 3-13. Fiberglass insulation in the first floor ceiling	43
Figure 3-14. Encasements of main and secondary beams	43
Figure 3-15. First floor ceiling sheets	43
Figure 3-16. Cutting plywood ceiling sheets around stair-case opening	43

Figure 3-17. Placing composite beam at roof of the second floor	44
Figure 3-18. Detail of second floor engineered column, composite beam and roof joists	44
Figure 3-19. Roof joists fixed in place	44
Figure 3-20. Opening for AC unit in the roof	44
Figure 3-21. Roof sheets in place	44
Figure 3-22. Fiberglass insulation in second floor ceiling	44
Figure 3-23. Columns' encasements to accommodate the width of the wall assemblies frames	45
Figure 3-24. Roof of test hut	45
Figure 3-25. Sheathing MC metal pins	46
Figure 3-26. Stud MC probes	46
Figure 3-27. A group of wall assembly frames ready to be instrumented	47
Figure 3-28. Installation of MC probes in left stud	47
Figure 3-29. MC and TC wiring on different types of sheathings	48
Figure 3-30. MC and TC wiring organization on the sheathing	48
Figure 3-31. a) OSB sheathing gravimetric samples, b) plywood samples, c) fiberboard samples and d) stud gravimetric samples	49
Figure 3-32. Fit of gravimetric sample	49
Figure 3-33. Sample screws and boundary tape sample	49
Figure 3-34. Three Stucco wall assemblies installed inside test hut	50
Figure 3-35. Stud pieces under wall assemblies	50
Figure 3-36. Tyvek opening to collect samples	51
Figure 3-37. Removable wood siding(s) in a wood siding assembly	52
Figure 3-38. Removable wood siding	52
Figure 3-39. Inner part of a stucco window	53
Figure 3-40. Applying the first coat of stucco onto the sheathing	54
Figure 3-41. Stucco application finished	54
Figure 3-42. Wires coming out of wall assemblies	55
Figure 3-43. Thermo couple and moisture content terminal blocks	55
Figure 3-44. RH sensors installed	56
Figure 3-45. Close-up picture for an RH sensor	56
Figure 3-46. Load cell placed and net installed	57
Figure 3-47. Fiberglass installed	58

Figure 3-48. RH sensors embedded in the insulation	58
Figure 3-49. Vapor barrier installation	59
Figure 3-50. LC and water tray window installed	60
Figure 3-51. Filling the gaps with foam insulation	60
Figure 3-52. Cables organization beneath wall assemblies	61
Figure 3-53. HVAC system inside each floor in the test hut	61
Figure 3-54. Locations of wall assemblies on the first floor	62
Figure 3-55. Locations of wall assemblies on the second floor	63
Figure 4-1. Taking out a stucco window in a stucco wall assembly to access gravimetric samples	74
Figure 4-2. Collecting gravimetric samples in a stucco wall assembly	74
Figure 4-3. Removing a non-fixed wood siding in a wood siding wall assembly	74
Figure 4-4. Collecting gravimetric samples in a wood siding wall assembly	74
Figure 4-5. Removing the insulation cap for the containers' window in the door of the test hut	74
Figure 4-6. Containers' window opening in the door of the test hut	74
Figure 5-1. Total accumulative evaporation for the 31 wall assemblies	76
Figure 5-2. Calculated vapor pressure values for the 31 wall assemblies in the lower location inside the stud cavity (16" from the base of wall assembly) for the 5 test periods.	77
Figure 5-3. MC profiles for the 25 gravimetric samples in wall assembly 6 (OSB, stucco, and vapor barrier) for the 5 test periods	78
Figure 5-4. Different MC absorption conditions (right side) and the corresponding time sections in the MC profile plot (left side) for wall assembly 6 (OSB, stucco and vapor barrier) for the total experiment duration	85
Figure 5-5. Evaporation rates for the three types of sheathings with the same type of cladding (stucco) and without vapor barrier	87
Figure 5-6. Evaporation rates for wall assemblies 5, 7, 9 and their duplicate wall assemblies 17, 19, 21 (three types of sheathings with the same type of cladding of wood siding and with vapor barriers)	87
Figure 5-7. Effect of water injection on MC change for wall assembly #8 (plywood sheathing, with vapor barrier and stucco cladding)	89
Figure 5-8. Effect of vapor barrier on MC change for wall assemblies #10 (Fiberboard/Stucco with VB) and #16 (Fiberboard/stucco without VB)	90

Figure 5-9. Effect of sheathing material on MC change for wall assemblies #6 (OSB), #8 (plywood) and #10 (fiberboard), all with stucco cladding and vapor barrier.	91
Figure 5-10. Effect of cladding on MC change for wall assemblies #2 (no cladding), #7 (wood siding) and #8 (stucco), for configurations with plywood and vapor barrier.	92
Figure 5-11. Heights of gravimetric samples from the base of the wall assembly	97
Figure 5-12. Moisture absorption in 1 inch diameter sample vs height for the different wall assemblies with vapor barriers (period 2)	98
Figure 5-13. Moisture absorption percentage per one sample area vs. height for wall assemblies with vapor barrier (period 2)	99
Figure 5-14. Moisture absorption percentage per one sample area vs. height for stucco with vapor barrier wall assemblies (period 2)	100
Figure 5-15. Moisture absorption percentage per one sample area vs. height for wood siding with vapor barrier wall assemblies (period 2)	101
Figure 5-16. Averaged moisture absorption percentages of duplicate wall assemblies vs. height for the different types of sheathings configured with stucco and vapor barrier (period 2)	102
Figure 5-17. Averaged moisture absorption percentages of duplicate wall assemblies vs. height for the different types of sheathings configured with wood siding and vapor barrier (period 2)	103
Figure 6-1. Locations of gravimetric samples in the wall assemblies	107
Figure 6-2. Two cases of moisture absorption, where equilibrium moisture content EMC is reached in wall assembly 16 (b) but not in wall assembly 10 (a)	108
Figure 6-3. Accumulated evaporation amount for the EMC period for wall assembly 16	108
Figure 6-4. Divisions of zones in the components surrounding the stud cavity for the moisture mapping calculation method (view from outdoor through sheathing into stud cavity)	111
Figure 6-5. Surfaces moisture absorption by percentages of the total absorbed for the wall assemblies with vapor barriers (period 2)	113

Figure 6-6. Drying capacity percentages for the duplicate wall configurations for test Period 1	116
Figure 6-7. Drying capacity percentages for the duplicate wall configurations for test Period 2	116
Figure 7-1. Accumulated evaporation in period 2 for wall assembly 6 (OSB, stucco, and vapor barrier)	119
Figure 7-2. Calculated vapor pressure at the two RH sensors' heights in wall assembly 6 (OSB, stucco, and vapor barrier) for test period 2	120
Figure 7-3. RH vs. height profile for wall assembly 6 (OSB, stucco, and vapor barrier) for period 2.	121
Figure 7-4. Vapor pressure difference profile for wall assembly 6 (OSB, stucco, and vapor barrier)	122
Figure 7-5. Moisture content in the sheathing vs. height profile for wall assembly 6 (OSB, stucco, and vapor barrier) for period 2.	124
Figure 7-6. Sheathing permeance zones and locations of gravimetric samples	125
Figure 7-7. Evacuation vs. height profile for wall assembly 5 (plywood sheathing, vapor barrier, and wood siding) for test period 2.	130
Figure 7-8. Total evacuated vapor mass by (a) Mapping Method (MM) and (b) by Calculation Evacuation Method (CEM)for the different wall configurations with wood sidings and vapor barriers for test period 2.	133
Figure 7-9. Total evacuated vapor mass by (a) Mapping Method (MM) and (b) by Calculation Evacuation Method (CEM)for the different wall configurations with stucco and vapor barriers for test period 2.	133



## List of Tables

Table 2-1. Wall assemblies' configurations subjected to Montreal-type loading.	22
Table 2-2. Parameters to be measured	28
Table 2-3. Summary of sensor allocations	28
Table 4-1. Summary of test periods and loadings	67
Table 4-2. Evaporation rates of different samples for different periods	70
Table 5-1. Different parameters values in the lower (16") and upper (72") locations inside the stud cavities of the different wall assemblies for test period 2.	93
Table 5-2. Evaporation and calculated vapor pressure values for: a) upper location, b) lower location (period 2)	96
Table 6-1. Absorption of the components surrounding the stud cavity by percentages of the total moisture absorbed in period 2 using the mapping method (MM)	112
Table 6-2. Evaporation, absorption, evacuation and drying capacity for the different wall assemblies with vapor barriers for test periods 1	114
Table 6-3. Evaporation, absorption, evacuation and drying capacity for the different wall assemblies with vapor barriers for test periods 2	115
Table 7-1. Calculations steps using CEM to calculate the evacuation for wall assembly #5 (plywood sheathing, vapor barrier, and wood siding cladding) for test period 2	128
Table 7-2. Calculated evacuation and percentage of evacuation per zones for the duplicate wall configurations with vapor barrier for test period 2.	129
Table 7-3. Total evacuated vapor mass by the Calculation Evacuation Method (CEM) compared with vapor passing through the sheathing calculated by the Mapping Method (MM) for duplicate wall configurations with vapor barrier for test period 2	131

## Nomenclature

Symbol	Parameter	Units
$A$	area	$m^2$
DP	pressure difference	Pa
HR	humidity ratio	g/kg
$M$	permeance	$ng/Pa \cdot s \cdot m^2$
MC	moisture content	% mass
$M_{pi}$	permeance of outer layers	$ng/Pa \cdot s \cdot m^2$
$p$	vapor pressure	Pa
$r$	radius	m
RH	relative humidity	%
$RH_i$	indoor relative humidity	%
$RH_o$	outdoor relative humidity	%
T	temperature	$^{\circ}C$
$T_i$	indoor temperature	$^{\circ}C$
$T_o$	outdoor temperature	$^{\circ}C$
W	moisture content of the air	$kg_{\text{water vapor}}/kg_{\text{dry air}}$
$W$	mass of vapor	ng
$W_{di}$	calculated evacuated vapor mass per zone	ng
$\Delta p_{ci}$	vapor pressure difference between the vapor pressure in the stud cavity as a function of height and the outdoor vapor pressure	Pa
$\theta$	time	s

## Abbreviations

A/C	Air Conditioner
CEM	Calculated Evacuation Method
cfm	cubic feet per minute
CMHC	Canadian Mortgage and Housing Corporation
DAS	Data Acquisition System
DEI	Drying by Evaporation Index
DI	Drying Index
EDRA	Envelope Drying Rates Analysis
EMC	Equilibrium Moisture Content
HAM	Heat, Air, and Moisture
HVAC	Heating, Ventilation, and Air Conditioning
IRC	Institute for Research in Construction
LC	Load Cell
MC	Moisture Content
MDRY	Moisture Durability Reference Year
MEWS	Moisture Management in Exterior Walls Systems project
MM	Mapping Method
NBCC	National Building Code of Canada
NRC	National Research Council
OSB	Oriented Strand Board
RH	Relative Humidity
RTD	Resistive Temperature Detector
TC	Thermo Couple
TMY	Typical Meteorological Year
TRY	Typical Reference Year
PVC	Polyvinyl Chloride

# Chapter 1

## INTRODUCTION

### 1.1 Context of the research project

Building envelope design is currently based on sets of proven-by-experience practices, application of passed-down principles and simplistic calculation evaluation. The lack of appropriate means for designers to assess the durability of their building envelope design has led to premature failures such as those in Vancouver (Barrett 1998), Seattle, and New Zealand, where climatic wet conditions exist. Durability of building envelopes are seriously threatened by moisture. If temperature and relative humidity conditions are appropriate, the accumulation of moisture within hygroscopic materials such as wood and wood products can produce a breeding ground for decay fungi, and thus, leading to deterioration of building envelope components. Rain is the main source of moisture in the building envelope. The major causes of rain penetration into the building envelope are the defects in envelope junctions and joints. Field surveys have shown that the ingress of rainwater into the building envelope occurs primarily at the interface details between different components, such as window-wall details, deck perimeters, balconies and walkways (Ricketts and Lovatt, 1996). No matter how the rainwater penetrates into the building envelope, the results are leaks that follow unpredictable routes, and the resulting situation is a wet envelope that needs to dry out.

While building envelope failures in the field are frequent, little information is available on comparative drying potential of wood-frame walls. Therefore, studying the drying process of wet envelopes is of a great importance to the building science and industry to help generate guidelines for better designs. Before new tools can be proposed, more knowledge of building envelope behavior is required. Existing models and computer simulations are not yet widely used with confidence by industry to provide reliable predictions of the performance of various wall sections, especially when potential liability may be involved. Results from large-scale wall systems, tested under climatic conditions, can provide valuable data to gain a better

understanding of wall system behavior and increase the confidence level of users and designers (Fazio 2004).

## **1.2 Moisture management characteristics**

There are four characteristics involved in the moisture management related to building envelopes, or called the 4D's, which are deflection, drainage, drying and durability (Hazleden & Morris 1999).

*Deflection* relates to the outer skin of the envelope, such as cladding of walls and roofs or can be called the first line of defense against weather loads (in this case is the rain).

*Drainage* relates to water that passes the first line of defense (the cladding) and can be identified as the second line of defense, represented by the cavity or drainage space in some designs. This drainage space redirects water out of the envelope depending on the design of the space, as well as on gravity.

*Drying* concerns the water or moisture that passes these two lines of defense and enters the stud cavity, and to be removed through evaporation and diffusion since drainage of water from stud cavity does not occur by design.

*Durability* depends on materials properties and their capacity to resist deterioration under moisture loads by time.

The water journey into the building envelope can follow many paths and it is influenced by deflection and drainage. On the other hand, drying describes the journey of the water out of the building envelope in the form of vapor.

## **1.3 The water journey into the stud cavity**

Building envelopes have to be designed and constructed to deflect and drain (if the rain managed to pass the cladding) the bulk (i.e. 95-99%) of rain water hitting them (Hazleden & Morris 1999). Rain water can be driven through the exterior cladding by different forces: air pressure, capillarity, gravity, airflow, surface tension and kinetic energy. In many situations, rain water ingress is a result of a combination of several of these forces. Wall assemblies could

follow the rain screen design that adds an air cavity behind the cladding as a capillary break, or could be designed without such a cavity. In a typical exterior wall system with air cavity, the journey of the rain water penetration into the interior wythe of exterior walls can be divided into three sub journeys: crossing the cladding, spanning the air cavity and migrating into the inner wythe and thus the stud cavity, or could take the express journey by directly leaking inside the stud cavity in case of defaults in joints most of the time (under the windowsill for an example). Direct leakage can be considered as the major cause of water penetration problems inside the stud cavity.

In a normal situation, when rain hits the first line of defense or cladding, most of the rain is deflected away; some will pass and penetrate through defects mostly in junctions driven by the kinetic energy forces. Some will be absorbed by the exterior surface of the cladding and stored in pores, interstitial cracks, and joint interfaces between cladding units by the capillary action, thus giving the opportunity for other forces such as air pressure difference, airflow, and surface tension to drive water into the inside surface of the cladding.

The second step involves the rain water spanning across the air cavity, and if there is no air cavity behind the cladding, this step is achieved by default. Capillary and surface tension store the water in the pores and cracks of the cladding as mentioned before, which has been referred to as the reservoir effect (bell 2001). This reservoir storage provides an opportunity for water to be driven by air pressure difference across the air cavity. Moreover, capillarity drives water directly through some members of the wall assembly that bridge across the air cavity, such as the wall ties for cladding support, electric outlet boxes, shelf angles, furring, or mortar droppings. After water reaches the plane of the back-up wall (sheathing), it may intrude deeper in the third step. The main driving forces for moisture at this stage are capillarity, air pressure difference across, and moisture diffusion. If the moisture manages to penetrate the sheathing after the air cavity and weather resistive membrane fail to block this penetration, the moisture may be driven into the inner wythe of the wall and thus into the stud cavity by the air pressure difference (Mao et al. 2004).

Once the rain water penetrates through the defense lines of the outer wall into the stud cavity, it tends to run off the different components and concentrate at the bottom of the cavity. Here the first journey of water into the cavity ends and another journey starts - the drying journey which is the main concern of this study. The water at the bottom of the cavity will tend to find a way out through cracks, junctions or other openings between the different components. The repeated penetration and concentration of water will generate a moisture source at the bottom of the cavity mostly on the bottom plate. This moisture loading source is what has to be represented experimentally in a test method.

#### **1.4 Literature on previous experimental studies**

The main focus of this study is the drying characteristics of the different wall configurations of building envelope systems, specifically the drying capacity of the materials enclosing the stud cavity, thus the drying capacity of cavity itself when subjected to typical steady-state indoor and outdoor conditions. Because drying follows wetting, many attempts and methods have been established by researchers for stud cavity wetting before subjecting the specimens or the assemblies to the drying stage.

In the context of experimental testing, researchers used several procedures to introduce water into the building envelope for hygrothermal testing p

urposes. These wetting protocols can be grouped into four main procedures: spraying water on the exterior cladding surface, inserting water directly into the building envelope, and pre-wetting building envelope components (Teasdale-St-Hilaire & Derome 2005), in addition to another method that involves drying directly by evaporation from a wetting source. Another important aspect is the design of the experiment that involves a number of steps: wall assemblies (specimens), instrumentation, data collection methods, and loading conditions. These aspects are also reviewed along with the previous experiments.

## **1.4.1 Methods of water insertion into the building envelope (Wetting)**

### **1.4.1.1 Spraying the cladding of the building envelope**

A subtask of the Moisture Management in Exterior Walls Systems project (MEWS) was to perform a large number of water infiltration tests by subjecting different types of walls to simulated wind-driven rain at certain loads and for time periods according to current industrial standards. Three nominal spray rates at various static and dynamic wind pressure differences applied to four types of cladding were carried in the tests to predict the hygrothermal responses of several wall assemblies that are exposed to North American climate loads, and a range of water leakage loads (Lacasse et al. 2003).

Determination of the degree of water wicking up between the siding veneer laps was the objective of the study done by Tsongas et al. (1998) by developing a wind-driven rain simulation test methodology. The test ran for 7 days, where water was sprayed onto the test wall once a day for 15 minutes using two low-flow irrigation-type spray heads. The reason behind most of the studies that implemented spraying water on the exterior part of the building envelope was to test water penetration or infiltration resistance rather than having a wetting source to the inside of the building envelope. Therefore, this wetting method is not directly relevant, but it still worth mentioning since it is dealing with water penetration into the building envelope.

### **1.4.1.2 Direct insertion into the building envelope**

This method could allow for better control of insertion rates into the building envelope. The water would be introduced into the wall assembly as a one-time source, or by wetting the components on a scheduled basis prior to the drying phase to attempt to mimic more or less the on-site conditions. Two experimental methodologies were performed by Tsongas et al. (1998) to introduce water between the siding and building paper to observe the extent of lateral migration of water behind the sidings. The water insertion rates correspond to the amount of rain water estimated to enter the wall at the junction between the wood siding and concrete landing. In the first method, water inserted once and the wall was opened up after 24 hours. In



the second method, the amount of water introduced to simulate a water leak for a whole month in a rainy season. Using a flattened copper tube, water was injected between the sidings and the building paper for 12 hours/day for 2 days, then another rate of entry for 2 hours every 12 hours for 2 days again, and finally with a third rate for one hour a day for 24 days.

In the framework of the Envelope Drying Rates Analysis (EDRA) consortium, Lawton et al. (1999) developed a method to insert controlled amounts of water by means of a horizontal line of point sources at the top of the stud cavity. The water was injected via clear vinyl tube with holes drilled at 13mm intervals, and was covered with ABS pipe split in half lengthwise to direct the water onto the interior surface of the sheathing and prevent back splash. For the preliminary test, two specimens were constructed (one without air cavity and the other without stucco cladding to provide direct access to the sheathing for moisture readings using hand-held moisture meter) with an array of sensors to measure temperature, relative humidity and relative moisture content. Sufficient water was meant to be injected into the stud cavity to raise the MC of all wood elements by about 25%. Given that the specimens contained approximately 40kg of wood, 10 liters were injected, one liter at a time over a period of 16 days. For the main experiment, specimens were left for two weeks to stabilize under the test conditions (indoor temperature of 23°C, and outdoor temperature of 10°C). When starting the main test, water was injected into stud spaces by the rate of one liter per day for a total of 4 liters. Specimens were weighed before starting the test with a floor scale (precision 0.05 kg) and then weighed again using the same scale for the initial weights. MC readings then were taken using a moisture meter, adjacent to the moisture pins for calibration purposes, and on some other locations to obtain a more complete mapping of the moisture distribution in the sheathing. Sensors installed included brass moisture pins to measure MC of selected wood elements, duff gauges to measure RH, type T thermocouples to measure surface and air temperatures and another sensor to measure temperature and RH within the stud space.

This type of point insertion could create only one wetting pattern each time of injection and it is impossible to control these patterns or even predict them. And for a smooth run off and equal loading on the bottom plate, the sheathing must be perfectly vertical, while the bottom plate being perfectly horizontal. Another expected issue is the water seeping out of the specimens

(this was observed in the experiment by Lawton et al. 1999). Moreover, care must be taken in the design stage of the wetting insertion method to avoid potential absorption by the insulation.

Schumacher et al. (2003) conducted a study to examine the basic relationship between ventilation airflow and the drying of wetted wall systems in a lab environment. The main concern was to reduce the number of intentional variables to one, namely the convective airflow rate. The wetting system utilizes 15 double sheets of a thick, highly adsorptive paper that is reinforced with a plastic mesh. One side of the wetting paper is stapled to the sheathing. Each double sheet of wetting paper is served by one small diameter plastic injection tube sandwiched between the two sides of the folded paper. Water was supplied in three doses of 450g at 4 hour time intervals in order to insure that there is no liquid water leakage and that the water is evenly absorbed by the sheathing. The weight change of the test wall panel during the wetting and drying phases was measured using counterbalance weighing system (consists of a 5000g capacity load cell, counterbalance weights and a steel arm) with an accuracy of 5g or less. The sheathing MC change was monitored in 5 locations: top-center, middle-left, middle-center, middle-right, and bottom-center by electrical resistance-based moisture content sensors. The temperature was measured at the same previous 5 locations as well.

The easy wetting control of the wick fabric is an advantage; it makes it possible to recreate a more realistic rain infiltration. However, it may be difficult to ensure a good wick fabric/sheathing contact. Also it may be difficult in ensuring the uniformity of wick fabric wetting from panel to panel.

One of the objectives of Teasdale-St-Hilaire, Derome and Fazio (2003) was to determine the amount of moisture accumulated in each panel during the wetting phase. Water was introduced on the inside surface of the sheathing with a certain quantity, duration, and frequency to reflect water infiltration through a window defect to simulate rain penetration for Montreal weather patterns. Water was introduced into the stud space onto the top center interior face of the sheathing (point of insertion) to correspond to a window defect located in the middle of the windowsill. Moisture content was monitored by the use of electrical resistance moisture probes in the studs and bottom plate as well as in the sheathing with a total of 5 locations. In the studs

and bottom plate, sensors were inserted in a way such that the tips of the probes were at ¼" from the inner stud cavity surface. In the sheathing, smaller pins were used for the panel monitoring. Type T thermocouples were used to measure the temperature at locations adjacent to moisture content probes in the wood framing and sheathing at a depth of 6mm (¼"). Thermocouples were also used to monitor the temperature on the surface of the gypsum and of sheathing in the middle height of each assembly. Relative humidity within the stud space of the wall specimens was monitored using a capacitance type sensor with an accuracy of ±4%. During the wetting and drying phases of the tests, the pressure difference between the inside and the outside of the test hut was monitored with a micromanometer as well. Moisture content was monitored also using gravimetric samples (small cut outs from the material to be monitored) to determine the moisture content of the wood framing as well as the sheathing. Framing gravimetric samples were 13mm (½") in diameter and 13mm (½") in depth. In test 1, 6 framing gravimetric samples were installed in each specimen plus 9 sheathing gravimetric samples.

The resulting MC curves trace the gain in MC during the water injection into the stud cavity, the loss of moisture content during the following removal of moisture through evaporation and through movement of the water vapor out of the stud cavity, and redistribution of moisture within the specimen. These MC curves at isolated predetermined locations may or may not fall within the path of the wetting pattern that is a result from the water drip at the top of the panel. These wetting patterns vary from panel to panel. Therefore, for point insertion wetting, there is no uniform wetting pattern at the starting point of the test and before the drying cycle. Because it is difficult to measure the moisture remaining in the specimen, it would be difficult to use this method to compare the performance of the different wall configurations.

#### 1.4.1.3 Pre-wetting components by immersion

The Envelope Drying Rates Analysis (EDRA) project was performed in the framework of the Canadian Mortgage and Housing Corporation (CMHC)'s Best Practice Guide program to experimentally test and evaluate the potential of drying as a moisture management mechanism. Pre-wetting various wood and wood-based components within the inner wythe of the building

envelope was a different wetting approach used in the EDRA project by Hazleden & Morris (2001). Panels were constructed and cladded with instrumentation, not including interior finish plywood, polyethylene vapor barrier, insulation, and RH and temperature sensors. Dry panel weights were taken. Panels then were wetted by immersing (studs down) in a shallow tank of water such that the water level was within 6mm of the sheathing for 240 hours to achieve 25% to 30% MC by weight in studs and plates and 20% to 25% MC in OSB and plywood. The bare panels were then weighed after immersion, while the closing up components (insulation, vapor barrier, plywood interior finish, RH and temperature sensors) were weighed separately. After the test period was over, panels were removed from the chamber and immediately been weighed. Panels were then disassembled, the bare panels were weighed again as well as the closing components. During the test, measurements were taken electronically every 15 minutes through electronic monitoring. Each panel had the following instrumentation: one load cell, up to 22 MC points, up to 12 temperature points, and up to 2 RH points, all connected to the data acquisition system DAS.

In a study to assess the hygrothermal response of various components in wood-frame wall assemblies using hygIRC, Maref et al. (2004) conducted a large-scale laboratory test. The experiment consisted of two phases: immersion and stabilization. The immersion phase permitted the OSB to reach an elevated level of MC quickly by immersing the complete face of the specimen in a large water tank for three days. The stabilization phase was to insure that the MC throughout the component reached equilibrium. It took place after draining the water from the tank by leaving the specimens for two days to allow for even re-distribution of moisture into the OSB (the initial MC at the start of the test was assumed to be uniform for all the specimens). The change and the rate of change were monitored, in the total MC (drying) of critical wall assembly components (in OSB sheathing). The MC of the components was monitored on a continuous basis during the stabilization phase to ensure reaching the desired MC prior starting the test. The weight data has been used to determine weight loss over time in the OSB affixed to wood frame wall using precision weighing system for full-scale wall assemblies with nominal weights of up to 250kg approximately to the nearest gram.

In the two previous experiments (Hazleden & Morris 2001 and Maref et al. 2004) the panels were immersed to try and reach an elevated moisture content level. Then whole panels were weighed to monitor the drying capacity for the assembly. However water absorption represents relatively small amount compared to the weight of the whole panel and accuracy is hard to achieve when monitoring the evaporation of the panel.

A comparable method was used by Teasdale-St-Hilaire, Derome and Fazio (2004) but with only one wall component being immersed that is the bottom plate. The method involved the soaking of an insert as a second bottom plate, weighing the MC in the insert, and then placing it between the two vertical studs over the bottom plate of the wall specimen through an access door cut out in the drywall. The 6 inserts (one in each of the test wall panels) were of approximately the same weight, and cut from the same piece of spruce. They were immersed partially in water for 31 days to reach moisture content by weight of 55% with a 4% variation among the 6 insert pieces. Another gravimetric samples 13mm diameter by 13mm height each were initially saturated and then fitted into predrilled holes in the bottom plate insert as well as one more gravimetric sample in the sheathing. During the test under Montreal spring conditions (April and May), the 6 inserts and small gravimetric samples were weighed on a daily basis for 35 days. The pressure difference across the specimen was minimized and kept close to 0 for the test period. There was no intentional air leakage introduced in the specimens and no non-intentional air leakage was assumed. This approach represented a significant improvement, where the resulting curves provided a characteristic drying profile for each insert and sheathing gravimetric sample that was located adjacent to the bottom plate insert under specified conditions for the different wall systems. The amount of water that can be stored in the wood inserts is insufficient to activate all the processes contributing to the wetting and drying of the entire wall panel.

#### 1.4.1.4 Evaporation from a wetting source

Ojanen et al. (2002) studied the drying efficiency of a building envelope under 1-dimensional temperature and moisture gradient. Twenty structure frames were used in the test set-up in which the structure sections are installed. The main component under study was the wind

barrier (sheathing). Test structures were selected to include the most typical wind barrier materials in use, such as porous wood fiberboard, gypsum and plywood. Also, some other cases with additional exterior insulation with stucco, and one case having gypsum board with exterior mineral wool insulation without coating (cladding), and a reference case without any wind barrier (open case). The wetting source was a water vessel containing liquid water embedded in each structure frame. The experiment consisted of three different measuring periods with steady-state conditions, in the three periods with the same warm side temperature of 20°C (with less than  $\pm 0.5$  °C variance). The three measuring periods had the following cold side temperatures: -10°C (to represent winter conditions), +3°C and +12°C with about  $\pm 1$  °C variation from the set value. Drying of the structures was based only on diffusive moisture transport through the outer material layers and was monitored by weighing the whole installation frame of each structure section along with the initially contained water in the vessel. The result was presented as a moisture flux kg/s.m<sup>2</sup> out from each structure and these fluxes represent the drying efficiency of the different configurations. The relative humidity of the cold side air space was also monitored during the test for the different structures.

In this experiment, the loading conditions are well established to allow for comparative analysis between the different structures, but the limitation to one dimensional drying by the horizontal setup of the test structures does not describe the real drying process of a building envelope. .

### **1.5 In search of a common yardstick**

As seen in the literature, researchers have adopted different methodologies trying to study the wetting and drying of building envelopes experimentally. In the direct insertion methods, the water intrusion into the building envelope was intended, to a certain degree, to mimic that of a real life. At the same time, uniform distribution of moisture and equilibrium moisture content levels were expected, but, these types of point insertions could create only one wetting pattern each time of injection and it is impossible to control these patterns or even predict them. Therefore, wetting patterns tend to vary from panel to panel making it impossible to attain uniform distribution of moisture through the component. In addition, the expected seeping of

water out of the wall panel makes it hard to have the same initial wetting conditions for the different wall panels. Thus, a uniform basis for comparative analysis cannot be established.

In the direct insertion method by Schumacher et al. (2003), the objective of the wetting method was to insure even absorption of water in the sheathing rather than mimicking a real life wetting caused by rain water penetration. Other researchers had the same principle of trying to achieve uniform distribution of moisture in the test specimens using the immersion method. In this method, there is only one initial wetting source that will dry out eventually; this is the moisture already contained in the test specimen after immersion. The objective was to monitor the drying by weighing the whole wall panel. However water absorption rates vary from panel to panel making it hard to have the same initial wetting conditions. At the same time, these absorption rates represent relatively small amount compared to the weight of the whole panel. Therefore, accuracy is hard to achieve when monitoring the evaporation of the panel.

The above experiments considered only one source of wetting that is the runoff of penetrated rain water in the building envelope. In site situations, and as mentioned earlier, penetrated water into the stud cavity will run off the different components, concentrate at the bottom, and eventually leak out of the building envelope leaving a wet bottom plate behind that could act as a second moisture loading source. A pre-wetting by immersion method was adopted by Teasdale-St-Hilaire, Derome and Fazio (2004), but with only one wall component being immersed, that is the bottom plate insert. However, the amount of water that can be stored in the wood inserts is insufficient to activate all the processes contributing to envelope drying especially if the envelope components are not in moisture content equilibrium level; the water absorption rates may vary from insert to insert making it hard to have the same initial wetting conditions for the different wall panels, making it difficult to establish a uniform basis for comparative analysis.

Based on the previous literature, while the amount of water, location, and method of wetting varies from an experiment to another, they come short of providing a reliable common yardstick to evaluate the relative drying capacity and thus the performance of the different building envelope configurations.

Therefore, there is a need to establish a framework for large-scale building envelope testing under specific loading conditions that allows developing a common yardstick to evaluate the drying characteristics of different wall systems and thus compare the relative performance of different wall configurations.

### **1.6 Goal for the experimental study undertaken**

The experimental investigation undertaken is based on the hypothesis "that the data generated from large scale tests on various wall configurations will yield recognizable patterns that would enable researchers to identify mechanisms relating measurable building envelope parameters to movement and accumulation of moisture in wood-based building envelope systems and that the knowledge gained would support a design process that would better predict the performance of envelope systems" (Fazio 2004). Thus, the design of building envelopes would move from a thumb-rule mode towards an engineering approach.

### **1.7 Scope of the study**

This experimental investigation is part of a Collaborative Research and Development (CRD). The initial phases of the project involved the development of the following protocols: the loading protocol (Fazio 2004), the protocol on specimen (Derome & Fazio 2004), and the monitoring protocol (Rao 2004). This author was involved in tasks 1 to 5 and responsible for tasks 6 to 8 below:

1. Revising the instrumentation and design of the wall assemblies.
2. Test hut design.
3. Instrumentation and implementation of wall assemblies.
4. Implementation of the test hut.
5. Test methodology.
6. Data collection protocols.
7. Data analysis.



8. Development of patterns from the analysis of results to carry out comparative analyses of wall systems of different configurations

The experiment was designed and instrumented drawing from the knowledge base developed by the group from previous tests. The aim of this experimental investigation was to initiate and validate a new test method that would yield repeatable results and would enable the comparison of the relative drying capacity of building envelope systems with different configurations. Modeling was not part of the study nor was it funded by the sponsors

### **1.8 Objectives of the study**

This research aims to improve building design, and develop better products, by:

- Develop a test method to better characterize the relative hygrothermal performance of different wall configurations for the purpose of comparing them.
- Investigating the hygrothermal performance and the relationship between evaporation and evacuation of different full-scale wall assemblies in relationship to envelope configurations under the same climatic and loading conditions, thus, determining a yardstick to be used as an indicator of the drying capacity of the different configurations.
- Comparing the drying potential for the different wall configurations by quantifying the evacuation of these different building envelope systems.

## **Chapter 2**

### **DESIGN OF THE EXPERIMENT**

Drying capacity is the measure of the rate of movement of the moisture out of the stud cavity and it can serve as a common yard stick to evaluate the relative performance of different wall configurations (Fazio et al. 2006). Hence, the envelope system with the greater capacity to evacuate moisture from the stud cavity would be less susceptible to moisture driven damages. This drying capacity would vary according to the specific wall configuration and according to the climatic load applied such as temperature, relative humidity (indoor and outdoor), pressure difference across the wall, and initial moisture content distributed within the components of wall assemblies. Construction variables also affect the building envelope drying capacity. Notably, these include the air leakage of the construction; material properties, and pre-existing characteristics of the materials including moisture content, deficiencies, and holes.

The experiment involved full-scale wall assemblies that represent some of the most common building systems and configurations being used in the building industry. In the experiment, the wall configurations were reproduced in 31 wall assemblies that have been built and tested under pre-set loading conditions according to developed protocols. All 31 assemblies were subjected to the same test conditions that include a moisture source within the stud cavity and a set of climatic conditions. Each wall assembly is 2,477 mm (8'- 1½") high and 762 mm (2'-½") wide and is instrumented with: 12 pairs of moisture content pins to measure the moisture content in 12 preset locations; 18 thermocouples; and 25 gravimetric samples to measure the change in moisture content. The 31 assemblies represented different wall configurations of wall sections, from cladding to interior finish. Except for the insulated core, each layer is provided with two or more alternatives within available and normally used configurations.

## **2.1 Drying mechanism**

The capacity to evacuate moisture is one of the characteristics critical to the durability of the building envelope. This drying capacity could be more important than the amount of water that enters the cavity, and depends directly on the capacity of the wall assembly to evacuate the moisture. Drying occurs by drainage, by capillary action (redistribution of moisture within the adjacent materials), and by evaporation followed by diffusion through surrounding materials and transported by air leakage.

Water from a concentrated source, such as could be found on the bottom plate, can be redistributed to the surrounding regions and materials of the building envelope by capillary action, thus, increasing the moist exposure to evaporate within the stud cavity, and to a more limited extent, out of the cavity. Although, this redistribution plays a role in drying, the water migrating to the outer surface may be considered minor, and can be neglected for this study. Therefore, the major mechanism of moisture evacuation in this study would be the drying of specific envelope configurations by evaporation, diffusion and exfiltration of moisture in the vapor form (Fazio 2004).

## **2.2 Drying by Evaporation Index “DEI” and drying capacity**

Drying capacity could be assumed as the capability of a building envelope to evacuate moisture out of the stud cavity, as well as it could be identified as the drying potential, where the word capacity could be taken as an amount, thus the drying capacity could be a scientific measure of moisture evacuation out of the building envelope at any particular period of time under certain conditions. On the other hand, Drying by Evaporation Index or “DEI” is the measure of the rate of moisture movement out of the stud cavity, and is based on the relation between moisture evaporation inside the cavity and moisture evacuation out of the cavity. This measure is an indicator of the drying capacity and thus serves as a comparative indicator between different envelope system configurations.

This measure also varies according to the specific wall configuration and according to the loading applied. It can be said that it is a function of indoor & outdoor temperature, indoor &

outdoor relative humidity, pressure difference across the building envelope and the initial moisture content IMC distributed within the components of wall assembly. Construction variables, such as material properties, potential air leakage and pre-existing characteristics of the materials including moisture content, deficiencies, holes, straightness etc. will also affect the index (Fazio 2004).

## **2.3 Loading conditions**

The drying capacity is one of the main indicators of the wall system's susceptibility to moisture damage. Therefore, building envelope systems can be experimentally evaluated by comparing their drying capacities under certain conditions to obtain effective benchmarking results. For this test the variables to be studied are the different wall configurations, therefore, the other conditions have to be kept the same for the whole experiment period; these conditions are namely the climatic loading and the moisture loading.

### **2.3.1 Climatic loading**

Indoor conditions were set at:

- Temperature: 21°C
- RH: 35 %

Outdoor conditions:

- Temperature: 8°C
- RH 76%.

The reason behind setting the weathering conditions to steady state is to better understand the effect of other parameters, such as the different configurations as mentioned above to identify the relative performance, since understanding the behavior of systems under static loads before moving to dynamic loads is a common practice in engineering investigation<sup>1</sup>. The month of October for the city of Montreal (based on the weather data analysis by Candanedo et al. 2006) was selected as the primary month for the experiment since it is proposed as the month with

the worst conditions for drying potential. Since the study is investigating the possible worst drying conditions, all the wall assemblies are proposed to be facing the northern elevation, where there is no direct solar radiation.

### **2.3.2 Moisture loading**

Keeping the initial state as uniform as possible for the moisture loading is of a great importance. In literature, researchers had difficulties in providing the same initial wet conditions before starting the drying process, these unequal initial conditions make it hard to establish a common yardstick for the drying capacity of different wall configurations with which to compare the relative performance of different building envelope systems. Therefore, to establish the drying capacity, the test set up should have the following characteristics (Fazio 2004):

- "The moisture source should be uniform for all the assemblies in the experiment.
- The moisture source should be replenishable to provide enough moisture to establish moisture equilibrium in the components of the assembly, and to feed the drying mechanism.
- The testing should be continuous.
- The drying rate (or evaporation rate) should be monitored (weighed) on a continuous basis.
- The climatic loading parameters ( $T_i$ ,  $T_o$ ,  $RH_i$ ,  $RH_o$ ,  $DP$ ) should be monitored on a continuous basis.
- The interior of the stud cavity should have the minimum disturbance.

The following set up would fulfill the above conditions:

- A moisture source is to be placed over the bottom plate of the assembly between the two vertical studs.
- A method for water insertion into the moisture source with a minimum disturbance for the stud cavity.

---

<sup>1</sup> Unpublished report on Data analyses of test results and development of new methodologies for CRD hygrothermal test. Prepared by P., Fazio, A., Alturkistani, Q., Mao & J., Rao.

- The evaporation rate can be monitored and weighed on a continuous basis by sitting the moisture source on a load cell that is connected to a data acquisition system".

### Moisture source in the stud cavity

A water tray on a load cell, set on top of the bottom plate of the stud cavity, provides the moisture source where rain penetration tends to puddle. Figure 2-1 demonstrates the water tray and load cell. Load cells (SCAIME Type AG) were used to measure the weight of the water in each tray. The nominal rated capacity of these load cells is 1 kg. Their accuracy is 1/4 grams. The water tray as shown in the figure is made of 3mm (1/8") thick clear acrylic sheets. The outside dimensions are 343mm×114mm×38mm (13.5"×4.5"×1.5") to fit within the stud cavity. Each tray is divided into 5 compartments to provide three loading conditions of 1/3, 2/3 and 3/3 of the surface area of the tray. Water is added by means of small flexible tubes through a plastic window and then sealed during the test.

This water tray provides a uniform, measurable and repeatable moisture loading for the wall panels, and is not intended to directly simulate any particular pattern and condition of water penetration into the wall cavity nor to mimic the exact "real life" condition, rather, to highlight the drying process that would happen in a wetted stud cavity. The total amount of water evaporated includes the moisture added to the stud cavity, the moisture absorbed by different materials surrounding the stud cavity, and the water vapor leaving the stud cavity to either the indoor or outdoor environment (Fazio et al. 2006a). More detailed information about the load cell is given in Appendix C.

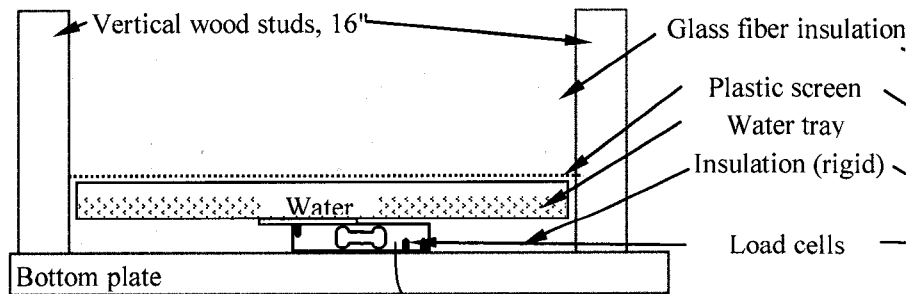


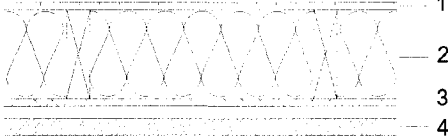
Figure 2-1. Water tray and load cell (source: Fazio et al. 2006a)

## 2.4 Specimens' protocol<sup>2</sup>

### 2.4.1 Different Wall Configurations

The 31 wall assemblies represent different wall systems and configurations of complete wall sections, from cladding to interior finish. Components of each wall system consist of four layers (Fig. 2-2):

1. *Interior finish* are the material(s) that provide(s) support for the finish coat, often paint, and provides control to vapor diffusion for cold climate loading;
2. *Insulated core* consists of wood studs and the insulation between the studs;
3. *Sheathing* consists of the sheets that close the inner wythe and provide lateral bracing to the wood frame;
4. *Cladding system* consists of the materials providing rain management, including cladding, air space (or no air space) and weather resistive membrane.

	#	Component	Material and configuration
	1	Interior finish	a. Polyethylene and painted gypsum, or b. Painted gypsum
	2	Insulated core	c. 38 mm x 140 mm @ 400 mm cc with glass fiber batt insulation
	3	Sheathing	d. Oriented strand board (OSB), e. Plywood f. Fiberboard, or g. Insulation sheathing (polystyrene)
	4	Cladding system	h. Wood siding on furring and spun bonded polyolefin, or i. Cement stucco on metallic lath and two layers of weather resistive membrane

Source: Protocol on Specimens (Derome, Fazio)

Figure 2-2. Different configurations to be tested

<sup>2</sup> Derome & Fazio 2004.

Except for the insulated core, each layer is provided with two opposite alternatives within the spectrum of available and normally used solutions. As a result, the following configurations were applied (Table 2-1):

1. interior finish:
  - Slightly vapor-tight system [a].
  - Highly vapor-tight system [b].
2. The insulated core has one option representing commonly used 2x6 wood frame structures with glass fiber insulation [c].
3. cladding system:
  - Totally vented cladding system with little moisture storage capacity [h].
  - Simple capillary break and high moisture storage capacity [i].
4. sheathing:
  - Low vapor permeability [d].
  - High vapor permeability [f].
  - Intermediate value [e].

Insulated sheathing [g], with low permeability and impact on temperature gradients, is introduced in a few assemblies in order to include commonly available systems. Table 2-1 shows the different wall assemblies' configurations subjected to Montreal-type loading. More information about material properties used in the test is included in Appendix A (Wu et al. 2007).



Table 2-1. Wall assemblies' configurations subjected to Montreal-type loading.

Interior Finish	Cladding System	Sheathing			
		OSB	Plywood	Fiberboard	Insulation
Painted gypsum with Polyethylene	No cladding	1*	2	3	4
	Wood siding	5 & 17	7 & 19	9 & 21	
		29 with insulation	30 with insulation	31 with insulation	
	Stucco	6 & 18	8 & 20	10 & 22	
Painted gypsum	Wood siding	11 & 23	13 & 25	15 & 27	
	Stucco	12 & 24	14 & 26	16 & 28	

\* Numbers in this table refer to assembly number

### 2.4.2 Wall assembly Frame Description and Dimensions

Each wall assembly, consists of a central bay (area of study) made up of two 38mm x 140mm 2x6 wood studs at 406mm (16") spacing sided by two guarded bays of 140mm (5½") each and a boundary frame made up of 19mm (¾") plywood boards to form a complete air separation between wall assembly frames. Figure 2-3 shows the general components of each wall assembly with all the dimensions including the overall height, width and depth for the wall assembly frame.

### 2.4.3 Construction Methods

Each wall assembly is constructed according to methods used in the field. Wall assembly frames are assembled using screws instead of nails for ease of disassembly. Wood studs are without any treatment; fiberglass insulation is forced fit between studs; polyethylene sheets are stapled; gypsum boards are installed using drywall screws as single piece for each wall assembly (so there is no junction taping); screws are covered with compound and sanded; paint is applied with rollers.

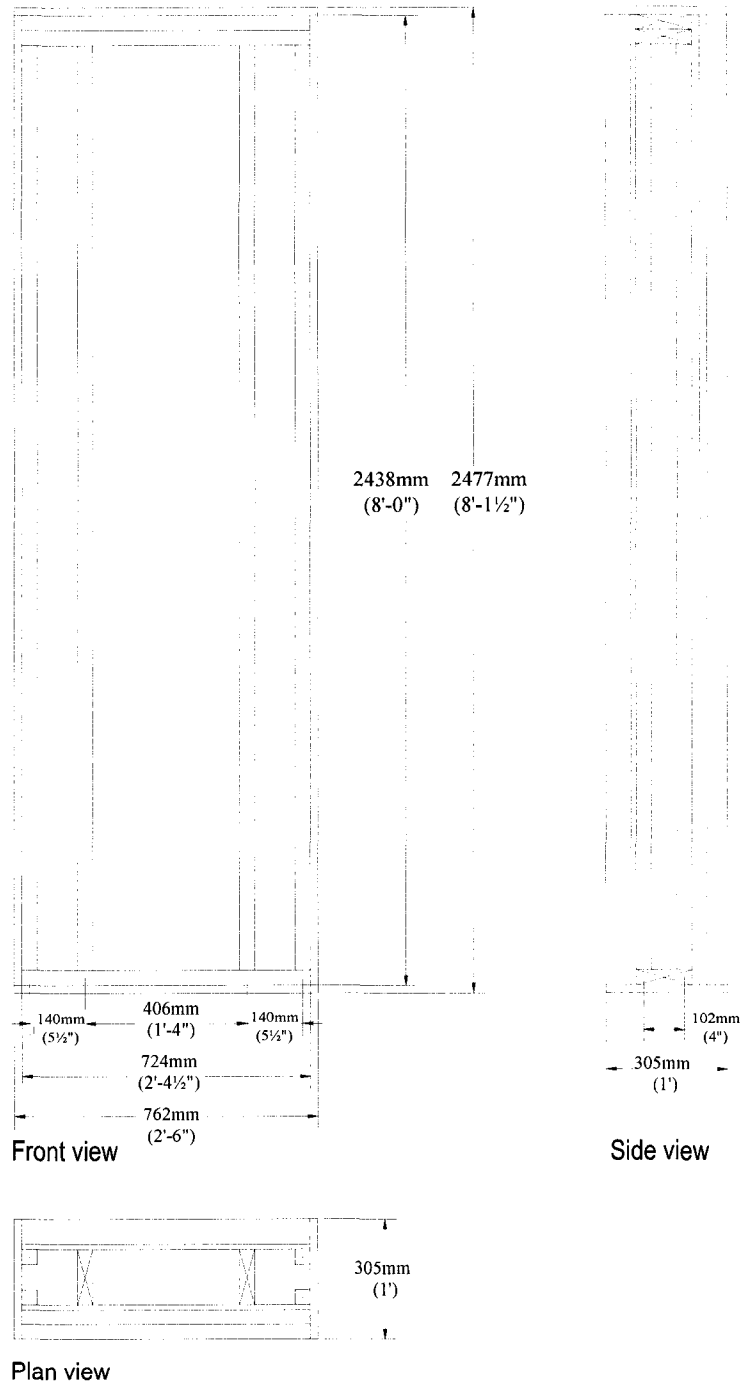


Figure 2-3. Wall assembly frame dimensions

## **2.5 Environmental chamber**

The environmental chamber is a large scale research facility that can be used for investigation of building envelope performances as a function of heat, air, and moisture transfer as well as the interaction between the building envelope and the indoor environment. Building envelope assemblies of up to 7.2m high and 4.1m wide can be tested in the chamber. The environmental chamber consists of two chambers to represent the dynamic outdoor and indoor conditions, the cold box and the hot box respectively. Between these two boxes, a rectangular frame is sandwiched, where building envelope assemblies can be built up or fixed (Fig. 2-4).

The walls of the chamber are made of 150mm foamed polyurethane boards and laminated between 0.8mm aluminum sheets outside and 0.8mm stainless steel sheets inside. The cold box chamber is 7.5m high, 4.4m wide and 3.6m deep. To simulate outdoor weather conditions, the temperature could be varied from -40°C to 50°C. The mechanical equipment includes a 5 ton compressor, a 25 kW re-heating heater, and a 12000 cfm recirculation fan. The hot box is 7.5m high, 4.4m wide and 6.1m deep. Temperature ranging from 5°C to 50°C can be maintained, and relative humidity percentages ranging from 10% to 90% can also be generated. The hot box is equipped with a 600 cfm air circulation system, a humidification system, and a fresh air supply/return damper (Fazio et al. 1997). For the experiment undertaken, the facility was used as one big cold climatic chamber where both the hot box and the cold box were joined forming a 7.5m high by 4.4m wide by 10.5m deep chamber to accommodate the two story test hut (Fig. 2-5).

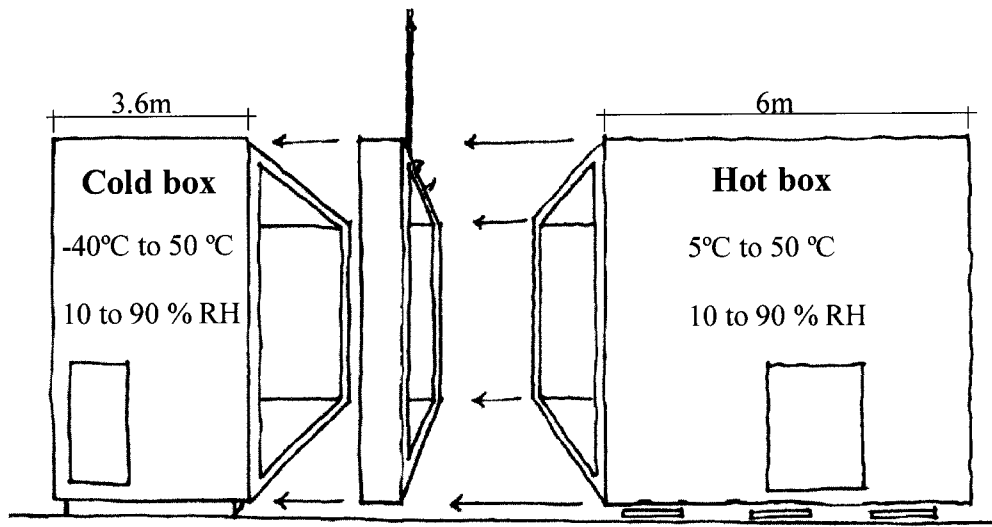


Figure 2-4. Schematic drawing of the environmental chamber (after Fazio et al. 1997)

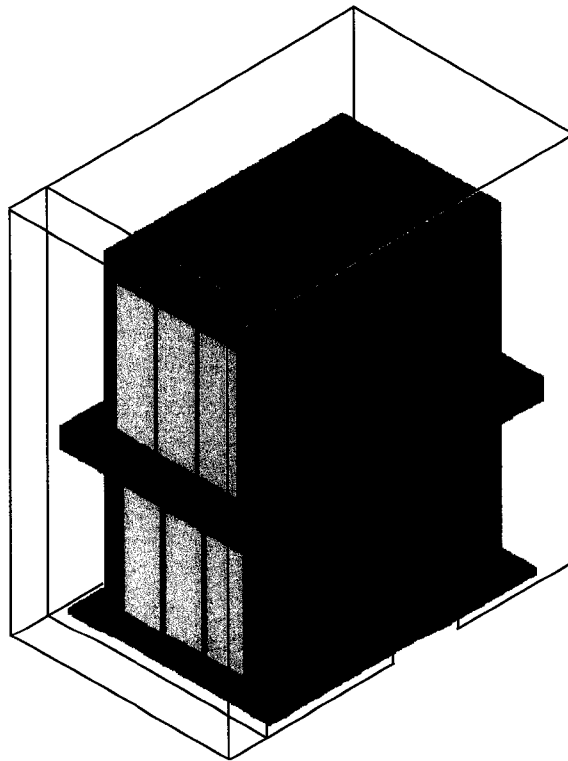


Figure 2-5. The two story test hut inside the environmental chamber

## 2.6 Hut Design

A test hut frame was designed to accommodate 31 wall assemblies in two stories, 15 in addition to the door assembly on the first floor and 16 wall assemblies on the second floor, using pre-engineered wood columns and beams. The interior dimensions of the environmental chamber were the start point for setting the hut frame dimensions as well as the final dimensions for the wall assemblies. The major elements of the hut were four 114mm x 140mm x 2642mm (4½" x 5½" x 8' 8") engineered wood columns for each floor, two 134mm x 241mm x 5442mm (5¼" x 9½" x 17' 10¼") composite engineered wood beams for the first floor, which are cantilevered to allow for a walkway through for the northern and southern sides in the second floor and two 134mm x 241mm x 4496mm (5¼" x 9½" x 14' 9") composite engineered wood beams for the second floor (roof). The eastern and western sides walkways were attained by the cantilevered 2x6 or 38mm x 140mm x 1003mm (1½" x 5½" x 12' 3½") joists. Beams and columns were rapped with wood sheets encasements to accommodate the depth of the frames of the wall assemblies. Figure 2-6 shows the test hut layout for the first floor in relation with the environmental chamber (Test hut drawings are presented in Appendix B).

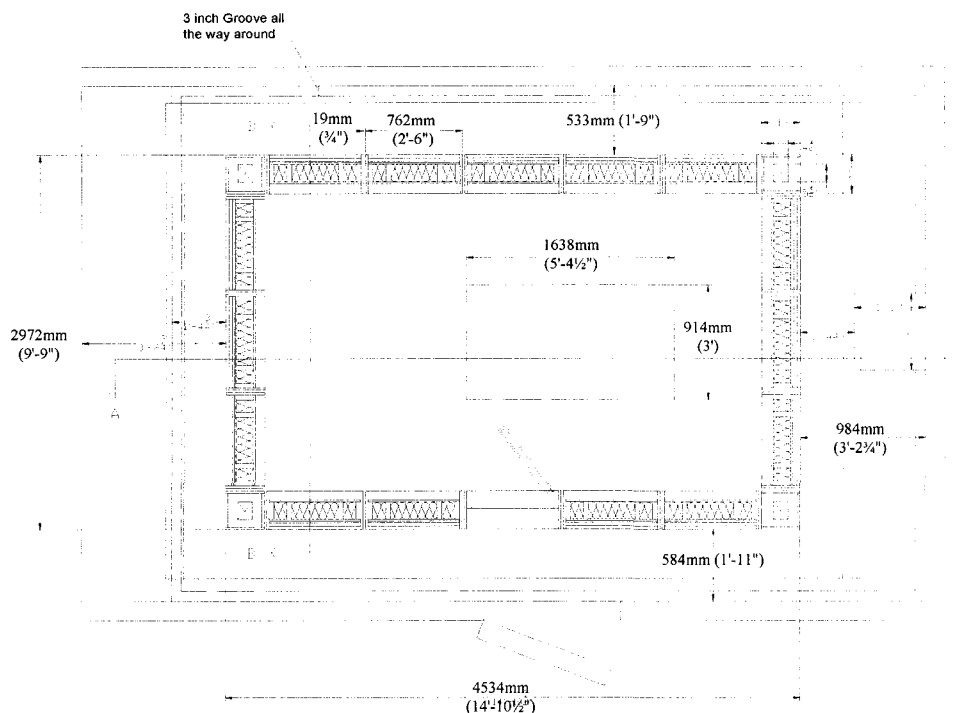


Figure 2-6. Test hut layout for the first floor

## 2.7 Design of Wall assembly

A Mock-up for the wall assembly frame was first constructed to demonstrate the possible configurations and to test the design of instrumentation on the wall assembly including all wiring and gravimetric samples (material cut outs to monitor MC change). Gravimetric samples comprise two parts, drilling the whole in the sheathing material and cutting-out the sample from another sheet of the same material. The gravimetric sample with little sanding should fit the hole flawlessly. For the stud gravimetric samples, a cavity of 13mm x 13mm x 13mm ( $\frac{1}{2}$ " x  $\frac{1}{2}$ " x  $\frac{1}{2}$ ") is made in the corner of the stud and plates for the cubic samples to fit. Moisture content probes can be installed easily on the sheathing, while in the stud, thin holes are to be drilled and then the probes are hammered into the stud until the desired depth. Because each moisture content probe has to be coupled with a thermo couple, another thin hole is drilled to insert the thermo couple to measure the temperature at the same depth of the moisture content probe.

Detailed drawings of the wall assembly were sent to Forintek in Quebec City, where the frames were first made. These drawings included dimensions and the steps to be followed to construct the wall assembly frame, plus details for what is needed for the instrumentation of each wall assembly. Forintek's part was to build the frames according to the following steps:

- Cut all the materials to the specified dimensions,
- Holes to be drilled in the left stud. There are three types of holes in different locations:
  - Moisture content probe holes.
  - Thermo couple holes.
  - RH sensors pass through holes.
- Cavities for stud cubic gravimetric samples to be made, 5 in the right stud, 1 in the top plate and 1 in the bottom plate,
- Openings to be drilled in all the sheathings for gravimetric samples (two drill bits with fixed diameter were provided),
- Assemble the frames without sheathings.

## 2.8 Monitoring parameters of Instrumentation

In the testing, several physical parameters are to be measured: weight, temperature, relative humidity, and moisture contents. Table 2-2 lists these parameters and the sensors used. Table 2-3 shows a detailed allocation of these sensors (Rao 2004):

Table 2-2. Parameters to be measured

Parameters	Sensor/Transmitter	Abbreviation
Weight	Load cell	LC
Temperature	Thermocouple	TC
Relative humidity	RH probe	RH
Moisture content	MC pin	MC
Moisture content	gravimetric sample	GR

Table 2-3 Summary of sensor allocations

Sensor	Per Specimen	Per Floor	Other	Usage	Total	MD*
LC	1		1	One per specimen and one for zero drift correction	32	2
RH	2			Two RH per specimen	66	4
		1		One per floor inside the test hut		
			2	Cold box and Hot box		
TC	15 (except specimen no. 4)			12 for temperature of MC sensors (4 in the stud and 8 on the sheathing) Note: in specimen no.4 there are 4 thermocouples in the stud only. 3 independent: 1 in the centre of cladding, 2 on dry wall.	545	16
		12		indoor and outdoor air temperature close to specimens (4")		
			2	air temperature over roof (2)		
	2			each RH probe has a temperature reading		
MC	12 (except specimen no. 4)			12 MC probes: 4 in the vertical stud; 8 on the sheathing. Note: in specimen no.4 there are 4 MC probes in the stud only.	364	12 chnl.
GR	25(except specimen no. 4)			7 cubic samples in stud specimen and 18 on the sheathing.	757	

Note: \* MD=module for DAS

To provide the most accurate representation of the parameters measured and the least interruption to the hygrothermal conditions of the samples, the design of the location, configuration, installation and wiring of different sensors considered the characteristics of the sensor types and the wall assemblies under testing. That was the case as well with the gravimetric samples. Most of the sensors for each wall assembly were instrumented separately before being installed in the test frame. The types and locations for different types of sensors and samples are presented with a description of purpose for each sensor:

### 2.8.1 Load Cell for measuring evaporation rate

The weight of a water tray at the bottom of the stud cavity of each test wall assembly is monitored continuously by one load cell. A diagram for the setup is shown in Figure 2-7. The water tray is made of 3mm (1/8") thickness clear acrylic sheets with dimensions to fit within the stud cavity. Water is added regularly by means of a thin flexible tube through the finishing layer (acrylic sheet window) that remains sealed during the test.

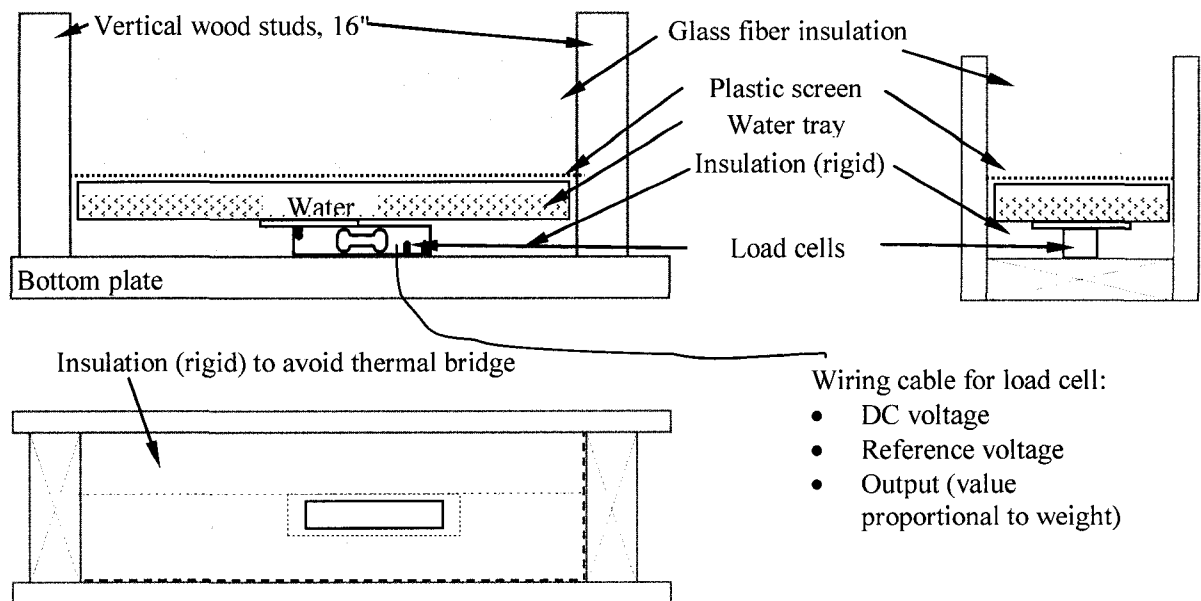


Figure 2-7. Weighing system with load cells (source: Fazio et al. 2006a)



### **2.8.2 Thermocouples in each wall assembly**

The majority of thermocouples originate from the wall assemblies. The thermocouple wiring uses a direct connection method, where the two copper and constantan conductors are twisted together, then the tip portion (where the temperature will be measured) of the twisted wires were soldered, and finally brushed with liquid tape to provide electrical insulation.

On each wall assembly, there are 15 thermocouple locations: one is on the cladding on the exterior side at the centre of the wall assembly, two on the gypsum board inside at the centre line 16 inches and 72 inches from the bottom end to measure the gypsum surface temperature at the same heights of the two relative humidity sensors inside the cavity. Four locations are in the stud and the remaining 8 locations are on the sheathing. These 12 thermocouples (in the stud and sheathing) are coupled with 12 moisture content probes (12 pairs of metal pins) to correct the moisture content readings. The exact locations for the thermocouples in the left stud and on the sheathing are shown in Figure 2-8.

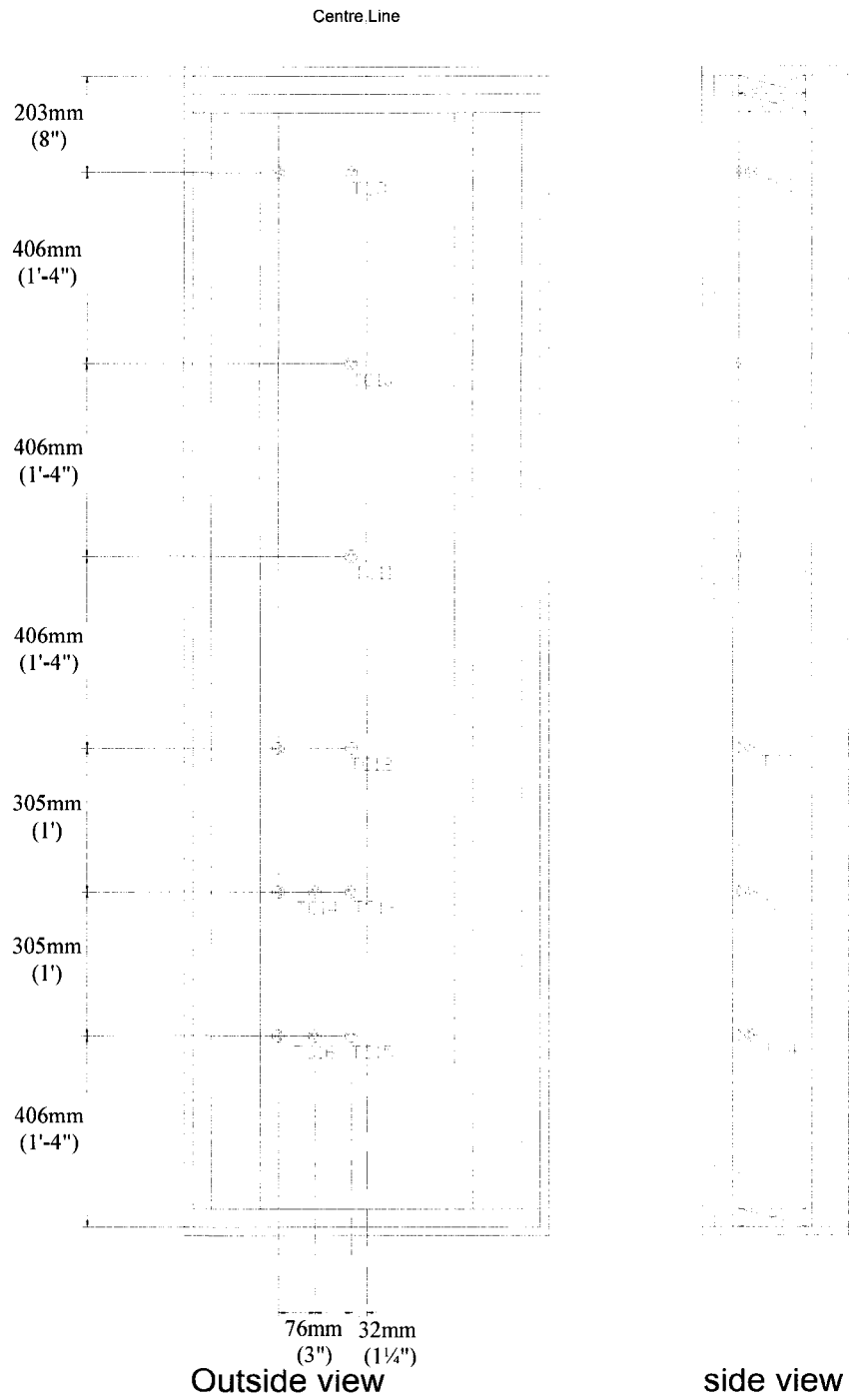


Figure 2-8. Thermocouple locations in the left stud and on sheathing of each wall assembly

### 2.8.3 Thermocouples for test hut

The other thermocouples are for air temperature close to the wall assemblies. There are 6 thermocouples outside the test hut at the perimeter about 102mm (4") from the wall assemblies, and 6 more thermocouples inside the hut with the same distance from wall assemblies for each floor. For these air temperatures, the thermocouple tip is shielded from radiation by a metal tube of 13mm (1/2") diameter (made from aluminum duct tape). Critical temperatures (such as test room temperatures) are measured by RTD (Resistive Temperature Detector) for precision and stability. Figures 2-9 and 2-10 show the locations for the 24 thermocouples inside and outside the test hut for both floors.

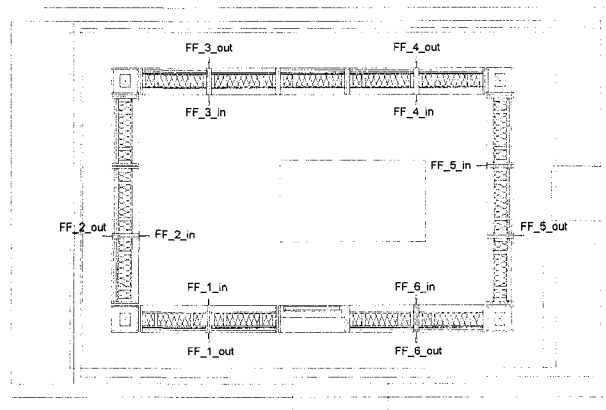


Figure 2-9. First floor air temperature thermocouple locations

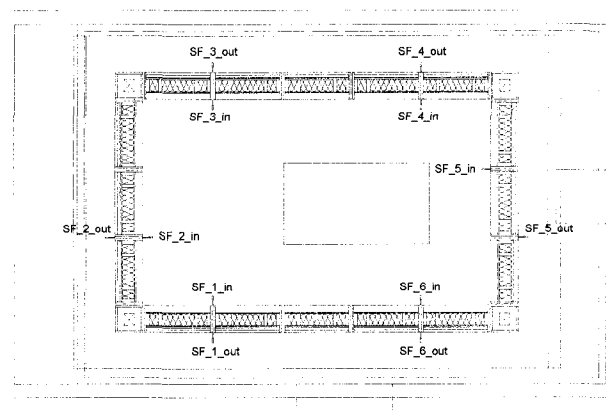


Figure 2-10. Second floor air temperature thermocouple locations

#### **2.8.4 Relative Humidity probes inside the Wall assembly**

On each wall assembly there were two RH probes on two different heights; 406mm (16") and 1829mm (72") from the base of the wall assembly. The relative humidity probe places a sensor and miniaturized transducer circuit in one small package. Both RH and temperature outputs are available on the probe wiring, where each probe has 4 wires and uses two AI channels. Two probes are installed in each wall assembly, and two more for each floor of the test hut. RH sensors use 4 AI modules (each 32 input channels) in total.

The RH probes are located inside the insulation cavity and the wires leading to the probes are fixed to the stud in the buffer zone area all the way down to the right corner of the assembly and grouped with the other wires. RH probes are hanged to taut nylon strings that were fixed across the two studs to provide more precise locations. A temperature sensor is embedded with each RH probe for measuring the temperature to determine the water vapor pressure from the simultaneously measured RH and temperature. Figure 2-11 indicates the locations of RH probes inside the wall assembly. Four more RH sensors are located in the cold box, hot box, first floor and second floor inside the test hut.

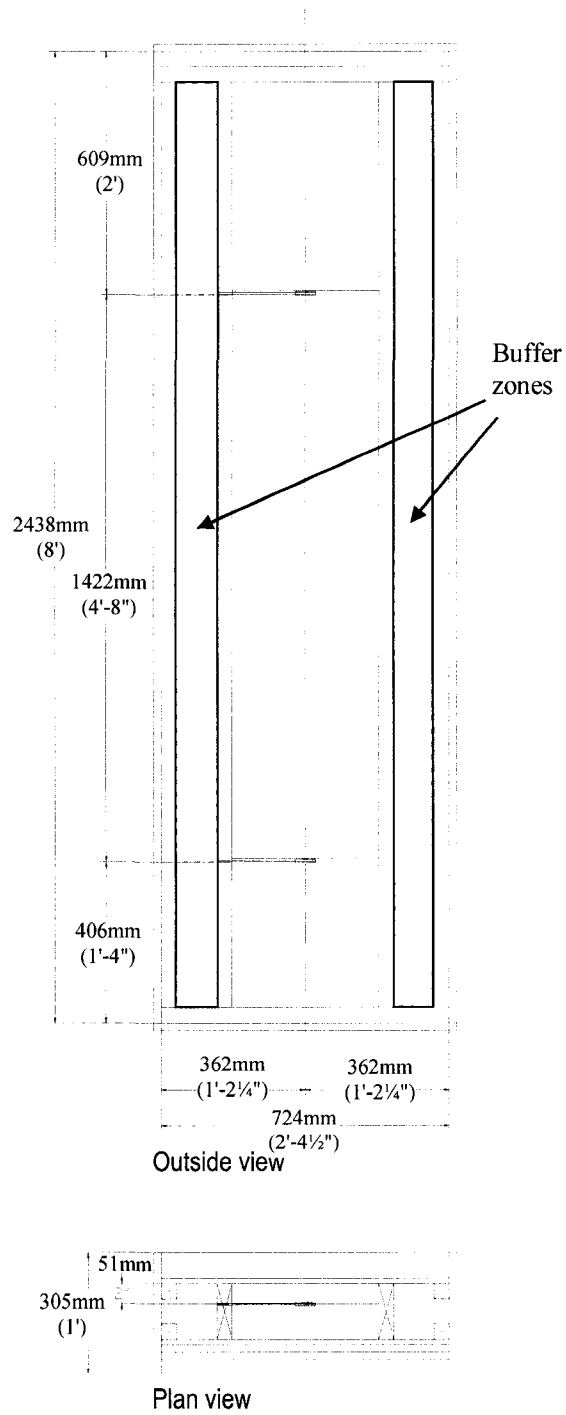


Figure 2-11. RH sensors positions in the wall assembly

### **2.8.5 Moisture content by metal pins**

Moisture contents of studs and sheathing are measured by resistive electronic moisture content transmitters. On each assembly, 12 probes (pairs of metal pins) were installed, with 4 in the stud (MC1, MC2, MC3 and MC4) and 8 on the sheathing (MC8, MC10, MC11, MC12, MC13, MC14, MC15 and MC16) at the locations shown in Figure 2-12. The number does not represent the order of MC probes or just a labeling name; it represents the location on the stud and sheathing, where these locations correspond to the gravimetric samples locations with respect to the centre line. On the sheathing, the customized pins used small gold-plated pins similar in size and shape to the pins inside the connector for parallel port printers, but with solid copper core. The holes on the sheathing for the pins were pre-punched using a hand-held moisture meter. For the stud, stainless-steel probes with insulated shank, 51mm or 2" in total length, were used. A pair of small diameter holes, 25mm (1") long, was drilled from the guarded zone side to a depth of 13mm (1/2") away from the central stud space side. The probes were then hammered into the stud till the tips of the probes were 6mm (1/4") from the stud surface on the cavity side. More detailed information about the MC pins is provided in Appendix C.

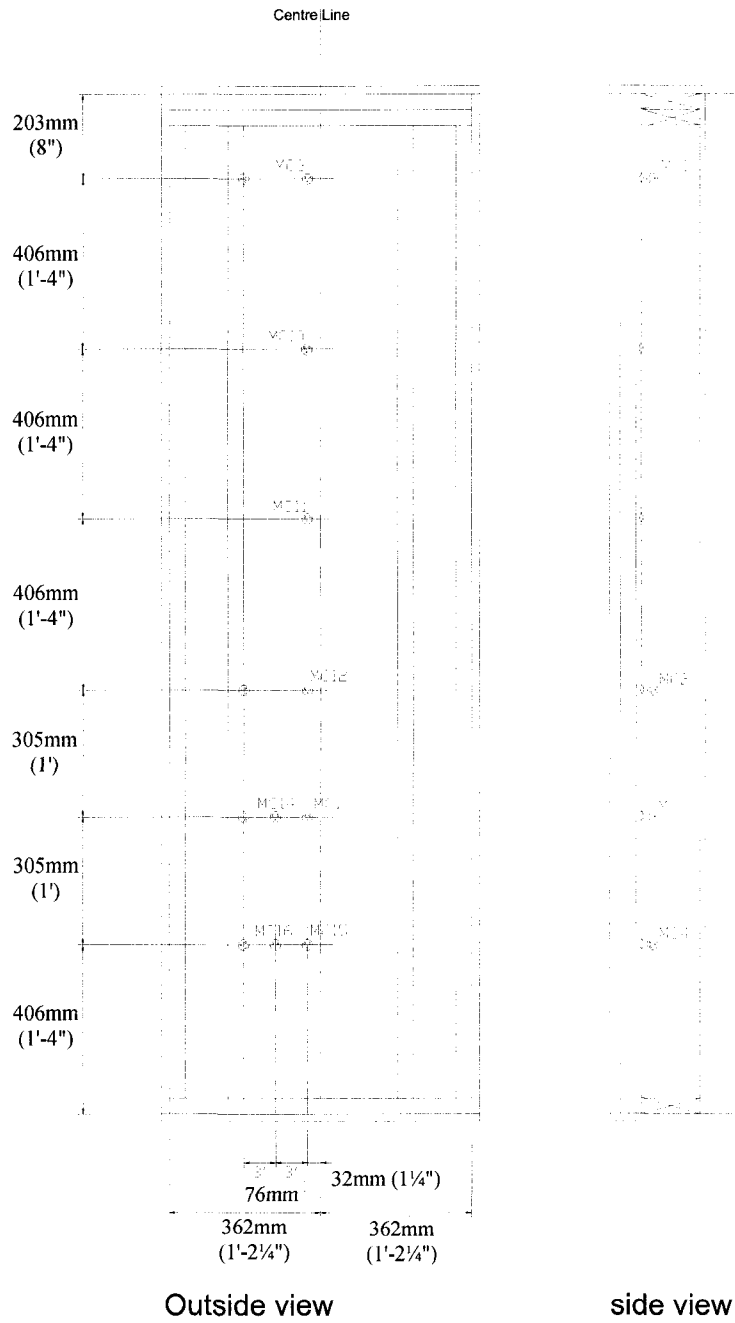
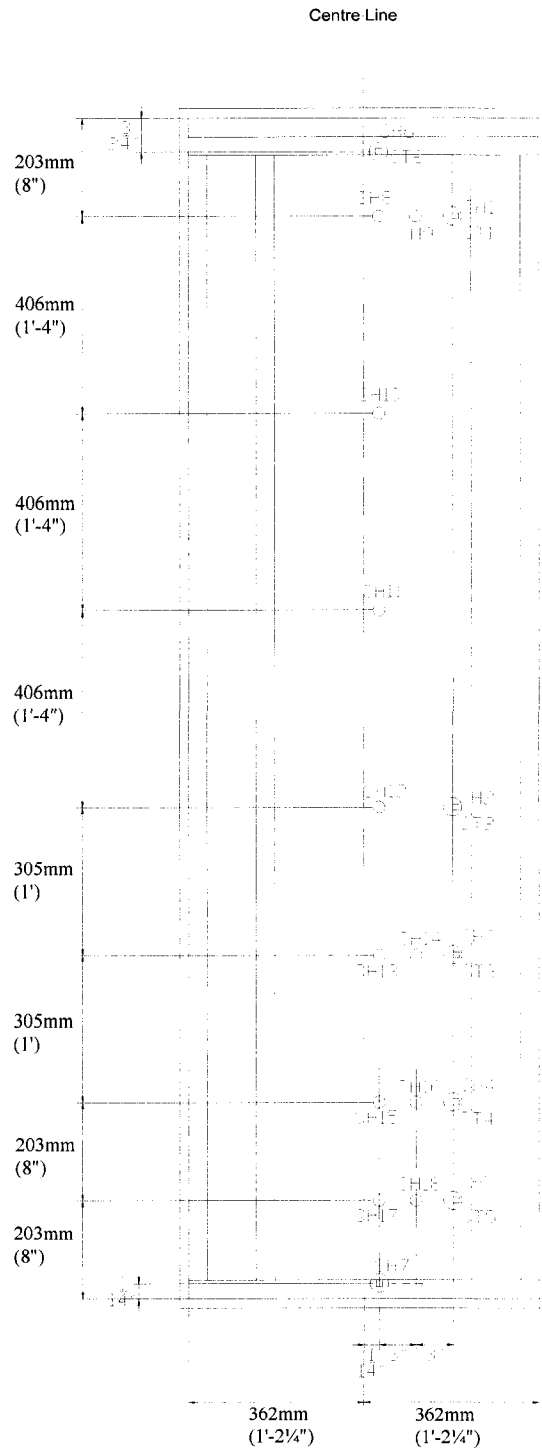


Figure 2-12. Locations of Moisture Content pins in the wall assembly

### **2.8.6 Moisture Content by gravimetric samples**

Moisture contents of the materials in the wall assemblies can also be monitored by gravimetric samples. These samples are circular cut-outs from the sheathing materials, and cubical cut-outs from the studs. These samples are used to measure the moisture content in wood studs and in the different sheathing materials. The moisture content of a gravimetric sample is determined as the ratio of the moisture contained within the sample to the mass of the oven dry sample. There are 25 gravimetric samples in each wall assembly frame (except wall assembly 4, where there are no samples in the sheathing); 7 samples in the wood studs (4 in the vertical stud, 1 in the top plate and 1 in the bottom plate); and 18 samples in the sheathing material. On each of the locations 1 to 7, there are two gravimetric samples, one cubical sample in the corner of the stud with the dimensions 13mm x 13mm x 13mm ( $\frac{1}{2}$ " x  $\frac{1}{2}$ " x  $\frac{1}{2}$ ") and one circular cut-out of the sheathing material with the diameter of 38mm ( $1\frac{1}{2}$ "), where these samples act as both, gravimetric samples and as caps to remove and reach the stud samples. The gravimetric samples in locations 8 to 18 are circular cut-outs from the sheathing material with the diameter of 25mm (1"). More samples were positioned in the lower part because they will experience more moisture accumulation being closer to the water tray. Figure 2-13 shows the exact locations for the gravimetric samples and their identification labels. "SH" stands for sheathing gravimetric samples and "ST" stands for the stud gravimetric samples.





**Outside view**

Figure 2-13. Locations of gravimetric samples in the wall assembly

## **2.9 Control of Test Conditions**

Conditions in the environment chamber and test hut need to be maintained during the testing periods. These conditions include: temperature and relative humidity. The methods of controlling these conditions include: automatic with industrial process controllers, simple thermostats, controls by DAS, and manual adjustment.

### **2.9.1 HVAC equipment**

Exterior conditions for the test huts are provided by heating and cooling equipment located in the cold box and hot box. The interior conditions of a hut are maintained by a small combined conditioning unit placed inside each test room. The equipment of the cold box contains an evaporator for cooling, an electrical heater for heating and centrifugal fan for air circulation. The HVAC equipment of the hot box can also be used to supplement cooling, heating, and air circulating when needed. The HVAC needs inside each test hut floor is provided by equipment placed inside a plywood box 914mm x 914mm x 1219mm (3' x 3' x 4'). The box is designed to distribute the air to surrounding evenly. An air-conditioning unit is placed on outside of the hut for each floor. Air in the test hut is circulated through the A/C unit to provide cooling. The control of these units is by the DAS. A specially design logic circuit board is use in conjunction with DAS to provide protection against water overflow (from drain pan of dehumidifier) and overheating in case of break down of the A/C unit. In addition, safety provisions are to be installed to cut off power to equipment and devices when abnormal situations occur. For example, when the cooling system fails and temperature in the large chamber rises to a preset value, the power to the heating equipment will be cut off to protest against further temperature increase in the chamber.

### **2.9.2 Data Acquisition System**

The functions of the Data Acquisition System "DAS" are (Rao 2004):

- 1) to monitor and save the conditions of wall assemblies under testing,
- 2) to maintain test conditions, and

- 3) to provide runtime display and plotting to assist the operator to judge the status of on-going testing.

The DAS has a total of 1,200 input channels and 22 output channels. Some reserves are allocated in DAS to replace channels that have problems during the testing. The configuration of the DAS was designed to be better suitable for the undertaken experiments. The improvements demonstrate in two aspects: distributed DAS and integrated measurement for moisture contents. The DAS consists of three data acquisition centers (DACs). A DAC here denotes a collection of data acquisition (DA) hardware that can read data from a large number of sensors and are located in one centralized chassis. A center could be a stand-alone DAS, it can also be just part of a DAS (for systems with multi-chassis). The three DACs are the current data acquisition system (DAC 0) and two remote DACs (DAC 1 and DAC 2). The DAC 0 will be used to measure RH, MC, test conditions, controller status, and other sensors in the chamber but out of the test huts. The two remote DACs will be placed in the two floors of the test hut, and measure mainly the thermocouples (Fig. 2-14).

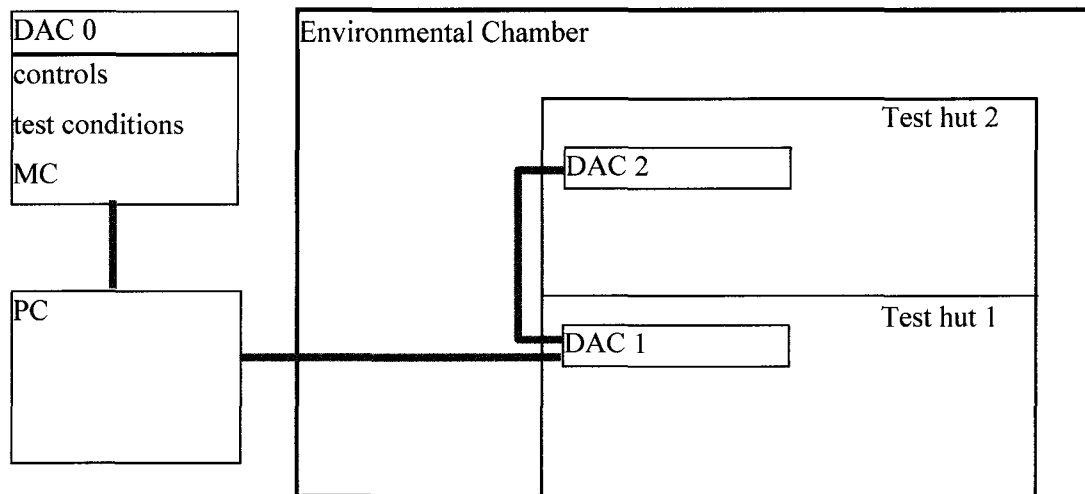


Figure 2-14. Diagram of DACs and data acquisition system

## Chapter 3

### IMPLEMENTATION

#### 3.1 Test Hut Construction

The test hut frame was constructed by two professional carpenters with students' help, according to the shop drawings with some of the details modified during construction. The following figures show the steps of construction of the hut frame.

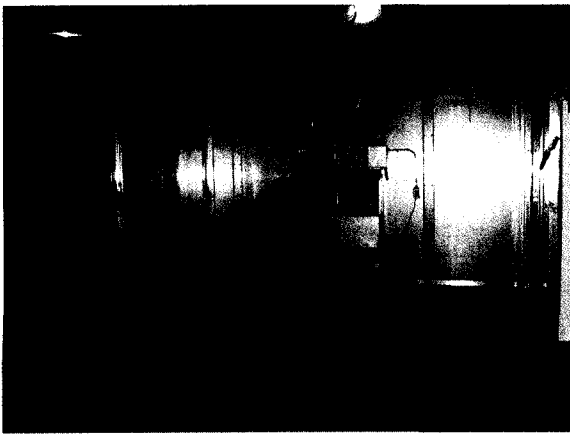


Figure 3-1. Environmental chamber before starting construction



Figure 3-2. Base studs and plywood footings for frame columns



Figure 3-3. Base studs and perimeter finished

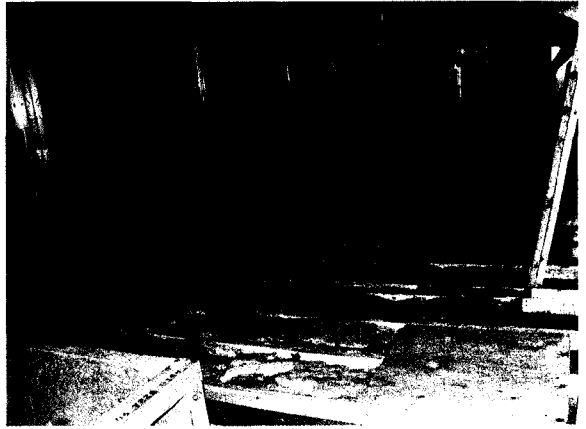


Figure 3-4. Base insulation



Figure 3-5. First floor flooring



Figure 3-6. Engineered columns fixing

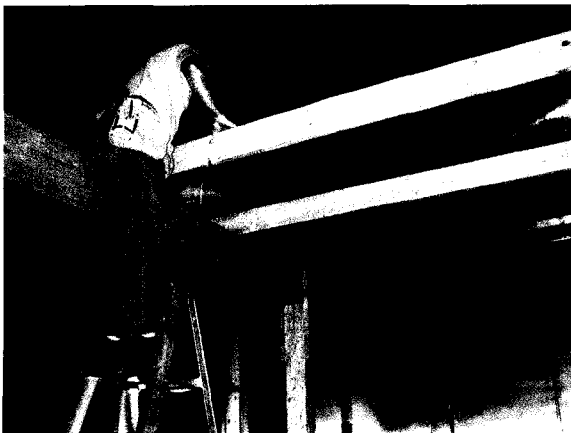


Figure 3-7. Joists installation supported by engineered composite beams



Figure 3-8. Cantilevered joists for second-floor walkway

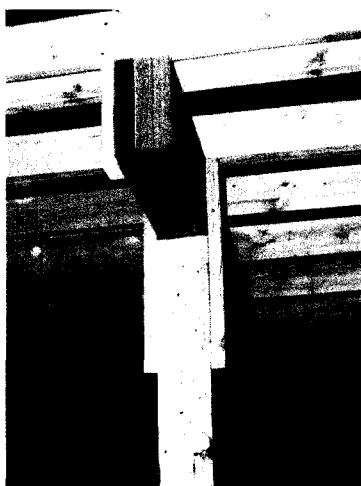


Figure 3-9. Composition of column, beam and joists



Figure 3-10. Flooring for the walkway on the second floor

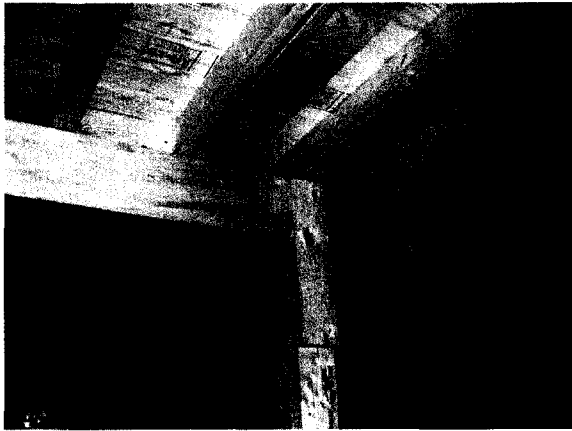


Figure 3-11. Composition of column, beam and joists with second floor flooring

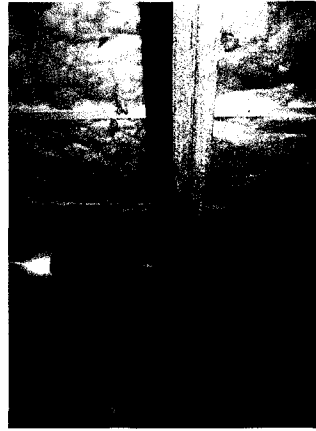


Figure 3-12. Fiberglass insulation beneath the walkway

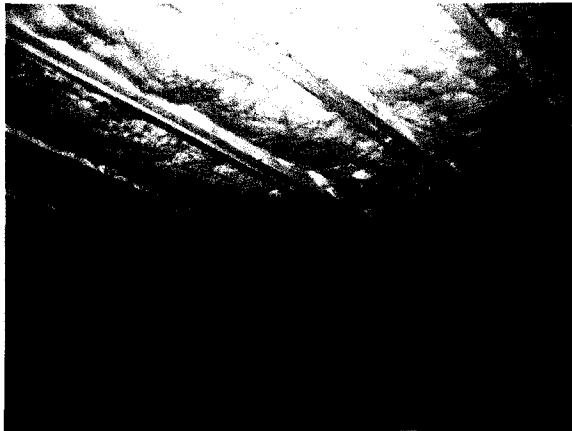


Figure 3-13. Fiberglass insulation in the first floor ceiling

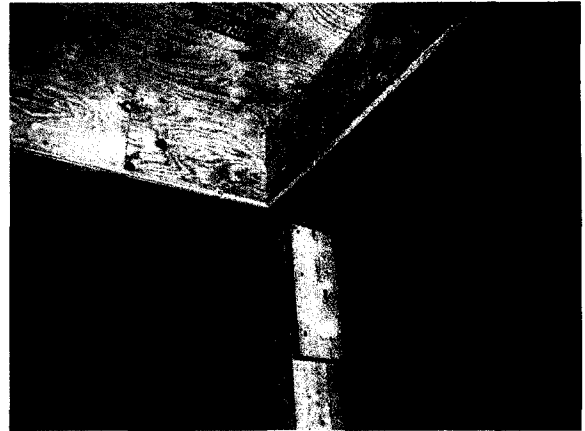


Figure 3-14. Encasements of main and secondary beams



Figure 3-15. First floor ceiling sheets



Figure 3-16. Cutting plywood ceiling sheets around stair-case opening



Figure 3-17. Placing composite beam at roof of the second floor



Figure 3-18. Detail of second floor engineered column, composite beam and roof joists



Figure 3-19. Roof joists fixed in place



Figure 3-20. Opening for AC unit in the roof



Figure 3-21. Roof sheets in place

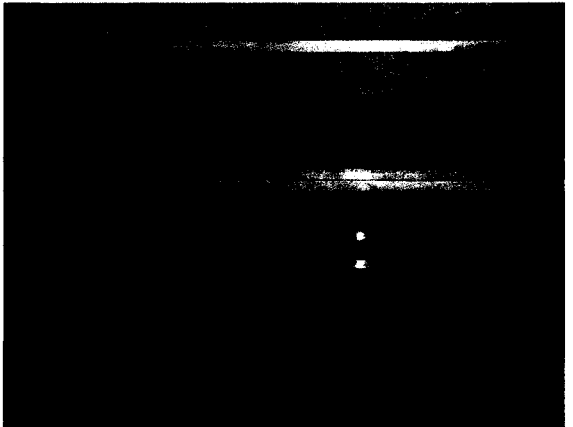


Figure 3-22. Fiberglass insulation in second floor ceiling



Figure 3-23. Columns' encasements to accommodate the width of the wall assemblies frames

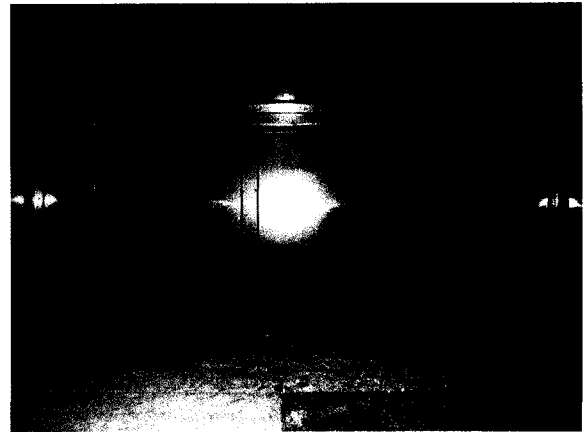


Figure 3-24. Roof of test hut



## 3.2 Wall assemblies implementation

### 3.2.1 Wall assemblies Instrumentation and Installation

The implementation of the instrumentation for the wall assemblies involved different tasks, from the set-up phase described earlier, to the preparation phase, and then to the implementation phase. The preparation phase included preparing and cutting all the wires for different parameters to the exact calculated lengths, this was done while the wall assembly frames were being prepared at Forintek. Figures 3-25 and 3-26 show the wires for the moisture content probes for both stud and sheathing. To better illustrate the whole process, the implementation of wall assemblies is described in the same order as they were instrumented and assembled.

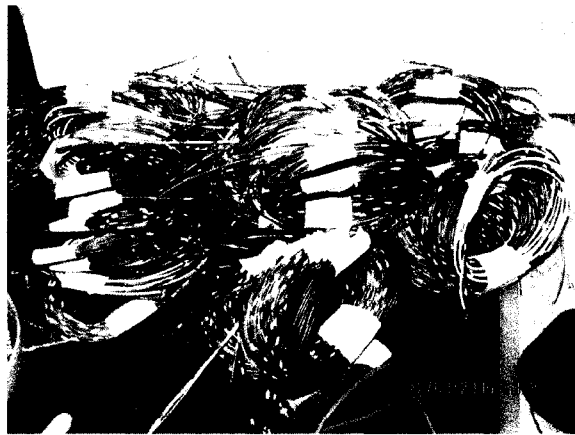


Figure 3-25. Sheathing MC metal pins

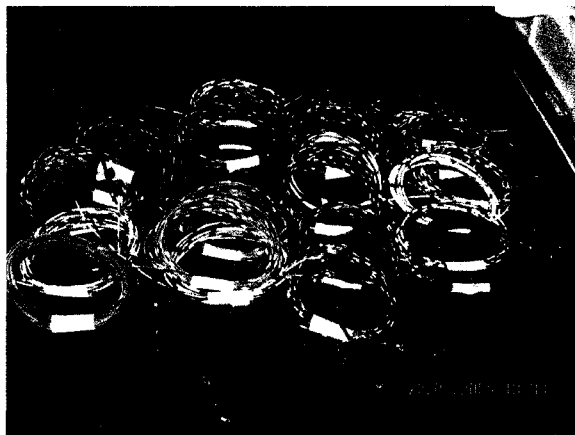


Figure 3-26. Stud MC probes

### 3.2.2 Wall frames

Wall frames were made at Forintek in Quebec city as mentioned earlier. The wall frames were then shipped to the lab in Montreal in several deliveries (Fig. 3-27).

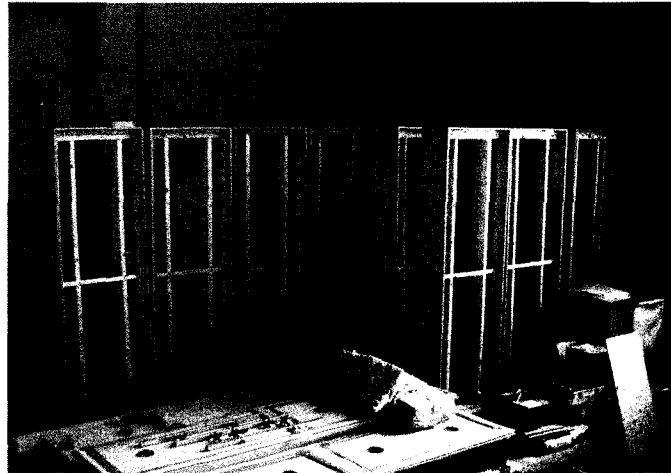


Figure 3-27. A group of wall assembly frames ready to be instrumented

### 3.2.3 Installation of MC probes in the stud

To install the MC probes in the stud, the whole frame was disassembled to take the left stud out. The MC probes were then hammered perpendicularly till the needed depth. The thermocouple wires were inserted at the same time after brushing the tip with liquid tape (Fig. 3-28). All the wires were then organized for the four locations in a way that they do not run over each other so it can be traceable.



Figure 3-28. Installation of MC probes in left stud

After installing the MC probes in the left stud, the frame was reassembled with checking the cavity spacing between the two studs (368mm or 14½” with a tolerance of 0.8mm 1/32”), which is important for placing the Load Cells and their nets.

### 3.2.4 Sheathing wiring and installation

Wires were organized on the sheathing to reach the various locations and to be traceable (Fig. 3-29). The hand-held MC unit was used to punch two tiny holes on the material for inserting the two gold pins (with wires already soldered on the end of the pins). Electrically conductive glue is used on the pins when inserting for maintaining good contact during and after insertion. Then, liquid tape is used as electrical insulation to cover the exposed metal ends.

All the wires were then directed towards the lower right corner inside the buffer zone and grouped to be taken out from the wall assembly (Fig. 3-30). Then the sheathings were installed to the wall assembly frames and were ready for cladding installation.

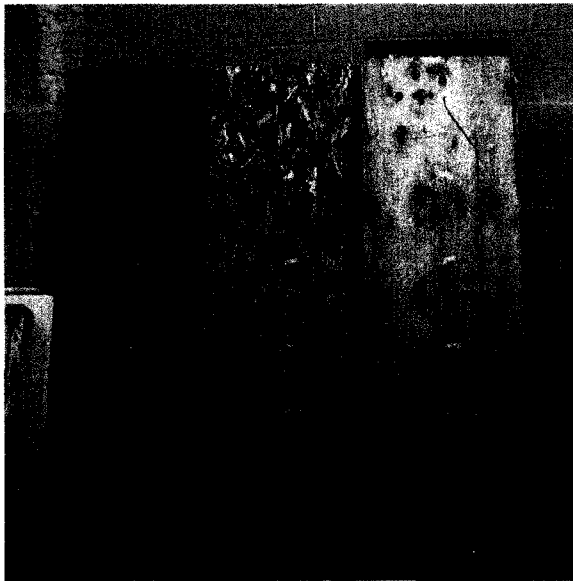


Figure 3-29. MC and TC wiring on different types of sheathings

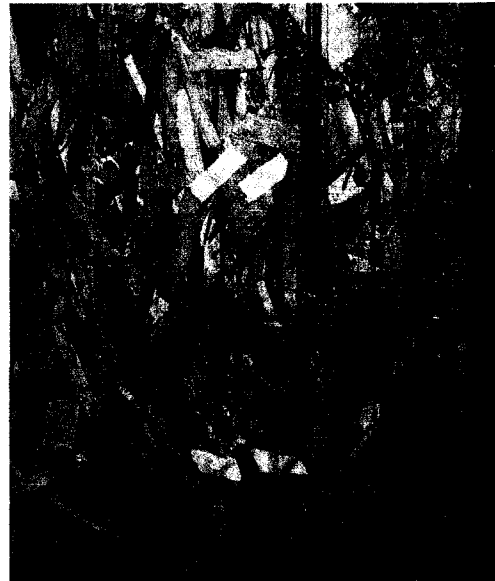


Figure 3-30. MC and TC wiring organization on the sheathing

### 3.2.5 Gravimetric samples preparation

Gravimetric samples were cut out from samples of the same sheathing materials used in the experiment (Fig. 3-31). Each sample was sanded down to fit a specific location (Fig. 3-32), and marked with an identification number. The same is done for the stud gravimetric samples.

*Sheathing samples* are taped around the perimeter and equipped with screws for ease of placement and removal. Two types of screws were used: a normal screw for the samples behind wood siding cladding, where there is an air gap (Fig. 3-33 right), and eye screws for the samples behind stucco cladding, where there is no gap between sheathing and cladding, installed in a way that they do not protrude over the surface (Fig. 3-33 left).

*Stud gravimetric samples* were first equipped with eye screws, and then painted with two coats of latex vapor barrier primer-sealer on the four sides in contact with the stud.

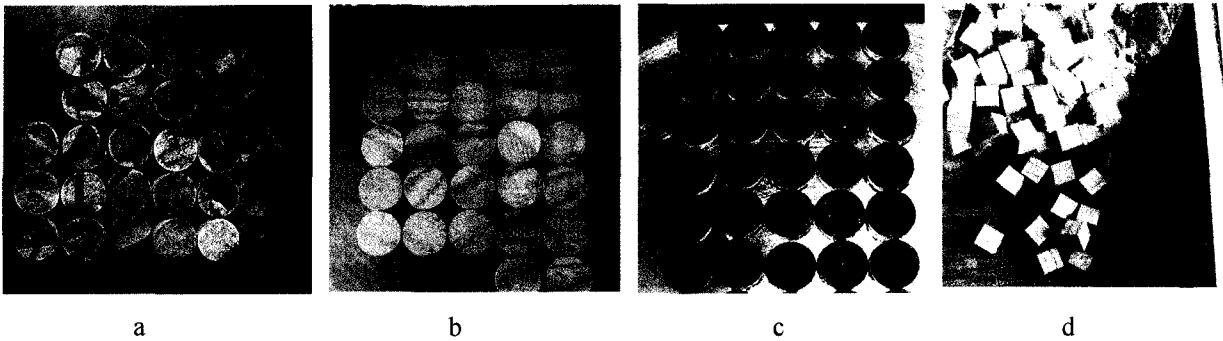


Figure 3-31. a) OSB sheathing gravimetric samples, b) plywood samples, c) fiberboard samples and d) stud gravimetric samples



Figure 3-32. Fit of gravimetric sample

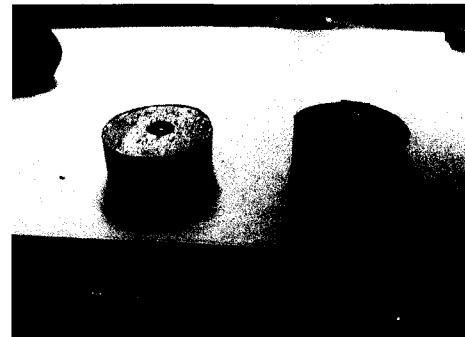


Figure 3-33. Sample screws and boundary tape sample

### 3.2.6 Installation of wall assemblies into the hut

The 12 stucco wall assemblies were installed first before stucco application, the remaining 15 wood siding wall assemblies and the 4 with no cladding assemblies were installed afterward. Small wood spacers were inserted between wall assemblies and in gaps between the assemblies and column/beam encasements to screw the wall assemblies in place. Figure 3-34 shows three stucco wall assemblies fixed in place.

Four pieces of 2x6 studs 127mm (5") high are cut and screwed under each wall assembly in the test hut to raise the wall assemblies off the floor to have space for passing and organizing the wires (Fig. 3-35).

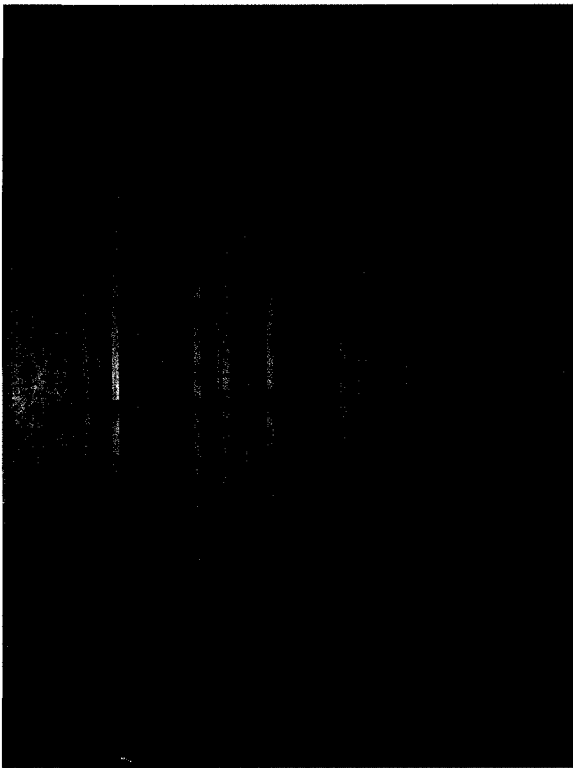


Figure 3-34. Three Stucco wall assemblies installed inside test hut

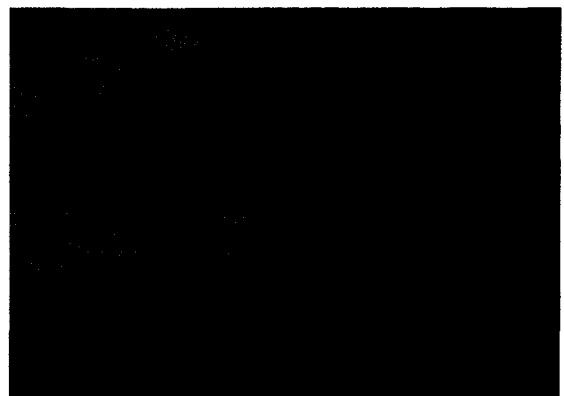


Figure 3-35. Stud pieces under wall assemblies

### 3.2.7 Cladding Installation

#### 3.2.7.1 Wood siding

Wood sidings were installed on the wall assemblies in the lab space with a help of a carpenter before installing the assemblies in the test hut. Then, the wall assemblies were installed in the test hut. For the gravimetric samples collection, instead of making windows in the wood sidings, the one or two whole wood sidings were made removable depending on sample' locations while the other sidings were fixed. The process of preparing the wood siding wall assemblies involved the following:

- Caulking was applied around the exterior perimeter of the sheathing.
- Tyvek paper (spun bonded polyolefin) was stapled to the sheathing after cutting openings for sample(s) removal. These openings were to be used many times for each gravimetric sample collection day. Therefore, the openings were taped in a way to continue being air tight (Fig. 3-36).
- Two 19mm x 38mm 1x2 furring strips are then installed at two vertical sides of the wall assembly.
- The fixed sidings then were screwed in place.

Figure 3-37 shows a wood siding wall assembly ready to be installed in the test hut as well as it shows the removable wood siding(s) for samples collection such as the one in Figure 3-38.

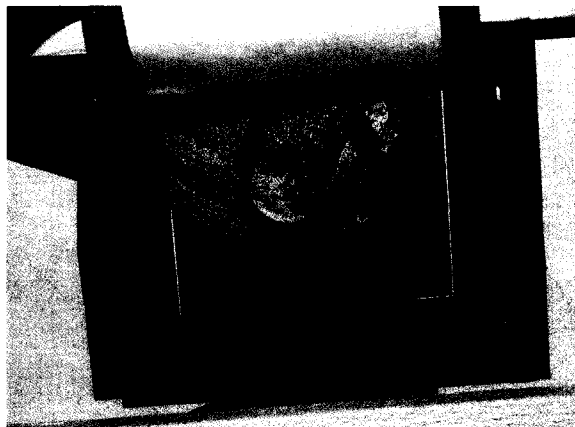


Figure 3-36. Tyvek opening to collect samples

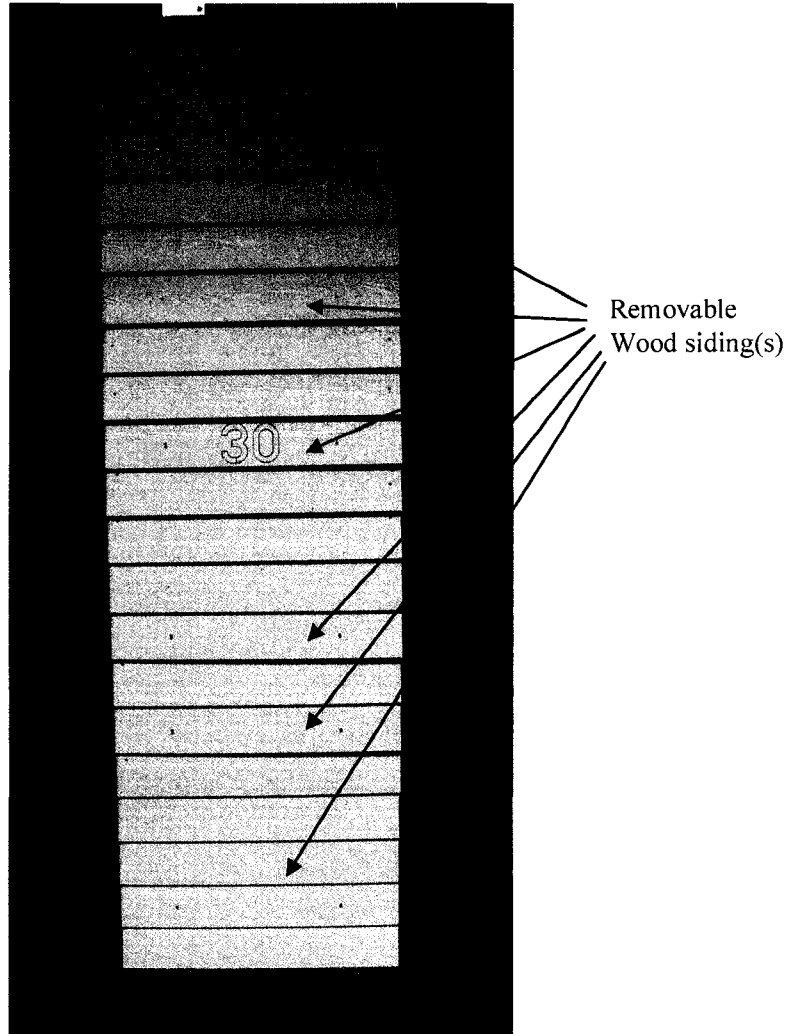


Figure 3-37. Removable wood siding(s) in a wood siding assembly



Figure 3-38. Removable wood siding

### 3.2.7.2 Stucco cladding

Stucco was applied by two specialized workers to the 12 stucco wall assemblies which had been installed and prepared in the test hut. Windows (Fig. 3-39) were made in the stucco to allow the removal of the gravimetric samples. On each wall assembly there were 7 stucco windows with three sizes depending on sample locations. These windows comprised: (i) two rectangular shape frames made of PVC strips cut to pre-determined dimensions and glued together, (ii) an outer frame that was fixed directly to the sheathing over the weather resistive membrane with flat head screws, and (iii) an inner frame that slides in and out to give access to the gravimetric samples (Fig. 3-39).

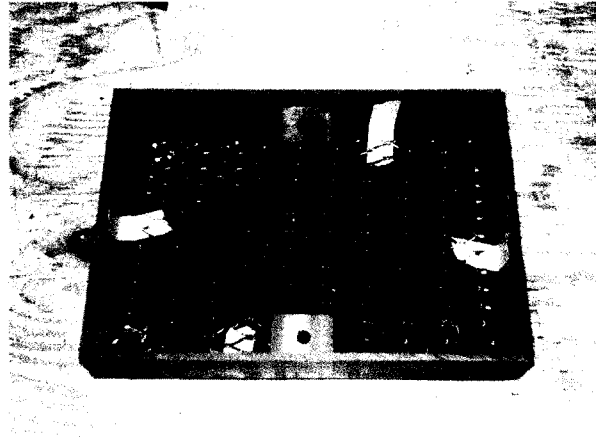


Figure 3-39. Inner part of a stucco window

The process of preparing the stucco wall assemblies involved the following:

- Two layers of construction felt paper (weather resistive membrane) were stapled to the sheathing. Openings were cut in the felt paper behind the stucco windows' locations for gravimetric samples removal.
- The outer frames for the stucco windows were fixed in place.
- Steel mesh was stapled over the felt paper. Openings were cut in the mesh to fit around the fixed plastic frames.
- The above steps were made outside the chamber in the lab space. Then, the wall assemblies were fixed in their locations inside the test hut.



- The inner parts of the stucco windows were inserted in the outer fixed frames and the small gaps in between the windows and the fixed frames were taped to avoid the intrusion of stucco while it was being applied. Then stucco was applied in three coats one day apart with a final thickness of about 25mm (1").

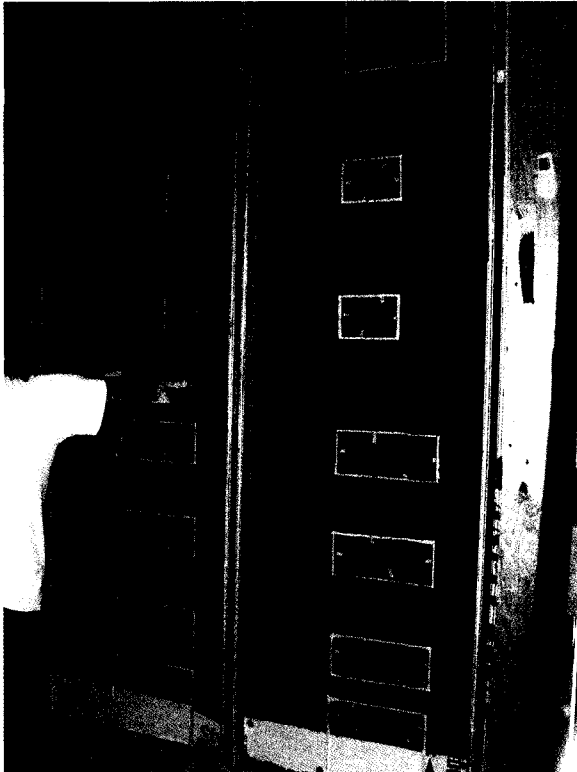


Figure 3-40. Applying the first coat of stucco onto the sheathing

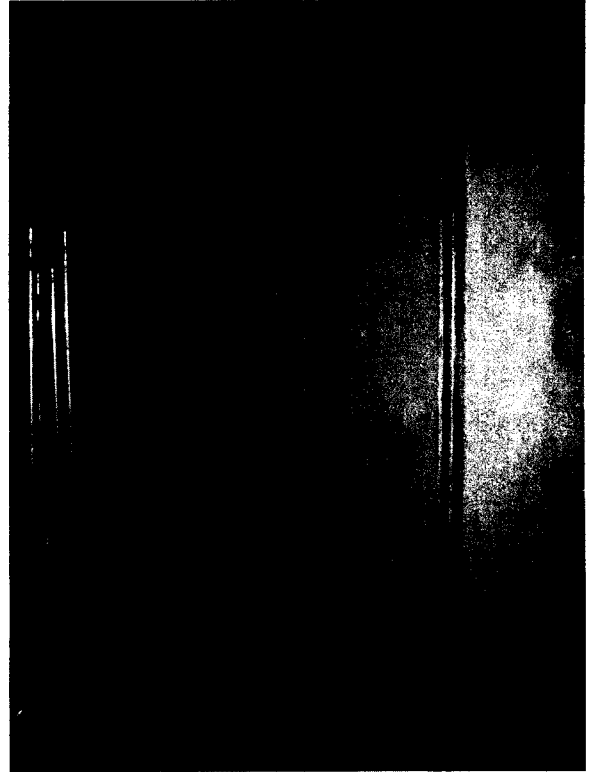


Figure 3-41. Stucco application finished

### 3.2.8 Connecting the wires to terminal blocks and DAS

Wiring to moisture content and thermo couple sensors were connected first and then tested to check for any faults. All wires were organized, grouped into the lower right corner and brought out of the assembly frame (Fig. 3-42), connected to the terminal blocks (Fig. 3-43), and then placed inside small boxes for protection. All the cables were organized beneath the wall assemblies to be protected from damage or from being stepped over.

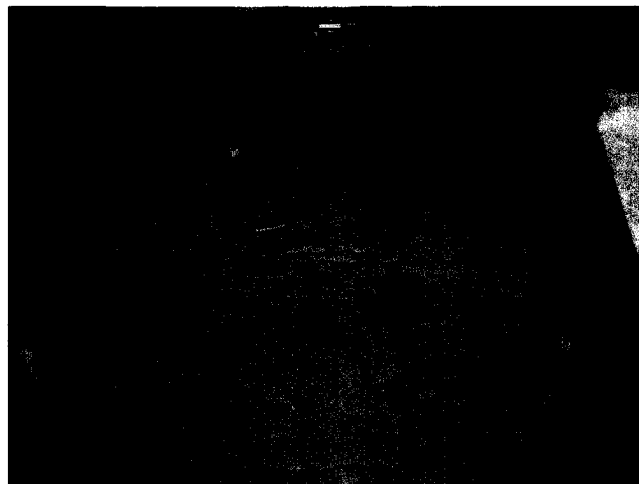


Figure 3-42. Wires coming out of wall assemblies

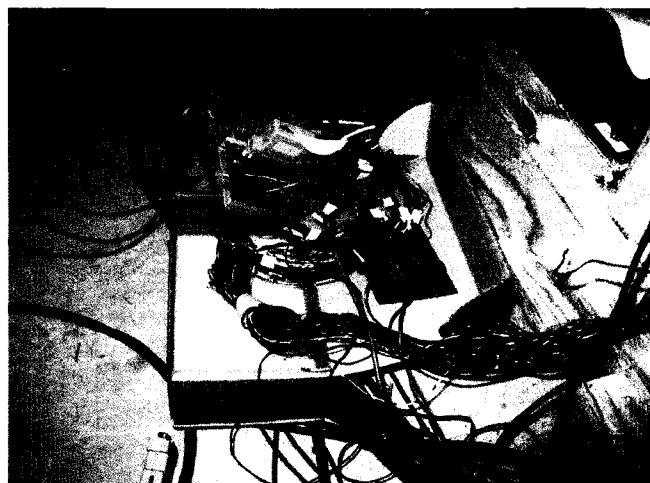


Figure 3-43. Thermo couple and moisture content terminal blocks

### 3.2.9 RH sensors installation

Two taut nylon strings were fixed across the two studs of each wall assembly at the heights of 406mm (16") and 1829mm (72"). The RH probes were cantered in the cavity (Fig. 3-44). Again, data readings were monitored and tested for RH sensors.



Figure 3-44. RH sensors installed

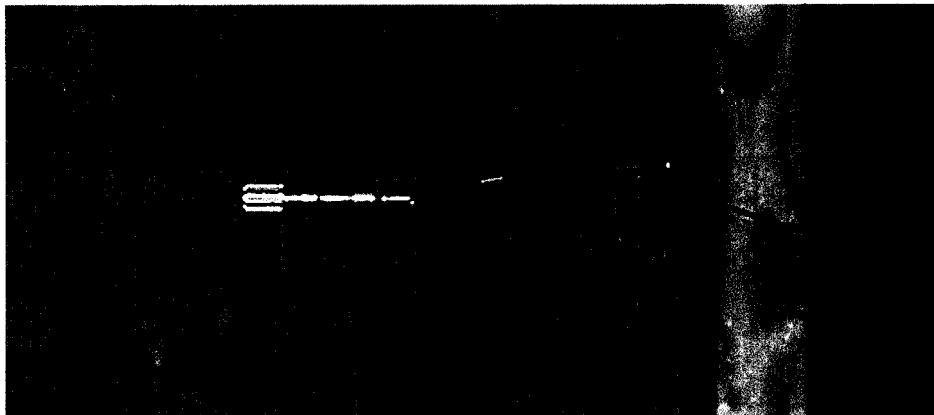


Figure 3-45. Close-up picture for an RH sensor

### **3.2.10 Installation of load cell (LC) and net below insulation**

Load cells were placed over the bottom plate in all the wall assemblies. The LC cable is passed through a hole drilled in the bottom plate and frame. All the load cells were checked and tested through the DAS. The nets above the load cells were installed to hold the fiberglass insulation in place and to prevent debris to fall in the water trays (Fig. 3-46).

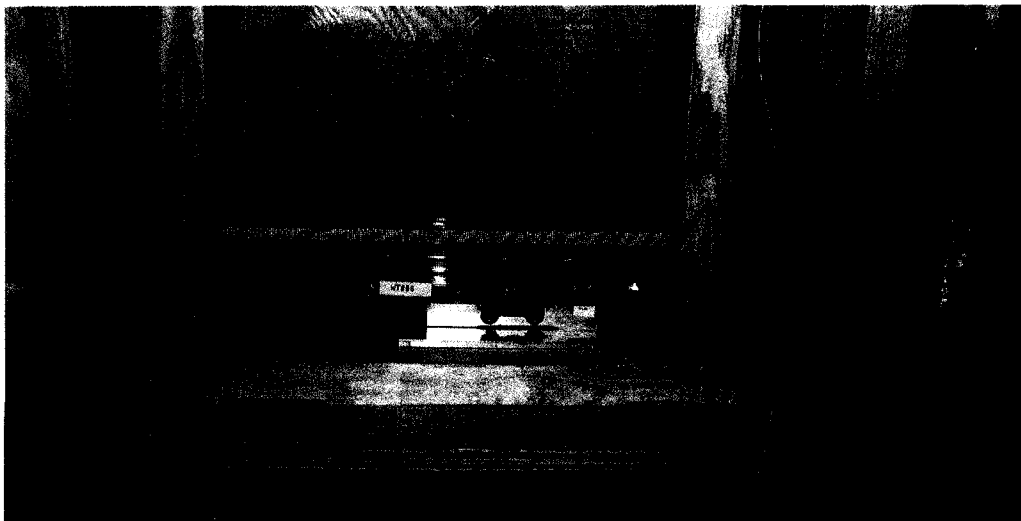


Figure 3-46. Load cell placed and net installed

### **3.2.11 Installation of fiberglass, vapor barrier and gypsum board**

After all of the wiring is done and all sensors checked through readings from the data acquisition system, all moisture content pins on the sheathings were brushed with liquid tape. Then, the fiberglass was installed (Fig. 3-47) taking care that the RH sensors were properly positioned within the insulation (Fig.3-48).



Figure 3-47. Fiberglass installed

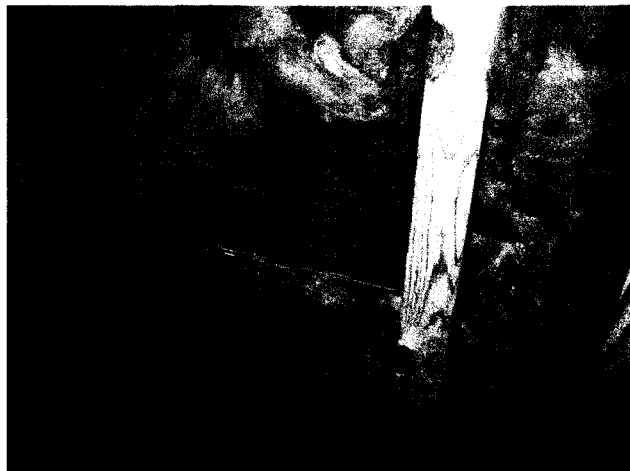


Figure 3-48. RH sensors embedded in the insulation

Polyethylene sheets were stapled to 19 wall assemblies according to Table. 2-1. A cut out was made in the sheet not to block the LC window (Fig. 3-49).



Figure 3-49. Vapor barrier installation

Gypsum boards were numbered for each wall assembly and cut to the specific dimensions. Small rectangular pieces were cut out at the bottom for the LC windows made of acrylic. All the boards were painted in the lab with one primer and two coats of paint applied one day apart. The gypsum boards were taken inside the hut and installed onto the wall assemblies, followed by caulking around the perimeters. Screws were covered with sealing compound which was then sanded.

### 3.2.12 LC and water tray windows installation

The last step in closing the wall assemblies was to fix the clear acrylic sheet window over the rectangular cut-out area on the drywall on each wall assembly. The acrylic window was fastened with four screws to the studs through the gypsum board. The window perimeter was sealed with clear peel-off caulking for easy removal to gain access to the moisture source assembly. Access holes were provided on the acrylic window, which would be opened to insert a plastic tube and add water to the water tray when required (Fig. 3-50).

### 3.2.13 Air tightness of the test hut

All the gaps beneath the wall assemblies were closed by fitting rigid insulation boards cut to size to provide thermal insulation and then caulked for air tightness. The same was done in the gaps around the AC units in both the first floor and on the roof. All other gaps between the wall assemblies and between the wall assemblies and column/beam encasements were filled with regular expanding foam insulation from both inside and outside (Fig. 3-51).



Figure 3-50. LC and water tray window installed

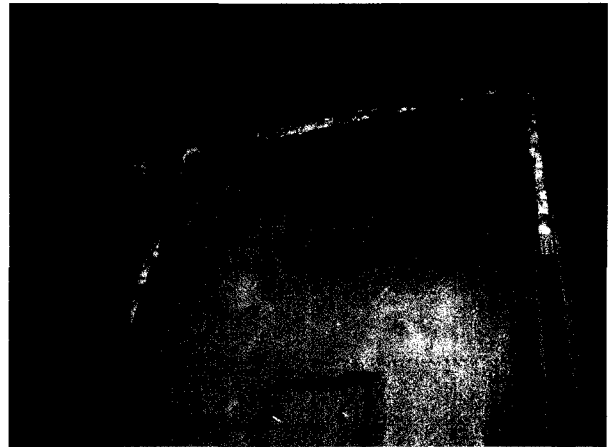


Figure 3-51. Filling the gaps with foam insulation

### 3.2.14 Organizing the wires beneath wall assemblies

After connecting and checking, all wires and cables were organized beneath the wall assemblies in a way that they cannot be damaged or stepped on. Plywood sheets were cut to fit and screwed to the bottom of the wall assemblies to protect the wiring and to provide access when required (Fig. 3-52).

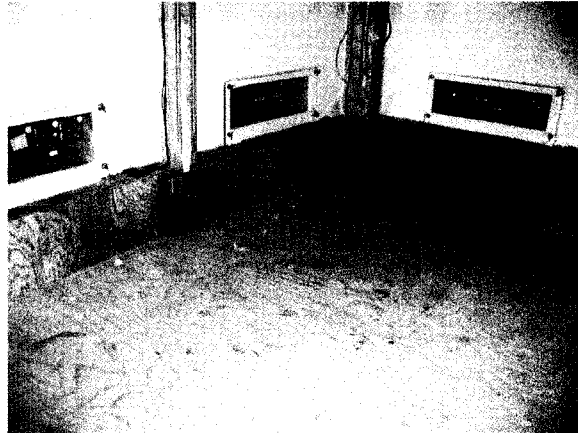


Figure 3-52. Cables organization beneath wall assemblies

### 3.2.15 HVAC System Inside the test hut for first and second floors

The HVAC box inside the first and second floors in the test hut included a heater, humidifier, and dehumidifier (Fig. 3-53) to maintain indoor conditions. A fan was fixed on top of the box to distribute the air evenly.

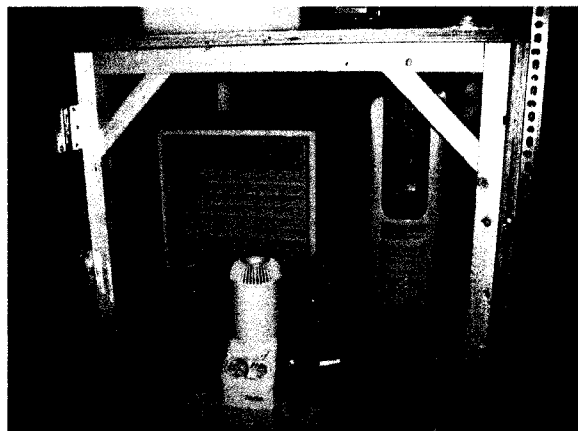


Figure 3-53. HVAC system inside each floor in the test hut



### 3.3 Locating wall assemblies inside the test hut

As stated earlier, there are 12 wall assemblies duplicates, 6 with stucco cladding and 6 with wood siding cladding (Table 2-1). First, the stucco wall assemblies were located in the northern and southern sides of the test hut, where there was more space for the stucco contractors to maneuver while applying the stucco. Second, wall assemblies 1, 2 and 3 were installed on the eastern side. These wall assemblies have no duplicates. Thirdly, wall assemblies 29, 30 and 31, also without duplicates, were installed on the second floor above 1, 2, and 3, respectively. Fourthly, wall assembly 4, the only one with polystyrene insulation board as the sheathing, was positioned on the second floor in the same location as the door on the first floor. Figures 3-54 and 3-55 show the locations of the wall assemblies on the first and second floors respectively.

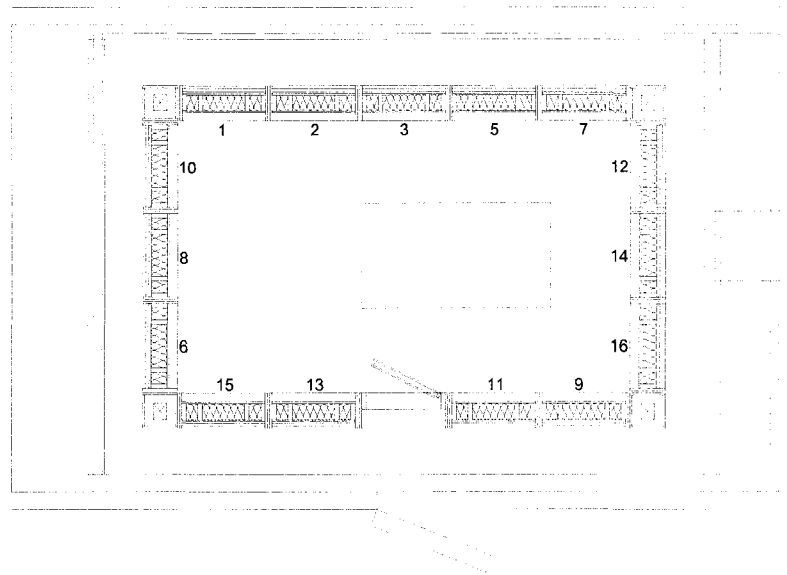


Figure 3-54. Locations of wall assemblies on the first floor

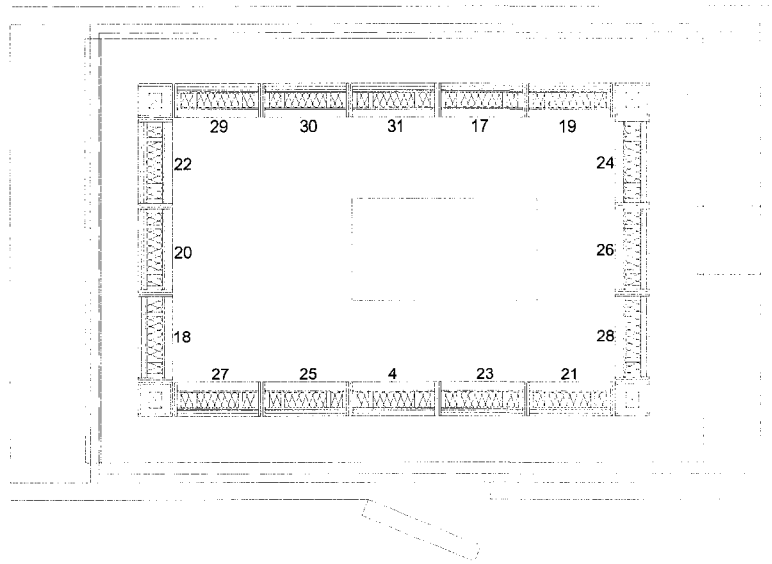


Figure 3-55. Locations of wall assemblies on the second floor

## Chapter 4

### TEST METHODOLOGY

The project in this thesis focused on an experimental study to develop new testing methodologies. The test methodology presented in this chapter includes the loading conditions including temperatures, relative humidities, and moisture source within the stud cavity. Five test runs are described. Indoor and outdoor conditions are maintained at steady state for the different test periods. The conditions adopted represent worst possible outdoor drying conditions as obtained from the weather analysis. A protocol to collect the 757 gravimetric samples was established to govern the collection of data from these samples on a weekly basis to monitor the moisture content change of the different materials in the wall assemblies.

#### 4.1 Weather data conditions

Indoor conditions were set at:

- Temperature: 21°C
- RH: 35 %

Outdoor conditions were based on the weather data analysis carried out by Candanedo et al. (2006). The 10% worst drying conditions were selected in the ranking years based on monthly average drying index “DI” for each month for the different test periods. For test periods 1 (1/3 pf water tray filled) and 2 (2/3 of water tray filled), conditions for the month of October were used since October emerged from the analysis as the month with the worst conditions for drying potential. The outside temperature and relative humidity RH were then obtained from the “Index Rank per Month” information. The year of 1977 was selected having the following outdoor conditions:

- Temperature: 8°C
- RH 76%.

## **4.2 Hygrothermal test – Montreal conditions**

### **4.2.1 Pre-conditioning of the test hut**

In early spring of 2005, before installing the wall assemblies into the test hut frame inside the environmental chamber, the materials for the wall assemblies were relatively dry. Pre-conditioning of the test hut started at 15:10 on April 17<sup>th</sup>, 2005 with the following conditions:

- Temperature:  $20 \pm 2$  °C
- RH: 40%

### **4.2.2 Establishment the base line**

The main objective of the period to establish the base line was to attain steady state conditions at the start of the test. The period to establish the base line started at 13:50 on June 29<sup>th</sup>, 2005 with the following outdoor conditions:

- Temperature: 8°C
- RH: 65 % (and set to 76% on July 8<sup>th</sup> at 10:45)

### **4.2.3 Test program**

#### **4.2.3.1 Test period 1**

After reached approximate steady state conditions for the test parameters ( $MC$ ,  $T_o$ ,  $T_i$ ,  $Rh_o$ , and  $RH_i$ ), test period #1 was started at 14:20 on July 18<sup>th</sup>, 2005 with the outdoor conditions set at  $T = 8\text{ }^\circ\text{C}$  and  $RH = 76\%$  corresponding to the month of October. Water was added to the middle compartment (1/3) of the trays at the bottom of the stud cavities. This test period lasted 12 weeks and two days.

#### **4.2.3.2 Test period 2**

Test period #2 started on October 12<sup>th</sup>, 2005 by adding water to the second compartment of the water tray, thus increasing the water surface area to 2/3 the tray total area. This test period lasted for 16 weeks. The climatic conditions were kept at  $T = 8\text{ }^\circ\text{C}$  and  $RH = 76\%$ .

#### **4.2.3.3 Test period 3**

On February 2<sup>nd</sup>, 2006, test period #3 started by changing the exterior weather conditions to those of the month of April in the Weather Data Analysis (Candanedo et al. 2006) representing spring conditions of  $T = 5\text{ }^\circ\text{C}$  and  $RH = 69\%$ . The test ran for four weeks till March 2<sup>nd</sup>, 2006.

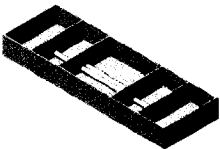
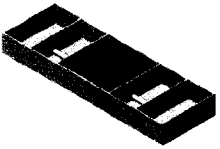
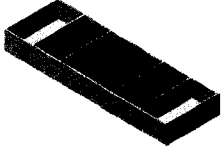
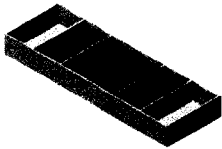
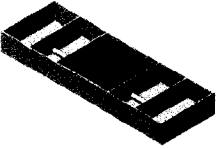
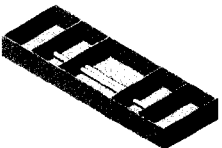
#### **4.2.3.4 Test period 4**

Test period #4 ran for four weeks, from the 2<sup>nd</sup> till the 30<sup>th</sup> of March 2006, to simulate the month of May in the Weather Data Analysis with outdoor conditions set at  $T = 12\text{ }^\circ\text{C}$  and  $RH = 70\%$ . The moisture load was reduced to 1/3 the surface area of the water tray.

#### **4.2.3.5 Test period 5**

In test period #5 conditions were set to dry the wall assemblies under June outdoor conditions of  $T = 17^\circ\text{C}$  and  $RH = 68\%$  and no water in the trays. This test period ran for four weeks from March 30<sup>th</sup> to April 27<sup>th</sup>, 2006.

Table 4-1. Summary of test periods and loadings

Test periods	Dates and duration	Loading conditions	
		Climatic loading	Moisture loading
Establishing baseline	29/6/2005 – 18/7/2005 19 days	8 °C 76% RH	
# 1 October conditions	18/7/2005 – 12/10/2005 12 weeks	8 °C 76% RH	
# 2 October conditions	12/10/2005 – 2/2/2006 16 weeks	8 °C 76% RH	
# 3 April conditions	2/2/2006 – 2/3/2006 4 weeks	5 °C 69% RH	
# 4 May conditions	2/3/2006 – 30/3/2006 4 weeks	12 °C 70% RH	
# 5 June conditions, drying	30/3/2006 – 27/4/2006 4 weeks	17 °C 68% RH	

### **4.3 Gravimetric samples protocol**

Moisture contents of the materials in the wall assemblies were monitored manually by 757 gravimetric samples. The MC of a gravimetric sample is determined as the ratio of the moisture contained within the sample to the mass of the oven dry sample. Since most of the data analysis to be performed is based on the data gathered from the gravimetric samples, the accuracy of the readings of these gravimetric samples is of a great importance in order for the results to be reliable. Different measures were taken into consideration in the development of the gravimetric samples protocol to enhance the accuracy of the data.

#### **4.3.1 Initial moisture content of gravimetric samples**

All samples were placed within the chamber under controlled conditions for 6 weeks to acquire the same initial moisture contents as the other materials in the wall assemblies. Typically two samples for each material were oven dried to set a preliminary benchmark for the dry weight of the samples. The following initial moisture content values were calculated and assumed for all the samples:

- OSB: 3.8%
- Plywood: 4.9%
- Fiberboard: 5.1%
- Stud: 4.0%

#### **4.3.2 Collection Process of Gravimetric Samples**

There are 757 gravimetric samples to be collected, weighed, and replaced once a week. Due to this large number of samples, a procedure was established consisting of: removing the gravimetric sample from the assembly components, taking it to the scale, weighing it, taking it back, and re-installing it. This procedure was to be performed as quickly as possible to prevent the sample from gaining or losing moisture. The duration of this procedure is referred to as the gravimetric “sample travel time”.

### **4.3.3 Samples enclosure during collection process**

One way to collect the samples is to put them in “zip bags”, which could be considered the best enclosure for tightness with the minimal evaporation of the sample’s moisture content. However, collecting the samples in zip bags is a time consuming process. The bags have to be zipped open and closed three times in the whole process, in collecting, weighing, and re-installing. Moreover, the gravimetric sample’s identification number has to be checked twice, while weighing and re-installing, which will add more time to the “sample travel time” and consequently to the whole collecting process time.

The other option was to use simple plastic openable containers with movable dividers, where the dividers were arranged in a way that each sample has its own compartment. To have better moisture tightness, the dividers were fixed and sealed with epoxy glue. Gaskets were taped on the openable part of the container to ensure tightness when closing. Before using these plastic containers, the evaporation rate of the gravimetric samples inside has to be determined and compared to the evaporation rate of the samples inside zip bags for similar time periods.

### **4.3.4 Evaporation rate of samples (during collection process)**

A small test was carried out to determine and compare the evaporation rate of the gravimetric samples while being in zip bags and in the plastic container. Six samples, two OSB, two plywood, and two fiberboard samples were soaked in water for 18 hours to reach high moisture contents because samples with high moisture contents will experience higher evaporation rates. The test was held inside the test hut. The parameters were 21°C and 35% RH inside the test hut and 8°C and 77% RH outside the test hut. Table 4-2 shows the evaporation rates according to time and the change in moisture content ( $\Delta MC$ ) in different time intervals. It was concluded from table 4-2 that in extreme wet conditions of 77% MC in the plywood and 51% MC in the fiberboard, when using the plastic trays, the evaporation rate could reach 1% for plywood and fiberboard gravimetric samples after 60 minutes; hence, it was decided to keep the “sample travel time” at 60 minutes or less.



Table 4-2. Evaporation rates of different samples for different periods

enclosure	material	dry weight  (g)	after soaking the samples in water							
			0 minutes		10 minutes		20 minutes		60 minutes	
			weight (g)	MC %	weight (g)	$\Delta$ MC%	weight (g)	$\Delta$ MC%	weight (g)	$\Delta$ MC%
Zip bag	OSB	3.259	4.511	38	4.507	0.123	4.500	0.338	4.489	0.675
	Plywood	2.661	4.751	79	4.747	0.150	4.742	0.338	4.736	0.564
	Fiberboard	1.459	2.254	54	2.251	0.206	2.247	0.480	2.238	1.096
Container	OSB	3.636	4.839	33	4.830	0.248	4.821	0.495	4.807	0.880
	Plywood	2.566	4.551	77	4.542	0.351	4.533	0.701	4.524	1.052
	Fiberboard	1.564	2.369	51	2.365	0.256	2.359	0.639	2.352	1.087

#### 4.3.5 Gravimetric samples collection procedure

A procedure was developed after testing a few methods for the collection process. This procedure consists of the following:

##### 4.3.5.1 Collecting personnel

Four students worked in the collecting process; each student had a specific job to do as follows:

- *The Collector* was responsible for collecting the gravimetric samples from the wall assembly and put them in the containers.
- *The Transporter* was responsible for taking the containers from the collector to the Weigher and then take them back to the Re-installer, as well as writing some notes if there was any problem with the gravimetric samples.
- *The Weigher* stayed inside the test hut to weigh the gravimetric samples in the scale and record the data in the tables.
- *The Re-installer* was responsible for putting back the gravimetric samples in the wall assembly.

#### 4.3.5.2 Collecting containers

Because of the size of the container and to make the “sample travel time” shorter, two containers were developed to collect the samples from each wall assembly, “Top” and “Bottom” containers, where the samples in each wall assembly were grouped into top portion samples and bottom portion samples. There are 11 samples in the top portion and 14 samples in the bottom portion. These samples were arranged in the container’s compartments in a way that the collector always starts collecting the samples from top to bottom and from left to right in the wall assembly. So the collector goes by the order of the samples in the wall assembly and starts filling the compartments that have the same order. The weigher goes in the same order while weighing the samples with a very fast check on the sample’s identification number, where the samples are listed in the recording tables in the same order (left to right and top to bottom).

#### 4.3.5.3 Order of collection

The collector always starts collecting the top portion samples, and when he finishes, he starts collecting the top portion samples of the next wall assembly. After getting back the samples, the re-installer starts installing back the samples in the top portion for the wall assembly from where samples were first collected. In this way the re-installer always follows the collector without running into each other. After finishing all the top portions for the wall assemblies, the collector starts collecting the bottom portion samples from the first wall where he first started collecting the top portion samples from and in the same order until he reaches the last wall assembly in the first floor. The same procedure is done for the wall assemblies in the second floor.

#### 4.3.5.4 Containers' window:

To avoid opening and closing the hut door too many times during the collection process, which would affect the indoor conditions, a small window was made in the door (with a gasket in the perimeter to insure air tightness when closed) to transfer the samples' containers in and out. This window is just big enough to transfer the containers between the transporter and the weigher (Figs. 4-5 and 4-6).

#### 4.3.6 Gravimetric "Samples' Travel Time"

As mentioned above, the most important factor in the samples collection process is the "sample travel time". This is the time needed for each gravimetric sample to travel from the original location in the wall assembly to the scale to be weighed and then back to be re-installed in its location. The travel time for the sample depends on several factors: whether it is at the top or bottom of the wall assembly, type of cladding, stucco or wood siding; whether there is another layer of rigid insulation sheathing or not, and whether it is on the first or second floor. Many traveling times were recorded. The average travel time was about 5.5 minutes with a maximum of 7 minutes in worst cases. Going back to table 4-2, it can be seen that the highest change in moisture content (margin of error) in 10 minutes is less than  $\frac{1}{2}$  %.

#### 4.3.7 Errors encountered with gravimetric samples

With the use of a high precision scale, the error in reading due to the accuracy of the weighing scale is negligible. However, errors can be introduced due to installation and the sampling procedure. The small gravimetric sample in a cut-out hole in the tested wall assembly may not have the same moisture content as would be in the wall assembly at that specific location had the hole for the sample no been made. For example, the original hygrothermal behavior of the wall assembly could be affected due to sample installation, e.g. the contact between the sample and material can diminish the liquid transport and thus affect the overall moisture transport in the components of the wall assembly (Teasdale-St-Hilaire 2006). Some air leakage may occur through the crack between sample and material, thus depositing condensation moisture around the edges of the sample.

To minimize these types of errors, all sheathing samples were taped around the perimeter to prevent moisture transport and hygrothermal interaction between the gravimetric sample and its surrounding in the sheathing material. The taping ensured that the moisture gain in the gravimetric samples is attained by vapor diffusion. The stud gravimetric samples were painted with two coats of INSUL-AID latex vapor barrier primer-sealer on the four sides making contact with the stud. Other types of errors include recording mistakes of scale readings due to the large number of samples and the breaking and splitting of small pieces of samples were kept to a minimum by using some adjusting procedures.



Figure 4-1. Taking out a stucco window in a stucco wall assembly to access gravimetric samples

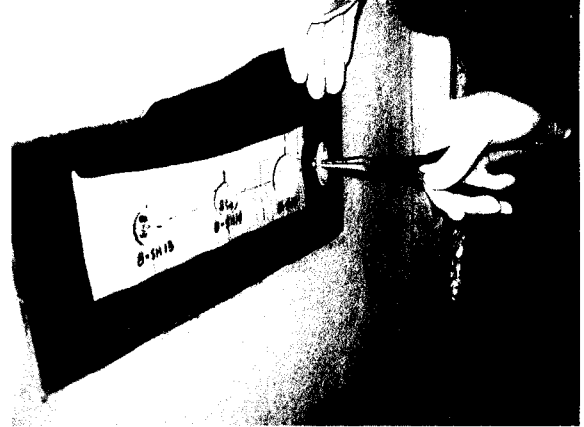


Figure 4-2. Collecting gravimetric samples in a stucco wall assembly



Figure 4-3. Removing a non-fixed wood siding in a wood siding wall assembly



Figure 4-4. Collecting gravimetric samples in a wood siding wall assembly

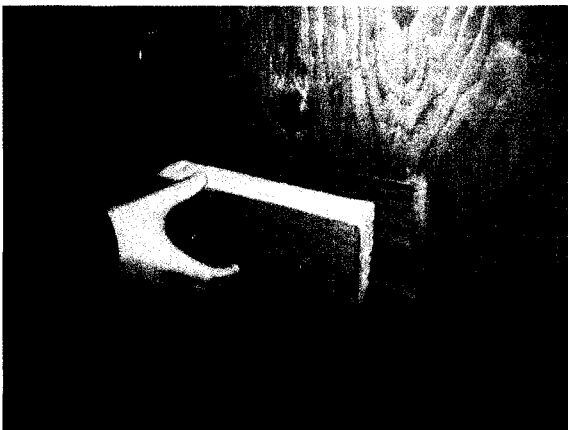


Figure 4-5. Removing the insulation cap for the containers' window in the door of the test hut

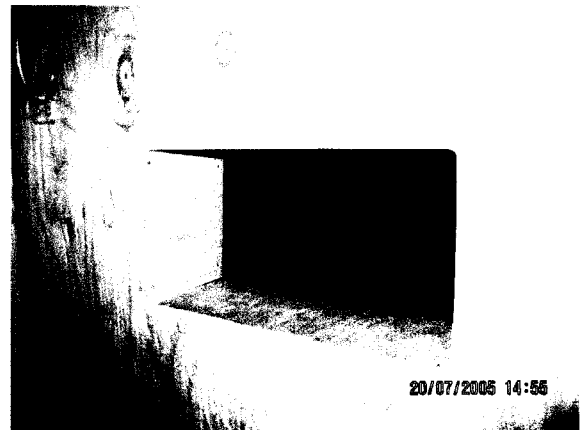


Figure 4-6. Containers' window opening in the door of the test hut

## Chapter 5

### RESULTS & COMPARATIVE ANALYSIS

In this chapter, samples of the different types of data outputs that are used through out the different chapters of the study are presented. Comparative parametric analyses are carried out between the different wall configurations by illustrating the effect of a specific parameter on the MC change while the other parameters are kept constant. The MC information is also used to perform comparative analysis on the moisture absorption vs. height for the different wall configurations. More data analysis is carried out for the stud cavity conditions of the different wall assemblies.

The MC readings from the metal pins were not used in this study since high levels of moisture content occurred in the lower parts of the sheathings, especially in the wall assemblies with stucco cladding. The resistive MC metal pins can only measure MC between 6% to wood fiber saturation (about 28% depends on wood species). Values measured above the fiber saturation are not exact reading (Rao 2004). Hence, the MC readings from the gravimetric samples, being more accurate than those obtained from the moisture pins, are presented and discussed throughout this study.

#### 5.1 Types of results

The data generated for the different parameters through the DAS include: weight of moisture source, temperature, relative humidity, moisture content. The data base contains all the readings for the different parameters recorded every 10 minutes for the whole 5 test periods in addition to the period to establish the base line. For each parameter over 43 000 reading point was recorded. The accumulated evaporation from the water trays inside the 31 wall assemblies was monitored by recording the readings of the load cells. Thermocouple (TC) readings were generated for the locations inside and outside the test hut to monitor the indoor and outdoor conditions. Four hundred and fifty seven TCs were also installed in the wall assemblies.

Relative humidity (RH) readings were recorded for the indoor and outdoor conditions. Two locations inside each stud cavity of the 31 wall assemblies were also monitored for RH. The data base also contains all the electronic moisture content readings generated for the sheathings and stud components of the different wall assemblies.

### 5.1.1 Accumulative evaporation

During the experiment, the DAS recorded the weight of the water tray on a continuous basis at 10-minute intervals. The evaporation rates for all the wall assemblies were recorded within a gram of accuracy for the whole test period. Figure 5-1 shows the accumulated evaporation values for the 31 wall assemblies for test period 1 and part of test period 2. The accumulated evaporation curves for each of the 31 wall assemblies are presented in Appendix D for the whole experiment period.

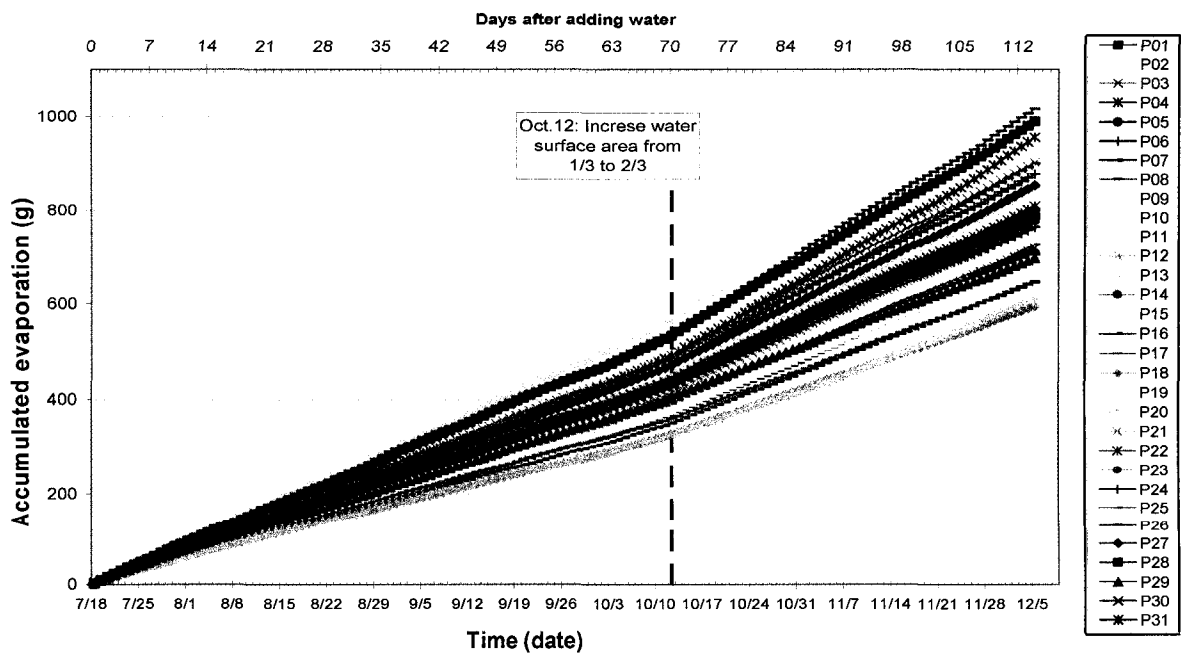


Figure 5-1. Total accumulative evaporation for the 31 wall assemblies

### 5.1.2 Relative humidity readings

On each wall assembly, there were two RH sensors to measure the relative humidity as well as the temperature for the two locations (406mm or 16" and 1829mm or 72" from the bottom) inside the building envelope (Fig. 2-8). These RH and temperature readings were used for vapor pressure calculations inside the stud cavities for the different wall assemblies. Figure 5-2 shows the calculated vapor pressures in the lower location inside the stud cavity for all the wall assemblies for the 5 test periods. It can be noted that the vapor pressure for test periods 1, 2, 3, and 4 (with moisture loading) for all the wall configurations was higher than both the interior and exterior vapor pressures.

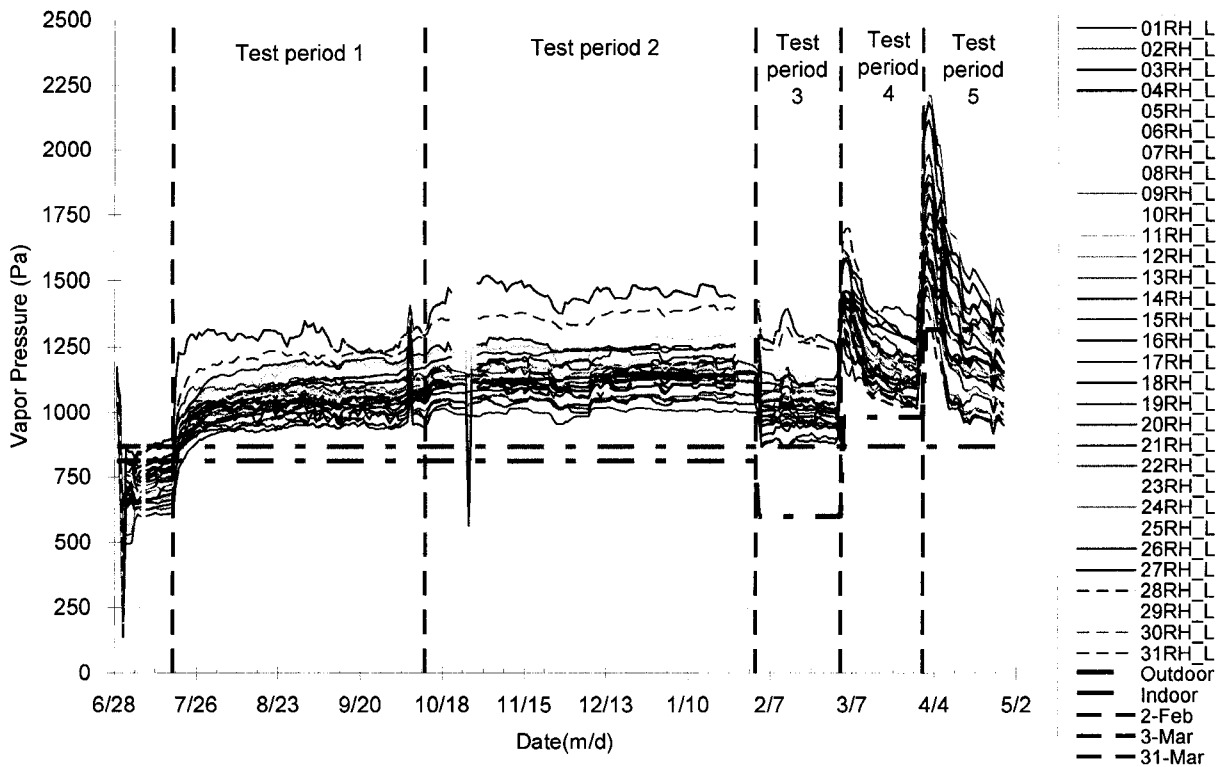


Figure 5-2. Calculated vapor pressure values for the 31 wall assemblies in the lower location inside the stud cavity (16" from the base of wall assembly) for the 5 test periods.



### 5.1.3 Moisture content profiles by gravimetric samples

The moisture contents in the 25 gravimetric samples in each of the 31 wall assemblies were calculated and plotted for the total duration of the experiment. Figure 5-3 shows one example of MC profiles for the 5 test periods for wall assembly 6 with OSB sheathing, stucco cladding, and a vapor barrier for the 25 gravimetric samples. The MC profiles for all the 31 wall assemblies for the whole experiment period are presented in Appendix E.

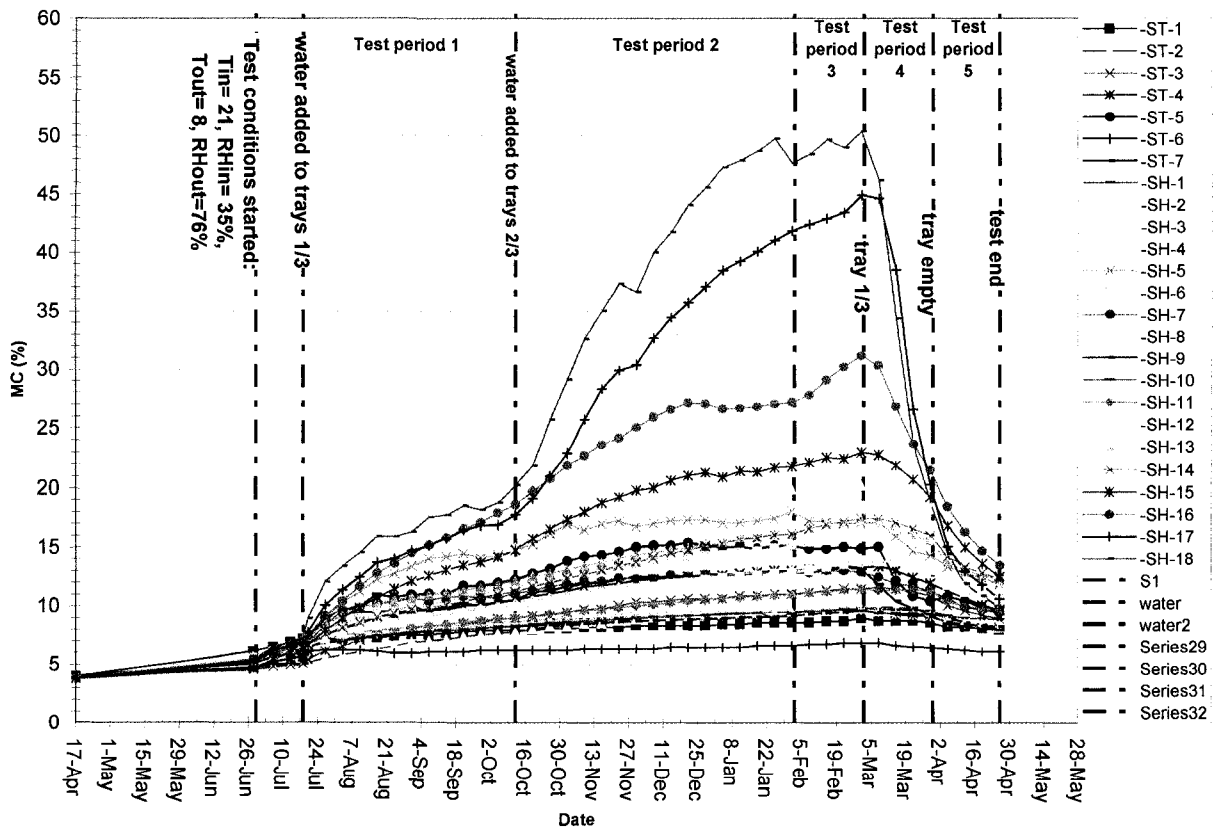
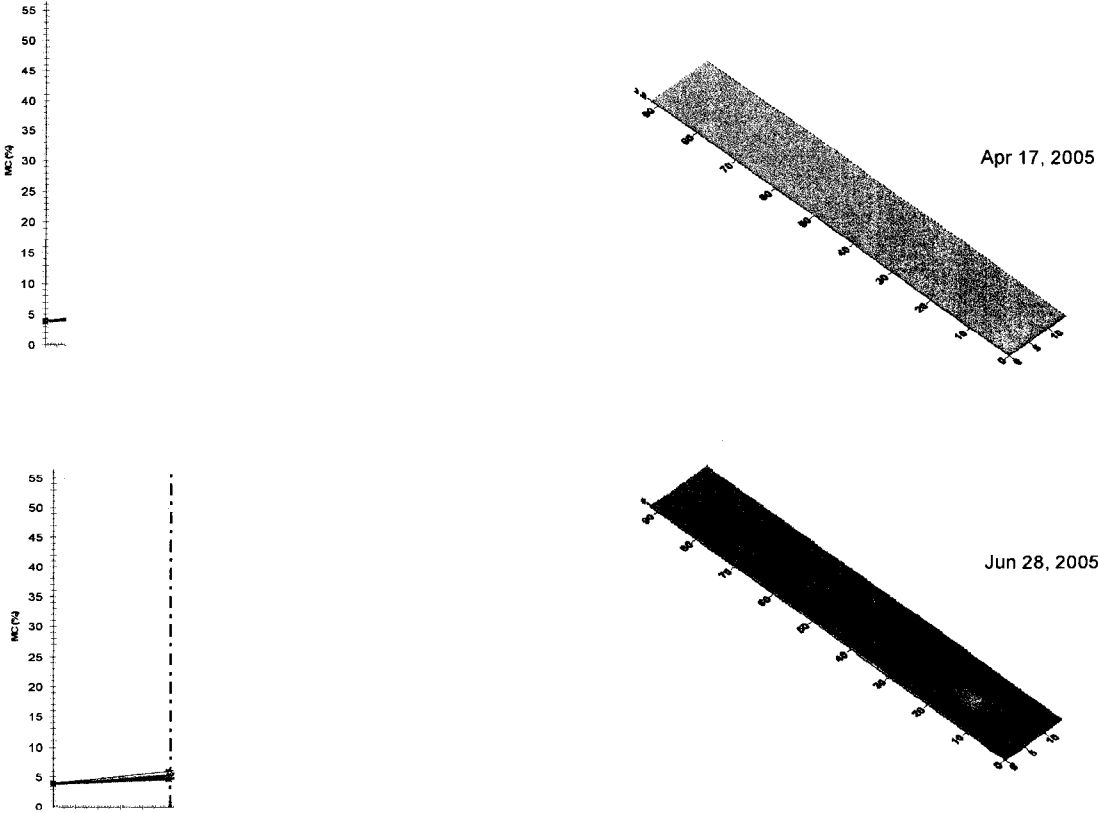
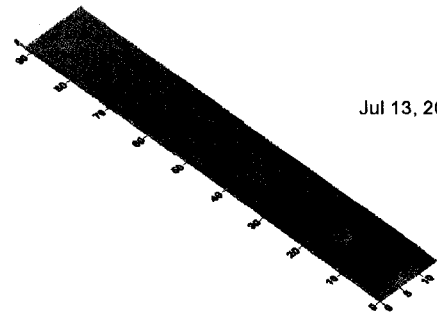
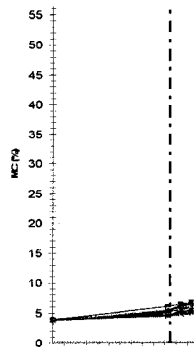


Figure 5-3. MC profiles for the 25 gravimetric samples in wall assembly 6 (OSB, stucco, and vapor barrier) for the 5 test periods

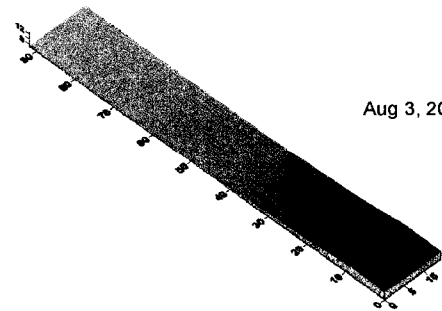
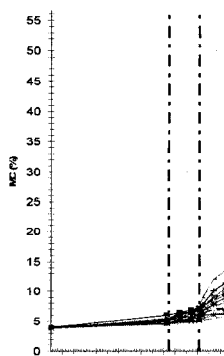
Using Surfer® 8 software<sup>5</sup>, the moisture content for the sheathing was mapped and has been presented graphically to understand and visualize the MC absorption distribution in the sheathing. This representation was based on the MC of the sheathing gravimetric samples and will be presented in frames, where each frame represents the MC in the sheathing for a certain day. MC Readings were collected once a week. The frames were generated for every second data collection day (every two weeks) for the 5 test periods and the baseline establishment period shown in Figure 5-3. Figure 5-4 shows the different MC absorption conditions (right side) as well as the corresponding time sections in the MC profile plot (left side) for wall assembly 6 (OSB, stucco and vapor barrier) for the total experiment duration. This wall assembly was chosen because it provided the worst case scenarios.



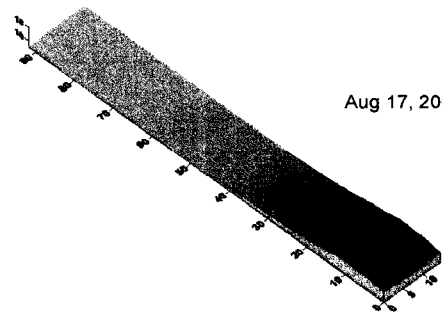
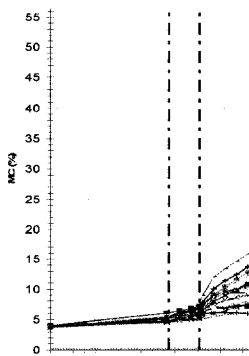
<sup>5</sup> By Golden software, Colorado.



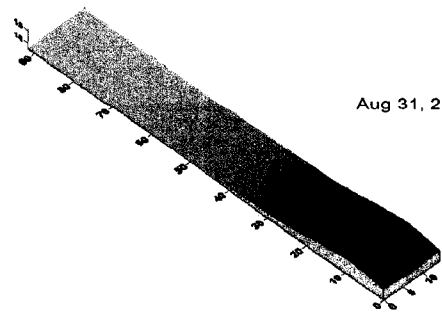
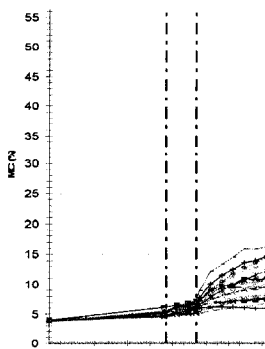
Jul 13, 2005



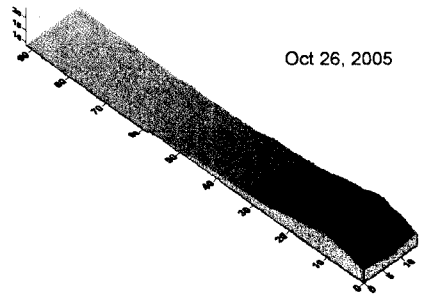
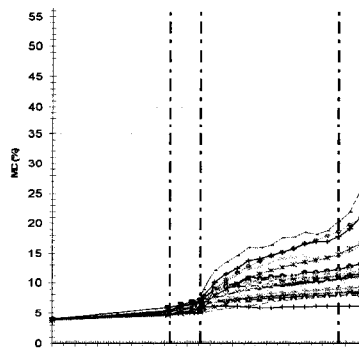
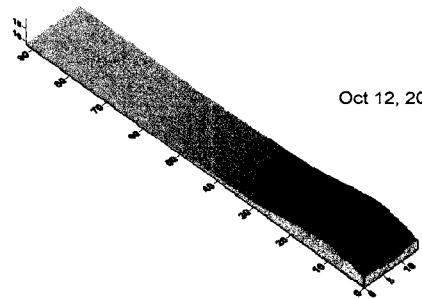
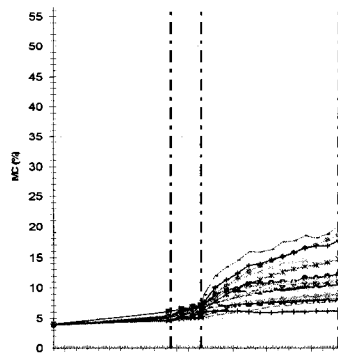
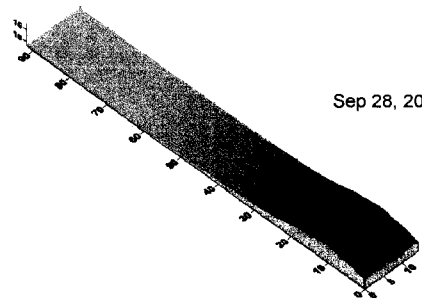
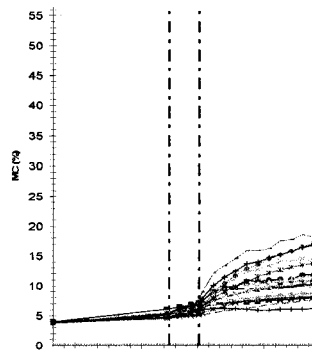
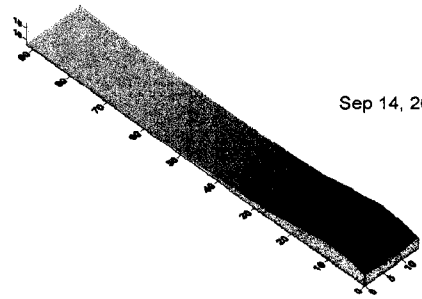
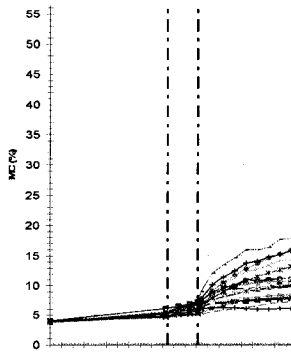
Aug 3, 2005

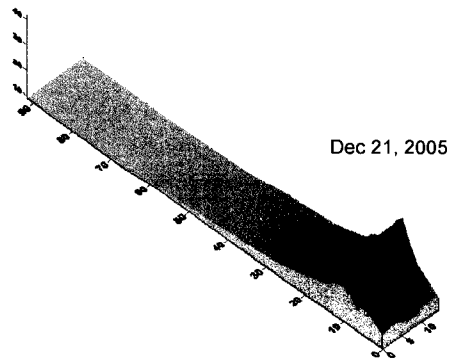
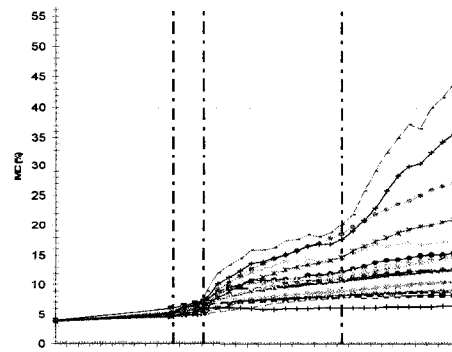
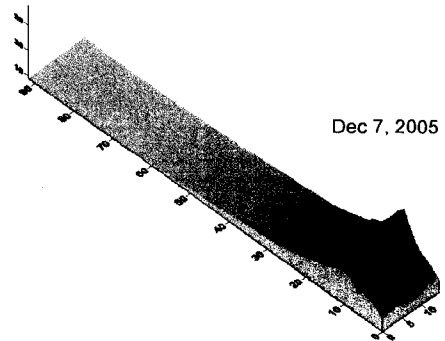
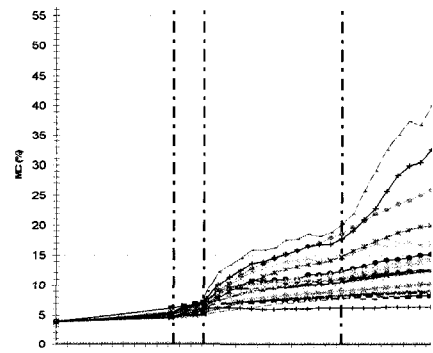
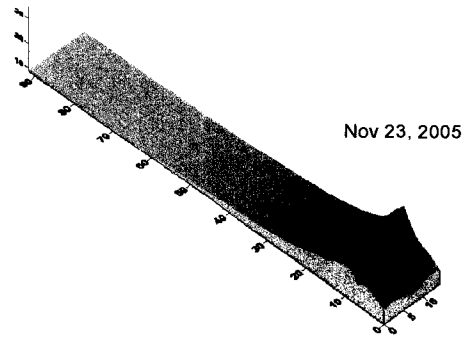
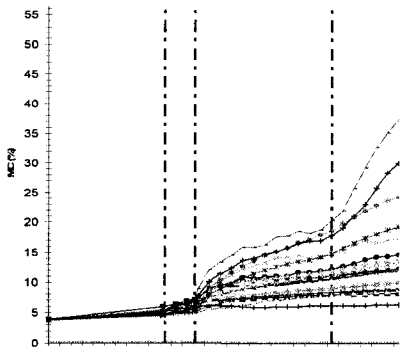
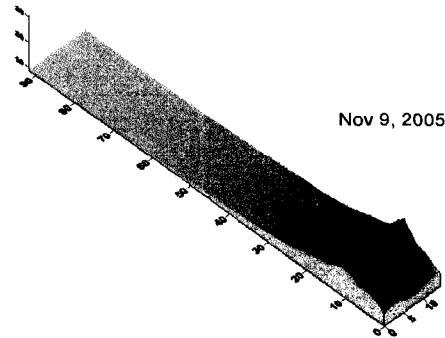
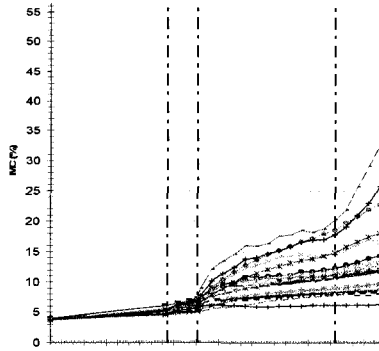


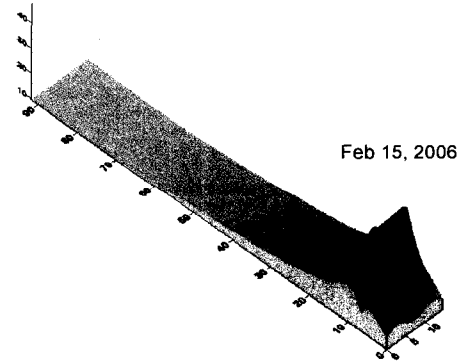
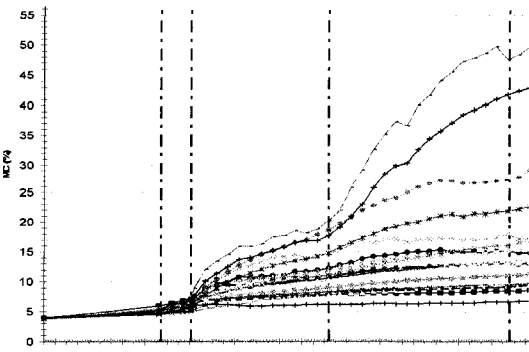
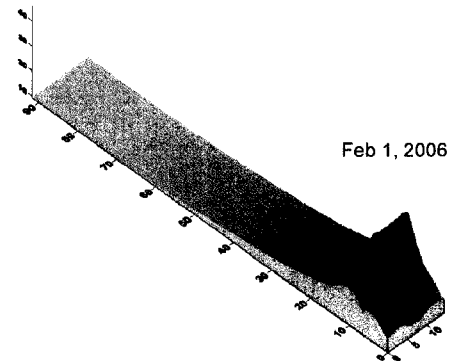
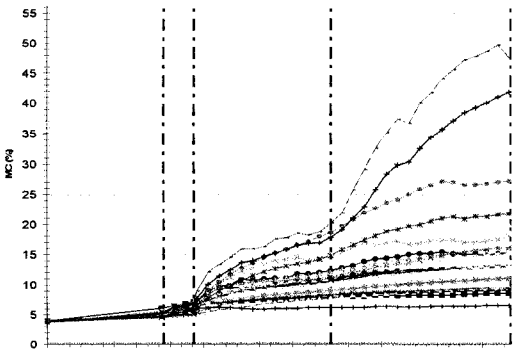
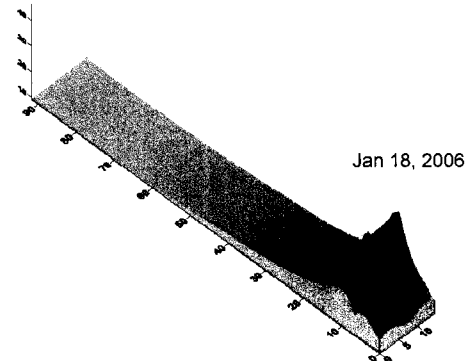
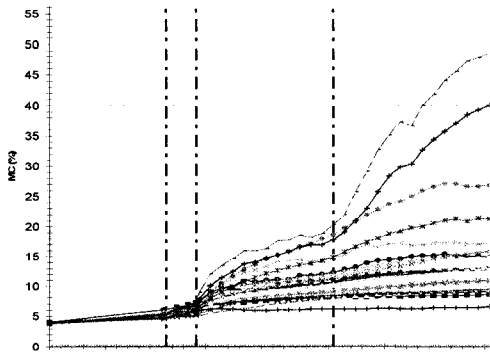
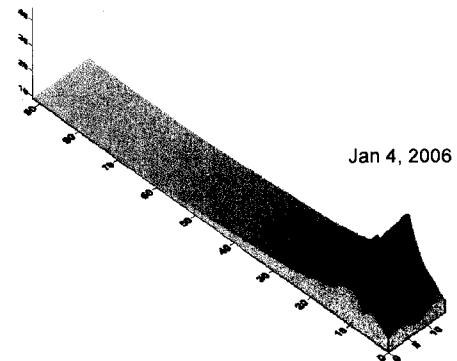
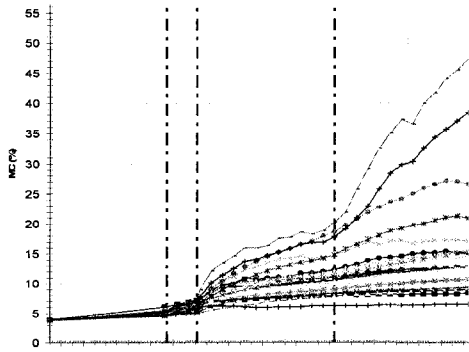
Aug 17, 2005

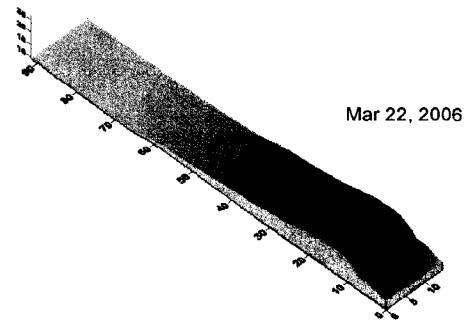
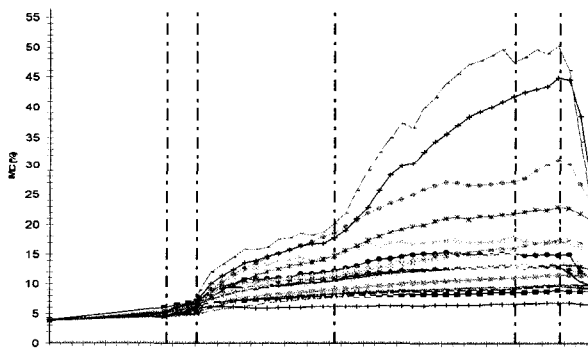
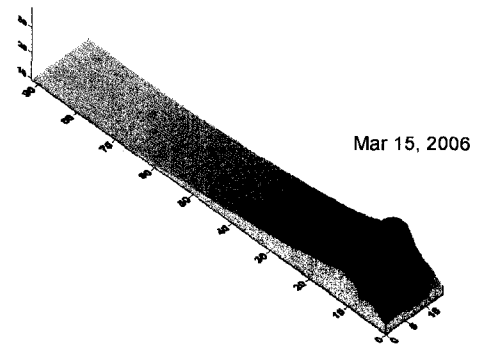
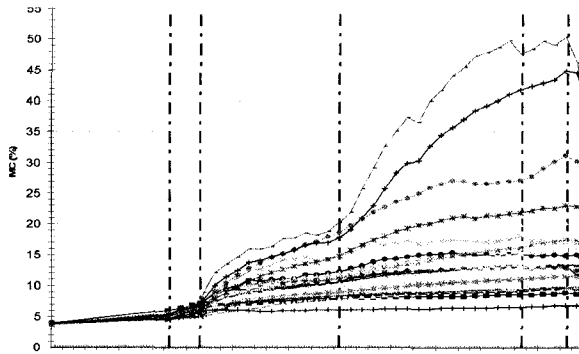
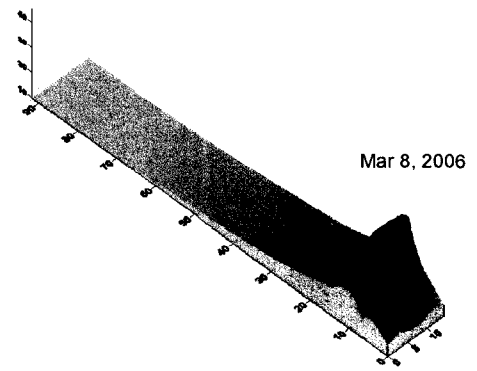
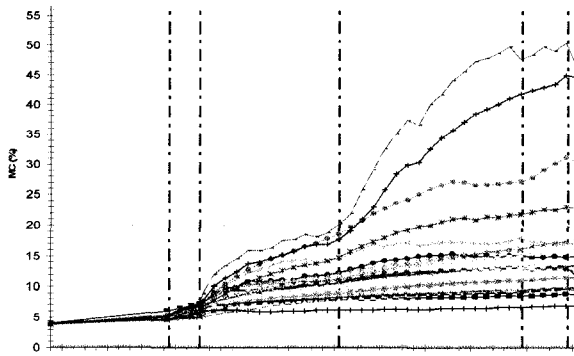
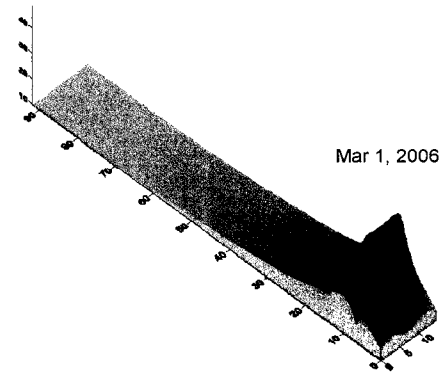
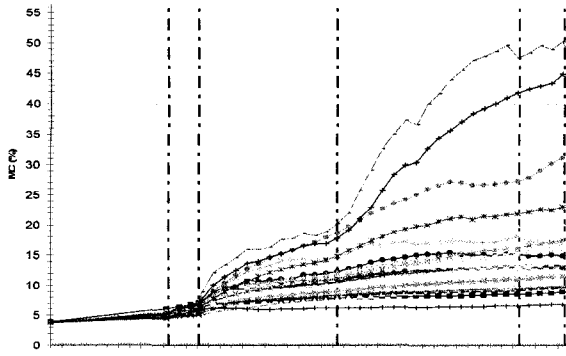


Aug 31, 2005









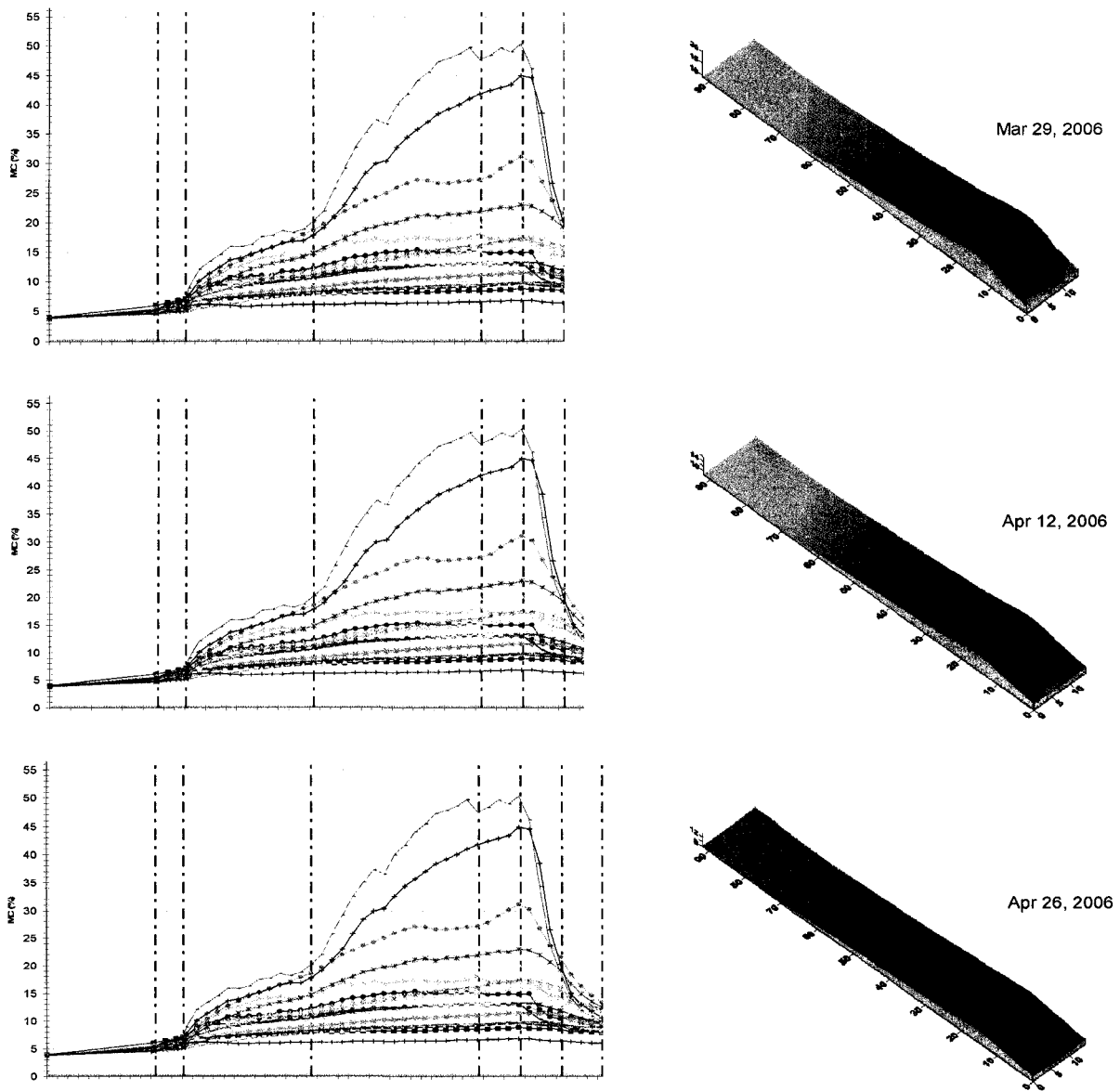


Figure 5-4. Different MC absorption conditions (right side) and the corresponding time sections in the MC profile plot (left side) for wall assembly 6 (OSB, stucco and vapor barrier) for the total experiment duration



## **5.2 Comparative data analysis for test period 1**

The aim of the comparative data analysis is to perform different types of comparative studies to evaluate the relative performance of the different configurations and thus the different building systems, where the relative performance of these systems is important to move the design of building envelope systems from a thumb-rule approach to an engineering approach. Comparative analyses were carried out for test period 1 (See Fig. 5-3). These comparative studies were applied on a number of wall assemblies with different configurations to study the effect of certain parameters on the relative performance of these wall configurations.

### **5.2.1 Evaporation rates for different wall configurations**

The evaporation rates for the time period of July 18<sup>th</sup> to September 7<sup>th</sup>, 2005 (in test period 1) of all the assemblies form consistent trends, but with different average daily evaporation rates or slopes for the different wall assemblies (Figs 5-5 & 5-6). This rate difference is attributed to the micro environments above the water surface that are governed by the characteristics of the wall panels, to the properties of materials around the stud cavity in the assemblies, to the difference in water temperature in the trays that varies according to different configurations, and to potential air leakage in the wall panels as stated in protocol on loading (Fazio 2004). The air leakage of the assemblies was limited to the air movement across the sheathing (and stucco cladding) through cracks in joints and gravimetric sample holes under stack effect, since the cracks around screws on the drywalls were well sealed with caulking.

The evaporation rate was typically higher for the fiberboard sheathings followed by the plywood and the OSB sheathings (Figs 5-5 & 5-6b). In several instances, this pattern breaks down due to the influence of other factors on the drying capacity such as possible air leakage. For example, the OSB-sheathed wall panel had a higher evaporation rate than the plywood-sheathed wall assembly in Figure 5-6a.

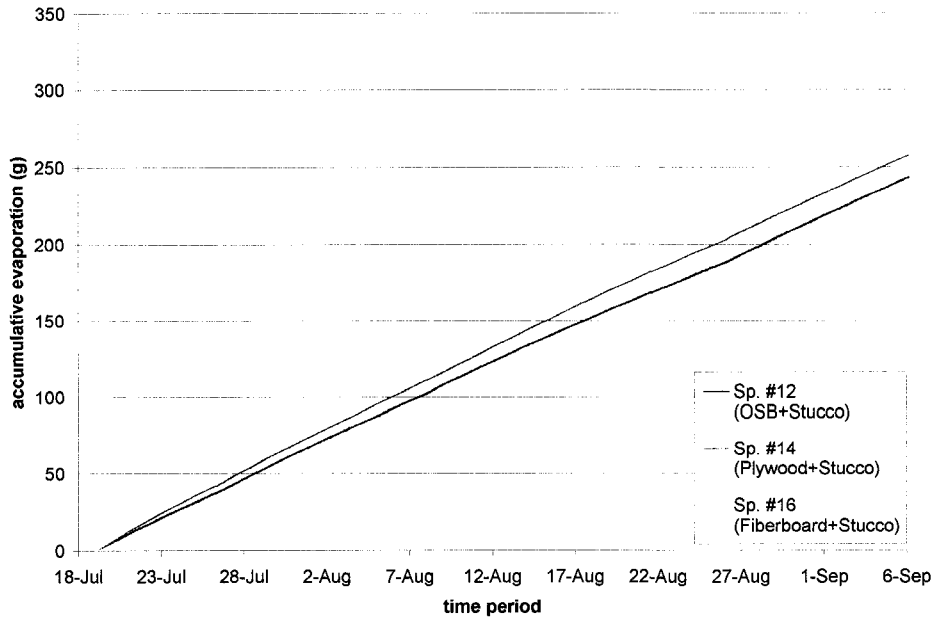


Figure 5-5. Evaporation rates for the three types of sheathings with the same type of cladding (stucco) and without vapor barrier

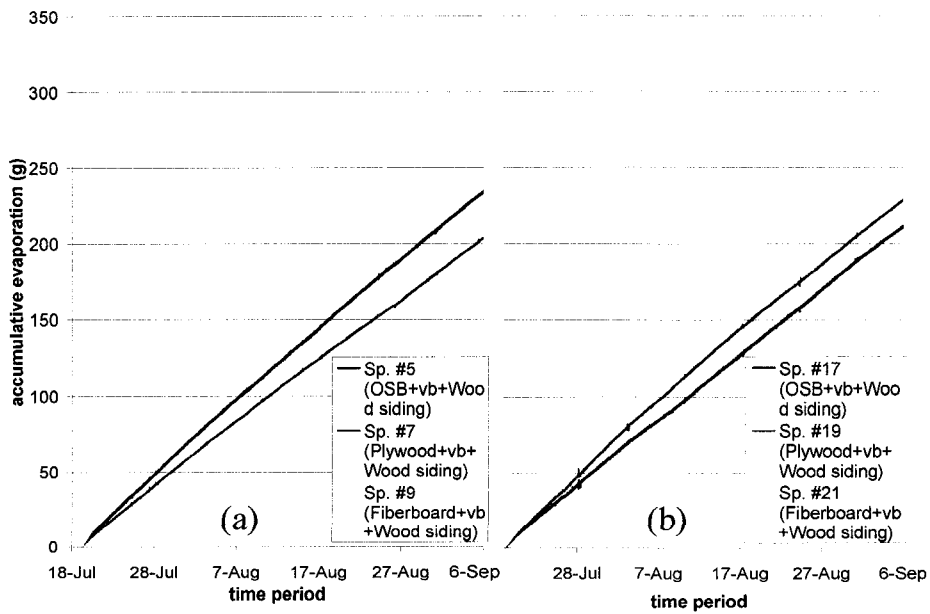


Figure 5-6. Evaporation rates for wall assemblies 5, 7, 9 and their duplicate wall assemblies 17, 19, 21 (three types of sheathings with the same type of cladding of wood siding and with vapor barriers)

### **5.2.2 Comparative parametric analysis**

Under moisture and climatic loadings applied, different wall configurations yield different drying capacities which can be influenced as well by the other parameters of the building envelope assemblies. By holding some of these parameters constant and varying others, the relative impact of each parameter can be established. Moreover, a comparative correlation can be established between the wall configuration and its drying capacity or drying evaporation index “DEI”, since a uniform climatic loading is applied to all of the assemblies.

In this section, MC data (by gravimetric samples) for sheathing, right stud, top and bottom plates are presented and discussed to perform comparative studies between the different wall assemblies by illustrating the effect of a specific parameter on the MC change while the other parameters are kept the same. Each time, data were presented and compared for a number of wall assemblies that have the same configuration with only one variable to check the effect of this variable on the MC change for the gravimetric samples analyzed.

### 5.2.2.1 Effect of adding water to the trays on MC

Figure 5-7 shows the MC profiles of the 25 gravimetric samples of assembly #8 (plywood sheathing, with vapor barrier and stucco cladding) for the period from Apr. 17<sup>th</sup> to Sep. 7<sup>th</sup>, 2005. The MCs increase at different rates over the three stages: (i) preconditioning of the assemblies, (ii) the test conditions with no water in wall assemblies, and (iii) the test condition with water added to the trays (moisture loading). Two general patterns in the rates of MC increases were observed: one at the start of the test conditions and the other at the time the water was injected into the trays. The effect of water injection was different for gravimetric samples at different locations. The profiles indicate that the MC in the gravimetric samples in the lower part of sheathing and stud close to the evaporation source increased significantly, while the change was less evident for the other samples in the upper regions of the assembly. These results indicate that moisture from the water tray at the bottom plate would create in the cavity a profile of the RH, which varies from close to 100% in the neighboring of the water to a much lower level near the top of the cavity. This phenomenon was observed in all the wall assemblies.

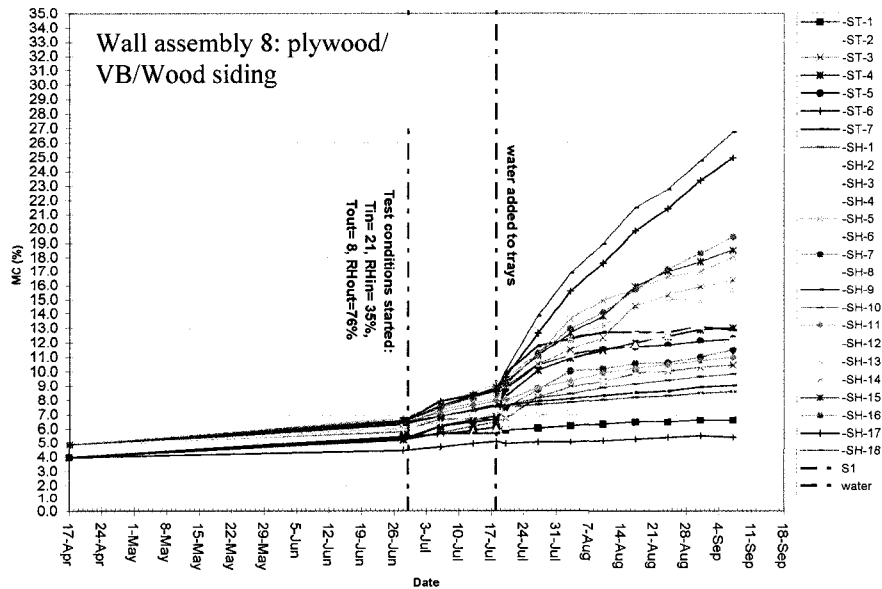


Figure 5-7. Effect of water injection on MC change for wall assembly #8 (plywood sheathing, with vapor barrier and stucco cladding)

### 5.2.2.2 Effect of vapor barrier on MC

The MC in the sheathing typically increases in assemblies with the vapor barrier. The comparative plots of MC profiles for assemblies #10 (Fiberboard/Stucco with VB) & #16 (Fiberboard/stucco without VB) are presented in Figure 5-8. The effect of the vapor barrier in assembly #10 can be seen by the significantly higher MC changes in gravimetric samples, especially SH-17 and SH-18 at the lower region of the stud cavity. It was expected that when the permeance of the sheathing material is high, as it is for fiberboard, then the effect of permeance of the vapor retarder is less. This, however, does not apply to the case of stucco with no air cavity between cladding and sheathing. In the case of Assembly #16 (Fiberboard/stucco without VB), the absence of the vapor barrier allowed moisture in the cavity to dry to the interior of the test hut as well as to the exterior.

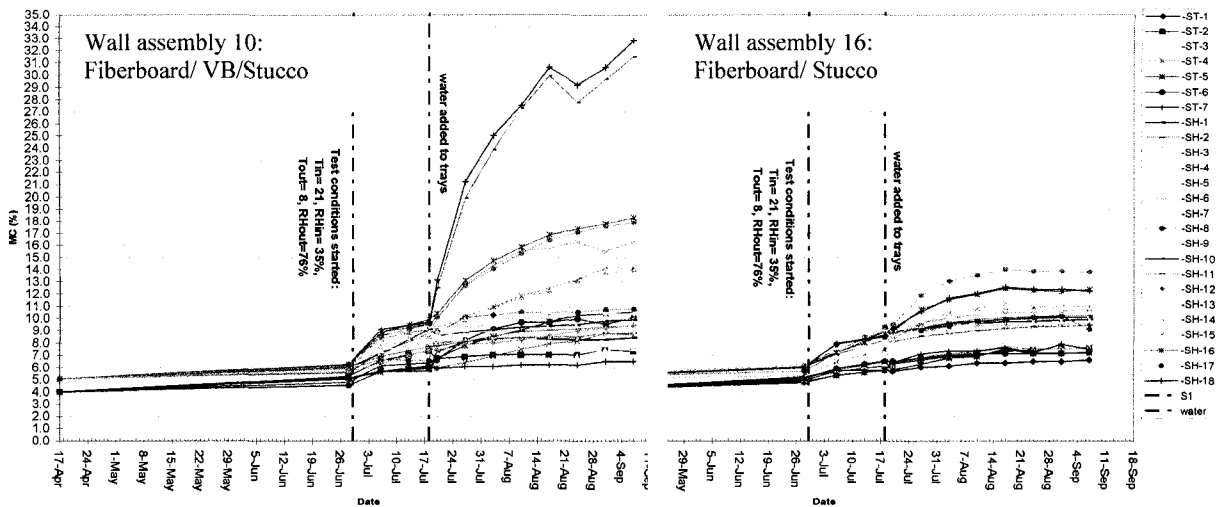


Figure 5-8. Effect of vapor barrier on MC change for wall assemblies #10 (Fiberboard/Stucco with VB) and #16 (Fiberboard/stucco without VB)

### 5.2.2.3 Effect of sheathing material on MC

Figure 5-9 shows the MC absorption in the different sheathing materials of the wall panels when the sheathing is combined with stucco without a cavity. All the three assemblies have stucco, vapor barrier, and different sheathing: #6 with OSB, #8 with plywood and #10 with fiberboard sheathing. The gravimetric samples from the fiberboard have the highest moisture accumulation followed by plywood and OSB samples, whereas one would expect the reverse with the least moisture accumulation occurring in the assembly with the fiberboard. The presence of the stucco as the cladding type causes the fiberboard to retain relatively high concentrations of moisture.

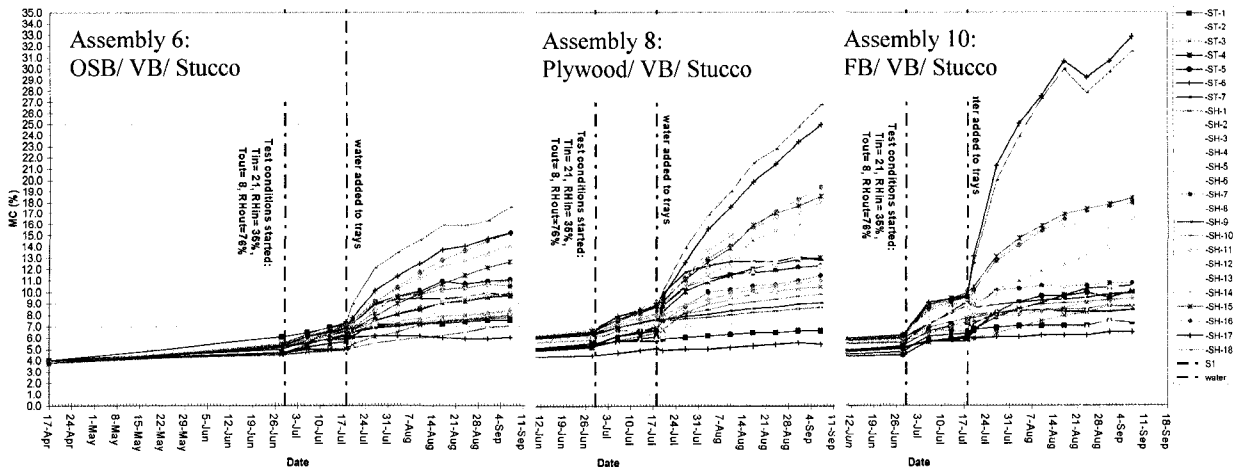


Figure 5-9. Effect of sheathing material on MC change for wall assemblies #6 (OSB), #8 (plywood) and #10 (fiberboard), all with stucco cladding and vapor barrier.

### 5.2.2.4 Effect of type of cladding on MC

The effect of cladding on the MC change is presented in Figure 5-10 for three assemblies, all having plywood sheathings and vapor barrier, but with different cladding types: assembly #2 with no cladding, #7 with wood siding, and #8 with stucco. The gravimetric samples behind the stucco had higher moisture absorption followed by samples with no cladding followed by samples behind wood siding having a cavity of 19mm (¾") air gap. The higher moisture

absorption in the sheathing with stucco is likely due to the fact that there is no cavity between the sheathing and the stucco to allow ventilation drying.

The existence of an air cavity behind the cladding would enhance the drying mechanism, especially if there is ventilation which would contribute to drying; the higher the rate of ventilation the greater the drying potential. This air ventilation will be driven through the air cavity by one or the combination of two forces, either by air pressure differential induced by wind or thermal buoyancy. In theory, exterior air ventilation offers three major benefits (Schumacher et al. 2003):

- The flow of outside air, which is relatively dry, promotes convective drying of both surfaces surrounding the air cavity.
- The ventilating air can provide the evaporation heat necessary to enhance the evaporation process as water evaporates at the surface of the sheathing membrane.
- Water vapor diffusing through the inner wall can bypass the vapor diffusion resistance of the cladding and be carried away directly to the outside.

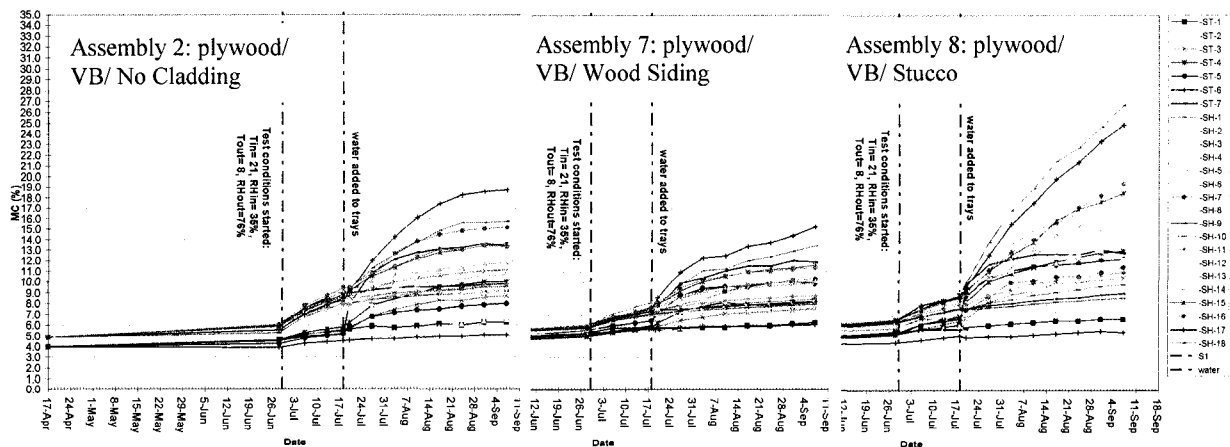


Figure 5-10. Effect of cladding on MC change for specimens #2 (no cladding), #7 (wood siding) and #8 (stucco), for configurations with plywood and vapor barrier.

### 5.3 Data analysis for the stud cavity conditions in test period 2

The internal conditions in the stud cavity were affected mainly by the evaporation of the moisture loading source at the bottom of the cavity. In this section, the different parameters were analyzed to understand the relationships between them. Table 5-1 lists the different parameters for test period 2: accumulated evaporation, averaged RH readings, averaged temperature readings, humidity ratios, and vapor pressures. The relative humidity and temperature values were averaged for the duration of test period 2 for the data collected from the two RH+T sensors, upper 1829mm (72") and lower 406mm (16"), while the humidity ratio and vapor pressure values were calculated from the RH and T values.

Table 5-1. Different parameters values in the lower (16") and upper (72") locations inside the stud cavities of the different wall assemblies for test period 2.

Assembly	Evaporation(g)	RH (%)		T (°C)		Humidity ratio (g/kg)		vapor pressure (Pa)	
		upper	lower	upper	lower	upper	lower	upper	lower
#5	640	40.0	60.7	18.5	17.7	5.03	8.07	809	1290
#17	593	39.1	62.3	16.9	17.8	4.95	7.48	796	1201
#6	783	43.8	63.5	17.1	16.5	5.11	7.72	825	1237
#18	542	40.9	60.5	16.4	16.0	4.61	7.03	746	1129
#7	624	41.4	56.9	19.0	17.3	5.08	7.80	816	1248
#19	642	37.0	63.4	17.3	18.2	4.80	7.81	775	1254
#8	982	53.2	57.3	17.9	15.8	5.94	7.33	954	1174
#20	603	41.9	65.2	16.6	15.8	4.67	7.68	754	1235
#9	1022	44.1	54.7	18.5	17.4	5.45	7.26	873	1159
#21	849	46.8	57.8	16.7	16.7	5.53	6.84	890	1099
#10	829	47.4	59.7	17.4	17.2	5.78	7.40	932	1190
#22	759	48.7	63.0	16.5	15.2	5.23	7.37	842	1183
#1	665	44.7	55.5	17.4	15.6	4.92	6.87	794	1103
#2	656	46.3	55.0	18.0	15.5	5.06	7.07	814	1138
#3	716	40.9	49.8	18.2	17.5	5.08	6.48	820	1037
#30	712	38.8	69.0	17.4	18.4	5.10	8.56	822	1372
#31	739	40.8	58.6	17.3	18.1	5.26	7.21	846	1158



### **5.3.1 Accumulative Evaporation values**

For all the wall assemblies with different configurations, evaporation rate values ranged from 542g to 1022g. Different configurations were expected to have different evaporation rates, and at the same time, duplicate wall assemblies were expected to have similar evaporation rates. Seven of the 12 duplicates had a percentage difference of less than 10% in the evaporation rates, 2 duplicates had a difference of less than 20%, two more duplicates had a difference of about 44%, and only one duplicated had a difference of 63%. The duplicate assemblies with the highest difference in evaporation rates (63%) were assemblies 8 & 20 configured with plywood, vapor barrier and stucco. For wall assemblies with vapor barriers, generally, the evaporation rates in the assemblies in the first floor were higher than the evaporation rates in their corresponding duplicate assemblies on the second floor, thus, the differences in the evaporation rates may be attributed to stack effect, and to air movement caused by the fans of the environmental chamber, as well as on the make up of the wall assemblies.

### **5.3.2 Average relative humidity values in the stud cavities**

For wall assemblies with vapor barriers, it was observed that the average relative humidity values in the stud cavities in the lower location ranged from 54.7% to 69.0%. Wall assemblies with OSB and wall assemblies with stucco had the higher values with a range from 57.3% to 65.2%. For the assemblies with board insulation (29, 30 & 31), the RH values were the highest, especially for OSB and plywood, ranging from 68.1% to 69.0%.

For the upper location in the stud cavities, the RH values ranged from 37% to 48.7% except for assembly 8 with 53.2%. RH decreases with distance from the moisture source at the bottom of the cavity. The decreases of RH values from the lower to upper locations were about 20% for the OSB and OSB with stucco assemblies. A lower decrease of about 12% was observed for the fiberboard assemblies. Again, the highest differences of 30% were in assemblies with OSB and plywood plus insulation sheathing boards (assemblies 29 and 30). The decrease of RH in the upper location was only about 4% in the case of assembly 8 sheathed with plywood and clad with stucco. A possible vertical air flow due to air leakage may be the reason behind

the relatively high RH value in the upper location and the relatively high evaporation rate of 982g for assembly 8. This possible air flow may account for the higher absorption of moisture in the middle regions' gravimetric samples, which is different from the general trend of high absorption in the lower parts' gravimetric samples.

### **5.3.3 Averaged temperature values in the stud cavities**

For temperature readings from the two RH + T sensors in the two locations in the stud cavities, the temperatures in the lower locations were generally lower than those in the upper locations. It was also observed that the temperature readings in the first floor assemblies were higher than those in the second floor assemblies. This trend was also confirmed by comparing the temperature values of the duplicate assemblies. The temperature readings for assemblies with wood siding were higher than the readings for assemblies with stucco. This was expected since wall assemblies with wood sidings had an air cavity between sheathing and cladding that increased the total R value for the configuration. These temperature gradients between the upper and lower locations inside the stud cavities of the different wall assemblies were generally in the range of about 1°C.

### **5.3.4 Averaged vapor pressure values in the stud cavities**

The following parameters are related: temperature, relative humidity, vapor pressure, and humidity ratio. The evaporation was the main driver in the stud cavities of the different wall assemblies. Table 5-2 shows the vapor pressure values for the upper (5-2a) and lower (5-2b) locations. The values are presented in an ascending order for vapor pressure values. It can be noted that the evaporation rates had the major effect on the relative humidity and thus the vapor pressure values. Therefore, the vapor pressure depends mainly on evaporation, thus, the higher the evaporation, the higher the vapor pressure.

Table 5-2. Evaporation and calculated vapor pressure values for: a) upper location, b) lower location (period 2)

a			b		
	evaporation (g)	vp (P)		evaporation (g)	vp (P)
#18	542	746	#3	716	1037
#20	603	754	#21	849	1099
#19	642	775	#1	665	1103
#1	665	794	#18	542	1129
#17	593	796	#2	656	1138
#5	640	809	#31	739	1158
#2	656	814	#9	1022	1159
#7	624	816	#8	982	1174
#3	716	820	#22	759	1183
#30	712	822	#10	829	1190
#6	783	825	#17	593	1201
#22	759	842	#20	603	1235
#31	739	846	#6	783	1237
#9	1022	873	#7	624	1248
#21	849	890	#19	642	1254
#10	829	932	#5	640	1290
#8	982	954	#30	712	1372

### 5.3.5 Convection inside the stud cavities

Convection inside the stud cavity was not measured in this test, but, it was limited to the buoyancy induced convection inside the stud cavity since the drywall is totally sealed. This convection can still be examined by checking the temperature values recorded in the upper and lower locations inside the stud cavity. The temperature gradients between the upper and lower locations for the different wall assemblies were generally in the range of about 1°C as mentioned above, which means that the convection was very small and probably had no major effect inside the stud cavity.

## 5.4 Moisture absorption vs. height analysis for test period 2

As seen in the last section that evaporation from the moisture loading source at the bottom of the stud cavity determined the internal conditions in the stud cavity. In this section, the moisture absorption in the sheathing material vs. height is analyzed based on the evaporation values for the different wall configurations for test period 2.

To study the relationship between moisture absorption and height (distance from water tray), the absorption rates are calculated for the 7 heights corresponding to the heights of the

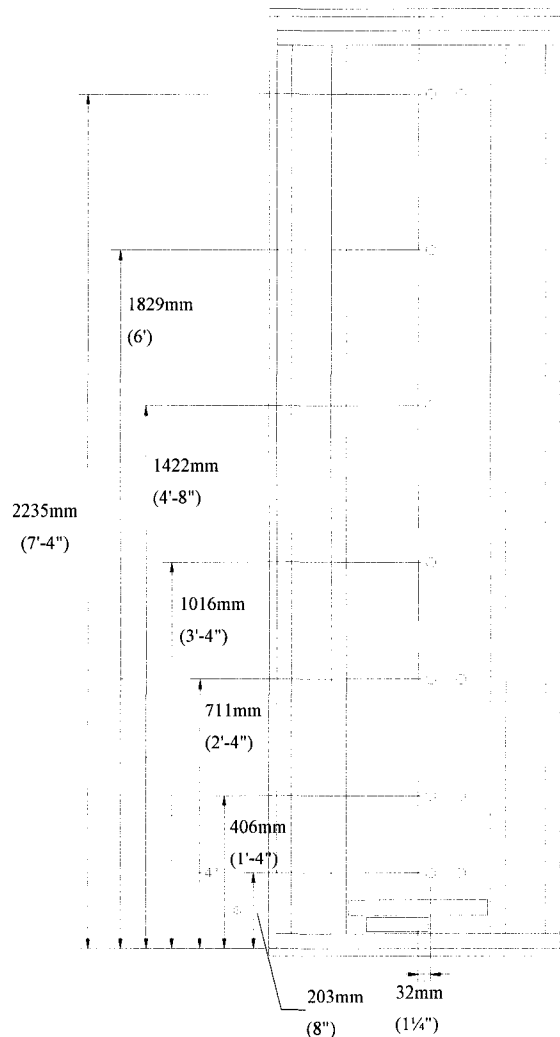


Figure 5-11. Heights of gravimetric samples from the base of the wall assembly

gravimetric samples as shown in Figure 5-11. At each of the 7 heights, the absorption value was calculated as the average absorption of the samples that fall in the same x-axis. The profile of moisture absorption vs. height is then plotted for period 2 (Fig. 5-12) for the wall assemblies with vapor barriers. The absorption values were in grams per 1 inch diameter sample. The decrease of moisture absorption with height can be clearly seen for all the sheathings in the different wall assemblies with different configurations.

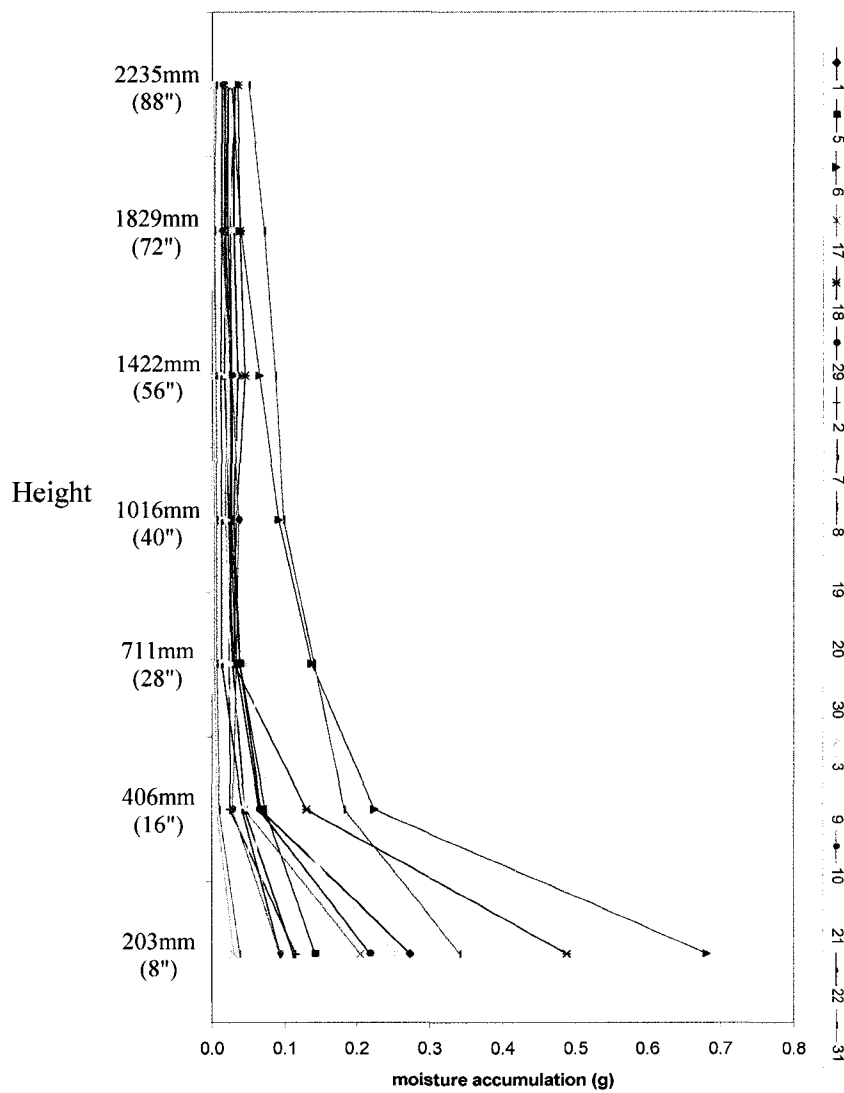


Figure 5-12. Moisture absorption in 1 inch diameter sample vs. height for the different wall assemblies with vapor barriers (period 2)

### 5.4.1 Moisture absorption percentage of total evaporation

For comparative analysis purposes, the relation between moisture absorption and height can be re-plotted as a percentage of moisture absorption in the samples to the total evaporated moisture. The moisture absorptions of sheathing gravimetric samples at different heights in each wall assembly were divided by the total evaporated moisture from the water tray at the bottom of that assembly. Figure 5-13 shows the percentage of moisture absorption vs. height profiles for the wall assemblies with vapor barrier.

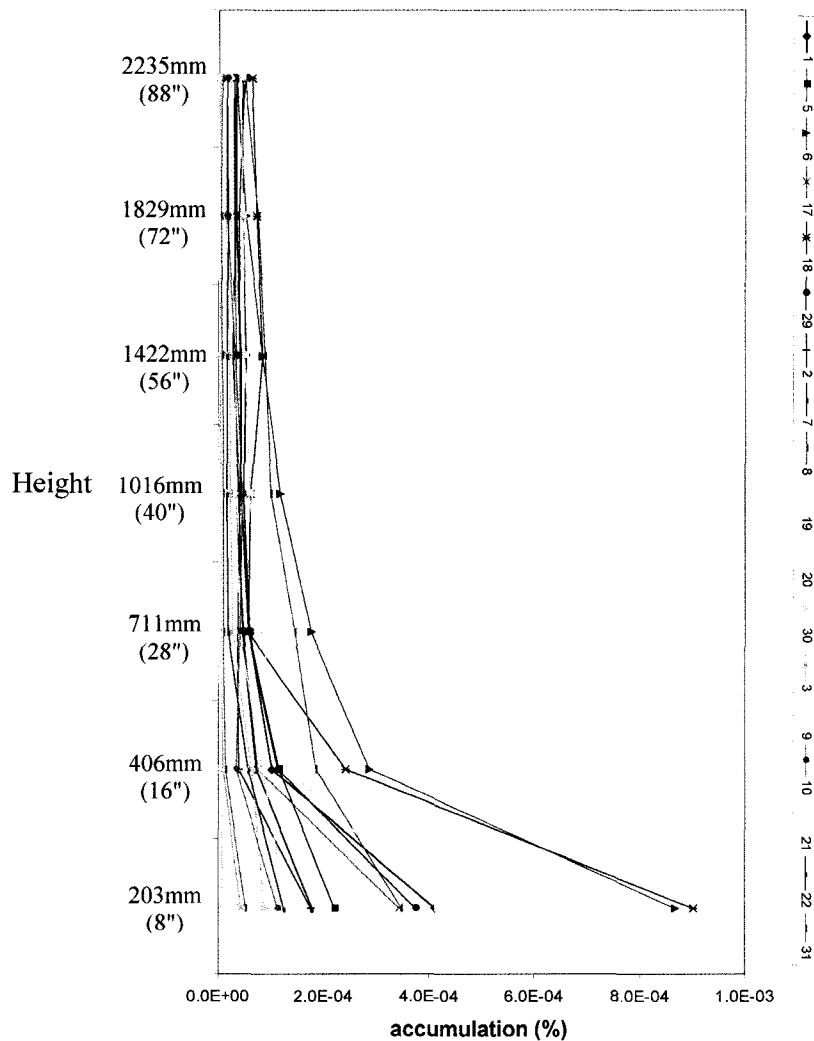


Figure 5-13. Moisture absorption percentage per one sample area vs. height for wall assemblies with vapor barrier (period 2)

- *Absorption analysis of sheathings behind stucco cladding*

If the type of cladding is taken as a comparative parameter on the different types of sheathings for walls having vapor barriers, then the effect of stucco cladding on each type of sheathing can be analyzed. In Figure 5-14, there are three pairs of profiles representing the three stucco-vapor barrier duplicates. The good agreement between duplicate profiles can be noticed, where the OSB sheathing has the highest percentage of moisture absorption to the total evaporated, followed by the plywood sheathing and then fiberboard sheathing. The ratio of absorption rates for the three types of sheathings are approximately 1:3:8.

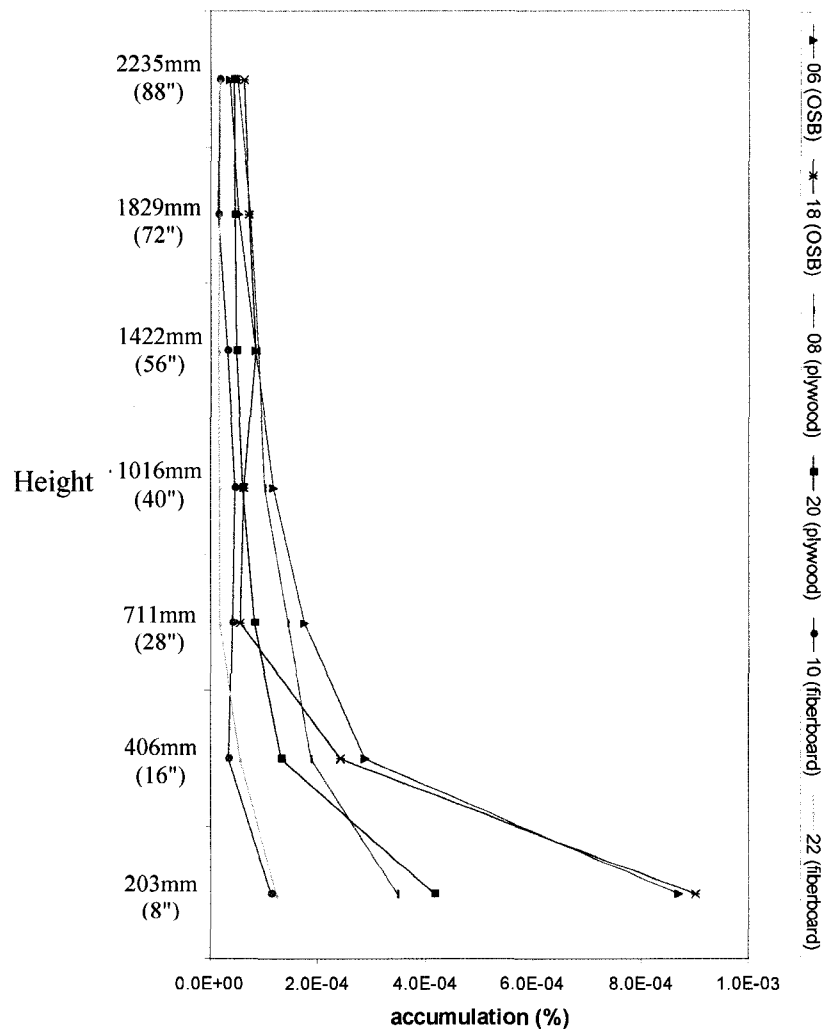


Figure 5-14. Moisture absorption percentage per one sample area vs. height for stucco with vapor barrier wall assemblies (period 2)

- *Absorption analysis of sheathings with Wood siding*

In the case of wood siding, OSB had the highest percentages of absorption followed by plywood and then fiberboard. On the other hand, OSB and plywood had significantly higher absorption percentages than the fiberboard as shown in Figure 5-15. This is attributed to the material characteristics for the three types of sheathings.

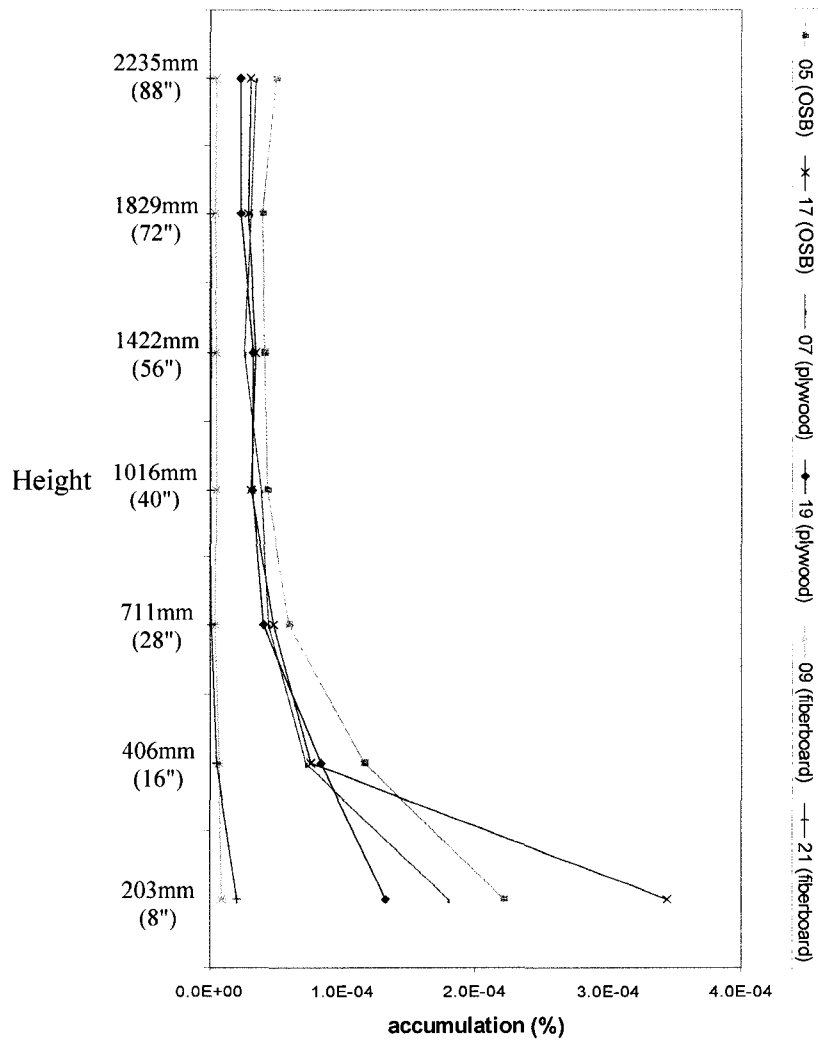


Figure 5-15. Moisture absorption percentage per one sample area vs. height for wood siding with vapor barrier wall assemblies (period 2)



### 5.4.2 Averaged moisture absorption percentages vs. Height

According to the previous analysis, there were good trend agreements between the moisture absorption values with respect to height in sheathings for the duplicate assemblies. For easier comparisons, the values were averaged for the duplicate assemblies. Figure 5-16 shows the averaged moisture absorption values with respect to height for the different types of sheathings configured with stucco and vapor barrier.

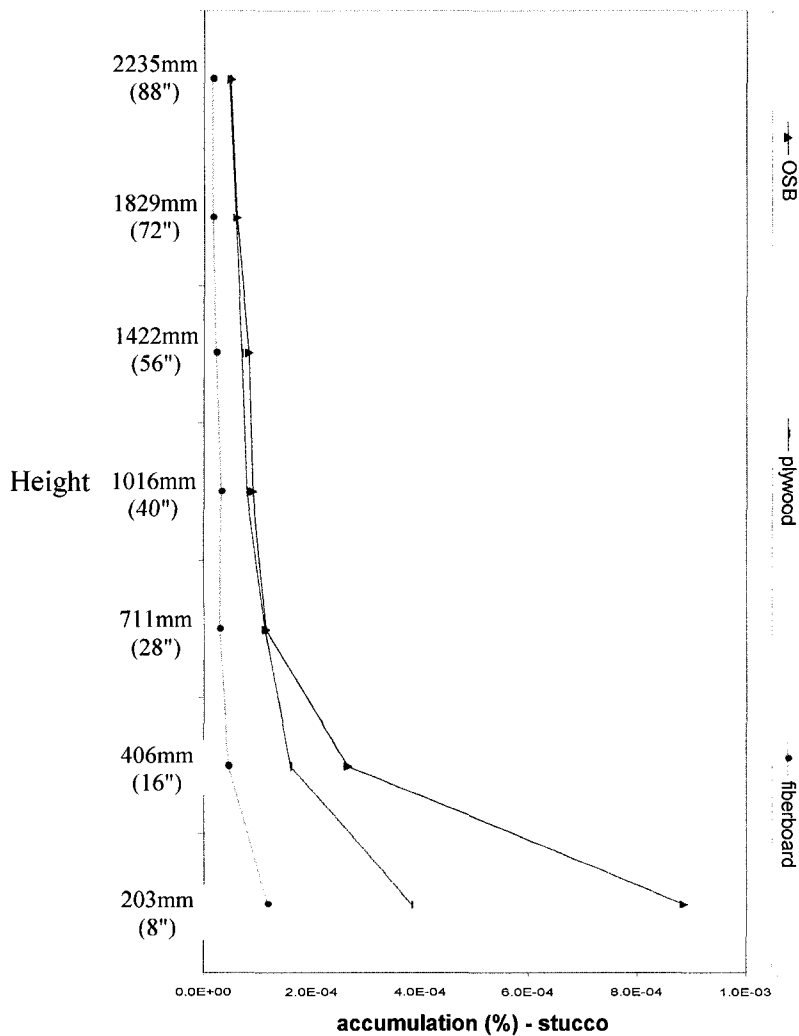


Figure 5-16. Averaged moisture absorption percentages of duplicate wall assemblies vs. height for the different types of sheathings configured with stucco and vapor barrier (period 2)

Figure 5-17 shows the averaged moisture absorption values with respect to height for the different types of sheathings and configured with wood siding and vapor barrier.

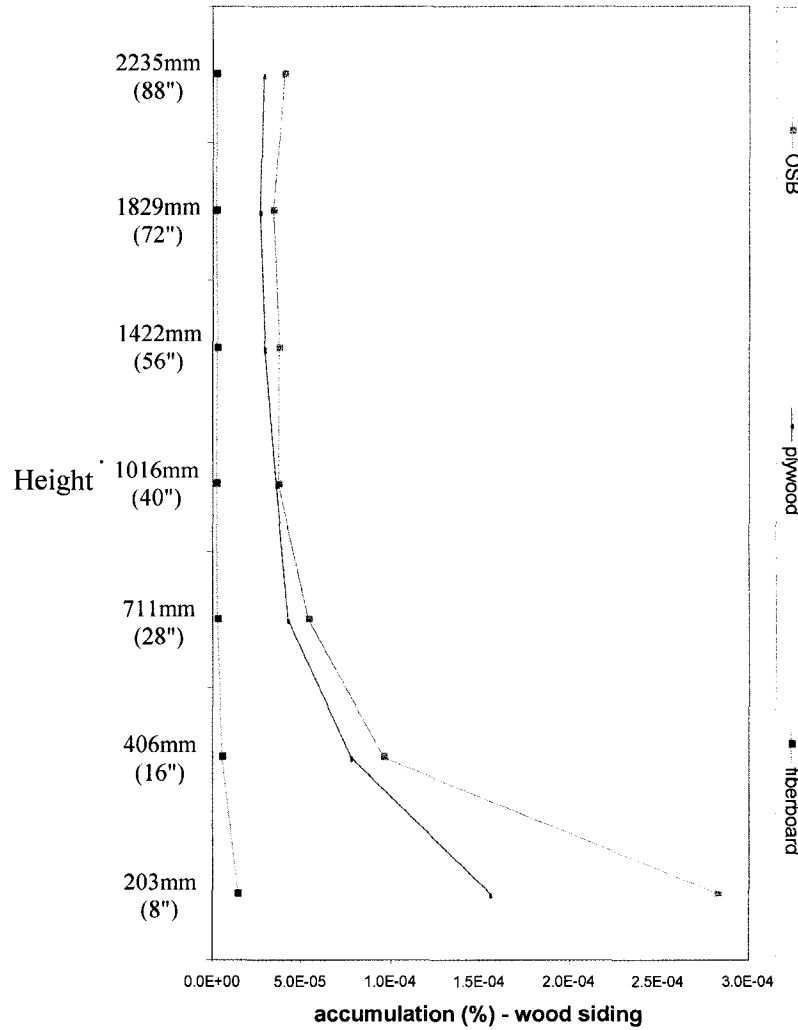


Figure 5-17. Averaged moisture absorption percentages of duplicate wall assemblies vs. height for the different types of sheathings configured with wood siding and vapor barrier (period 2)

## **Chapter 6**

### **DRYING CAPACITY**

The capacity to evacuate moisture is one of the characteristics required to ensure the durability of the building envelope. The envelope system with the greater capacity to evacuate moisture in the stud cavity will have a greater drying capacity and be less susceptible to moisture driven damages. In this experiment, the performance of an assembly is reflected in the evaporation rate of the moisture source, which can be related to the “building envelope drying capacity” of the assembly. This capacity is a measure of the rate of movement of the moisture out of the stud cavity and it can serve as a common yard stick to evaluate the relative performance of different wall configurations using the Drying by Evaporation Index "DEI" as a tool. In this chapter, a calculation by mapping method "MM" is presented. This calculation method was initiated to investigate the relations among moisture absorbed by components surrounding the stud cavity, thus estimating the moisture transported out of the cavity through the sheathing material, which is part of the total water evaporated from the tray. This MM method was applied on test periods 1 and 2 only since the objective of the study is to investigate the performance of the different building configurations in the worst drying potential conditions.

#### **6.1 Introduction of DEI (Drying by Evaporation Index)**

##### **6.1.1 Total evaporated moisture and drying capacity**

The total amount of water evaporating from the water source includes the moisture added to the stud cavity, the moisture absorbed by different materials surrounding the stud cavity, and the water vapor leaving the stud cavity to either the indoor or outdoor environment (Fazio et al. 2006). It is assumed that a minimal amount of moisture will remain in the cavity with the existence of the vapor pressure difference being the driving force for evacuating the evaporated vapor out of the stud cavity. Therefore, part of the evaporated vapor will find its way outside of the cavity while the other part will be captured by the materials surrounding the stud cavity,

namely: the sheathing, the drywall (with the absence of vapor barrier), vertical studs and top and bottom plates.

### **6.1.2 DEI and drying capacity**

Drying by Evaporation Index or “DEI” is the measure of the rate of moisture movement out of the stud cavity, and it is a function of moisture "evaporation" inside the cavity and moisture "evacuation" out of the cavity. This index will vary according to the specific wall configuration and according to the climatic load applied as mentioned earlier.

On the other hand, drying capacity or drying potential can be identified as the capacity of a building envelope to evacuate moisture out of the stud cavity, where the drying capacity can be quantified using the DEI as a tool. Thus the drying capacity could be a quantitative measure of moisture evacuation out of the building envelope under a predetermined set of conditions.

## **6.2 Equilibrium Moisture Content EMC**

In literature and as mentioned above, experiments dealt with two individual main phases wetting and then drying. The purpose of the wetting phase, or the pre-conditioning, or the combination of the two is to ensure that the building envelope components were brought to elevated moisture content. EMC is defined as the moisture content level at which a substance is neither gaining nor losing moisture. So, if a substance is no longer releasing or gaining moisture, equilibrium exists. This EMC level depends on the relative humidity and temperature (vapor pressure) of the air surrounding the substance. Thus, if remaining long enough in contact with air where the relative humidity and temperature remain constant, the moisture content will also reach a level and become constant at the EMC value. Every combination of relative humidity and temperature has an associated value of EMC, where it increases with increasing relative humidity (Simpson W. 1999).

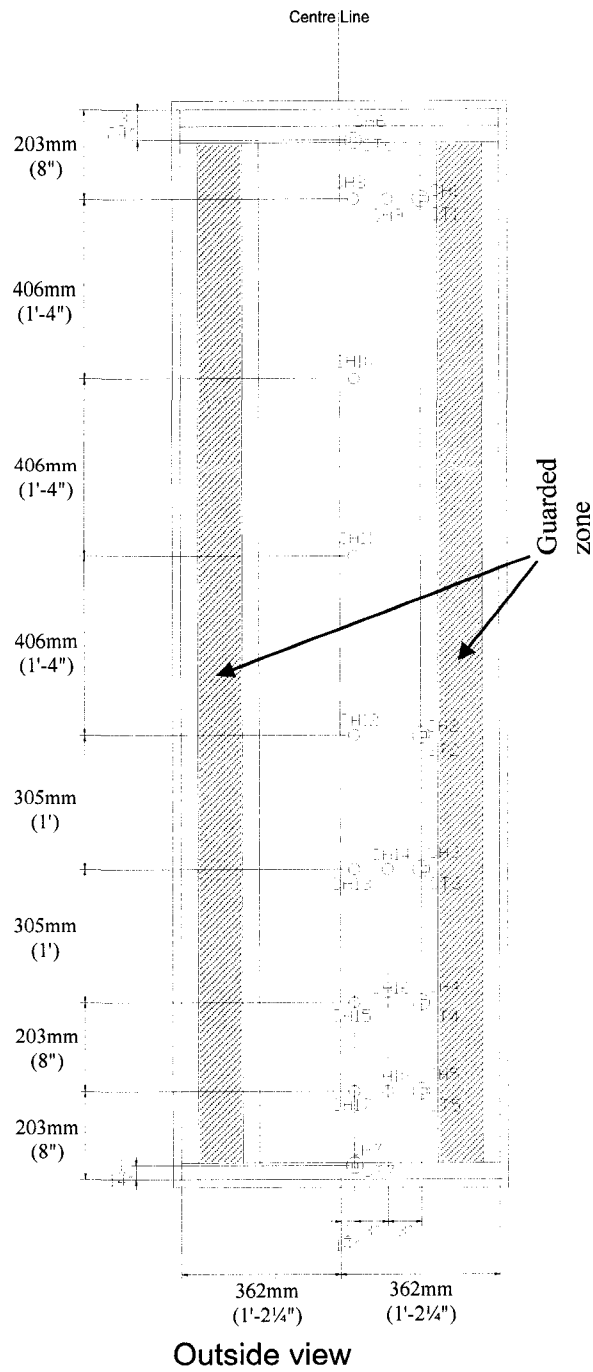
### **6.2.1 Wetting and drying**

This study has two phases: wetting and drying. The drying of the stud cavity is based on the evaporated moisture from the water source at the bottom of the cavity (evaporation). This

amount of moisture is continuously monitored through the DAS. The amount of moisture leaving the cavity is referred to as the evacuation; it is part of the total evaporation and represents the drying phase. As the evaporation is taking place, the surrounding components are wetted by retaining a certain amount of the vapor as it diffuses out of the cavity driven by the vapor pressure difference. This wetting of surrounding materials continues until the equilibrium moisture content EMC is reached and the surrounding materials are no longer gaining or losing moisture. At this stage, it can be said that the amount of evaporated moisture represents the amount of drying or evacuating out of the stud cavity.

### **6.2.2 Correlation between evaporated moisture and DEI**

In order to establish the drying by evaporation index (DEI) for a wall assembly and thus identify the drying capacity, a correlation between the evaporation rate (evaporation), and the amount of moisture leaving the cavity (evacuation) has to be identified. After the EMC has been reached, the slope of the evaporation rate is deemed to represent the rate of water vapor exiting the stud cavity. For example, Assembly #16 reached a steady-state when the MC for the 25 gravimetric samples (Fig. 6-1) located in the surrounding materials stopped increasing. This state is represented by the horizontal profiles in Figure 6-2b. At this equilibrium, the water evaporated for the same EMC time period represents the amount of moisture leaving the wall and is referred to as the evacuated moisture (Fig. 6-3). Therefore, if equilibrium is reached, it is easy to establish the DEI directly as a function of evaporation and evacuation. In the experiment, most of the wall assemblies reached the EMC at some stage. However, assemblies having stucco cladding on OSB and plywood sheathing continued to absorb moisture and did not reach EMC during the test periods, thus, making it difficult to establish the DEI. In this case, where moisture content equilibrium is not reached, a new factor has to be determined to establish the DEI that is the “absorption”. Absorption is the portion of evaporation absorbed in the materials surrounding the stud cavity. If this amount could be estimated, then the evacuated portion can be quantified accordingly from which the DEI can then be established.



SH: gravimetric samples in sheathing  
 ST: cubical gravimetric samples in wood studs

Figure 6-1. Locations of gravimetric samples in the wall assemblies

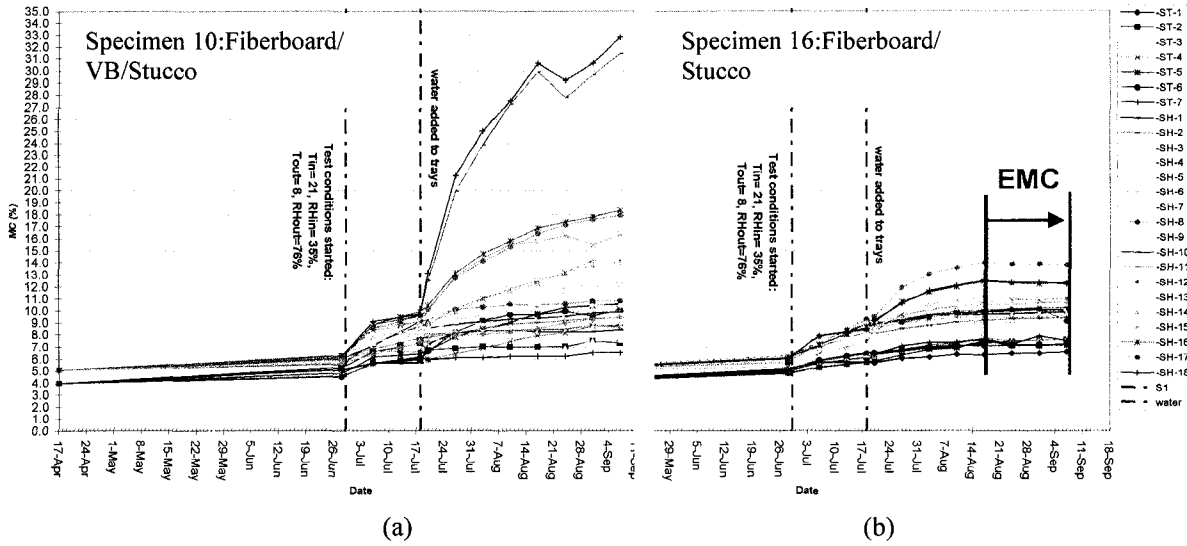


Figure 6-2. Two cases of moisture absorption, where equilibrium moisture content EMC is reached in wall assembly 16 (b) but not in wall assembly 10 (a)

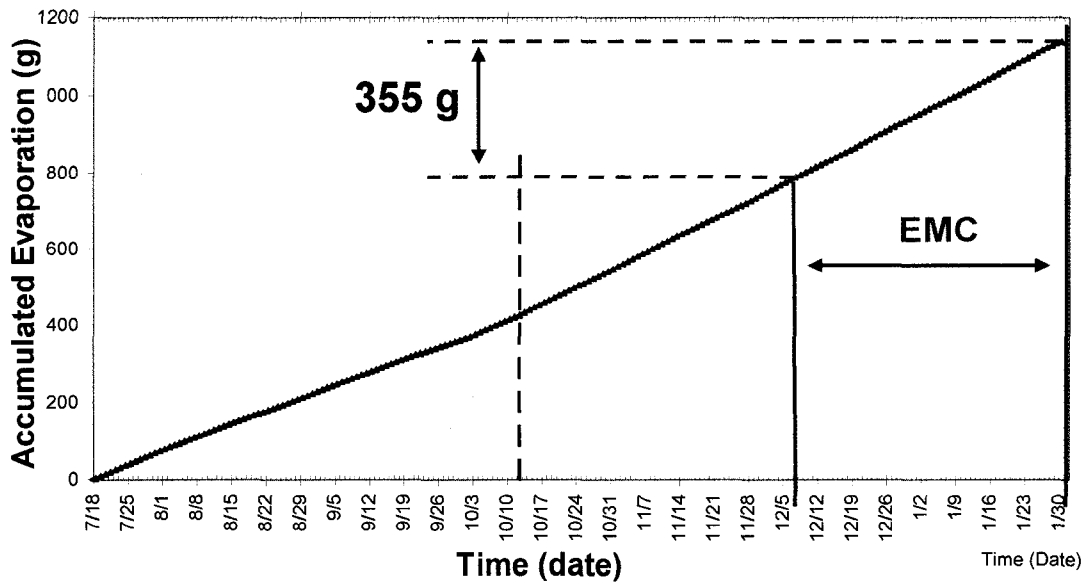


Figure 6-3. Accumulated evaporation amount for the EMC period for wall assembly 16

### **6.3 Absorption by the Mapping Method MM calculations**

The absorption-evaporation ratio concept investigates the amounts of moisture being generated inside the stud cavity and the amount of moisture stored in the different components surrounding the stud cavity. The moisture generation can be obtained simply from the monitored weight change of the water tray. The moisture absorption is obtained through a more complex estimation procedure employing interpolation and area-weighted average of gravimetric sample data. There are 6 components surrounding the cavity that have the potential to absorb moisture from within the stud cavity. These components are the sheathing, right and left vertical wood studs, top and bottom plates, and drywall. Since there are no gravimetric samples in the gypsum boards (no MC monitoring), only the assemblies having vapor barriers are included in this calculation method. In cases when EMC is reached, there is no further absorption and the evaporation equals the evaporation.

#### **6.3.1 MM calculation assumptions**

In this calculation method, the following assumptions are made:

- The vapor barriers prevent any significant moisture transport from cavity to indoor and negligible moisture content changes in the drywall.
- The moisture gain in the stud cavity, due to increase in RH in the air and absorption in the fiberglass insulation, is negligible for the long duration under consideration.
- Judging from the little amounts of moisture captured by the gravimetric samples in the studs, the moisture captured in the wood studs is considered to be indicative of surface accumulation and not of penetration all the way through the studs.
- The moisture accumulation is uniform with respect to the center line axis, thus the moisture accumulation in the side that contains the gravimetric samples of the sheathing is assumed to be the same as the other side. Similarly, the two studs are considered to have identical moisture distribution.



### 6.3.2 Calculation steps

As mentioned above, it will be assumed that the presence of perfectly installed vapor barriers leads to negligible moisture transport from cavity to indoor and negligible moisture content changes in the drywall. The moisture absorption thus occurs on the remaining 5 components. The following procedure is used to obtain the moisture absorbed by the surrounding components:

- The *top plate* is assumed to have uniform MC as the sole gravimetric sample on it.
- The *bottom plate* has only one gravimetric sample. The change in the average moisture content of the entire bottom plate is set to be 80% of the change in the gravimetric sample. This percentage is based on the following considerations and on typical MC gradients monitored in the bottom sheathing region. The bottom plate is divided into two constant MC zones. The central zone has 40% of the total area and its MC equals that of the gravimetric sample. The outer zone with 60% area is further away from the center of the evaporation area of the water tray and is expected to have less moisture accumulation. The accumulation rate in this zone is assumed to be 60% of the middle zone.
- *Vertical studs (2) and sheathing*: Only one of the vertical studs has 5 gravimetric samples. The sheathing board has 18 gravimetric samples on one side of the center vertical line. The sheathing is assumed to have symmetrical MC distribution with respect to the central line. For both sheathing and vertical studs, the surfaces are divided into a number of zones. While the studs are divided in only vertical directions, the sheathing is divided into regular and non-equal rectangular zones, as shown in Figure 6-4. For a zone having a gravimetric sample within the zone, the MC of the zone is assumed to be uniform and equal to that of the gravimetric sample. For a zone with no gravimetric sample, its MC value is calculated from interpolation of adjacent zones. The average MC values in a component are calculated from the area-weighted average MC of all the zones.

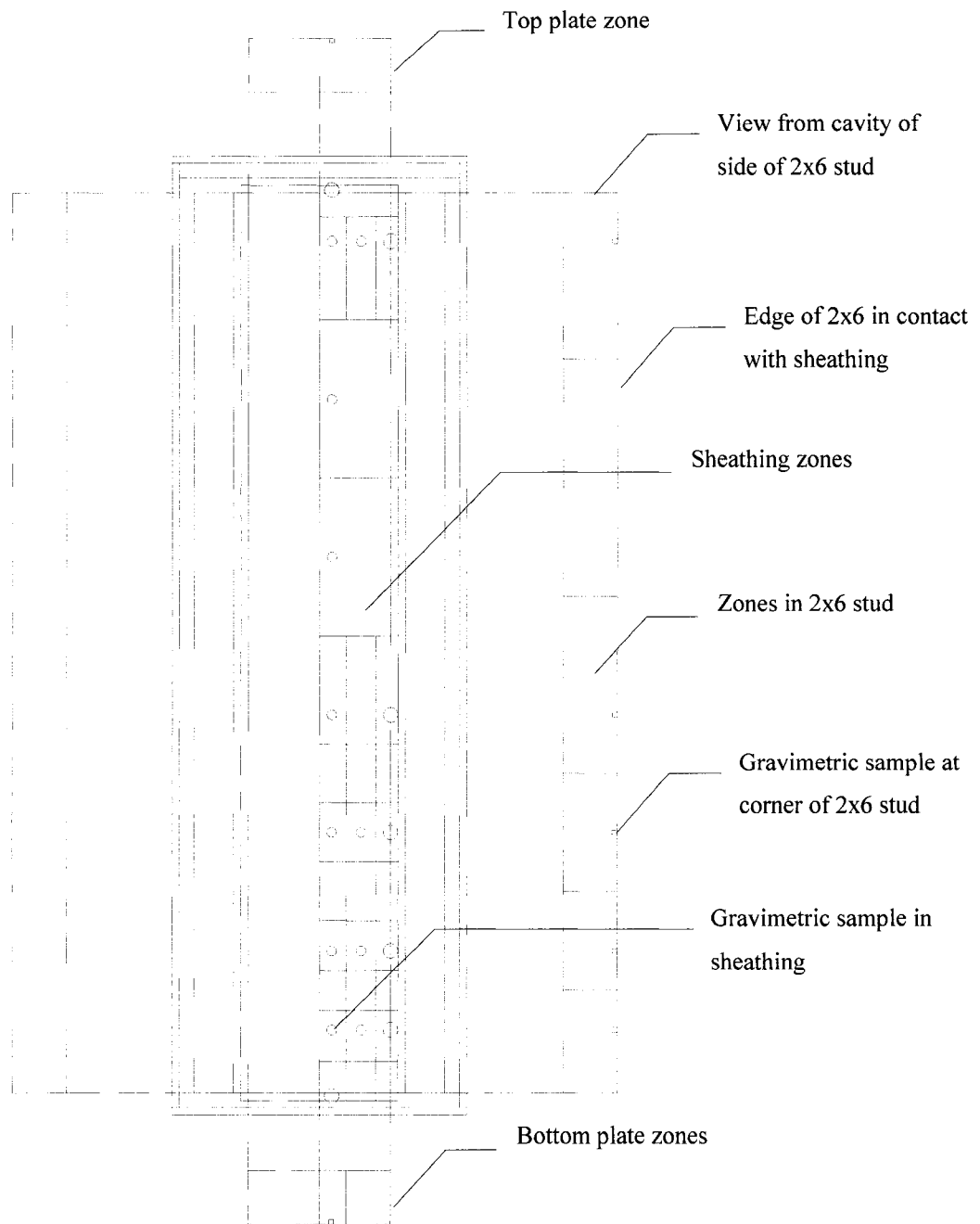


Figure 6-4. Divisions of zones in the components surrounding the stud cavity for the moisture mapping calculation method (view from outdoor through sheathing into stud cavity)

## 6.4 Surfaces absorption

Table 6-1 shows the percentages of absorption by the components surrounding the stud cavity for wall assemblies that have vapor barriers for period 2 of the experiment. The relative good agreement in the average absorption percentages of the duplicate assemblies is noteworthy.

Similarities in the absorption percentages in the sheathings of pair-equivalent wall panels can be noted with percentage differences varying from 3% to 6% in 3 of the pairs, from 9% to 10% in 2 of the pairs and 16 % in only one of the pairs. Since each of the pair-equivalent was on a different floor level, some of the difference may be attributed to the stack effect; part of the difference may be attributed to the make up of the specimens and some to air movement in the test chamber. Sheathings with stucco cladding accumulate more moisture than those with wood siding cladding. The increase of absorption in the OSB and plywood sheathings with stucco was about 9%. In the case of fiberboard, the fiberboard sheathing with stucco absorbed 18% more than the fiberboard sheathing with wood siding.

Table 6-1. Absorption of the components surrounding the stud cavity by percentages of the total moisture absorbed in period 2 using the mapping method (MM)

Assembly #	Configuration (all with VB)	Percentage of total absorbed (%)			
		top plate	Right & left studs	bottom plate	sheathing
5	OSB-wood siding	3	21	3	74
17	OSB-wood siding	1	24	4	71
6	OSB-stucco	0	16	1	82
18	OSB-stucco	1	19	4	77
7	plywood-wood siding	2	26	0	72
19	plywood-wood siding	1	26	3	70
8	plywood-stucco	1	18	1	81
20	plywood-stucco	1	24	1	74
9	fiberboard-wood siding	4	50	0	46
21	fiberboard-wood siding	0	54	0	54
10	fiberboard-stucco	1	36	0	63
22	fiberboard-stucco	3	40	1	57
1	OSB-no cladding	0	12	37	51
29	OSB-insul.-wood siding	1	20	6	73
2	plywood-no cladding	1	18	16	65
30	plywood-insul.-wood siding	1	25	8	66
3	fiberboard-no cladding	0	47	5	48
31	fiberboard-insul.-wood siding	2	45	0	54

Figure 6-5 shows the surfaces accumulation by percentages of the total accumulated moisture in materials surrounding the stud cavity for wall assemblies with vapor barrier and cladding for period 2. The results were presented as bar charts for better comparison between the absorption percentages of the different components for the duplicate wall assemblies.

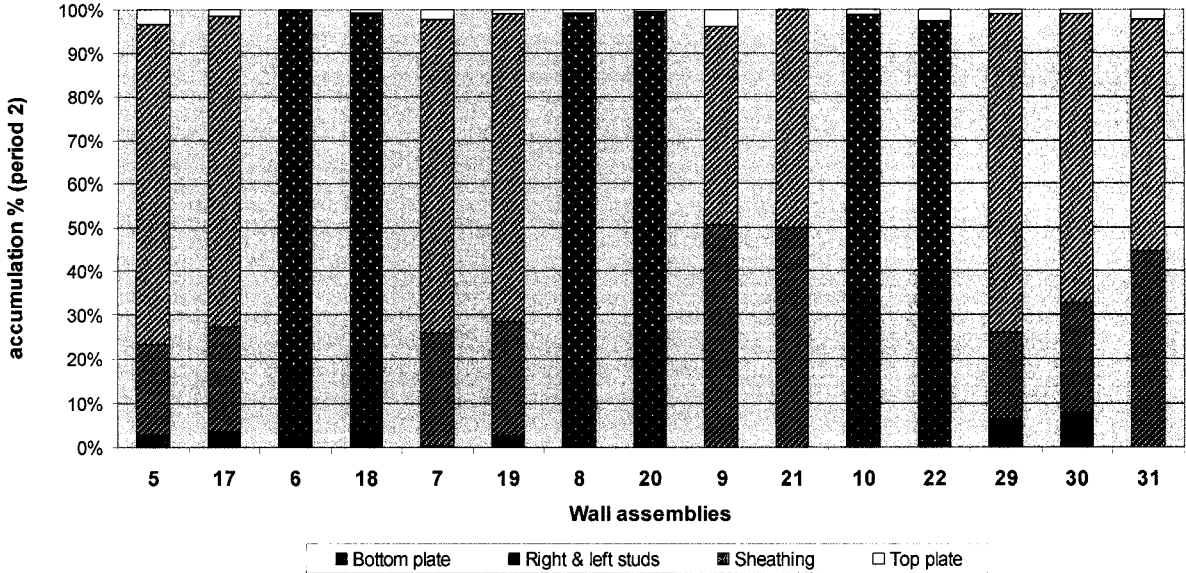


Figure 6-5. Surfaces moisture absorption by percentages of the total absorbed for the wall assemblies with vapor barriers (period 2)

## 6.5 Drying capacities for different wall configurations

The mapping method calculations were performed on the different wall assemblies using the gravimetric data for test periods 1 and 2. The climatic loading was for October conditions with 8°C and 76% RH. The moisture loading was 1/3 of the water tray surface area for test period 1 and 2/3 for test period 2. The DEI is defined as the measure tool for the ratio of the evaporation evacuated to the total evaporation, thus determining the drying capacity. It captures the capacity of an envelope to remove internal moisture and, therefore, it can indicate the drying capacity of this envelope.

The estimated drying capacities from the data of test periods 1 and 2 are summarized in Tables 6-2 and 6-3 respectively. The results are arranged to facilitate the comparisons between duplicate assemblies. The drying capacities of duplicates are displayed, in Tables 6-2 and 6-3,

Table 6-2 Evaporation, absorption, evacuation and drying capacity for the different wall assemblies with vapor barriers for test period 1.

Assembly #	Configuration (all with VB)	Evaporation (g)	Absorption (g)	Evacuation (g)	Drying capacity (%)
1	OSB-no cladding	376	278	98	26
29	OSB-insul.-wood siding	406	182	224	55
5	OSB-wood siding	392	235	157	40
17		360	169	191	53
6	OSB-stucco	488	354	134	27
18		328	238	90	27
2	plywood-no cladding	344	232	112	33
30	plywood-insul.-wood siding	442	97	345	78
7	plywood-wood siding	351	192	159	45
19		392	199	193	49
8	plywood-stucco	537	432	105	20
20		328	237	91	28
3	fiberboard-no cladding	374	41	333	89
31	fiberboard-insul.-wood siding	434	67	367	85
9	fiberboard-wood siding	567	87	480	85
21		495	57	438	88
10	fiberboard-stucco	446	198	248	56
22		435	179	256	59

in two adjacent rows with the same text shading. The bar charts in Figures 6-6 and 6-7 display the estimated drying capacities of the six (6) duplicates (pairs) in Tables 6-2 and 6-3. It can be observed that duplicate assemblies have the same moisture drying capacity to the exterior, within 13 % margin in test period 1 and 4% margin in test period 2. These margins can be attributed to experimental errors. On the other hand, the differences in the drying capacities of different wall configurations are significantly larger. This drying capacity similarity for walls with same configurations and the variation of drying capacities for walls with different configurations make the DEI a good indicator to compare the drying performance of building envelopes with different configurations.

Table 6-3 Evaporation, absorption, evacuation and drying capacity for the different wall assemblies with vapor barriers for test period 2.

Assembly #	Configuration (all with VB)	Evaporation (g)	Absorption (g)	Evacuation (g)	Drying capacity (%)
1	OSB-no cladding	665	323	342	51
29	OSB-insul.-wood siding	583	126	457	78
5	OSB-wood siding	640	110	522	82
17		593	106	476	80
6	OSB-stucco	783	321	459	59
18		542	214	297	55
2	plywood-no cladding	656	120	537	82
30	plywood-insul.-wood siding	712	76	636	89
7	plywood-wood siding	624	84	526	84
19		642	81	551	86
8	plywood-stucco	982	272	710	72
20		603	141	446	74
3	fiberboard-no cladding	716	20	696	97
31	fiberboard-insul.-wood siding	739	29	710	96
9	fiberboard-wood siding	1022	20	1002	98
21		849	7	843	99
10	fiberboard-stucco	829	99	730	88
22		759	73	672	89

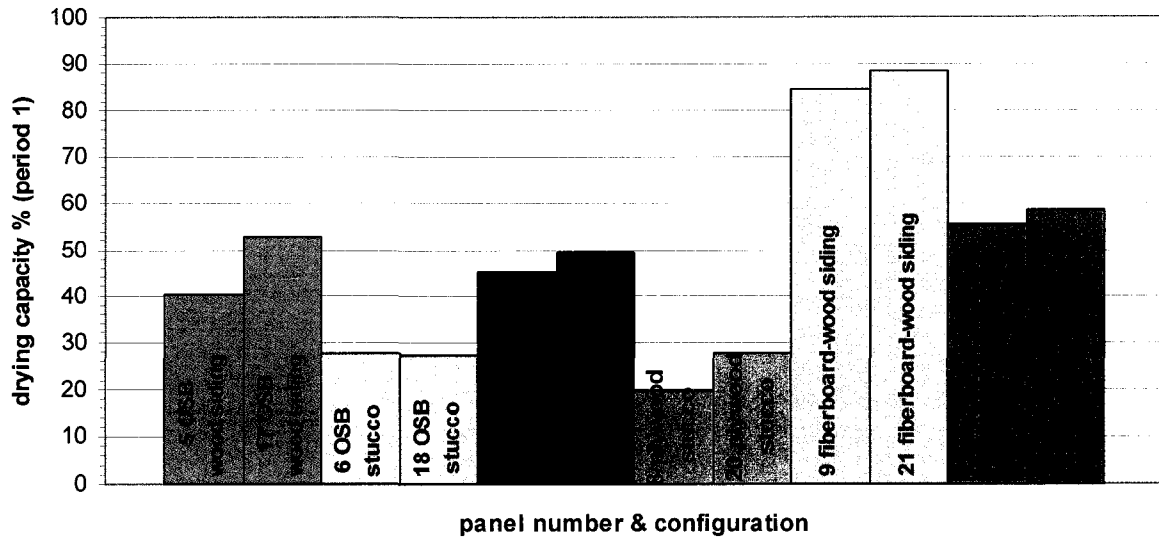


Figure 6-6. Drying capacity percentages for duplicate wall configurations for test period 1

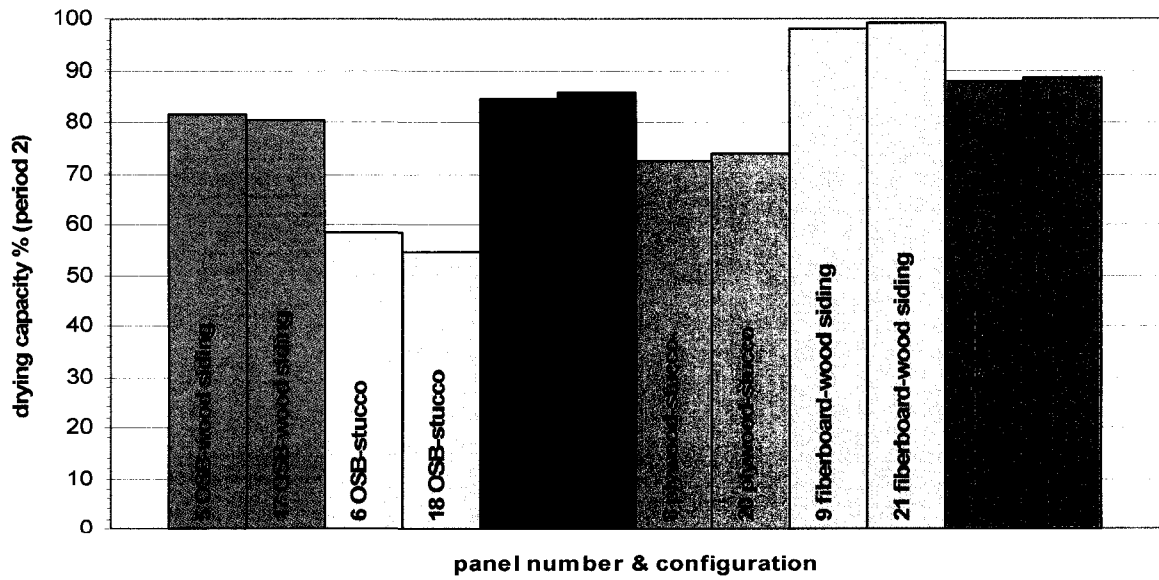


Figure 6-7. Drying capacity percentages for duplicate wall configurations for test period 2

Based on these estimated drying capacity values, the relative drying performance of the wall assemblies can be evaluated. For example, the results for the assembly sheathed with fiberboard and cladded with wood siding show a drying capacity of 85-88% in test period 1 and 98-99% in test period 2. This means that for the conditions adopted for this study, 85 to 88% of the moisture in the stud cavity dries out in the course of test period 1 and 98 to 99% dries out in the course of test period 2.

By comparing the drying capacities for period 2 in this study, the wall configuration showing the best overall drying performance is the assembly sheathed with fiberboard and cladded with wood siding, followed by the assembly sheathed with fiberboard and stucco cladding (88-89%), the assembly with plywood sheathing and wood siding (84-86%), the assembly with OSB and wood siding (80-82%), the assembly with plywood and stucco (72-74%). The worst configuration is the assembly sheathed with OSB and cladded with stucco having a drying capacity of 55-59%.

Stucco cladding had a negative effect on the drying capacity of different configurations in the test, because it acts as a vapor retarder layer when compared to the same configurations but with wood siding that have an air gap to enhance the drying. For test period 2, the stucco cladding (#10 and 22 in Table 6-3) lowered the drying capacity of the assembly with fiberboard sheathing relatively by about 11% compared to the assembly with wood siding (#9 and #21). Similarly, in the case of the plywood sheathing assembly, the relative difference was about 15%. The biggest effect was in the case of the assembly with OSB sheathing with a relative difference of 33-38%.

An experimental validation procedure for the mapping method, that involved cutting material samples from the wall assemblies, was scheduled to be carried out after the test completion. This procedure did not take place since the test set-up and the wall assemblies were used by another team to carry out a different test.



## **Chapter 7**

# **MOISTURE EVACUATION FROM STUD CAVITIES OF BUILDING ENVELOPES**

As discussed in the previous chapter, the mapping method calculates the evacuation through the sheathing material only. This evacuation value through the sheathing is important since sheathing is the critical layer where moisture damage can occur. None the less, it is also important to find out the evacuation through the outer layers namely the cladding, the weather resistive membrane and the sheathing. A Calculation Evacuation Method (CEM) is introduced in this chapter to calculate the evacuation through the outer layers of the building envelope, where CEM takes into account the non-linear profile with height of the absorbed vapor mass as well as the vapor pressure profile arising from the moisture source located at the bottom of each wall cavity.

### **7.1 In-cavity profiles due to moisture loading**

In site situations where rain water penetrates into the stud cavity of the building envelope and concentrates at the bottom, the wet bottom plate becomes a moisture loading source. This moisture evaporates creating a vapor pressure profile that decreases with height and causes a corresponding absorption-evacuation mass profile through the sheathing. In this experiment, such profiles were observed and studied to analyze the evacuation process through the building envelope's outer layers, and thus, evacuation of the different wall assemblies could be quantified. All the analyses were carried out for test period 2.

#### **7.1.1 Vapor pressure profiles**

The vapor pressures are mainly the result of the evaporation from the moisture loading source at the bottom of the cavity. Figure 7-1 shows an example of the accumulated evaporation for assembly 6 (which has OSB sheathing, stucco cladding, and vapor barrier) for test period 2.

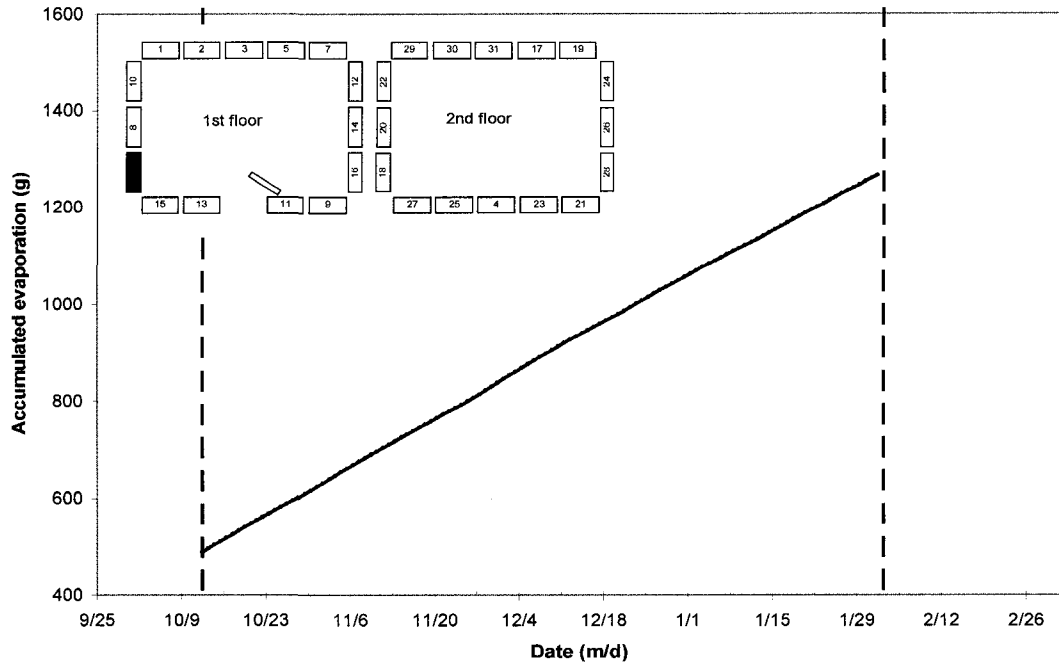


Figure 7-1. Accumulated evaporation in period 2 for wall assembly 6 (OSB, stucco, and vapor barrier)

Figure 7-2 shows the calculated vapor pressures based on the relative humidity and temperature values measured by the two RH sensors at the two locations (406mm or 16" and 1829mm or 72" from the bottom) in each of the stud cavities of the 31 wall assemblies. Since there were only two RH sensors on each wall assembly, at least a third point is needed to be able to determine the vapor pressure profile inside the stud cavity (even though more points would increase the accuracy of the profile).

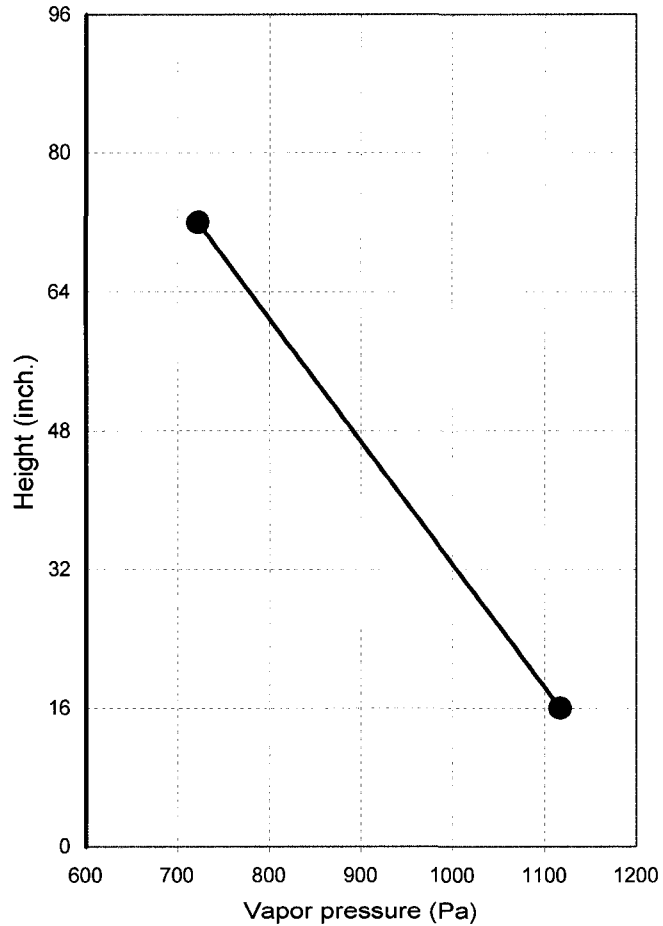


Figure 7-2. Calculated vapor pressure at the two RH sensors' heights in wall assembly 6 (OSB, stucco, and vapor barrier) for test period 2

### 7.1.2 Relative humidity profiles

To obtain the vapor pressure profile in respect to height, a third location is taken at just above the water level of the water tray at a height of 4½" from the base of the assembly. At this point, it is assumed that near saturation condition of 98% relative humidity is sustained. The fitting curves for the relative humidity profiles inside the stud cavities vs. height were plotted for the wall assemblies with vapor barriers. The RH profile vs. height for assembly 6 (OSB sheathing, stucco cladding, and vapor barrier) is shown in Figure 7-3.

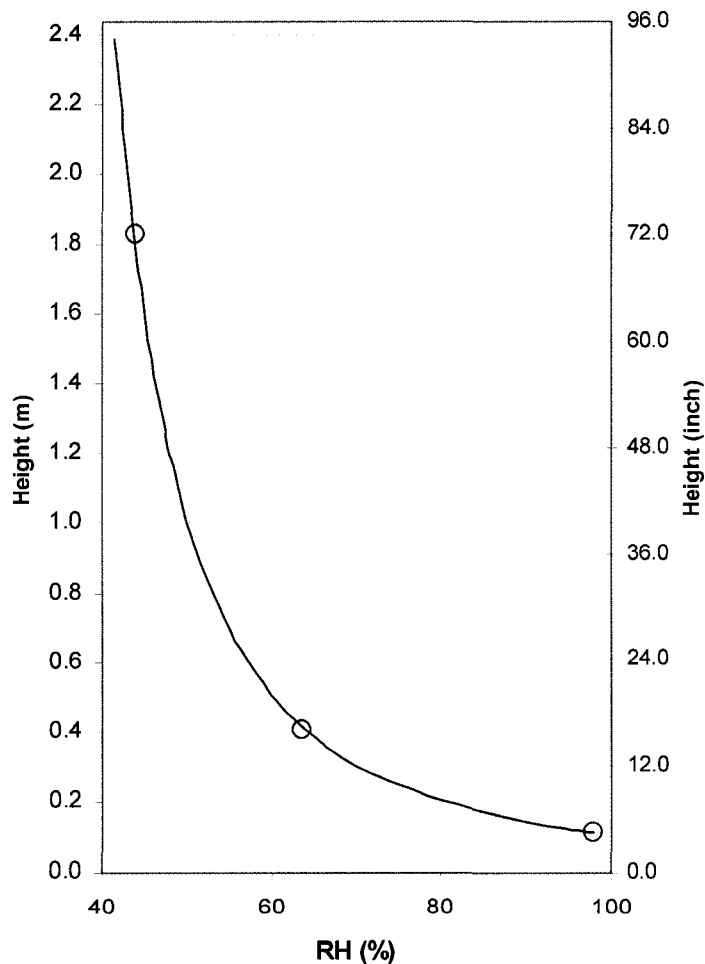


Figure 7-3. RH vs. height profile for wall assembly 6 (OSB, stucco, and vapor barrier) for period 2.

### 7.1.3 Vapor pressure difference profiles

After getting the vapor pressure profiles, the fitting curves<sup>6</sup> for the vapor pressure difference between the stud cavity and outside vs. height were then plotted for the wall assemblies with vapor barriers. Figure 7-4 shows one example that is the vapor pressure difference profile for wall assembly 6 (OSB sheathing, stucco cladding, and vapor barrier). The moisture loading source at the bottom of the cavity creates a nonlinear vapor-pressure difference profile with maximum value at the bottom of the cavity and minimum value at the top of the cavity.

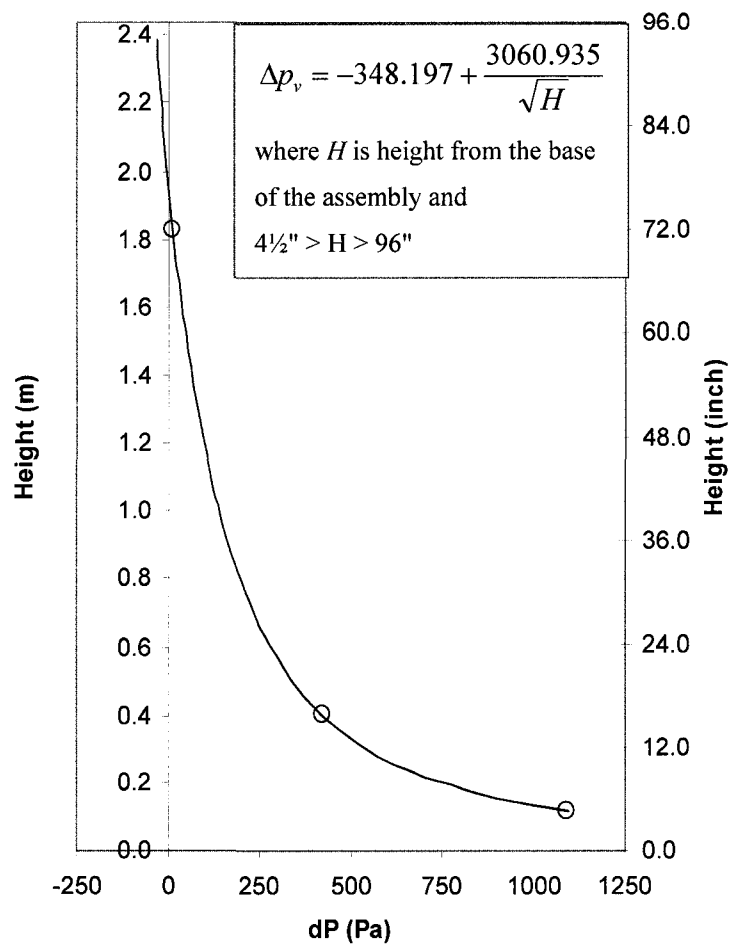


Figure 7-4. Vapor pressure difference profile for wall assembly 6 (OSB, stucco, and vapor barrier)

<sup>6</sup> Using TableCurve 2D® Automated Curve Fitting Software by Systat Software, Inc.

## 7.2 Vapor evacuation by the Calculated Evacuation Method "CEM"

Permeance of building envelope layers is used to describe the rates of vapor diffusions under the vapor pressure differential between the two sides. When the envelope permeance,  $M$  (ng/Pa·s·m<sup>2</sup>) is known over a given period of time,  $\theta$  (s), and under a constant vapor pressure differential, the mass of vapor transport,  $W$  (ng), can be calculated from Fick's law of diffusion:

$$W = M \cdot A \cdot \theta \cdot (P_1 - P_2) \quad (\text{Eq. 1})$$

where  $p_1$  and  $p_2$  are the vapor pressures on the two sides of the layer(s) (Pa). In this equation the vapor pressures are typically assumed to be constant in the planes perpendicular to the wall depth. Thus, the vapor pressures at the bottom and top of the stud cavity (along the plane coincident to the inner sheathing surface) are considered to be the same; i.e., the permeance is the same per unit area of the panel.

This condition was found not to be true in the investigation carried out in this study, where the moisture source was located at the bottom plate in the stud cavity. This moisture source gave rise to non linear RH and vapor pressure profiles, which varied from a maximum value at the bottom of the cavity to a minimum at the top of the cavity. Since permeance varies with RH, the permeance of the sheathing can be expected to vary in accordance with the RH and vapor pressure profiles. These variables have been incorporated in the calculation of the amount of water diffusing (evacuation) through the outer layers of the assembly to the outdoor, including the sheathing, weather barrier, and cladding. This calculation method is referred to herein as the Calculated Evacuation Method (CEM) to distinguish it from the evacuation by the Mapping Method (MM) explained previously, which considers the diffusion through the sheathing only.

### 7.2.1 Moisture content vs. height

In the CEM the evacuation of vapor through the outer layers depends mainly on the vapor pressure and on the permeance, which in turn varies with moisture content. This moisture content changes with height and depends on the vapor pressure difference between the inside

of the stud cavity and the outdoor. Figure 7-5 shows the MC vs. height profile for wall assembly 6 (OSB, stucco, and vapor barrier). The MC profiles are curve fitted over seven data points. These profiles confirm the shapes of the vapor pressure profiles which have only three data points.

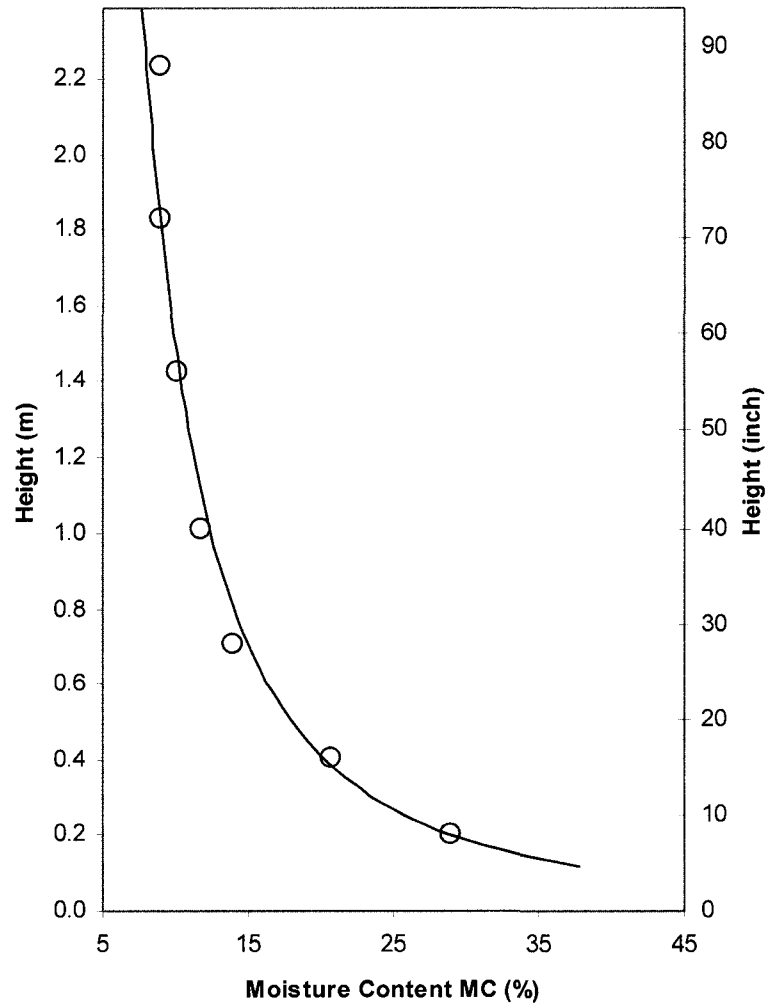


Figure 7-5. Moisture content in the sheathing vs. height profile for wall assembly 6 (OSB, stucco, and vapor barrier) for period 2.

### 7.2.2 Evacuation zones

The sheathing was divided into four zones of different sizes along the height (Fig. 7-6). The calculated evacuated vapor mass for each zone,  $W_{di}$  (g), is obtained by rewriting Eqn. 1 as

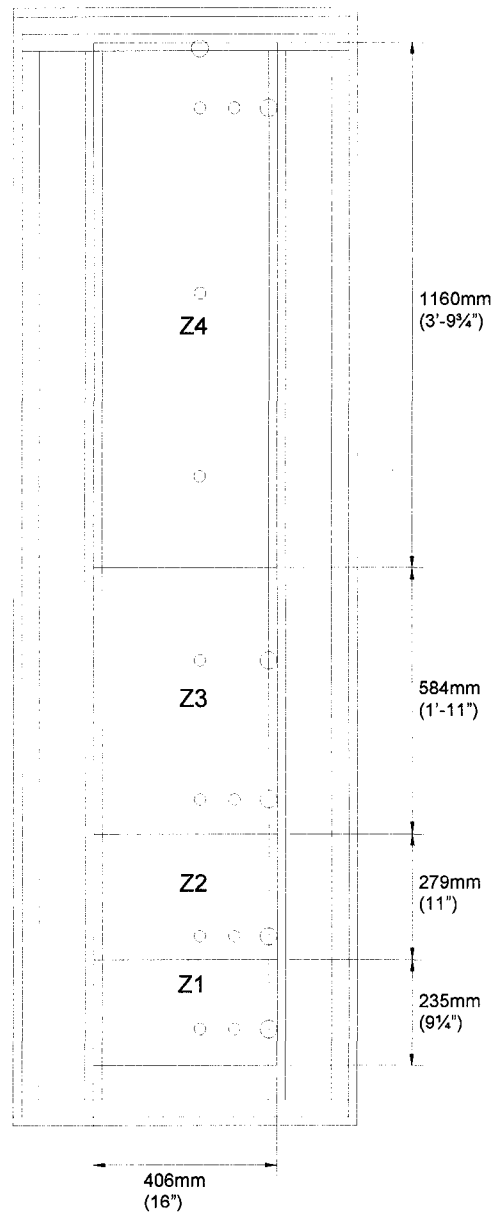


Figure 7-6. Sheathing permeance zones and locations of gravimetric samples



follows:

$$W_{di} = M_{pi} \cdot A_i \cdot \theta \cdot \Delta p_{ci} \quad (\text{Eq. 2})$$

where

$W_{di}$  = mass of the evacuated moisture passing through the outer layers in a specific zone, ng

$M_{pi}$  = permeance of outer layers for a zone from material properties, ng/Pa·s·m<sup>2</sup>

$A_i$  = zone area, m<sup>2</sup>

$\theta$  = time, s

$\Delta p_{ci}$  = vapor pressure difference between the vapor pressure in the stud cavity as a function of height corresponding to the zone and the outdoor vapor pressure, Pa

$i = 1$  to 4 zones.

Since the vapor pressure difference across the zone,  $\Delta p_{ci}$ , for Eq. 2 changes with height, as illustrated in the example of Figure 7-4, the average  $\Delta p_{ci}$  for the zone is calculated by integrating the vapor pressure difference over that zone.

### 7.2.3 Calculation steps

The material properties used in the calculations were taken from Kumaran (2002) and the material property data base generated by Wu, Kumaran and Fazio (2007) for the materials used in this study. The calculation steps using "CEM" to obtain the vapor evacuation for the 4 zones, and thus, the total vapor evacuation are as follows:

1. The average moisture content in the sheathing of a zone is calculated by integration over that specific zone using the MC profiles for the different wall assemblies (such as in the example of Figure 7-5);
2. The corresponding equilibrium RH value in the sheathing of the zone is looked up from the absorption isotherm for the sheathing material;

3. The average permeability for the zone is calculated by integrating the permeability over that zone based on the permeability vs. RH data curve for the sheathing material;
4. The total permeance is then calculated from the total resistance of the outer layers;
5. The average vapor pressure difference across the zone is calculated by integration over the height of that zone;
6. With the permeance value of the outer layers and cavity vapor pressure difference calculated in Steps 4&5 above, the evacuated vapor mass that passes over each zone ( $W_{di}$ ) is then calculated from Eq. 2. Calculations in Steps 1 to 6 above are performed for each of the 4 zones for the different wall assemblies;
7. The total evacuated vapor mass is the sum evacuations of the four zones for each wall assembly.

Table 7-1 is a case study to explain the calculations steps for wall assembly #5 (plywood sheathing, vapor barrier, and wood siding cladding).

Table 7-1. Calculations steps using CEM to calculate the evacuation for wall assembly #5 (plywood sheathing, vapor barrier, and wood siding cladding) for test period 2.

Step	Unit	Zones			
		Z1	Z2	Z3	Z4
Height	mm	235	279	584	610
Area	m <sup>2</sup>	0.096	0.114	0.237	0.248
1. Sheathing average moisture content (MC)	%	14.1%	11.3%	9.8%	8.6%
2. Corresponding RH, looked up from absorption isotherms for sheathing	%	84.5%	73.0%	67.0%	61.5%
3. Corresponding permeability, interpolation from sheathing material data	kg/Pa·s·m ×10 <sup>-12</sup>	3.23	2.22	1.83	1.53
Sheathing calculated permeance	ng/Pa·s·m <sup>2</sup>	277	191	157	132
Sheathing calculated resistance	Pa·s·m <sup>2</sup> /ng	0.0036	0.0052	0.0064	0.0076
Total calculated resistance for outer layers	Pa·s·m <sup>2</sup> /ng	0.0042	0.0059	0.0070	0.0082
4. Total calculated permeance for outer layers	ng/Pa·s·m <sup>2</sup>	236	171	143	121
5. Vapor pressure differential, from stud cavity to exterior	Pa	798.9	395.0	175.2	38.9
6. Evacuated vapor mass	g	179	74	58	3
7. Total calculated evacuation	g		314		

### 7.3 Results and evacuation profiles

Table 7-2 shows the calculated evacuation values for the 4 zones for the duplicate wall assemblies; it also shows the evacuation percentages. The evacuated vapor mass quantities, calculated for each zone for the duplicate wall assemblies, decrease with height. Differences, observed in the evaporations of duplicate wall assemblies, can be attributed to (i) stack effect since each of the pair-equivalent was on a different floor level; (ii) the make up of the wall assemblies and (iii) to different air movement in the test chamber.

Figure 7-7 shows the evacuation profile vs. height for wall assembly 5 (plywood sheathing, vapor barrier, and wood siding cladding). The typical evacuation profile demonstrates graphically the intensities of evacuation from the stud cavity to the outdoor with respect to height.

Table 7-2. Calculated evacuation and percentage of evacuation per zones for the duplicate wall configurations with vapor barrier for test period 2.

#	Configuration (all with VB)	Evacuation <i>Wdi</i> (g)				Percentage of evacuation (%)			
		Z1	Z2	Z3	Z4	Z1	Z2	Z3	Z4
5	OSB-wood siding	179	74	58	3	56	23	18	4
17	OSB-wood siding	161	51	38	-8	63	20	15	2
6	OSB-stucco	147	80	63	10	48	26	21	5
18	OSB-stucco	126	50	21	-32	64	25	11	0
7	plywood-wood siding	362	81	55	-10	72	16	11	1
19	plywood-wood siding	311	89	53	-7	68	19	12	1
8	plywood-stucco	230	126	149	111	37	20	24	18
20	plywood-stucco	228	92	41	-13	63	25	11	1
9	fiberboard-wood siding	488	240	253	225	41	20	21	19
21	fiberboard-wood siding	421	212	233	229	39	19	21	21
10	fiberboard-stucco	234	139	161	168	33	20	23	24
22	fiberboard-stucco	245	143	138	26	43	25	24	7

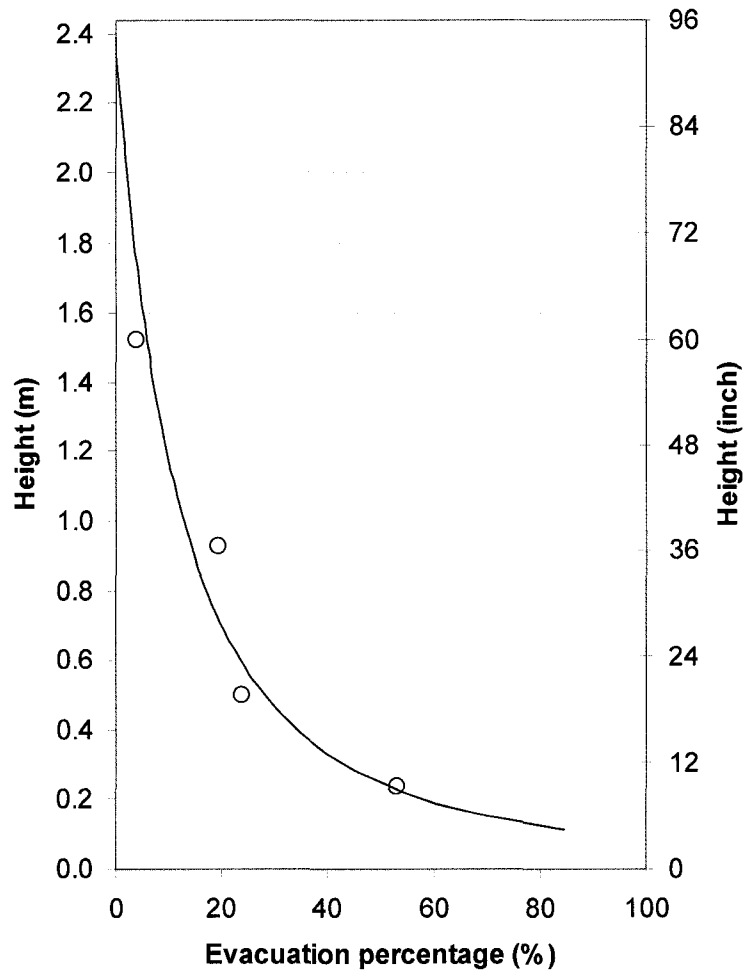


Figure 7-7. Evacuation vs. height profile for wall assembly 5 (plywood sheathing, vapor barrier, and wood siding) for test period 2.

## 7.4 Calculated Evacuation Method (CEM) vs. evacuation by Mapping Method (MM)

Table 7-3 shows the total evacuation vapor mass by the calculated evacuation method (CEM) compared with the vapor mass passing through the sheathing calculated by the mapping method (MM) for the duplicate wall assemblies. The mapping method (MM) provides the vapor evacuation through the sheathings (Figs. 7-8a and 7-9a), whereas the CEM provides the evacuation through the sheathing and outer layers including stucco cladding (Fig. 7-9b) and the evacuation through the sheathing and the weather resistive membrane since there is an air cavity behind the wood sidings (7-8b). Hence, all values in Table 7-3 calculated by the CEM except for wall assemblies 9 and 21 were lower than the values calculated by the MM. For the stucco wall assemblies, the difference between these two evacuations is considered to represent the absorption in the outer layers of the envelope especially the cladding.

Table 7-3. Total evacuated vapor mass by the Calculation Evacuation Method (CEM) compared with vapor passing through the sheathing calculated by the Mapping Method (MM) for duplicate wall configurations with vapor barrier for test period 2.

Assembly #	Configuration (all with VB)	Evacuation W (g)	
		CEM	MM
5	OSB-wood siding	314	522
17	OSB-wood siding	242	476
6	OSB-stucco	301	459
18	OSB-stucco	165	297
7	plywood-wood siding	487	526
19	plywood-wood siding	445	551
8	plywood-stucco	616	710
20	plywood-stucco	348	446
9	fiberboard-wood siding	1206	1002
21	fiberboard-wood siding	1096	843
10	fiberboard-stucco	701	730
22	fiberboard-stucco	552	672

As for the wood siding assemblies, in Figure 7-8, the evacuation values obtained by the CEM represent the evacuation values that are passing through the sheathing and the weather resistive membrane. Therefore, the difference is attributed to the condensation on the cold surface of the weather resistive membrane.

As for the fiberboard case with wood siding (wall assemblies 9 and 21), the evacuation values calculated by the CEM, were higher than those calculated by the MM. this was not expected and the reason behind that is attributed to the water vapor permeability properties of the fiberboard. Other than the OSB and plywood, the permeability values for the fiberboard are almost the same for the different relative humidity conditions (Appendix C), where the permeability value is  $1.82 \times 10^{-11}$  for 10% RH and for RH of 100% the permeability value is  $1.89 \times 10^{-11}$ . The MC in the sheathing is caused by the absorption and knowing that the upper zones experience much less vapor diffusion, therefore, the permeability values for the different zones did not represent the real permeability, and thus, ending up with a higher hypothetical diffusion values especially in the upper zones that increased the total evacuation value for the whole sheathing height.

Therefore, what can be compared between the evacuation values by the two methods is the consistency of the evacuation trends. On the other hand, the evacuation value through the sheathing is more important to be looked at since the sheathing is where the moisture damage could occur. It should be noted that these differences are highly sensitive to the permeability values used<sup>7</sup>.

---

<sup>7</sup> For the stucco, the permeability value was taken from the material property data base generated by Wu et al. (2007) for the materials used in this study. As for the wood siding, the permeability value was taken from Kumaran (2002).

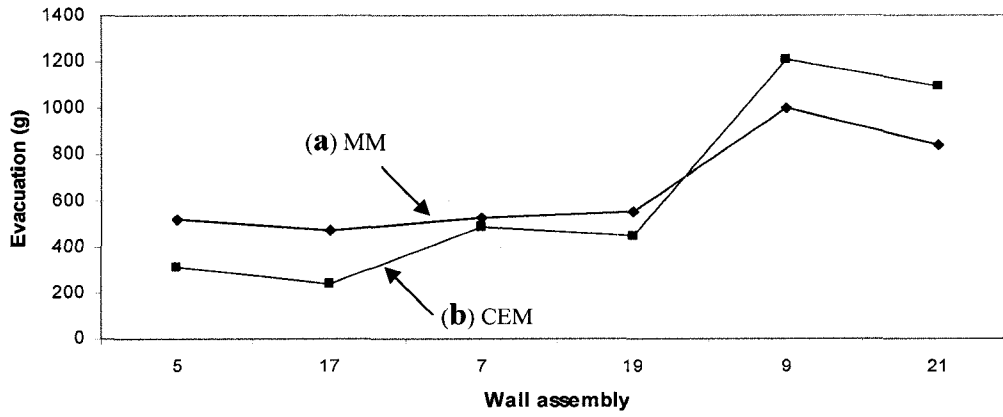


Figure 7-8. Total evacuated vapor mass by (a) Mapping Method (MM) and (b) by Calculation Evacuation Method (CEM) for the different wall configurations with wood sidings and vapor barriers for test period 2.

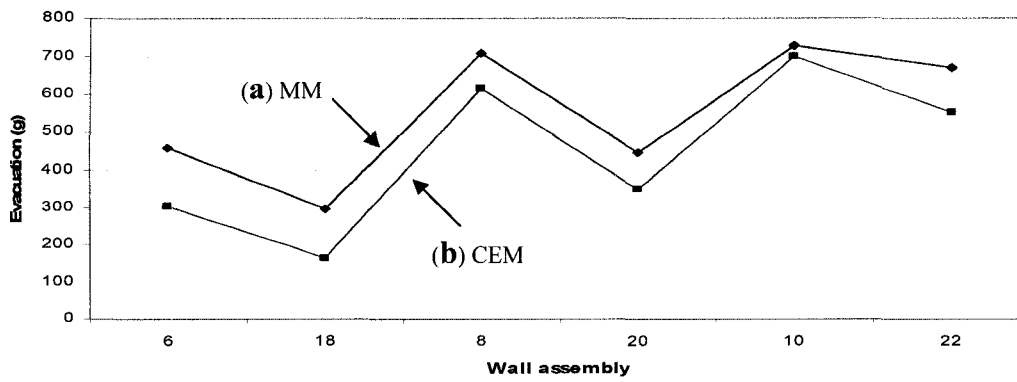


Figure 7-9. Total evacuated vapor mass by (a) Mapping Method (MM) and (b) by Calculation Evacuation Method (CEM) for the different wall configurations with stucco and vapor barriers for test period 2.



## **Chapter 8**

### **CONCLUSION**

The goal of the study was achieved by proving the hypothesis that the data generated from the large scale test on the various wall configurations would yield recognizable patterns relating measurable building-envelope parameters to movement and accumulation of moisture in wood-based building envelope systems. These recognizable patterns emerged from the raw data generated from the experiment and from the analysis of the data using parametric comparative analysis and new methods developed in the study.

A new testing method proposed by Fazio (2004) to establish the drying performance of building envelope wall systems has been implemented and validated by the candidate. The new test method consists of a water tray on a load cell placed on the bottom plate of the stud cavity as the moisture loading system. This new testing method was validated by results obtained using a Mapping Method "MM" and a Calculated Evacuation Method "CEM" developed by the author. The new testing method and analyses (method), with uniform, measurable and repeatable moisture loading source, can be used as a common yardstick to evaluate and compare the relative drying performance of building envelope wall systems of different configurations. Moreover, the method could be implemented by different users in different labs to confirm the drying performance of similar building systems used in different regions.

Since current building envelope design is based typically on sets of proven-by-experience practices, application of passed-down principles and simplistic calculation evaluation, the knowledge gained through this method would support a design process that better predicts the performance of envelope systems, thus moving the design of wood-based building envelope systems towards an engineering approach.

## 8.1 Contributions

### 8.1.1 New methods

- *Development of the Mapping Method "MM"*. The calculation by the mapping method yields profiles of moisture absorbed by the surrounding components in the stud cavity and thus, moisture evacuated from these stud cavities which can then be used to evaluate the relative drying performance of different building envelope systems as a whole assemblies.

The drying capacity is identified as the capacity of a building envelope to evacuate moisture out of the stud cavity, where the drying capacity can be quantified using the Drying by Evaporation Index "DEI" as a tool. DEI is the measure of the rate of moisture movement out of the stud cavity, and it is a function of moisture "evaporation" inside the cavity and moisture "evacuation" through the sheathing for specific time periods and climatic loadings. While evaporation is monitored by the new moisture loading system that is the water tray over the load cell, the evacuation is determined as the evaporation less the absorption of the materials surrounding the stud cavity that can be determined using the mapping method.

- *Developing the Calculated Evacuation Method "CEM"*. Since the mapping method calculates the evacuation through the sheathing material only, a Calculated Evacuation Method (CEM) was developed to calculate the evacuation through the outer layers of the building envelope including the sheathing, weather barrier, and cladding. CEM takes into account the non-linear profile with height of the absorbed vapor mass as well as the vapor pressure profile, where these profiles were due to the moisture source located at the bottom of each wall cavity. It was shown that moisture concentrating at the bottom plate, as it may happen as a result of the rain penetration, gives rise to non linear RH and vapor pressure profiles within the stud cavity, which vary from a maximum value at the bottom of the cavity to a minimum at the top of the cavity. Since permeance varies with RH, the permeance of the sheathing also varies in accordance

with the RH and vapor pressure profiles. These variables have been incorporated in the CEM calculations to determine the amount of water evacuating by diffusion through the outer layers of the assembly to the outdoor.

The relatively high level of agreement and repeatability in the results between duplicates provides confidence in using the MM and the CEM methods to study the relative drying performance of the different building envelope wall configurations.

### **8.1.2 Experimental innovations**

- The significance of this study arises from the overall management of the experiment in the macro scale that was the result of the combination of well developed aspects in the micro scale. These aspects covered the different protocols that are: the specimens' protocol (Derome and Fazio 2004), the loading protocol (Fazio 2004), and the monitoring protocol (Rao 2004). These protocols were combined with the test methodology and data collection methods to reveal a unique and state-of-the-art experimental method.
- The different wall configurations included in 31 wall assemblies are representative of building envelope systems widely used in North America. This number of assemblies permitted a comparative parametric analysis study for the different wall configurations and to perform a comparative analysis between duplicates to attain a significant and reliable benchmarking data.
- The uniqueness of the assembly instrumentation revealed a state-of-the-art design of data collection points on each assembly: 12 pairs of moisture content pins to measure the moisture content in 12 preset locations, 8 on the sheathing and 4 on the left stud; 17 thermocouples, 12 of them to measure the temperature in the 12 locations of moisture content pins (results from the moisture pins have not been analyzed in this thesis); 1 load cell to monitor the water being evaporated from the water tray; 2 relative humidity sensors; and 25 gravimetric samples to measure the change in moisture content, 18 samples in the sheathing, 5 in the right stud, and 2 samples in the top and bottom plates.

This extensive design of instrumentation was useful to study the hygrothermal performance of the wall assemblies.

- The well developed gravimetric samples protocol including the collection procedure, samples' enclosure, and travel time added reliability to the data generated. The gravimetric samples allowed manual monitoring for the moisture content of the materials surrounding the stud cavity in different locations on a continuous basis.

## **8.2 Limitations and future work**

Some factors affected the data and the analysis in the experiment undertaken to some extent. Factors such as stack effect since the wall assemblies and the duplicates in particular were on different floor levels, the make up of the wall assemblies, air leakage and air movement in the test chamber. Some recommendations could be helpful for future experiments:

- The main air fan in the cold box side caused a slight uneven distribution of temperature as well as causing uneven air distribution. Therefore, modifying the air handling system may improve air and temperature distribution.
- The duplicate wall assemblies should be placed next to each other to make sure they experience the same conditions and to avoid the stack effect.
- As for the make up of the wall assembly, some differences will always occur in the construction. However, these may be minimized with more attention and time given to the assembly of the wall panel.
- All the gravimetric samples should have the same size of 1½" in diameter instead of having both 1" and 1½". The larger size would be easier to make, easier to handle in the collection process, have less risk of broken small pieces, and be better for the analysis. Moreover, the bigger size gravimetric samples would have better fit in the gravimetric sample hole, and this would decrease the air leakage around the sample even though it has a longer perimeter.

- An option to improve the moisture distribution is to increase the number of stud gravimetric samples, especially at the bottom plate, and on the other stud components. The size of the samples could be reconsidered.
- Additional parameters to be studied would include varying stud depth from 2x6 (used in this study) to 2x4, introducing seasonal loadings, and cutting and weighing the wall samples at the end of the test to validate the mapping method described above.
- Since it is not an easy task to monitor the air leakage in the wall assemblies, a practical solution is to use thermographic imaging to monitor the air leakage to some extent as well as monitoring the locations of leakage.

Other recommendations could involve the time and budget constrains:

- The large number of wall assemblies could be reduced to save time and budget. One of the suggestions is to eliminate the wall assemblies without vapor barriers since the wall assemblies with vapor barriers showed a higher potential for moisture accumulation problems. Thus, the study would be focused on the different configurations with vapor barriers.
- The reduction of wall assemblies would give the opportunity to a better use of the instruments such as the RH sensors. The less number of wall assemblies means more sensors in each assembly. 4 relative humidity sensors may be needed in each wall cavity to have more information points that can be used for better analysis for the vapor pressure profiles inside the stud cavity.

### 8.3 Related publications

Alturkistani, A., Fazio, P., Rao, J. & Mao, Q. 2007. A new test method to determine the relative drying capacity of building envelope panels of various configurations. A paper accepted in the *Building and Environment Journal*.

Alturkistani, A., Fazio, P., and Rao, J. 2007. Evacuation profiles due to evaporation of moisture sources in the stud cavity of building envelope panels of various configurations. *IEA Annex 41*, Porto meeting, October 22-24.

Fazio, P., Mao, Q., Ge, H., Alturkistani, A., & Rao, J. 2007. Test method to measure the relative capacity of wall panels to evacuate moisture from their stud cavity. *Journal of Architectural Engineering, ASCE*, 13(4), December.

Fazio, P., Mao, Q., Alturkistani, A., Vera, S., & Rao, J. 2006. Establishing a uniform and measurable moisture source to evaluate the drying capacity of building envelope systems. *Research in Building Physics and Building Engineering: Proceedings of the Third International Conference in Building Physics (IBPC3)*. Montreal, August 27 to 31, pp. 369-377.

Fazio, P., Rao, J., Alturkistani, A., & Ge, H. 2006. Large scale experimental investigation of the relative drying capacity of building envelope panels of various configurations. *Research in Building Physics and Building Engineering: Proceedings of the Third International Conference in building Physics (IBPC3)*. Montreal, August 27-31. pp. 361-368.

## References

- Alturkistani, A., Fazio, P., Rao, J. & Mao, Q. 2007. A new test method to determine the relative drying capacity of building envelope panels of various configurations. A paper submitted to *Building and Environment Journal*.
- Alturkistani, A., Fazio, P., and Rao, J. 2007. Evacuation profiles due to evaporation of moisture sources in the stud cavity of building envelope panels of various configurations. *IEA Annex 41*, Porto meeting, October 22-24.
- ASHRAE. 2001. Handbook of Fundamentals. American Society of Heating, Refrigerating and Air-Conditioning Engineers. Atlanta, GA.
- ASTM. 2000. E331-00. Standard test method for water penetration of exterior windows, curtain walls, and doors by uniform static air pressure difference. *American Society for Testing and Materials*. West Conshohocken, PA, 04(11), pp. 51-54.
- ASTM. 1992. ASTM D4442-92. Standard test method for direct moisture content measurement of wood and wood-base materials. *American Society for Testing and Materials*. West Conshohocken, PA, 05.
- Barrett, D. 1998. The renewal of trust in residential construction: an inquiry into the quality of condominium construction in British Columbia. *Government of the Province of British Columbia*.
- Beaulieu, P., Bomberg, M., Cornick, S., et al. 2002. *Final report from Task 8 of MEWS Project (T8-03) – Hygrothermal response of exterior wall systems to climate loading: methodology and interpretation of results for stucco, EIFS, masonry and siding clad wood-frame walls*. IRC-RR-118. Institute for Research in Construction. National Research Council Canada. Ottawa, Canada.
- Bell, G. 2001. A framework for quantifying the water penetration resistance of exterior wall cladding. *International Conference on Building Envelope Systems and Technologies*. pp. 95-100.
- Bomberg, M. & Brown, W. 1993. Building envelope: Heat, air and moisture interactions. *Journal of Thermal Insulation and Building Envelopes*. Technomic Publishing, Manchester, PA, vol. 16, April, pp. 306-311.
- Brown, W., Adams, P., Tonyan, T. & Ullett, J. 1997. Exterior management in exterior wall claddings. *Journal of Thermal and Building Envelopes*. Technomic Publishing, Manchester, PA, vol. 21, July, pp. 23-43.
- Candanedo, L., Derome, D., and Fazio, P. 2006. Analysis of Montreal 30-year weather data to select loading conditions for large-scale tests on wall panel systems. *Research in Building Physics and Building Engineering: Proceedings of the Third International Conference in Building Physics (IBPC3)*. Montreal, August 27 to 31, pp. 959-966.

Derome, D. & Fazio, P. 2004. Protocol on specimens for the project to develop data on the relationship between measurable, physical building envelope parameters and movement, accumulation and evacuation of moisture in wood-based building envelope systems. NSERC Collaborative Research & Development (CRD) grant. Unpublished internal report, Concordia University, Montreal, Quebec.

Derome, D. & Fazio, P. 1998. Large scale testing of two flat roof assemblies insulated with cellulose. *Journal of Architectural Engineering*, 6(1), pp. 12-23.

Desmarais, G., Derome, D. & Fazio, P. 1998. Experimental set-up for the study of air leakage patterns. *Thermal Performance of the Exterior Envelopes of Buildings VII*, Clearwater Beach, Florida, pp. 99-108.

Desmarais, G. 2000. Impact of added insulation on the hygrothermal performance of leaky exterior wall assemblies. M. A. Sc. Thesis. Concordia University. Montreal, Quebec, Canada.

Djebbar, R. van Reenen, D. & Kumaran, M. 2001. Environmental boundary conditions for long-term hygrothermal calculations. *Performance of Exterior Envelopes of Whole Buildings VIII, Conference Proceedings*, Clearwater Beach, Florida, ASHRAE, Dec. 2-7, 13 p.

Fazio, P., Mao, Q., Ge, H., Alturkistani, A., & Rao, J. 2007. Test method to measure the relative capacity of wall panels to evacuate moisture from their stud cavity. *Journal of Architectural Engineering, ASCE*, 13(4), December.

Fazio, P., Mao, Q., Alturkistani, A., Vera, S., & Rao, J. 2006a. Establishing a uniform and measurable moisture source to evaluate the drying capacity of building envelope systems. *Research in Building Physics and Building Engineering: Proceedings of the Third International Conference in Building Physics (IBPC3)*. Montreal, August 27 to 31, pp. 369-377.

Fazio, P., Rao, J., Alturkistani, A., & Ge, H. 2006b. Large scale experimental investigation of the relative drying capacity of building envelope panels of various configurations. *Research in Building Physics and Building Engineering: Proceedings of the Third International Conference in building Physics (IBPC3)*. Montreal, August 27-31. pp. 361-368.

Fazio, P. 2004. Protocol on loading for the project to develop data on the relationship between measurable, physical building envelope parameters and movement, accumulation and evacuation of moisture in wood-based building envelope systems. NSERC Collaborative Research & Development (CRD) grant. Unpublished internal report, Concordia University, Montreal, Quebec.

Fazio, P., Athienitis, A., Marsh, C., & Rao, J. 1997. Environmental chamber for investigation of building envelope performance. *Journal of Architectural Engineering*. Vol. 3, no. 2, pp. 97-102.

Fazio, P., Derome, D. & Rao, J. 2001. Review and framework for large-scale laboratory studies on wetting and drying of building envelopes. *Canada-Japan Housing R&D Building Envelope Experts Meeting*.

Fazio, P., Derome, D., Gerbasi, D., Athienitis, A., & Depani, S. 1998. Testing of flat roofs insulated with cellulose insulation. *Thermal Performance of the Exterior Envelopes of Buildings VII, Conference Proceedings*, ASHRAE, Clearwater Beach, Florida, Dec. 6-10, pp. 3-13.



Geving, S. & Uvsløk, S. 2000. Moisture Conditions in Timber Frame Roof and Wall Structures. *Test house measurements for verification of heat, air and moisture transfer models. Project Report 273-2000*, BYGGFORSK, and Norwegian Building Research Institute, Oslo, Norway, 50p.

Geving, S. & Thue, J. 1996, Measurements and Computer Simulations of Hygrothermal Performance of Lightweight Roofs, in: Proceedings of the 4th Symposium of Building Physics in Nordic Countries, September 9-10, Espoo, Finland, pp. 541-548.

Geving, S. & Karagiozis, A. 1996, Field Measurements and Computer Simulations of the Hygrothermal Performance of Wood Frame Walls. In: Geving, S. 1997. Moisture Design of Building Constructions, Hygrothermal Analysis Using Simulation Models, Part II: Collection of papers and reports, NTNU Trondheim, Norway, Ph.D. Thesis, June 1997. Faculty of Civil and Environmental Engineering, Department of Building and Construction Engineering, NTNU, Norway.

Handegord, G. 1982. Air leakage, ventilation, and moisture control in buildings. *Moisture Migration in Buildings*, ASTM STP 779. M. Lieff & H. R. Trechsel, Eds., American Society for Testing and Materials, pp. 223-233.

Hazleden, D. & Morris, P. 1999. Designing for Durable Wood Construction: the 4 Ds. *8th International Conference On Durability of Building Materials and Components*, May 30 - June 3, Vancouver, Canada

Hazleden, D. & Morris, P. 2001. The Influence of Design on Drying of Wood-Frame Walls under Controlled Conditions. *Performance of Exterior Envelopes of Whole Buildings VIII: Integration of Building Envelopes, Conference Proceedings, ASHRAE*, Clearwater Beach, Florida, Dec. 2-7, pp. 18.

Hens, H. & Fatin, A. 1995. Heat-air-moisture design of masonry cavity walls: Theoretical and experimental results and practice. *ASHRAE Transactions*, ASHRAE, Atlanta, GA, vol. 101 pt. 1, pp. 607-626.

Hens, H. & Janssens, A. 1998. Application of a new type of air and vapor retarder in a self-drying sloped roof with a cathedral ceiling. *Thermal Performance of the Exterior Envelopes of Buildings VII*, Clearwater Beach, Florida.

Hutcheon, N. & Handegord G. 1983. Building science for a cold climate. NRCC.

Karagiozis, A. & Salonvaara, M. 2001. Hygrothermal system-performance of a whole building. *Building and Environment*, 36(6), 779-787.

Korsgaard, V. & Rode, C. 1992. Laboratory and practical experience with a novel water-permeable vapor retarder. *Thermal Performance of the Exterior Envelopes of Buildings V, Conference Proceedings, ASHRAE*, Clearwater Beach, Florida, Dec. 7-10, pp. 480-490.

Kumaran, M., Lackey, J., Normandin, N., van Reenen, D & Tariku, F. 2002. A thermal and moisture transport property database for common building and insulating materials, *ASHRAE website, Research Project Report 1018-RP*.

Lacasse, M., O'Connor, T., Nunes, S. & Beaulieu, P. 2003. Report from Task 6 of MEWS Project: Experimental Assessment of Water Penetration and Entry into Wood-Frame Wall Specimens-Final Report. Ottawa, Ont.: *National Research Council, Institute for Research in Construction, RR-133*, Feb., 308 p. <http://irc.nrc-cnrc.gc.ca/fulltext/rr133/>

Lawton, M., Brown, W., & Lang, A. 1999. Stucco-Clad Wall Drying Experiment. *Canadian Mortgage and Housing Corporation*, Vancouver, B.C., Research report no. 5972204.00, April.

Lawton, M. & Scott, D. 1995. Envelope durability problems in high-humidity buildings. *Thermal Performance of the Exterior Envelopes of Buildings VI, Conference Proceedings*, ASHRAE, Clearwater Beach, Florida, Dec. 4-8, pp. 197-205.

Mao, Q., Rao, J., & Fazio, P. 2004. Effect of capillary on rainwater penetration in the building envelope. *Originally published in the CIB World Building Congress*, May 2-7, Toronto, Ontario.

Maref, W., Lacasse, M. & Kourglicof, N. 2001. A Precision weighing system for helping assess the hygrothermal response of full-scale wall assemblies. *Performance of Exterior Envelopes of Whole Building VIII: Integration of Building Envelopes*. Clearwater Beach, Florida., pp. 1-7, December 12, 2001 (NRCC-45202).

Maref, W., Lacasse, M. & Booth, D. 2004. Large-scale laboratory measurements and benchmarking of an advanced hygrothermal model. *CIB Conference*, Toronto, Ontario, May 2-7, pp. 1-10.

Morrison Hershfield. 1996. *Survey of building envelope failures in the coastal climate of British Columbia*, Canadian Mortgage and Housing Corporation, Vancouver, B. C.

Morrison Hershfield. 1992. Moisture content in Canadian wood-house construction: Problems, research and practice from 1975-1992, CMHC.

National Building Code of Canada. 1995. *National Research Council of Canada*, Ottawa, Ontario, Canada.

Ogle, R. & O'Connor, J. 1995. Failure of the building envelope: Two case studies. *Thermal Performance of the Exterior Envelopes of Buildings VI, Conference Proceedings*, ASHRAE, Clearwater Beach, Florida, Dec. 4-8, pp. 55-66.

Ojanen, T., Salonvaara, M. & Simonson, C. 2002. Integration of simplified drying tests and numerical simulation in moisture performance analysis of the building envelope. *6th Symposium on Building Physics in the Nordic Countries*. June 17, Trondheim, Norway.

Ojanen, T. 1998. Improving the drying efficiency of timber frame walls in cold climates by using exterior insulation. *Thermal Performance of the Exterior Envelopes of Buildings VII, Conference Proceedings*, ASHRAE, Clearwater Beach, Florida, Dec. 6-10, pp. 155-164.

Rao, J. 2004. Protocol on monitoring in the CRD project excluding mold to develop data on the relationship between measurable, physical building envelope parameters and movement, accumulation and evacuation of moisture in wood-based building envelope systems. NSERC Collaborative Research & Development (CRD) grant. Unpublished internal report, Concordia University, Montreal, Quebec.

Ricketts, D. & Lovatt, J. 1996, Survey of Building Envelope Failures in the Coastal Climate of British Columbia. *Canadian Mortgage and Housing Corporation*, Vancouver, B.C. pp.43.

Schumacher, C., Shi, X., Davidovic, D., Burnett, E. & Straube, J. 2003. Ventilation drying in wall systems. *Proceedings of the Second International Building Physics Conference: Research in Building Physics*, A.A. Balkema Publishers, Leuven, Belgium, September 14-18, pp. 479-486.

Simpson, W. 1998. Equilibrium moisture content of wood in outdoor locations in the United States and worldwide. Res. Note FPL-RN-0268. Madison, WI: U.S. Department of Agriculture, Forest Service, Forest Products Laboratory.

Straube, J., & Burnett, E. 2001. Chapter 5: Overview of Hygrothermal Analysis Methods. ASTM Manual 40-Moisture Analysis and Condensation Control in Building Envelopes, American Society of Testing and Materials, Philadelphia.

Straube, J. 2001. The influence of low-permeance vapor barriers on roof and wall performance. *Thermal Performance of the Exterior Envelopes of Buildings VIII, Conference Proceedings*, ASHRAE, Clearwater Beach, Florida, Dec. 2-7, 12 p.

Teasdale-St-Hilaire. 2006. Hygrothermal performance of different wood-frame wall assemblies wetted by simulated rain infiltration. PhD Thesis, Department of Building, Civil and Environmental Engineering, Concordia University, Montreal, Canada.

Teasdale-St-Hilaire, A., Derome, D. & Fazio, P. 2003. Development of an experimental methodology for the simulation of wetting due to rain infiltration for building envelope testing. *Proceedings of the 2nd International Building Physics Conference*, Balkema, Leuven, Belgium, Sept. 14-18, pp. 455-462.

Teasdale-St-Hilaire, A., Derome, D. & Fazio, P. 2004. Behavior of wall assemblies with different wood sheathings wetted by simulated rain infiltration, *Performance of the Exterior Envelopes of Whole Buildings IX, Conference Proceedings*, ASHRAE, Clearwater Beach, Florida, Dec. 5-10.

Teasdale-St-Hilaire, A., Derome, D. & Fazio, P. 2005. Investigating the role of the vapor retarder in the drying response of wood-frame walls wetted by simulated rain infiltration. *10<sup>th</sup> ICBEST*. May, Ottawa, Ontario.

Teasdale-St-Hilaire, A. & Derome, D. 2005. State-of-the-Art Review of Simulated Rain Infiltration and Environmental Loading for Large-Scale Building Envelope Testing. ASHRAE Trans., vol. 111, pt. 2, paper no. 4821, p. 389-401.

Tsongas, G., Govan, D. & McGillis, J. 1998. Field observations and laboratory tests of water migration in walls with shiplap hardboard siding, *Thermal Envelopes VII/Moisture—Practices*, pp. 469-483.

Tsongas, G. & Olson, J. 1995. Tri State homes: a case study of extensive decay in the walls of older manufactured homes with exterior vapor retarder. *Thermal Performance of the Exterior Envelopes of Buildings VI*, Orlando, Florida, pp. 207-218.

Wu, Y., Kumaran, M., & Fazio, P. 2007. Moisture buffering capacities of five North American building materials. Accepted by the *Journal of Testing and Evaluation*.

## Appendix A

### MEASURED HYGROTHERMAL PROPERTIES OF BUILDING MATERIALS

The measured hygrothermal properties presented in this appendix were carried out by Wu et al (2007).

#### A.1. Hygrothermal Properties of Gypsum Board

**Thickness:**  $(12.60 \pm 0.11)$  mm

**Density:**  $(592 \pm 5)$  kg/m<sup>3</sup>

Table A.1 Thermal conductivity of gypsum board

Specimen thickness (mm)	Hot Surface Temperature (°C)	Cold Surface Temperature (°C)	Mean Temperature (°C)	Conductivity (Wm <sup>-1</sup> K <sup>-1</sup> )
12.43	6.60	-3.14	1.73	0.15
12.43	29.60	19.25	24.43	0.15
12.51	5.27	-3.49	0.89	0.15
12.51	29.59	19.02	24.31	0.14

Table A.2 Results from sorption isotherm measurement of gypsum board

RH, %	Temperature, °C	Moisture Content, kg/kg
100, Vacuum Saturation	Lab at 22 (1)	1.36 (0.12), 29 specimens
96.1 (1)	22.8 (0.1)	0.027 (0.001), 4 specimens
89.2 (1)	23.2 (0.1)	0.014 (0.0002), 4 specimen
70.4 (1)	23.2 (0.1)	0.0082 (0.0001), 4 specimen
50.1 (1)	23.2 (0.1)	0.0048 (0.0001), 4 specimen
33.5 (1)	22.4 (0.1)	0.0035 (0.0001), 4 specimen

Table A.3 Results from desorption isotherm measurement of gypsum board

RH, %	Temperature, °C	Moisture Content, kg/kg
93.8 (1)	23.1 (0.1)	0.126 (0.001), 4 specimens
91.1(1)	23.1 (0.1)	0.028 (0.0002), 4 specimen
70.8 (1)	23.2 (0.1)	0.024 (0.0001), 4 specimen
49.5 (1)	23.3 (0.1)	0.020 (0.0001), 4 specimen
33.1 (1)	22.4 (0.1)	0.019 (0.0001), 4 specimen

Table A.4 Dry cup measurements of gypsum board

Specimen Thickness mm	Chamber RH %	Chamber Temperature °C	WVT Rate kg/s·m <sup>2</sup>
12.62	50.0 (1)	23.2 (0.1)	3.08E-06 (2.8E-08)
12.48	50.0 (1)	23.2 (0.1)	2.94E-06 (1.8E-08)
12.63	50.0 (1)	23.2 (0.1)	2.94E-06 (2.4E-08)
12.62	70.4 (1)	23.1 (0.1)	4.71E-06 (7.1E-08)
12.48	70.4 (1)	23.1 (0.1)	4.53E-06 (5.4E-08)
12.63	70.4 (1)	23.1 (0.1)	4.50E-06 (5.9E-08)
12.62	89.8 (1)	23.1 (0.1)	5.72E-06 (5.7E-08)
12.48	89.7 (1)	23.1 (0.1)	5.57E-06 (3.9E-08)
12.63	89.8 (1)	23.1 (0.1)	5.46E-06 (1.1E-08)

Table A.5 Wet cup measurements of gypsum board

Specimen Thickness mm	Chamber RH %	Chamber Temperature °C	WVT Rate kg/s·m <sup>2</sup>
12.46	70.5 (1)	23.1 (0.1)	2.28E-06 (2.1E-09)
12.55	70.5 (1)	23.1 (0.1)	2.28E-06 (3.2E-09)
12.48	70.5 (1)	23.1 (0.1)	2.34E-06 (8.3E-09)
12.46	89.7 (1)	23.1 (0.1)	1.06E-06 (1.6E-08)

12.55	89.7 (1)	23.1 (0.1)	1.12E-06 (1.5E-08)
12.48	89.7 (1)	23.1 (0.1)	1.10E-06 (9.8E-09)

Table A.6 Derived water vapor permeability of gypsum board

RH %	Permeability kg/m·s·Pa	RH %	Permeability kg/m·s·Pa
10	3.00E-11	60	3.94E-11
20	3.17E-11	70	4.17E-11
30	3.34E-11	80	4.42E-11
40	3.53E-11	90	4.68E-11
50	3.73E-11	100	4.96E-11

Table A.7 Water absorption of gypsum board

Square Root of Time, s <sup>1/2</sup>	Water Absorption Kg/m <sup>2</sup>
7.8	0.08 (0.04)
13.4	0.27 (0.11)
19.0	1.00 (0.28)
23.2	1.55 (0.40)
26.8	2.17 (0.48)
30.0	2.80 (0.59)
32.9	3.14 (0.61)
35.5	3.51 (0.64)
40.3	4.02 (0.60)
44.5	4.33 (0.45)
50.2	4.62 (0.27)
55.3	4.80 (0.22)
66.2	5.08 (0.22)
78.6	5.36 (0.23)

Through the linear regression of the first linear part of the absorption curve, the absorption coefficient of gypsum board is calculated, and the value is  $0.16 \pm 0.04 \text{ kg/m}^2\text{s}^{1/2}$ .

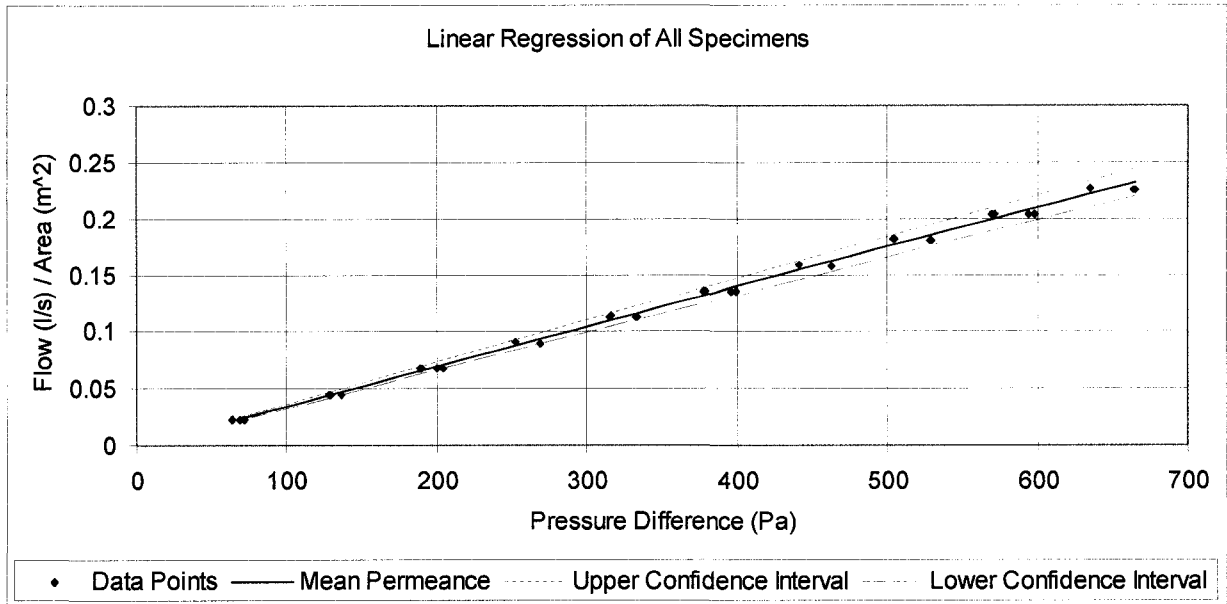


Figure A.1 The dependence of airflow rate on pressure difference for gypsum board

At the range of pressure differences from 100 to 700 Pa, the flow rate varies with pressure difference.

The air permeability of gypsum board under test is  $(5.2 \pm 0.3) \text{ E-08 kg/m}\cdot\text{Pa}\cdot\text{s}$ .

## A.2. Hygrothermal Properties of Oriented Strand Board

**Thickness:**  $(11.64 \pm 0.72)$  mm

**Density:**  $(664 \pm 46)$  kg/m<sup>3</sup>

Table A.8 Thermal conductivity of OSB

Specimen thickness (mm)	Hot Surface Temperature (°C)	Cold Surface Temperature (°C)	Mean Temperature (°C)	Conductivity (Wm <sup>-1</sup> K <sup>-1</sup> )
11.41	12.10	0.26	6.18	0.087
11.41	31.89	18.54	25.21	0.091
11.37	12.08609	0.366293	6.23	0.088
11.37	31.82672	18.57836	25.20	0.091

Table A.9 Results from sorption isotherm measurement of OSB

RH, %	Temperature, °C	Moisture Content, kg/kg
96.1 (1)	22.8 (0.1)	0.25 (0.02), 4 specimens
89.2 (1)	23.2 (0.1)	0.16 (0.002), 4 specimen
70.4 (1)	23.2 (0.1)	0.11 (0.002), 4 specimen
50.1 (1)	23.2 (0.1)	0.062 (0.0003), 3 specimen
33.5 (1)	22.5 (0.1)	0.047 (0.001), 4 specimen

Table A.10 Results from desorption isotherm measurement of OSB

RH, %	Temperature, °C	Moisture Content, kg/kg
100, Vacuum Saturation	Lab at 22 (1)	1.36 (0.12), 29 specimens
93.7 (1)	23.1 (0.1)	0.25 (0.008), 4 specimens
91.2 (1)	23.0 (0.1)	0.19 (0.002), 4 specimen
70.4 (1)	23.1 (0.1)	0.12 (0.002), 4 specimen
49.7 (1)	23.3 (0.1)	0.084 (0.001), 3 specimen
32 (1)	22.4 (0.1)	0.058 (0.001), 4 specimen



Table A.11 Dry cup measurements of OSB

Specimen Thickness mm	Chamber RH %	Chamber Temperature °C	WVT Rate kg/s·m <sup>2</sup>
11.54	49.95 (1)	23.25 (0.1)	8.60E-05 (1.75E-06)
11.65	49.95 (1)	23.25 (0.1)	1.07E-04 (1.87E-06)
11.59	49.95 (1)	23.25 (0.1)	1.02E-04 (1.91E-06)
11.54	70.38 (1)	23.21 (0.1)	1.69E-04 (1.81E-06)
11.65	70.38 (1)	23.21 (0.1)	1.99E-04 (1.88E-06)
11.59	70.38 (1)	23.21 (0.1)	1.87E-04 (2.18E-06)
11.54	89.88 (1)	23.07 (0.1)	2.03E-04 (4.10E-06)
11.65	89.88 (1)	23.07 (0.1)	2.27E-04 (2.73E-06)
11.59	89.88 (1)	23.07 (0.1)	2.20E-04 (4.58E-06)

Table A.12 Wet cup measurements of OSB

Specimen Thickness mm	Chamber RH %	Chamber Temperature °C	WVT Rate kg/s·m <sup>2</sup>
11.54	70.38	23.18	3.12E-04 (3.09E-06)
11.65	70.38	23.18	2.43E-04 (4.18E-06)
11.59	70.38	23.18	1.82E-04 (5.52E-06)
11.54	89.88	23.06	3.23E-04 (5.48E-06)
11.65	89.88	23.06	2.90E-04 (5.53E-06)
11.59	89.88	23.06	2.58E-04 (5.68E-06)

Table A.13 Derived water vapor permeability for OSB

RH %	Permeability kg/m·s·Pa	RH %	Permeability kg/m·s·Pa
10	2.95E-13	60	1.46E-12
20	4.05E-13	70	2.01E-12
30	5.58E-13	80	2.78E-12
40	7.67E-13	90	3.85E-12
50	1.06E-12	100	5.35E-12

Table A.14 Water absorption of OSB

Square Root of Time, s <sup>1/2</sup>	Water Absorption Kg/m <sup>2</sup>
7.7	0.020 (0.002)
13.4	0.030 (0.002)
17.3	0.037 (0.002)
20.5	0.045 (0.004)
24.5	0.050 (0.005)
30.0	0.061 (0.59)
34.6	0.074 (0.008)
38.7	0.078 (0.007)
42.4	0.082 (0.008)
49.0	0.094 (0.007)
54.8	0.103 (0.008)
60.0	0.111 (0.008)
64.8	0.118 (0.011)
81.2	0.141 (0.014)
94.9	0.166 (0.016)
112.2	0.194 (0.021)
135.7	0.237 (0.028)
155.9	0.275 (0.034)
291.4	0.686 (0.109)
312.8	0.754 (0.115)

Through the linear regression of the first linear part of the absorption curve, the absorption coefficient of OSB is calculated, and the value is  $0.0018 \pm 0.0002 \text{ kg/m}^2\text{s}^{1/2}$ .

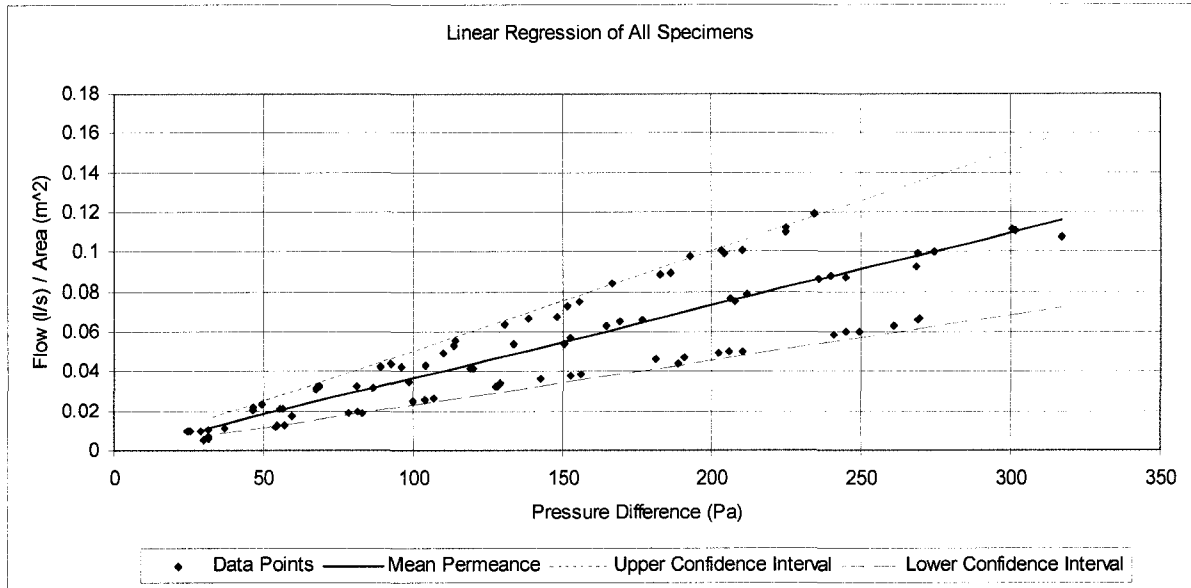


Figure A.2 The dependence of airflow rate on pressure difference for OSB

At the range of pressure differences from 20 to 300 Pa, the flow rate varies with pressure difference.

The air permeability of gypsum board under test is  $(5.1 \pm 1.9) \text{ E-}09 \text{ kg/m}\cdot\text{Pa}\cdot\text{s}$ .

### A.3. Hygrothermal Properties of Plywood

**Thickness:**  $(12.57 \pm 0.37)$  mm

**Density:**  $(456 \pm 30)$  kg/m<sup>3</sup>

Table A.15 Thermal conductivity of plywood

Specimen thickness (mm)	Hot Surface Temperature (°C)	Cold Surface Temperature (°C)	Mean Temperature (°C)	Conductivity (Wm <sup>-1</sup> K <sup>-1</sup> )
12.69	2.86	-3.51	-0.32	0.084
12.69	32.51	19.62	26.07	0.089
12.49	2.86	-3.68	-0.41	0.081
12.49	31.81	19.70	13.11	0.086

Table A.16 Results from adsorption isotherm measurement of plywood

RH, %	Temperature, °C	Moisture Content, kg/kg
100, Vacuum Saturation	Lab at 22 (1)	1.29 (0.11), 29 specimens
96.2 (1)	22.7 (0.1)	0.28 (0.027), 4 specimens
89.2 (1)	23.2 (0.1)	0.17 (0.005), 4 specimen
70.5 (1)	23.2 (0.1)	0.12 (0.002), 4 specimen
50.1 (1)	23.2 (0.1)	0.072 (0.0003), 4 specimen
33.5 (1)	22.5 (0.1)	0.058 (0.0003), 4 specimen

Table A.17 Results from desorption isotherm measurement of plywood

RH, %	Temperature, °C	Moisture Content, kg/kg
93.7 (1)	23.1 (0.1)	0.27 (0.005), 4 specimens
90.0 (1)	22.9 (0.1)	0.20 (0.001), 4 specimen
70.4 (1)	23.1 (0.1)	0.14 (0.001), 4 specimen
49.7 (1)	23.3 (0.1)	0.095 (0.002), 4 specimen
33.0 (1)	22.4 (0.1)	0.066 (0.001), 4 specimen

Table A.18 Dry cup measurements of plywood

Specimen Thickness mm	Chamber RH %	Chamber Temperature °C	WVT Rate kg/s·m <sup>2</sup>
13.04	49.98 (1)	23.21 (0.1)	8.69E-08 (1.07E-09)
13.15	49.98 (1)	23.21 (0.1)	1.41E-07 (3.02E-10)
12.08	49.98 (1)	23.21 (0.1)	6.67E-08 (4.09E-10)
13.04	70.40 (1)	23.15 (0.1)	1.83E-07 (9.58E-10)
13.15	70.40 (1)	23.15 (0.1)	2.94E-07 (4.52E-09)
12.08	70.40 (1)	23.15 (0.1)	1.69E-07 (9.75E-10)
13.04	89.15 (1)	23.18 (0.1)	3.63E-07 (6.05E-09)
13.15	89.15 (1)	23.18 (0.1)	4.97E-07 (1.00E-08)
12.08	89.15 (1)	23.18 (0.1)	3.72E-07 (4.59E-09)

Table A.19 Wet cup measurements of plywood

Specimen Thickness mm	Chamber RH %	Chamber Temperature °C	WVT Rate kg/s·m <sup>2</sup>
12.18	70.36 (1)	23.13 (0.1)	6.13E-07 (5.51E-09)
12.09	70.36 (1)	23.13 (0.1)	6.12E-07 (8.65E-09)
12.06	70.36 (1)	23.13 (0.1)	5.19E-07 (9.87E-09)
12.18	89.08 (1)	23.19 (0.1)	4.57E-07 (7.02E-09)
12.09	89.08 (1)	23.19 (0.1)	4.76E-07 (5.68E-09)
12.06	89.08 (1)	23.19 (0.1)	3.95E-07 (4.66E-09)

Table A.20 Derived water vapor permeability for plywood

RH %	Permeability kg/m·s·Pa	RH %	Permeability kg/m·s·Pa
10	1.01E-13	60	1.86E-12
20	1.80E-13	70	3.37E-12
30	3.22E-13	80	6.18E-12
40	5.77E-13	90	1.16E-11
50	1.03E-12	100	2.26E-11

Table A.21 Water absorption of plywood

Square Root of Time, s <sup>1/2</sup>	Water Absorption Kg/m <sup>2</sup>
7.8	0.026 (0.004)
11.0	0.042 (0.004)
15.5	0.055(0.018)
20.5	0.065 (0.038)
24.5	0.075 (0.041)
27.9	0.081 (0.047)
32.9	0.089 (0.055)
37.2	0.099 (0.061)
44.5	0.115 (0.073)
52.0	0.129 (0.082)
60.0	0.143 (0.090)
64.3	0.152 (0.097)
73.1	0.169 (0.110)
89.7	0.195 (0.125)
109.5	0.239(0.147)
127.0	0.275 (0.160)
150.6	0.343 (0.170)
168.6	0.406 (0.191)
295.4	1.018 (0.533)
309.4	1.095 (0.563)
323.2	1.174 (0.588)
336.3	1.260 (0.599)

Through the linear regression of the first linear part of the absorption curve, the absorption coefficient of plywood is calculated, and the value is  $0.0020 \pm 0.0013 \text{ kg/m}^2\text{s}^{1/2}$ .

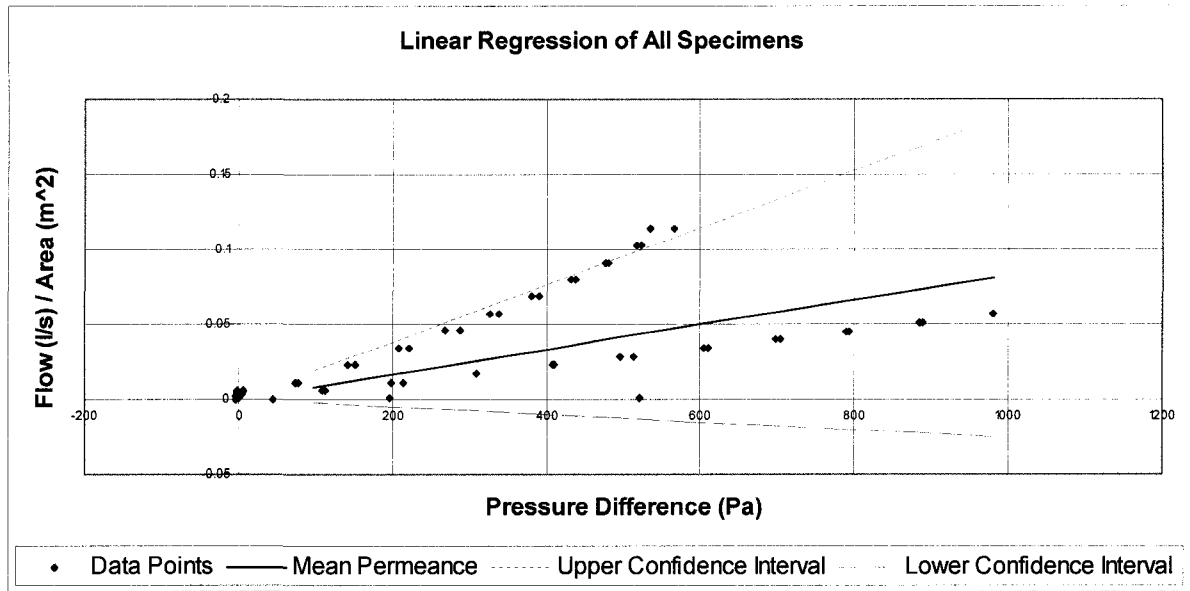


Figure A.3 The dependence of airflow rate on pressure difference for plywood

At the range of pressure differences from 20 to 1000 Pa, the flow rate varies with pressure difference.

The air permeability of gypsum board under test is  $(1.3 \pm 1.7) \text{ E-}09 \text{ kg/m}\cdot\text{Pa}\cdot\text{s}$ .

#### A.4. Hygrothermal Properties of wood fiberboard

**Thickness:**  $(10.84 \pm 0.11) \text{ mm}$

**Density:**  $(279 \pm 3) \text{ kg/m}^3$

Table A.22 Thermal conductivity of fiberboard

Specimen thickness (mm)	Hot Surface Temperature (°C)	Cold Surface Temperature (°C)	Mean Temperature (°C)	Conductivity ( $\text{Wm}^{-1}\text{K}^{-1}$ )
10.66	4.62	-2.94	0.84	0.0457
10.66	14.90	7.17	11.03	0.0463
10.72	15.67	7.22	11.44	0.0471
10.72	32.01	17.86	24.93	0.0485

Table A.23 Results from sorption isotherm measurement of fiberboard

RH, %	Temperature, °C	Moisture Content, kg/kg
100, Vacuum Saturation	Lab at 22 (1)	3.597 (0.046), 29 specimens
96.2 (1)	22.7 (0.1)	0.276 (0.027), 4 specimens
89.2 (1)	23.2 (0.1)	0.174 (0.005), 4 specimen
70.5 (1)	23.2 (0.1)	0.119 (0.002), 4 specimen
50.1 (1)	23.2 (0.1)	0.072 (0.0003), 4 specimen
33.5 (1)	22.5 (0.1)	0.058 (0.0003), 4 specimen

Table A.24 Results from desorption isotherm measurement of fiberboard

RH, %	Temperature, °C	Moisture Content, kg/kg
93.7 (1)	23.1 (0.1)	0.297 (0.01)
91.2 (1)	23.0 (0.1)	0.188 (0.002)
70.4 (1)	23.1 (0.1)	0.120 (0.001)
49.5 (1)	23.2 (0.1)	0.083 (0.001)
33.0 (1)	22.4 (0.1)	0.055 (0.001)

Table A.25 Dry cup measurements of fiberboard

Specimen Thickness mm	Chamber RH %	Chamber Temperature °C	WVT Rate kg/s·m <sup>2</sup>
11.00	50.05 (1)	23.20 (0.1)	2.00E-06 (1.28E-08)
11.11	50.05 (1)	23.20 (0.1)	2.06E-06 (1.93E-08)
11.02	50.05 (1)	23.20 (0.1)	2.12E-06 (2.11E-08)
11.00	70.39 (1)	23.15 (0.1)	2.78E-06 (7.71E-09)
11.11	70.39 (1)	23.15 (0.1)	2.87E-06 (8.98E-09)
11.02	70.39 (1)	23.15 (0.1)	2.94E-06 (8.51E-09)
11.00	89.74 (1)	23.07 (0.1)	3.70E-06 (2.27E-08)
11.11	89.74 (1)	23.07 (0.1)	3.79E-06 (2.99E-08)
11.02	89.74 (1)	23.07 (0.1)	3.84E-06 (2.76E-08)



Table A.26 Wet cup measurements of fiberboard

Specimen Thickness mm	Chamber RH %	Chamber Temperature °C	WVT Rate kg/s·m <sup>2</sup>
10.94	70.46	23.10	1.25E-06 (2.16E-08)
10.93	70.46	23.10	1.24E-06 (1.81E-08)
11.00	70.46	23.10	1.28E-06 (2.05E-08)
10.94	89.52	23.11	5.09E-07 (1.23E-08)
10.93	89.52	23.11	5.13E-07 (1.22E-08)
11.00	89.52	23.11	5.11E-07 (1.48E-08)

Table A.27 Derived water vapor permeability for fiberboard

RH %	Permeability kg/m·s·Pa	RH %	Permeability kg/m·s·Pa
10	1.82E-11	60	1.88E-11
20	1.85E-11	70	1.89E-11
30	1.86E-11	80	1.89E-11
40	1.87E-11	90	1.89E-11
50	1.88E-11	100	1.89E-11

Table A.28 Water absorption of fiberboard

Square Root of Time, s <sup>1/2</sup>	Water Absorption Kg/m <sup>2</sup>
7.75	0.012 (0.006)
13.42	0.022 (0.008)
18.97	0.028 (0.008)
25.69	0.035 (0.008)
35.50	0.042 (0.008)
43.13	0.049 (0.010)
55.32	0.065 (0.009)

70.57	0.084 (0.010)
84.14	0.106 (0.011)
94.55	0.129 (0.015)
112.78	0.183 (0.029)
129.38	0.255 (0.046)
148.19	0.353 (0.069)
161.37	0.428 (0.078)

Through the linear regression of the first linear part of the absorption curve, the absorption coefficient of plywood is calculated, and the value is  $0.0012 \pm 0.0001 \text{ kg/m}^2\text{s}^{1/2}$ .

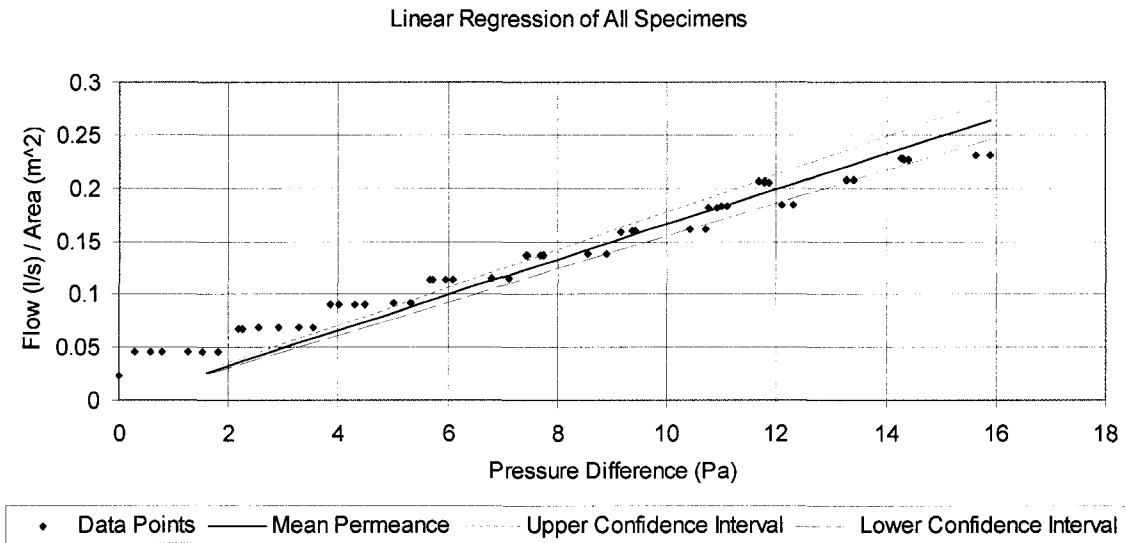


Figure A.4 The dependence of airflow rate on pressure difference for fiberboard

At the range of pressure differences from 0 to 16 Pa, the flow rate of all test specimens linearly varies with the pressure difference. The air permeability of fiberboard under test is  $(2.2 \pm 0.2) \text{ E-07 kg/m}\cdot\text{Pa}\cdot\text{s}$ .

### A.5. Hygrothermal Properties of spruce wood stud

**Density:**  $(465 \pm 20) \text{ kg/m}^3$

Table A.29 Thermal conductivity of spruce wood stud

Specimen thickness (mm)	Hot Surface Temperature (°C)	Cold Surface Temperature (°C)	Mean Temperature (°C)	Conductivity ( $\text{Wm}^{-1}\text{K}^{-1}$ )
37.48	12.25	-2.69	4.78	0.095
37.48	34.89	15.27	25.08	0.099
37.45	14.64	-2.33	6.16	0.096
37.45	34.90	15.32	25.11	0.098

Table A.30 Results from sorption isotherm measurement of spruce wood stud

RH, %	Temperature, °C	Moisture Content, kg/kg
93.7 (1)	23.1 (0.1)	0.24 (0.006), 4 specimens
91.2 (1)	23.0 (0.1)	0.17 (0.002), 4 specimens
70.4 (1)	23.2 (0.1)	0.12 (0.001), 4 specimens
49.7 (1)	23.1 (0.1)	0.08 (0.0005), 4 specimens
33.1 (1)	22.4 (0.1)	0.054 (0.001), 4 specimens

Table A.31 Results from desorption isotherm measurement of spruce wood stud

RH, %	Temperature, °C	Moisture Content, kg/kg
100, Vacuum Saturation	Lab at 22 (1)	1.57 (0.13), 29 specimens
93.7 (1)	23.1 (0.1)	0.28 (0.03), 4 specimens
90.0 (1)	23.2 (0.1)	0.19 (0.004), 4 specimens
70.4 (1)	23.1 (0.1)	0.14 (0.002), 4 specimens
49.9 (1)	23.3 (0.1)	0.10 (0.001), 4 specimens
33.1 (1)	22.4 (0.1)	0.071 (0.001), 4 specimens

Table A.32 Dry cup measurements of spruce wood stud

Specimen Thickness mm	Chamber RH %	Chamber Temperature °C	WVT Rate kg/s·m <sup>2</sup>
38.48	50.06	23.30	5.41E-08 (5.91E-10)
38.35	50.06	23.30	4.03E-08 (6.06E-10)
38.05	50.06	23.30	3.89E-08 (5.77E-10)
38.48	70.59	23.19	1.02E-07 (7.38E-10)
38.35	70.59	23.19	8.62E-08 (7.91E-10)
38.05	70.59	23.19	8.94E-08 (1.76E-09)
38.48	90.82	22.99	2.36E-07 (3.42E-09)
38.35	90.82	22.99	2.12E-07 (2.57E-09)
38.05	90.82	22.99	2.29E-07 (3.48E-09)

Table A.33 Wet cup measurements of spruce wood stud

Specimen Thickness mm	Chamber RH %	Chamber Temperature °C	WVT Rate kg/s·m <sup>2</sup>
38.90	70.54	23.23	3.00E-07 (4.68E-09)
38.63	70.54	23.23	2.74E-07 (4.63E-09)
38.75	70.54	23.23	2.81E-07 (3.97E-09)
38.90	90.82	23.00	2.25E-07 (4.14E-09)
38.63	90.82	23.00	2.45E-07 (4.45E-09)
38.75	90.82	23.00	2.04E-07 (5.60E-08)

Table A.34 Derived water vapor permeability for spruce wood stud

RH %	Permeability kg/m·s·Pa	RH %	Permeability kg/m·s·Pa
10	2.92E-13	60	3.23E-12

20	5.05E-13	70	5.32E-12
30	8.02E-13	80	9.00E-12
40	1.26E-12	90	1.56E-11
50	2.00E-12	100	2.81E-11

Table A.35 Water absorption of spruce stud

Square Root of Time $s^{1/2}$	Water Absorption (Average of 4 specimens) $Kg/m^2$
7.7	0.34 (0.03)
15.5	0.38 (0.02)
20.5	0.45 (0.03)
24.5	0.53 (0.03)
30.0	0.58 (0.05)
34.6	0.64 (0.03)
38.7	0.68 (0.03)
42.4	0.75 (0.04)
49.0	0.83 (0.03)
60.0	0.95 (0.05)
73.5	1.07 (0.05)
84.9	1.20 (0.03)
94.9	1.31 (0.03)
112.2	1.54 (0.04)
127.3	1.69 (0.05)
140.7	1.86 (0.04)
153.0	2.02 (0.05)
296.0	3.89 (0.01)
302.3	3.97 (0.05)
325.2	4.36 (0.05)
723.0	5.11 (0.30)

Through the linear regression of the first linear part of the absorption curve, the absorption coefficient of spruce is calculated, and the value is  $0.0124 \pm 0.0001 \text{ kg/m}^2\text{s}^{1/2}$ .

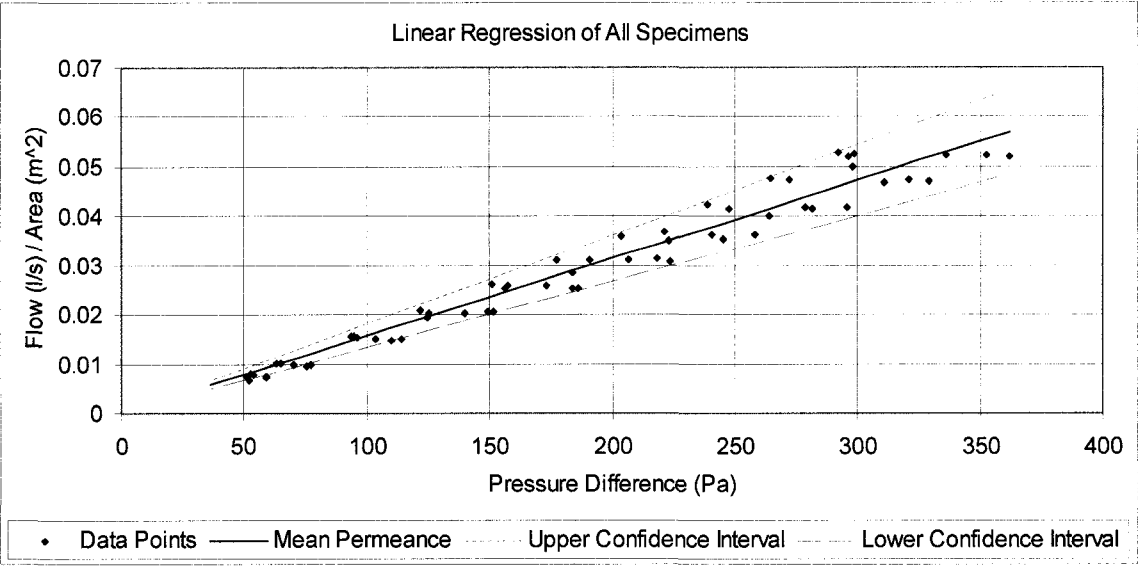


Figure A.5 The dependence of airflow rate on pressure difference for spruce stud

At the range of pressure differences from 50 to 350 Pa, the flow rate of two specimens increases with the pressure difference. The air permeability of spruce stud under test is  $(7.2 \pm 1.0) \text{ E-9 kg/m} \cdot \text{Pa} \cdot \text{s}$ .

## A.6. Hygrothermal Properties of extruded polystyrene foam sheathing

**Density:**  $(27.2 \pm 0.5) \text{ kg/m}^3$

**Thickness:**  $(26.3 \pm 0.7) \text{ mm}$

Table A.36 Thermal conductivity of EPS

Specimen thickness (mm)	Hot Surface Temperature (°C)	Cold Surface Temperature (°C)	Mean Temperature (°C)	Conductivity ( $\text{Wm}^{-1}\text{K}^{-1}$ )
25.88	16.29	-6.17	5.61	0.0258
25.88	34.60	13.47	24.04	0.0279
26.51	14.89	-4.99	4.95	0.0259
26.51	36.41	15.80	26.11	0.0280

Table A.36 Results from sorption isotherm measurement of EPS

RH, %	Temperature, °C	Moisture Content, kg/kg
96.2 (1)	22.7 (0.1)	0.003 (0.001), 3 specimens
89.2 (1)	23.2 (0.1)	0.003 (0.001), 3 specimens
70.3 (1)	23.2 (0.1)	0.003 (0.001), 3 specimens
50.1 (1)	23.2 (0.1)	0.002 (0.002), 3 specimens
33.2 (1)	22.4 (0.1)	0.002 (0.001), 3 specimens

Table A.37 Dry cup measurements of EPS

Specimen Thickness mm	Chamber RH %	Chamber Temperature °C	WVT Rate $\text{kg/s}\cdot\text{m}^2$
26.64	50.16 (1)	23.30 (0.1)	5.34E-08 (9.39E-10)
25.67	50.16 (1)	23.30 (0.1)	5.59E-08 (6.44E-10)
25.67	50.16 (1)	23.30 (0.1)	5.52E-08 (7.68E-10)
26.64	70.90 (1)	23.24 (0.1)	8.28E-08 (1.19E-09)
25.67	70.90 (1)	23.24 (0.1)	8.29E-08 (1.13E-09)
25.67	70.90 (1)	23.24 (0.1)	8.30E-08 (1.77E-09)

26.64	90.83 (1)	23.04 (0.1)	1.03E-07 (1.97E-09)
25.67	90.83 (1)	23.04 (0.1)	1.04E-07 (7.98E-10)
25.67	90.83 (1)	23.04 (0.1)	1.02E-07 (1.52E-09)

Table A.38 Wet cup measurements of EPS

Specimen Thickness mm	Chamber RH %	Chamber Temperature °C	WVT Rate kg/s·m <sup>2</sup>
26.64	70.40 (1)	23.00 (0.1)	3.26E-08 (6.37E-10)
25.67	70.40 (1)	23.00 (0.1)	3.27E-08 (4.82E-10)
25.67	70.40 (1)	23.00 (0.1)	3.37E-08 (2.40E-10)
26.64	91.18 (1)	22.98 (0.1)	1.09E-08 (1.94E-10)
25.67	91.18 (1)	22.98 (0.1)	1.05E-08 (2.92E-10)
25.67	91.18 (1)	22.98 (0.1)	1.02E-08 (3.58E-10)

Table A.39 Derived water vapor permeability for EPS

RH %	Permeability kg/m·s·Pa	RH %	Permeability kg/m·s·Pa
10	1.03E-12	60	1.08E-12
20	1.04E-12	70	1.09E-12
30	1.05E-12	80	1.10E-12
40	1.06E-12	90	1.11E-12
50	1.07E-12	100	1.12E-12

Extruded polystyrene foam sheathing has very low water absorption rate. Therefore, the partial immersion test of this material is hard to carry out. In addition, the test specimens are impermeable and no measurable airflow obtained for pressure differences up to several kPa.



## A.7. Hygrothermal Properties of Asphalt Impregnated Paper

**Density:**  $(1033 \pm 17) \text{ kg/m}^3$

**Thickness:**  $(0.64 \pm 0.016) \text{ mm}$

Table A.40 Dry cup measurements of asphalt impregnated paper

Specimen Thickness mm	Chamber RH %	Chamber Temperature °C	WVT Rate kg/s·m <sup>2</sup>
0.65	50.10	23.31	6.24E-08 (1.20E-09)
0.63	50.10	23.31	7.40E-08 (1.14E-09)
0.62	50.10	23.31	1.44E-07 (1.43E-09)
0.65	70.50	23.26	1.11E-07 (1.57E-09)
0.63	70.50	23.26	1.29E-07 (1.23E-09)
0.62	70.50	23.26	2.40E-07 (2.01E-09)
0.65	90.50	23.13	2.62E-07 (1.17E-09)
0.63	90.50	23.13	2.81E-07 (8.06E-10)
0.62	90.50	23.13	4.25E-07 (1.22E-09)

Table A.41 Wet cup measurements of asphalt impregnated paper

Specimen Thickness mm	Chamber RH %	Chamber Temperature °C	WVT Rate kg/s·m <sup>2</sup>
26.64	70.30	23.25	4.47E-07 (3.85E-09)
25.67	70.30	23.25	4.41E-07 (4.79E-09)
25.67	70.30	23.25	4.90E-07 (5.80E-09)
26.64	89.77	23.21	3.36E-07 (5.14E-09)
25.67	89.77	23.21	3.44E-07 (4.94E-09)
25.67	89.77	23.21	3.69E-07 (6.60E-09)

Table A.42 Derived water vapor permeability for asphalt impregnated paper

RH	Permeability	RH	Permeability
%	kg/m·s·Pa	%	kg/m·s·Pa
10	8.54E-16	60	2.82E-14
20	1.72E-15	70	5.70E-14
30	3.45E-15	80	1.16E-13
40	6.95E-15	90	2.38E-13
50	1.40E-14	100	4.99E-13

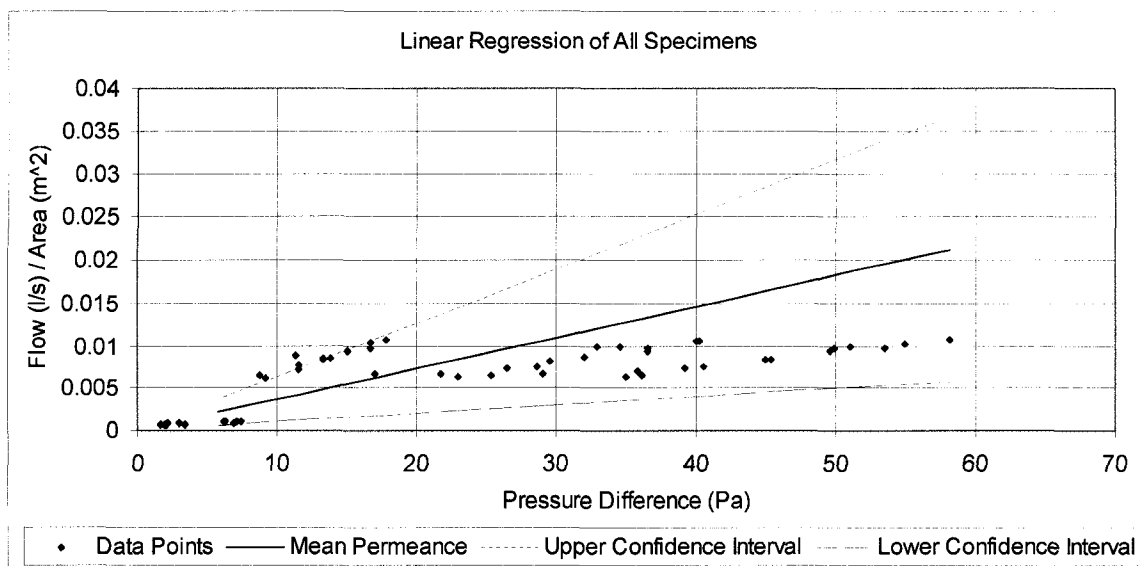


Figure A.6 The dependence of airflow rate on pressure difference for asphalt impregnated paper

At the range of pressure differences from 1 to 60 Pa, the flow rate of asphalt impregnated paper increases with the pressure difference. The air permeability of asphalt impregnated paper under test is  $(2.7 \pm 1.9) \text{ E-10 kg/m}\cdot\text{Pa}\cdot\text{s}$ .

## A.8. Hygrothermal Properties of Stucco

**Density:**  $(1411.98 \pm 65) \text{ kg/m}^3$

**Thickness:**  $(19.56 \pm 0.78) \text{ mm}$

Table A.43 Thermal Conductivity of Stucco

Specimen thickness (mm)	Hot Surface Temperature (°C)	Cold Surface Temperature (°C)	Mean Temperature (°C)	Conductivity ( $\text{Wm}^{-1}\text{K}^{-1}$ )
19.23	26.44	23.30	24.87	0.336
19.23	4.39	2.14	3.27	0.322
19.03	26.63	23.39	25.01	0.334
19.03	5.60	3.09	4.39	0.322

Table A.44 Results from sorption isotherm measurement of stucco

RH, %	Temperature, °C	Moisture Content, kg/kg
93.1 (1)	23.0 (0.1)	0.059 (0.001), 3 specimens
89.7 (1)	23.0 (0.1)	0.049 (0.001), 3 specimen
70.0 (1)	22.9 (0.1)	0.024 (0.004), 3 specimen
50.3 (1)	22.9 (0.1)	0.013 (0.0003), 3 specimen

Table A.45 Results from desorption isotherm measurement of stucco

RH, %	Temperature, °C	Moisture Content, kg/kg
100, Vacuum Saturation	Lab at 22 (1)	0.21 (0.01), 29 specimens
93.4 (1)	23.0 (0.1)	0.058 (0.001)
88.9 (1)	23.0 (0.1)	0.055 (0.002)
70.2 (1)	23.0 (0.1)	0.033 (0.0004)
50.3 (1)	23.0 (0.1)	0.022 (0.003)

Table A.46 Dry cup measurements of stucco

Specimen Thickness mm	Chamber RH %	Chamber Temperature °C	WVT Rate kg/s·m <sup>2</sup>
15.75	49.87	23.08	9.68E-07(3.29E-09)
15.28	49.87	23.08	1.04E-06(5.06E-09)
15.63	49.87	23.08	9.30E-07(4.29E-09)
15.75	70.40	23.10	1.42E-06(3.51E-09)
15.28	70.40	23.10	1.51E-06(1.04E-09)
15.63	70.40	23.10	1.36E-06(5.24E-09)
15.75	89.42	22.88	1.95E-06(1.78E-08)
15.28	89.42	22.88	2.11E-06(1.93E-08)
15.63	89.42	22.88	1.90E-06(2.18E-08)

Table A.47 Wet cup measurements of stucco

Specimen Thickness mm	Chamber RH %	Chamber Temperature °C	WVT Rate kg/s·m <sup>2</sup>
14.06	70.53	23.04	9.39E-07(6.10E-09)
13.96	70.53	23.04	9.82E-07(4.81E-09)
15.53	70.53	23.04	7.03E-07(2.72E-09)
14.06	87.82	23.12	2.49E-07(4.53E-09)
13.96	87.82	23.12	2.81E-07(5.12E-09)
15.53	87.82	23.12	1.57E-07(2.83E-09)

Table A.48 Derived water vapor permeability for stucco

RH %	Permeability kg/m·s·Pa	RH %	Permeability kg/m·s·Pa
10	1.27E-11	60	1.83E-11
20	1.37E-11	70	1.97E-11
30	1.47E-11	80	2.12E-11
40	1.58E-11	90	2.29E-11
50	1.7E-11	100	2.47E-11

Table A.49 Water absorption of stucco

Square Root of Time $s^{1/2}$	Water Absorption (Average of 4 specimens) $Kg/m^2$
7.75	0.68(0.17)
13.42	0.88(0.22)
17.32	1.01(0.26)
20.49	1.10(0.31)
23.24	1.18(0.33)
26.83	1.28(0.37)
30.00	1.35(0.39)
34.64	1.45(0.43)
38.73	1.54(0.46)
45.83	1.69(0.51)
51.96	1.80(0.55)
57.45	1.89(0.58)
62.45	1.97(0.60)
67.08	2.05(0.62)

Through the linear regression of the first linear part of the absorption curve, the absorption coefficient of stucco is calculated, and the value is  $0.088 \pm 0.022 \text{ kg/m}^2\text{s}^{1/2}$ .

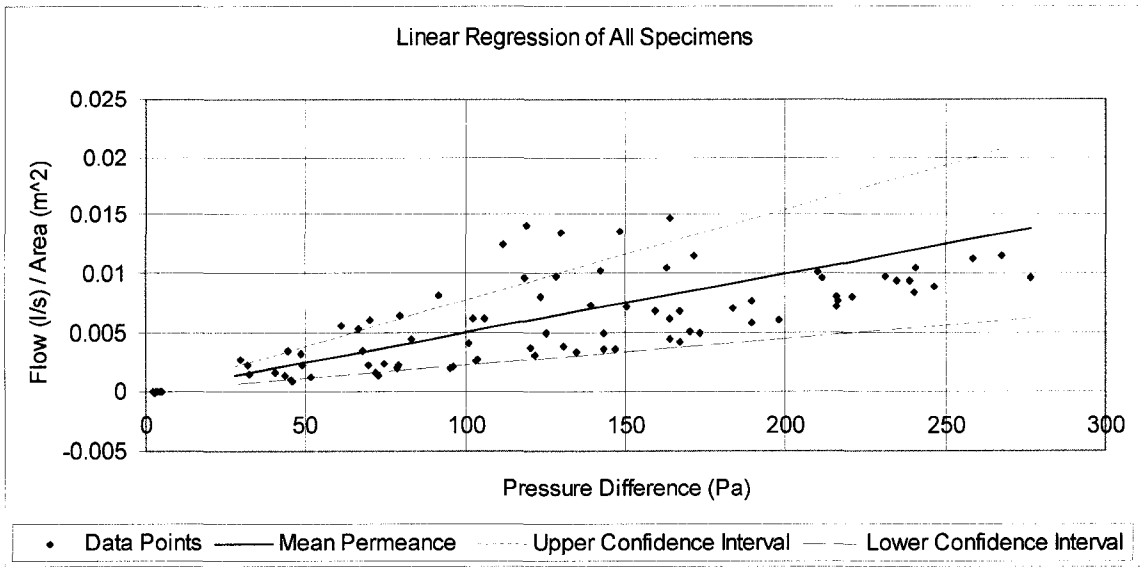


Figure A.7 The dependence of airflow rate on pressure difference for stucco  
 At the range of pressure differences from 30 to 270 Pa, the flow rate of stucco increases with the pressure difference. The air permeability of stucco under test is  $(1.2 \pm 0.7) \text{ E-09 kg/m}\cdot\text{Pa}\cdot\text{s}$ .

### A.9. Hygrothermal Properties of Glass Fiber Batt Insulation

**Density:**  $(11.51 \pm 0.09) \text{ kg/m}^3$

Table A.50 Thermal Conductivity of Glass Fiber Batt Insulation

Specimen thickness (mm)	Hot Surface Temperature (°C)	Cold Surface Temperature (°C)	Mean Temperature (°C)	Conductivity ( $\text{Wm}^{-1}\text{K}^{-1}$ )
127.04	15.14	-5.40	4.87	0.036
127.04	35.09	12.69	23.89	0.040
127.21	16.47	-5.17	5.65	0.036
127.21	35.19	13.17	24.18	0.040

### A.10. Hygrothermal Properties of Polyethylene sheet

**Density:**  $(1739 \pm 52) \text{ kg/m}^3$

**Thickness:**  $(0.153 \pm 0.003) \text{ mm}$

Table A.51 Dry cup measurements of polyethylene sheet

Specimen Thickness mm	Chamber RH %	Chamber Temperature °C	WVT Rate $\text{kg/s}\cdot\text{m}^2$
0.16	49.80	23.26	4.48E-09(3.17E-11)
0.15	49.80	23.21	4.03E-09(5.55E-11)
0.15	49.80	23.26	4.84E-09(3.76E-11)
0.16	70.38	23.04	6.56E-09(2.36E-10)
0.15	70.38	23.04	6.01E-09(1.43E-10)
0.15	70.38	23.04	6.69E-09(2.50E-10)
0.16	89.87	22.79	8.39E-09(1.32E-10)
0.15	89.87	22.79	7.96E-09(1.52E-10)
0.15	89.87	22.79	8.77E-09(7.32E-11)

Table A.47 Wet cup measurements of polyethylene sheet

Specimen Thickness mm	Chamber RH %	Chamber Temperature °C	WVT Rate kg/s·m <sup>2</sup>
0.15	70.51	23.20	2.53E-09(4.54E-11)
0.15	70.51	23.20	3.89E-09(4.14E-11)
0.15	70.51	23.20	1.88E-09(2.16E-11)
0.15	90.05	22.94	3.40E-09(5.14E-10)
0.15	90.05	22.94	4.24E-09(4.24E-09)
0.15	90.05	22.94	3.09E-09(5.39E-10)

Table A.48 Derived water vapor permeability for polyethylene sheet

RH %	Permeability kg/m·s·Pa	RH %	Permeability kg/m·s·Pa
10	4.47E-15	60	4.79E-15
20	4.59E-15	70	4.82E-15
30	4.66E-15	80	4.84E-15
40	4.71E-15	90	4.86E-15
50	4.75E-15	100	4.88E-15



# Appendix B

## TEST HUT DRAWINGS

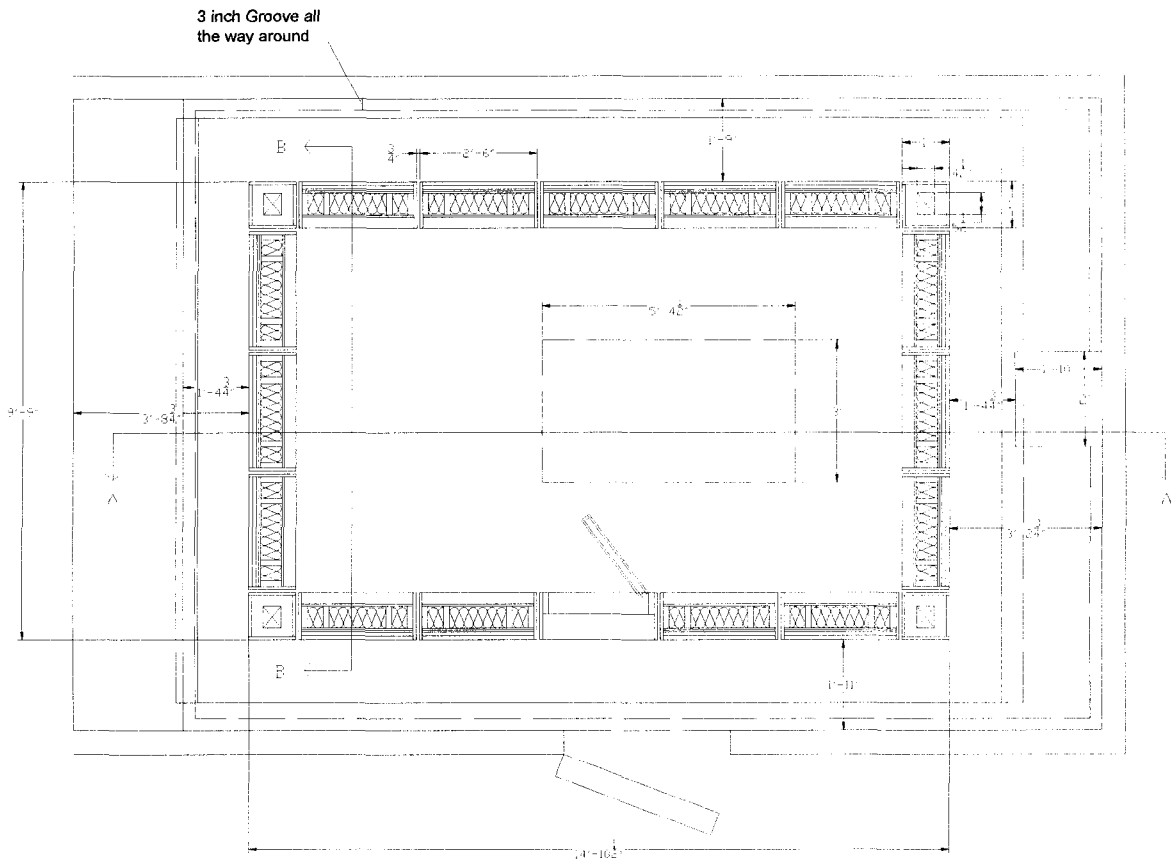


Figure B-1. Test hut layout for the first floor

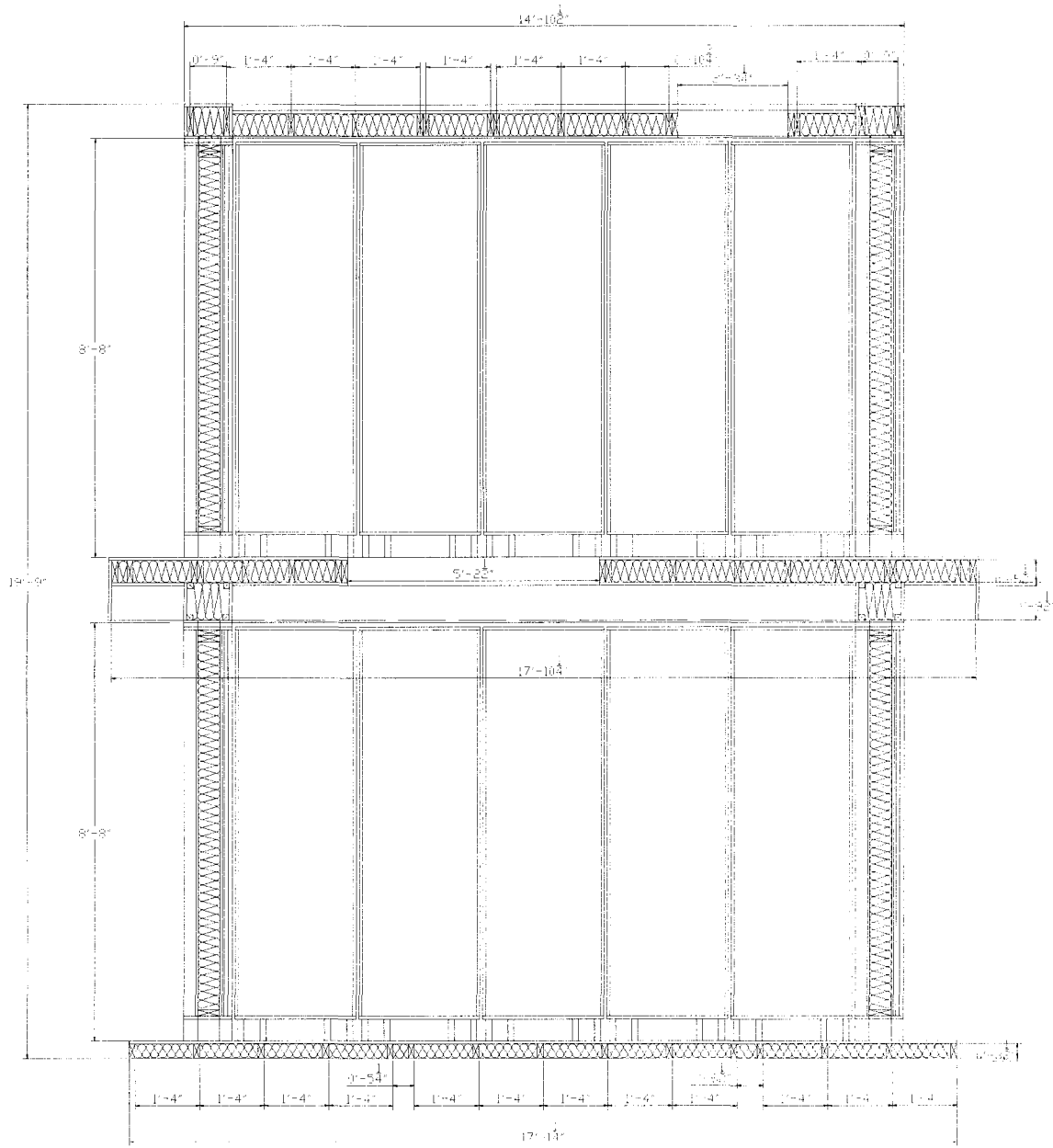


Figure B-2. Section A-A

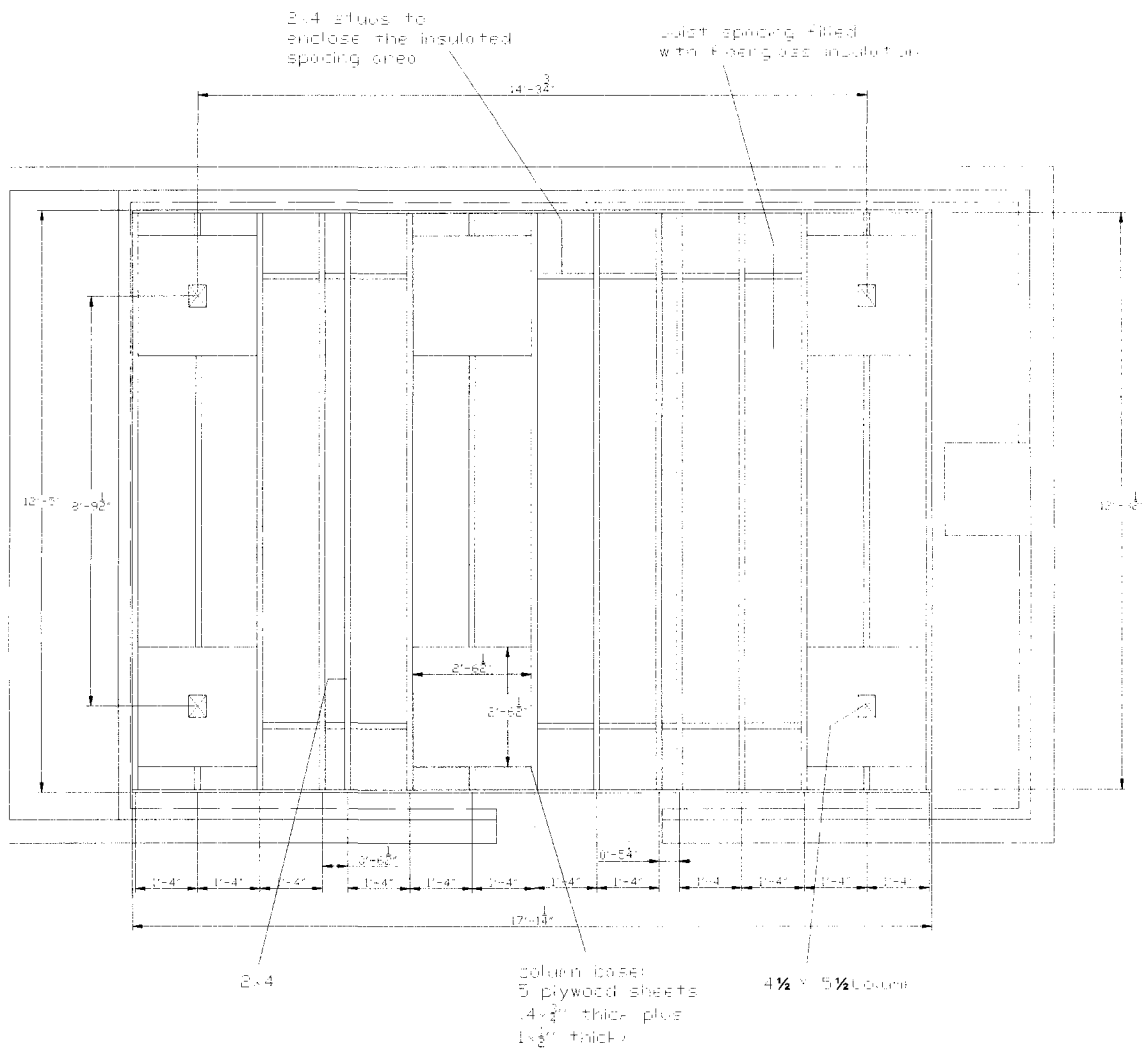
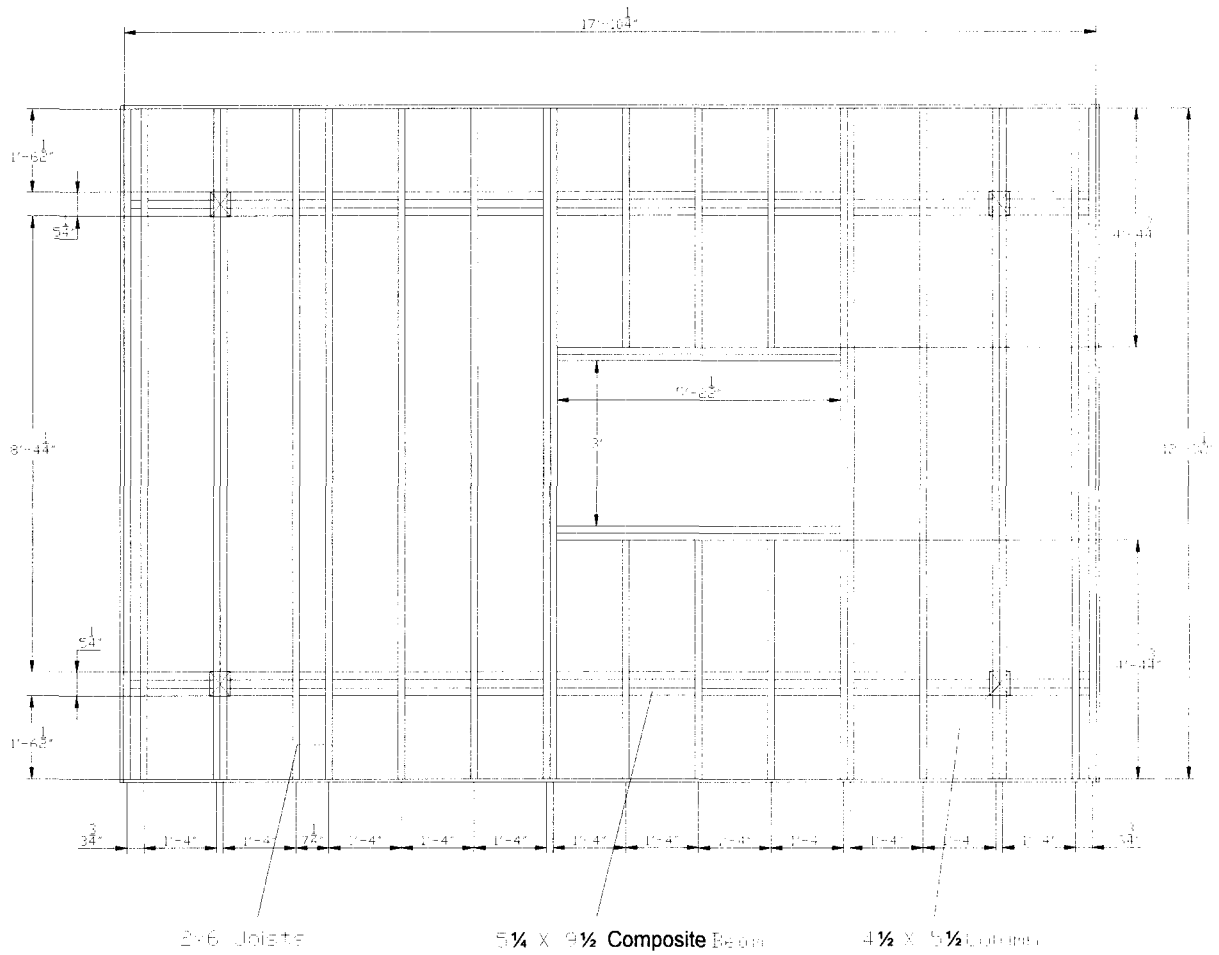


Figure B-3. First floor-structural



**Figure B-4. Second floor-structural**

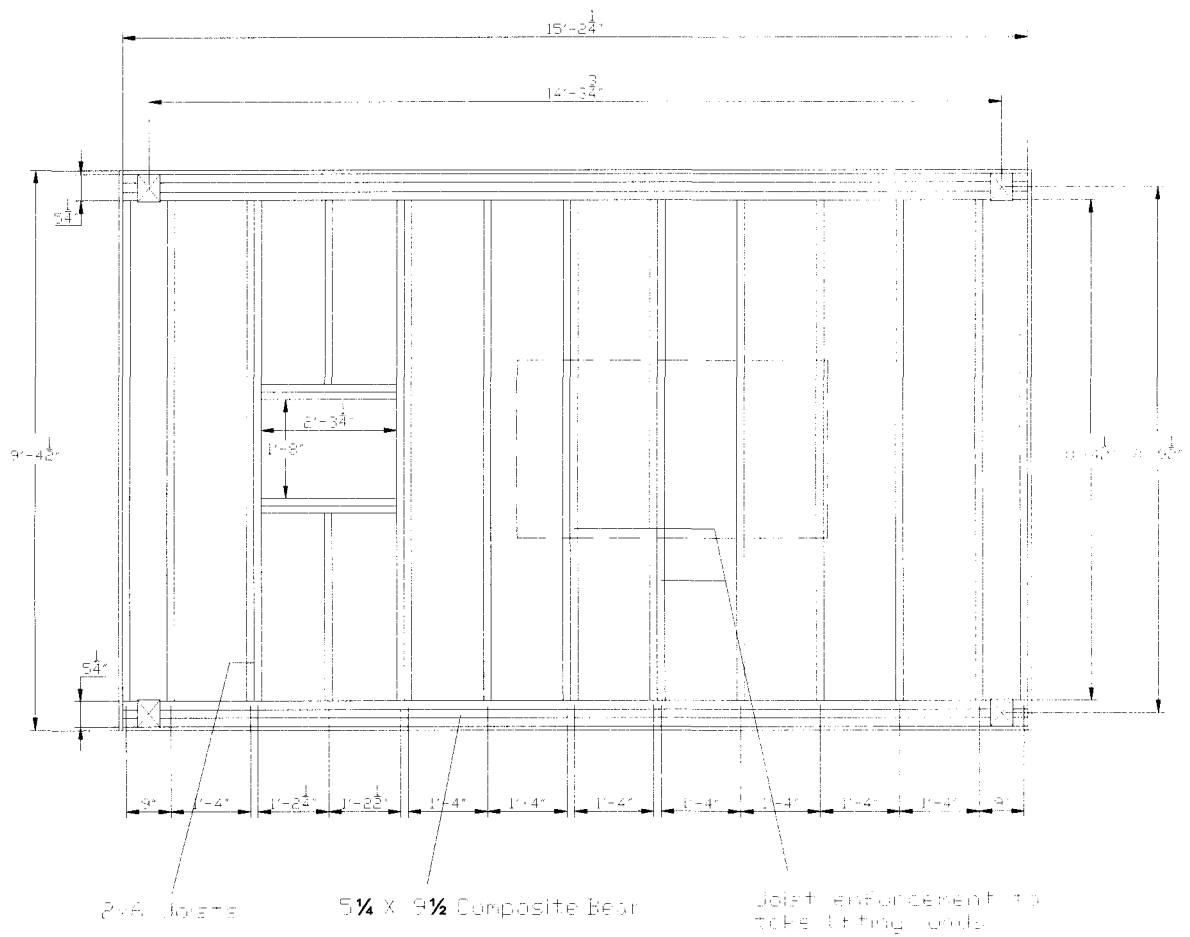


Figure B-5. Roof-structural

## Appendix C

### MONITORING PROTOCOL

In this appendix, some information is listed from the Protocol on monitoring in the CRD project prepared by Rao (2004).

#### **C.1 Load Cell for measuring evaporation rate**

Load cell (AG series by SCAIME, [www.scaleton.com](http://www.scaleton.com))

Capacity: 1 kg

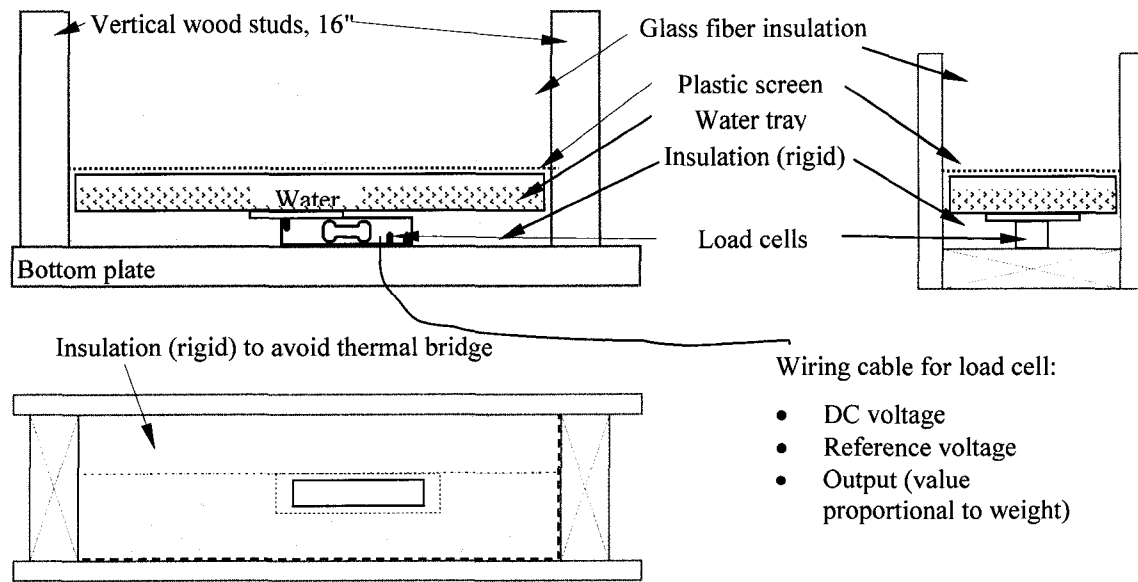
Sensitivity: ~2.00 mV/V

Accuracy: 1/4000

The weight of a water tray at the bottom in the insulation cavity of each test specimen is monitored continuously by one load cell. Details on the setup procedure for load cells are in the Loading Protocol. A diagram for the setup is shown in Figure C-1.

Each load cell has seven wires. The wires are connected to one 8-wire terminal block in the pass-through configuration of Figure 7a.

Load cell outputs are mini-volt signals. The sensitivity of the load cell is expressed x.xxx mini-volt per volt of applied input DC (direct current) power. For example, if a LC has a sensitivity of 1.98 and 10 VDC exact is applied to the LC, then the LC output should be 19.8 mV at the full load of 1 kg. The sensitivities of the LC are around 2.00 mV/V, but has slightly (1%) variations among sensors. The sensitivity is determined in the factory for each LC unit (identified with unique serial number).



**FigureC-1. A sketch of weighing system with load cells**

Since the wire from the power supply leading to the load cell has resistance, the voltage applied to the load cell is smaller than the voltage at the power supplier. This leads to the measurement of the reference voltage (terminals #3 & 4). Therefore, for each load cell, two measurements are taken by the DAS, one for the output and the other for the reference voltage. During data processing, the weight on a load cell is calculated by the following equation:

$$weight = \frac{output \times 10}{sensitivity \times reference\ voltage} \text{ (kg)}$$

Most of load cells have zero drift (permanent deformation in the load cell) if weights are applied continuously. To minimized this effect, one additional load cell is used to have a fixed weight applied to it, and is monitored together with other load cells. Any change in the measured values from the additional reference load cell is due to the zero drift, and is corrected in measured values of other load cells. (Note that this correction procedure implies that zero drifts are identical to all load cells). Experiences with trial runs on the evaporation wetting method show that the zero drift is very low and slow.

## C.2 Moisture content by metal pins

### Location

Moisture contents of studs and sheathing are measured by resistive electronic moisture content transmitters. Since the rain is not directly simulated in this test, moisture contents of siding and cladding are not monitored.

On each specimen, 12 probes (pairs of metal pin) are installed. One thermocouple is installed with each pair of MC pins to monitor the temperature. This temperature is needed to correct the electronic reading of MC transmitters.

**Table C-1. Sensor location for electronic moisture content probes**

#	Sensor	Material	Distance to bottom plate	Distance to centerline	Notes
1	nn_MC_C1	Sheathing	-0.75"	0	
2	nn_MC_C2		4"	0	
3	nn_MC_C3		1'	0	
4	nn_MC_C4		2'	0	
5	nn_MC_C5		4'	0	
6	nn_MC_C6		7'	0	
7	nn_MC_Q1		-.75"	4"	
8	nn_MC_Q2		4"	4"	
9	nn_MC_Q3		1'	4"	
10	nn_MC_S1	Stud	4"	7.25"	center of stud
11	nn_MC_S2		1'	7.25"	
12	nn_MC_S3		4'	7.25"	

### Installation of pins

To measure the moisture contents, pairs of metal pins are installed in wooden materials. The custom pins use small gold plate pins (similar in size and shape to the pins inside the connector for parallel port printers, but with solid copper core. The gold plating is for reducing corrosion). The pins have similar dimension as the pins on the hand-held moisture content meters.

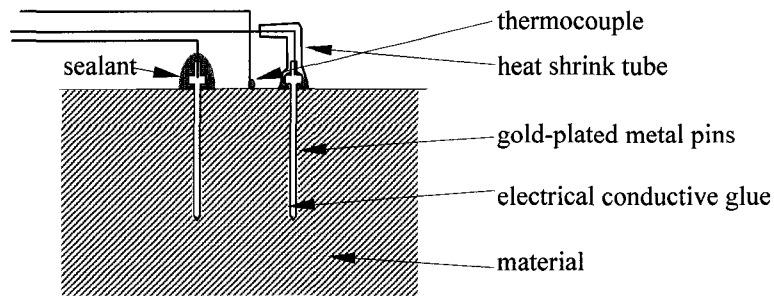
In installation, the hand-held MC unit is used to punch two tiny holes on the material for inserting two of the gold pins (with wires already soldered on the end of the pins). Electrically conductive glue is used on the pins when inserting for maintaining good contact. Liquid tape (electrical insulating) is used for covering the exposed metal ends. Additional



sealant (silicon caulking, for example) and/or heat shrink tubes may be used for conditions that are more stringent. The figure below shows a diagram of the installation.

Due to the tiny size and softness of the base metal, these pins should not be used for periods longer than 12 to 18 month in wet materials (close to fiber saturation).

In addition, commercially available metal pins designed for (resistive) moisture content measurement are also used. These pins are made from stainless steel and have different sizes for various depths into materials.



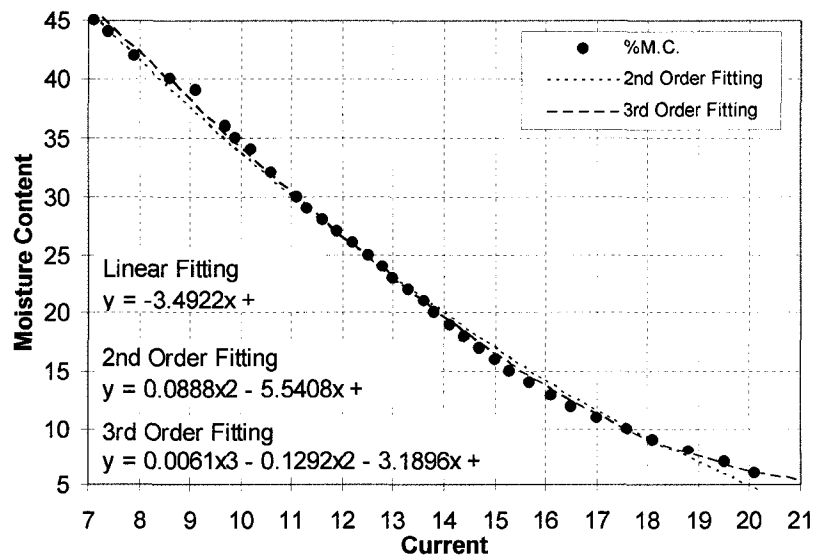
**FigureC-2. Installation of metal pins for moisture content**

#### MC measurement and calibrations

The measurement by resistive MC sensors relies in the relationship between moisture content of wood and electrical resistance in the wood. For spruce wood, the relation is shown in the following table and figure. The resistive MC sensor can only measure MC between 6% to wood fiber saturation (about 28% depends on wood species). Values measured above the fiber saturation are not exact reading.

**Table C-2. Calibration data for spruce wood**

Current (mA)	M.C. (%)	Current (mA)	M.C. (%)	Current (mA)	M.C. (%)
20.1	6	13.6	21	8.6	40
19.5	7	13.3	22	7.9	42
18.8	8	13.0	23	7.4	44
18.1	9	12.8	24	7.1	45
17.6	10	12.5	25	6.9	46
17.0	11	12.2	26	6.4	48
16.5	12	11.9	27	5.8	50
16.1	13	11.6	28	5.4	52
15.7	14	11.3	29	5.0	54
15.3	15	11.1	30	4.8	55
15.0	16	10.6	32	4.6	56
14.7	17	10.2	34	4.3	58
14.4	18	9.9	35	4.0	60
14.1	19	9.7	36		
13.8	20	9.1	39		



**FigureC-3. Moisture content sensor (MT-60) calibration curve**

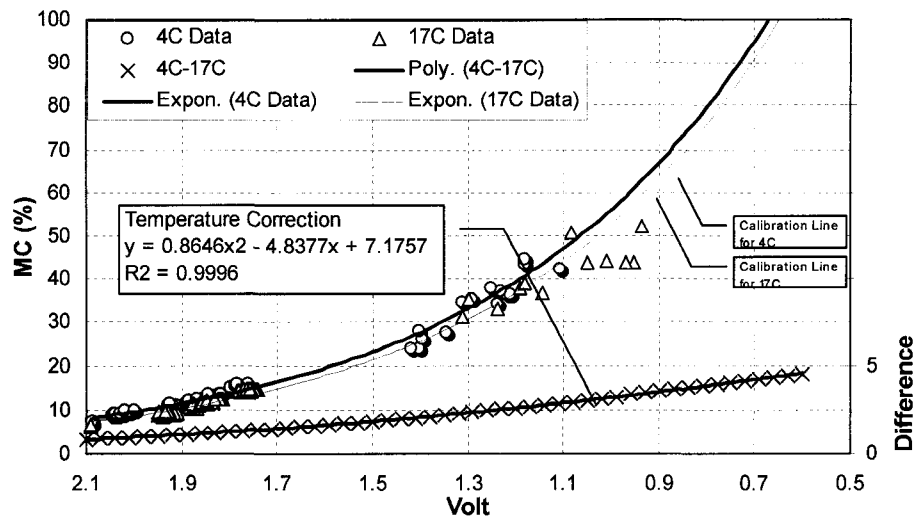
To ensure accuracy, a MC sensor needs three types of calibrations:

1. calibration of the transmitter,
2. species or material correction, and
3. temperature correction.

To verify a transmitter, there are two high-resistance resistors. Each resistor simulates a specific moisture content of wood. The operation is very easy and fast. This checking operation should be performed on all transmitters before a new experiment commences.

The resistances of different wood species at the same moisture content are influenced by the fiber density and composition, and are slightly different. Therefore, species correction is required if the wood measured is not the same as designated by the MC transmitter.

When wood products (plywood, OSB, etc.) are measured, a calibration curve is needed. The calibration process derives the relationship between the moisture contents and the electrical resistance measured by the transmitter. The resistance is very non-linear with respect to the water percentage. The MC transmitter current output is also non-linear but to a much lesser degree. The relation between the MC transmitter current output and the real moisture contents (measured by the gravimetry technique) in the wood is obtained at a number of conditions (of temperature and RH). A second-order or third-order regression equation can be used as the calibration curve. Figure C-4 shows such a curve for fiberboard. Calibration curves for plywood and OSB are being obtained.



**FigureC-4. Calibration of impregnated wood fibre Board**

The above calibration for fiber board was performed at two temperatures, 4 and 17°C. The empirical relation in the above figure can be fitted to an equation for easier data processing:

$$MC(\%) = 322.65 \cdot e^{-1.8094V} + \frac{17 - T}{14} [0.8646 * V^2 - 4.8377V + 7.1757]$$

The relationship between the resistance and the moisture contents in wood is also affected by the temperature of wood at which the measurement is made. A thermocouple is placed on the material close to each pair of pins. Temperature measured during the test will be used for calculating temperature correction. A correction table for spruce wood is shown below.

**Table C-3. Temperature correction for the MC sensors**

T (°C)	Moisture Contents							
	6%	7%	10%	15%	20%	25%	30%	35%
-20	3	4	5	7	11	13	15	18
-10	2	3	4	5	8	9	10	12
5	1	1	2	3	4	5	6	7
15	0	0	1	1	1	2	2	3
30	0	0	-1	-1	-1	-2	-2	-2

**Appendix D**  
**ACCUMULATED EVAPORATION**

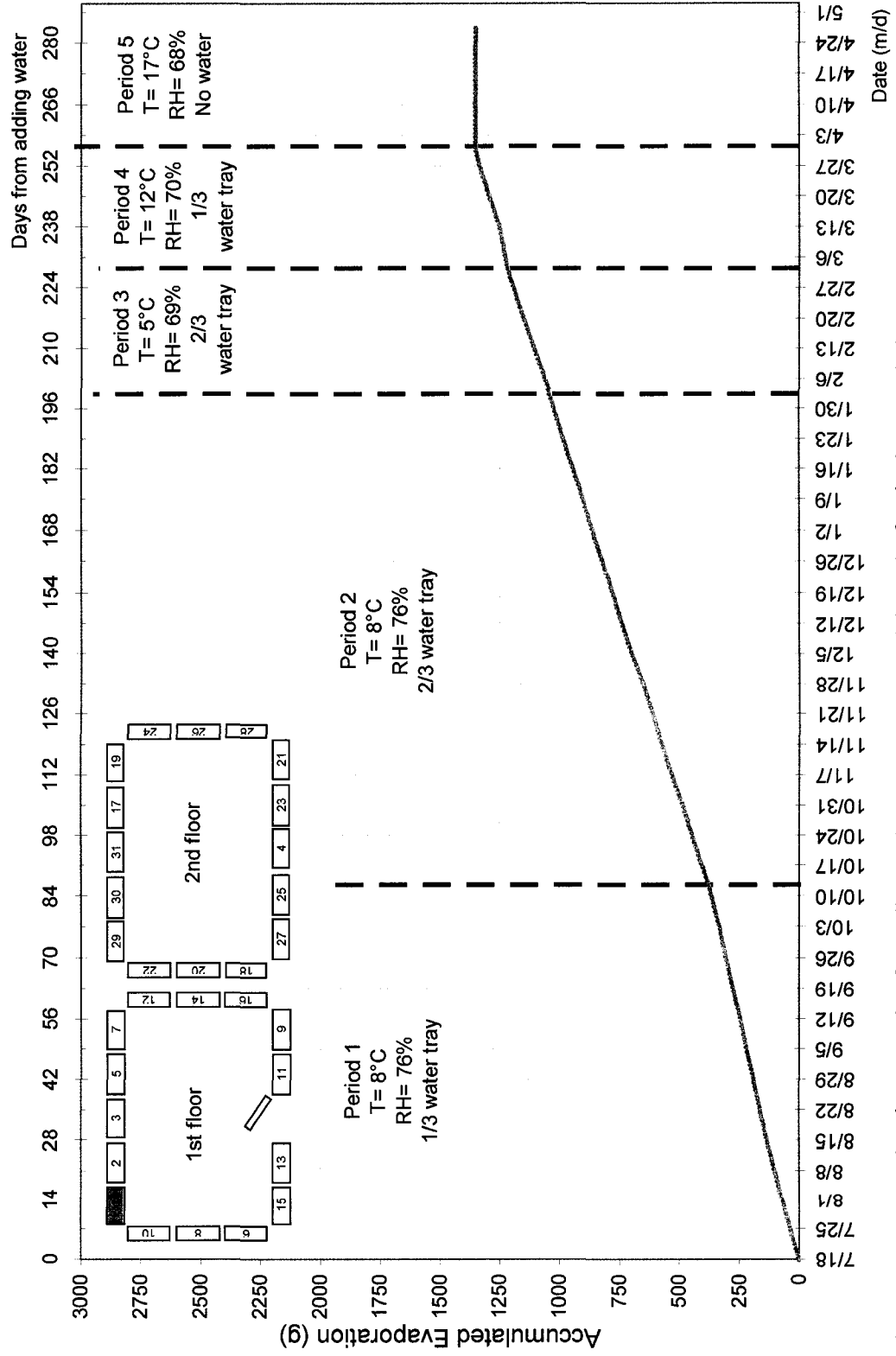


Figure B-1. Accumulated evaporation for wall assembly 01 (OSB, no cladding, vb) for the 5 test periods

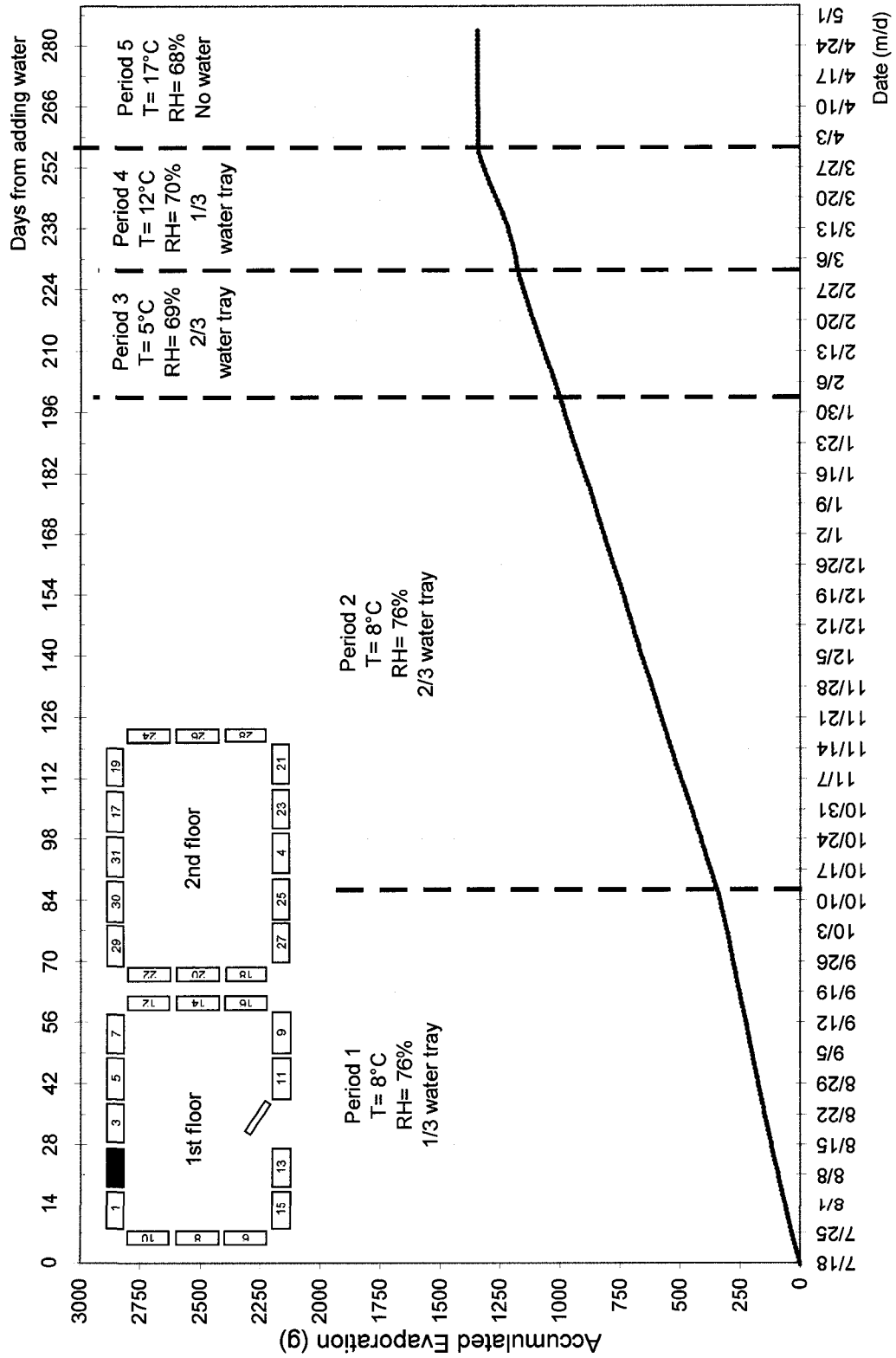


Figure B-2. Accumulated evaporation for wall assembly 02 (plywood, no cladding, vb) for the 5 test periods

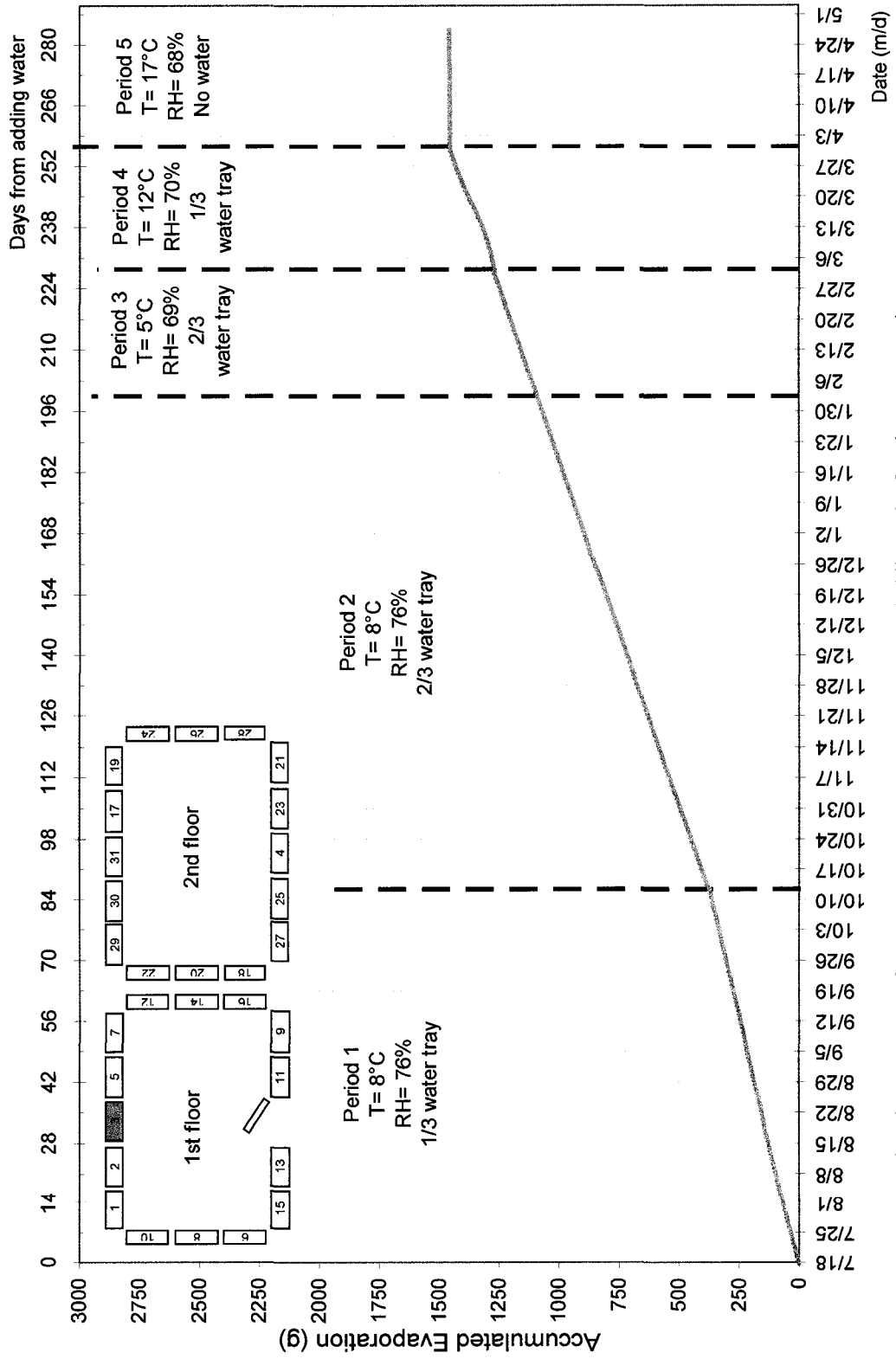


Figure B-3. Accumulated evaporation for wall assembly 03 (fiberboard, no cladding, vb) for the 5 test periods



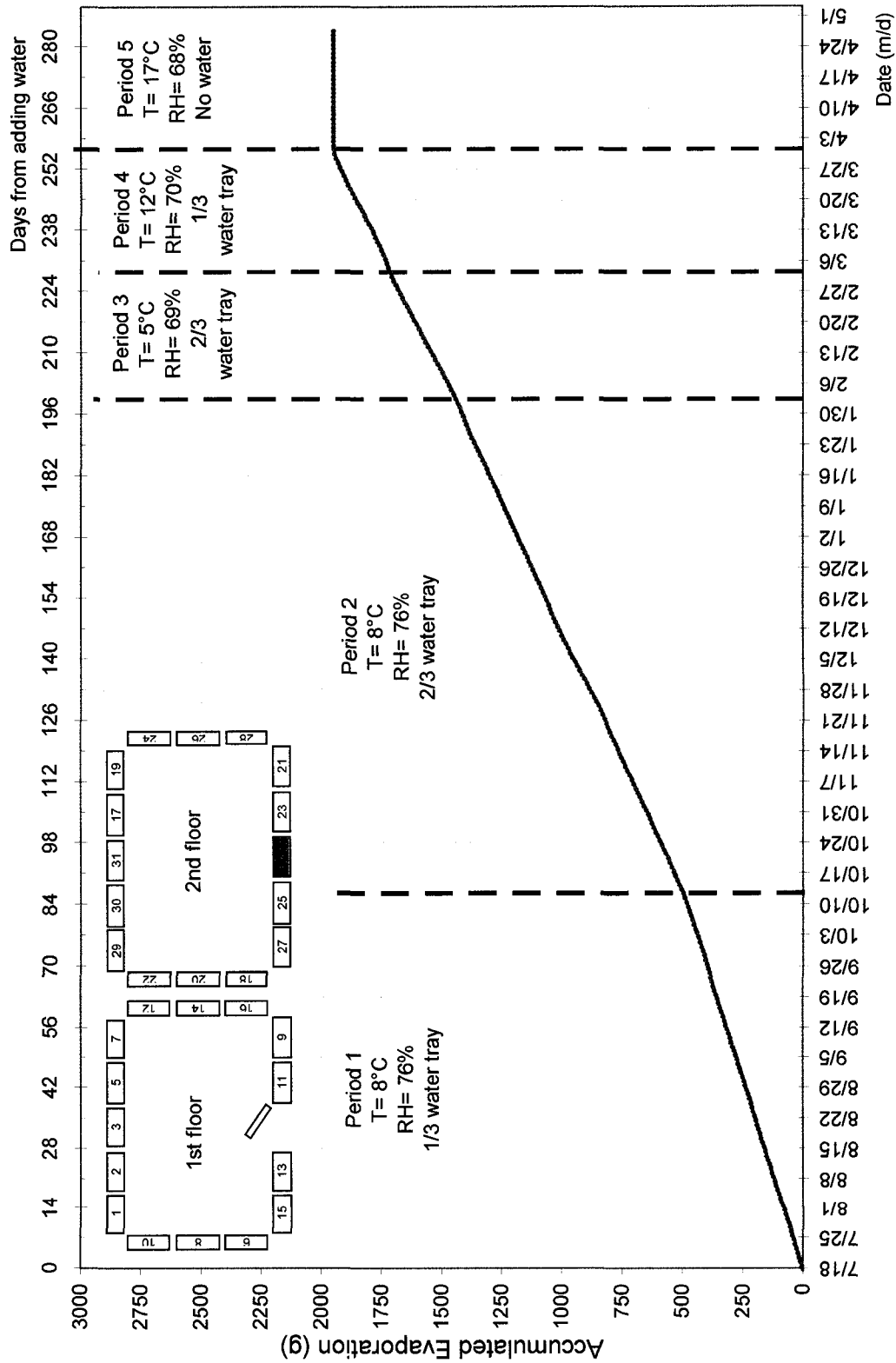


Figure B-4. Accumulated evaporation for wall assembly 04 (insulation board, no cladding, vb)

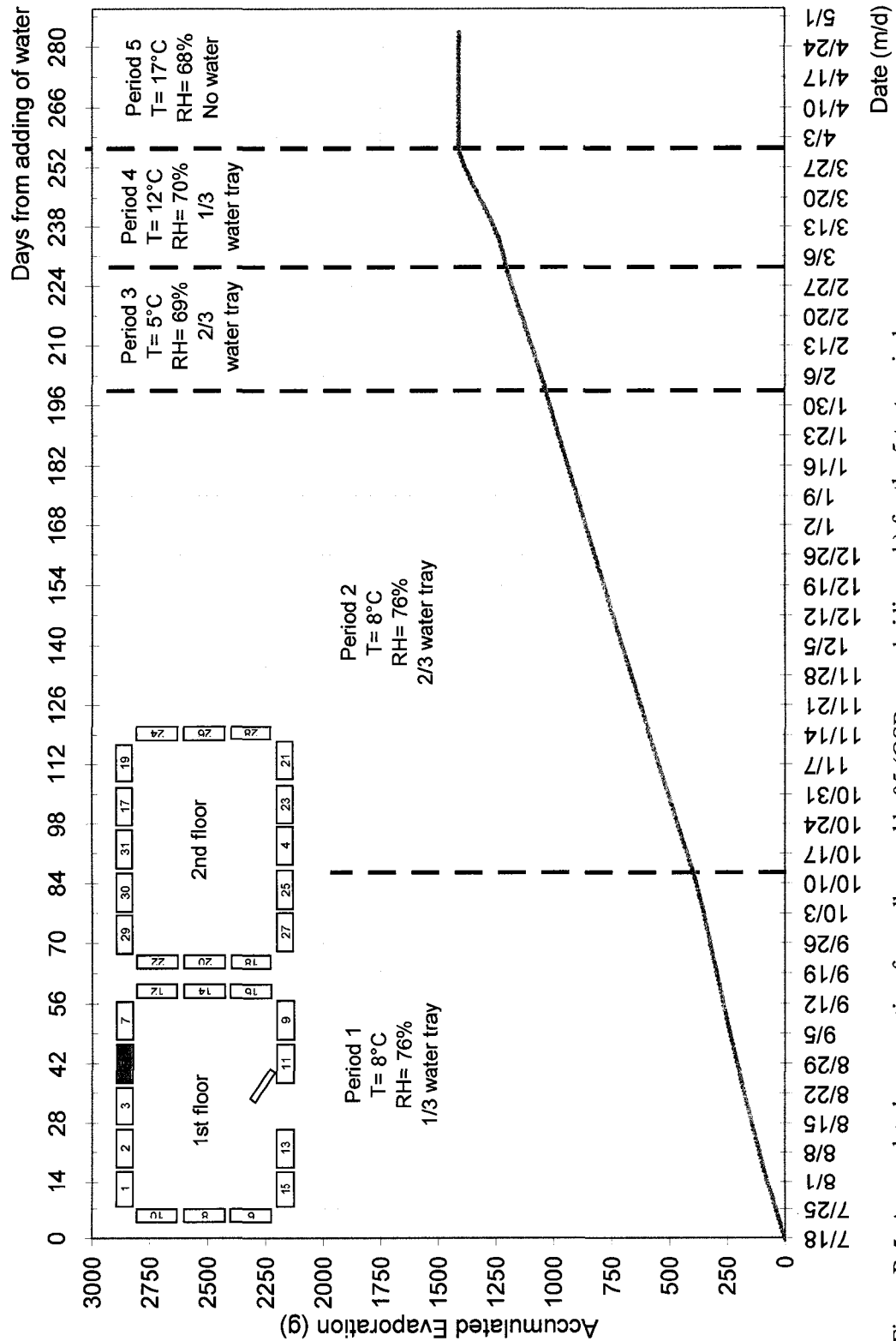


Figure B-5. Accumulated evaporation for wall assembly 05 (OSB, wood siding, vb) for the 5 test periods

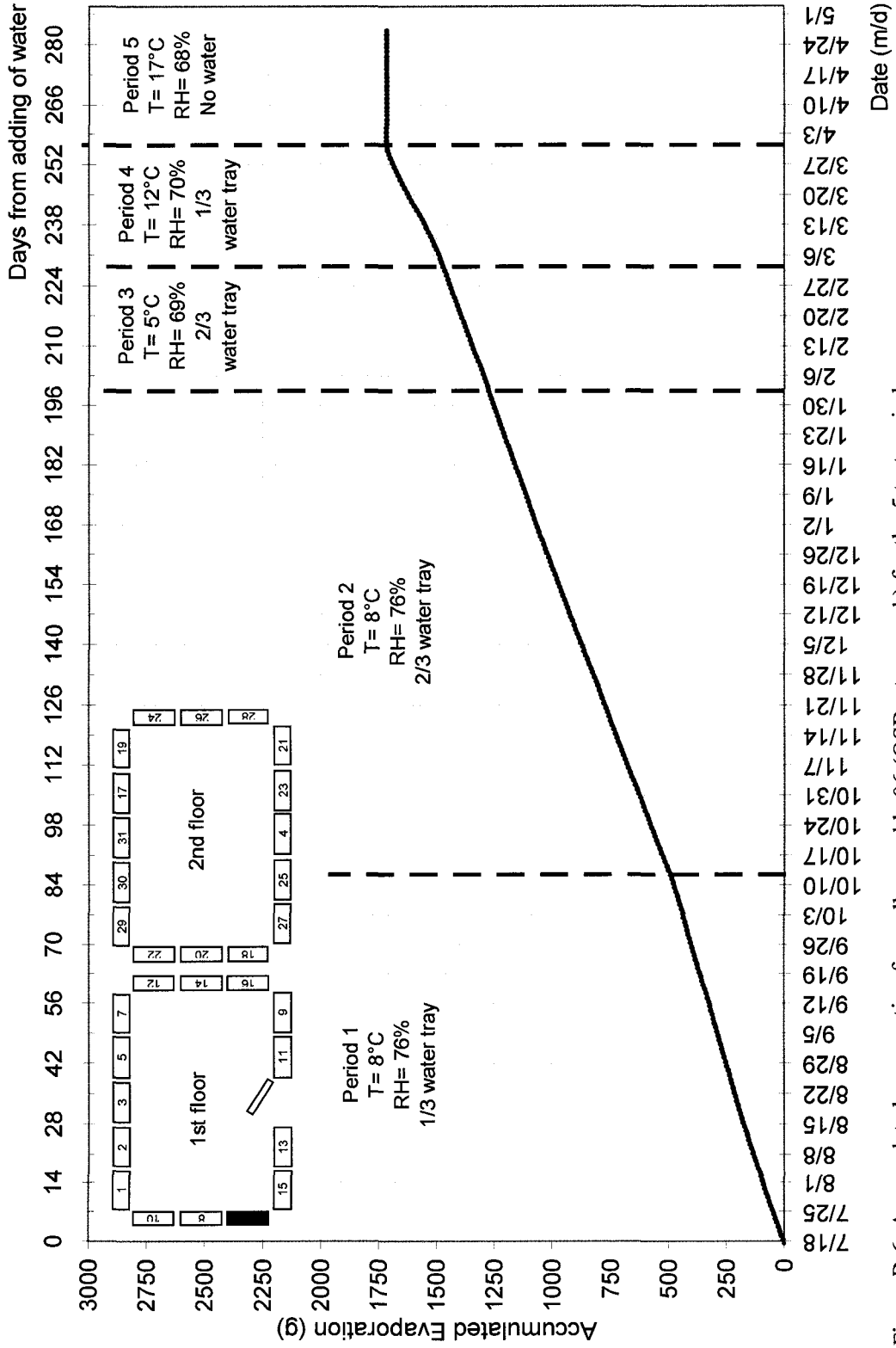


Figure B-6. Accumulated evaporation for wall assembly 06 (OSB, stucco, vb) for the 5 test periods

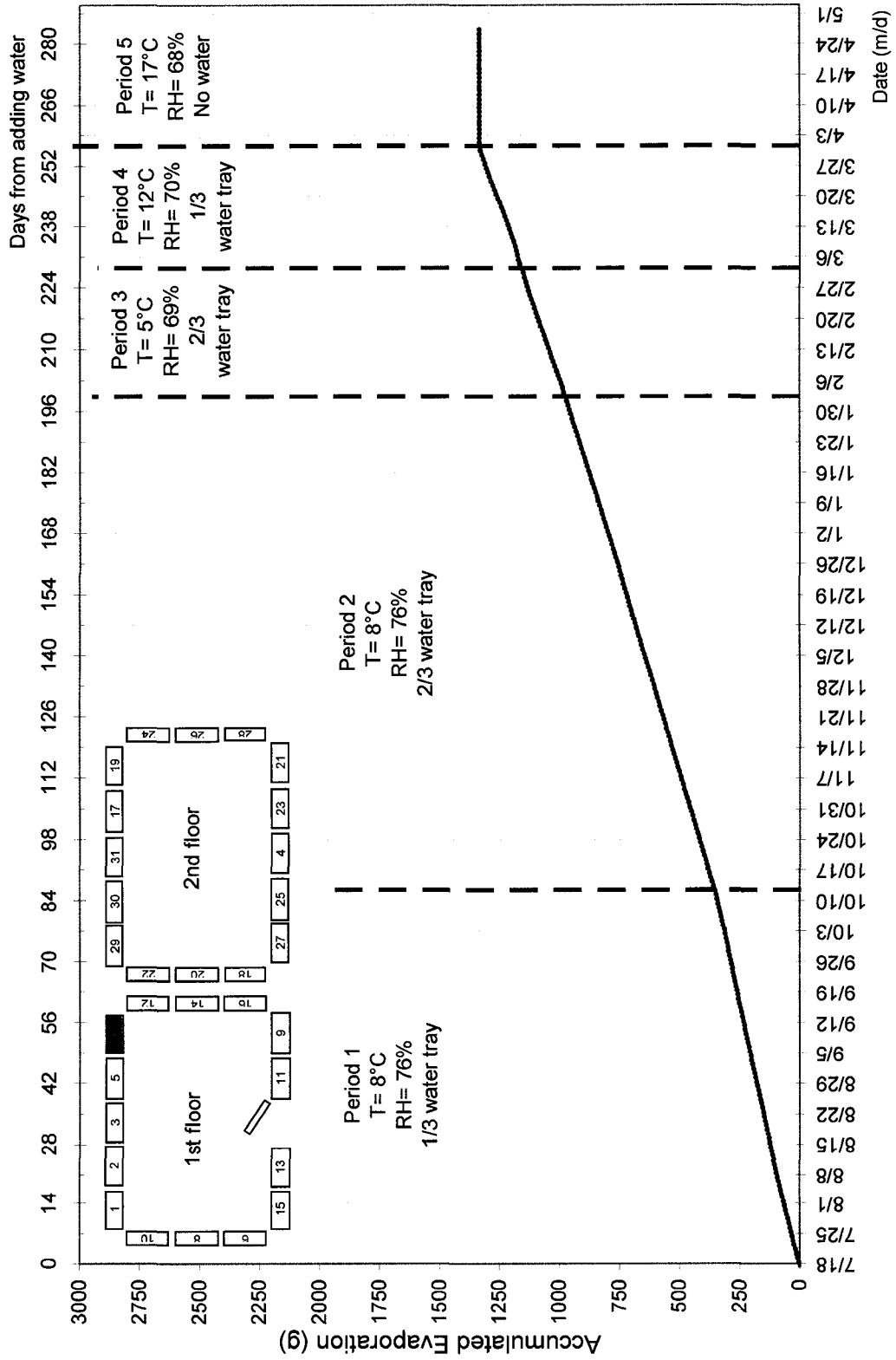


Figure B-7. Accumulated evaporation for wall assembly 07 (plywood, wood siding, vb) for the 5 test periods

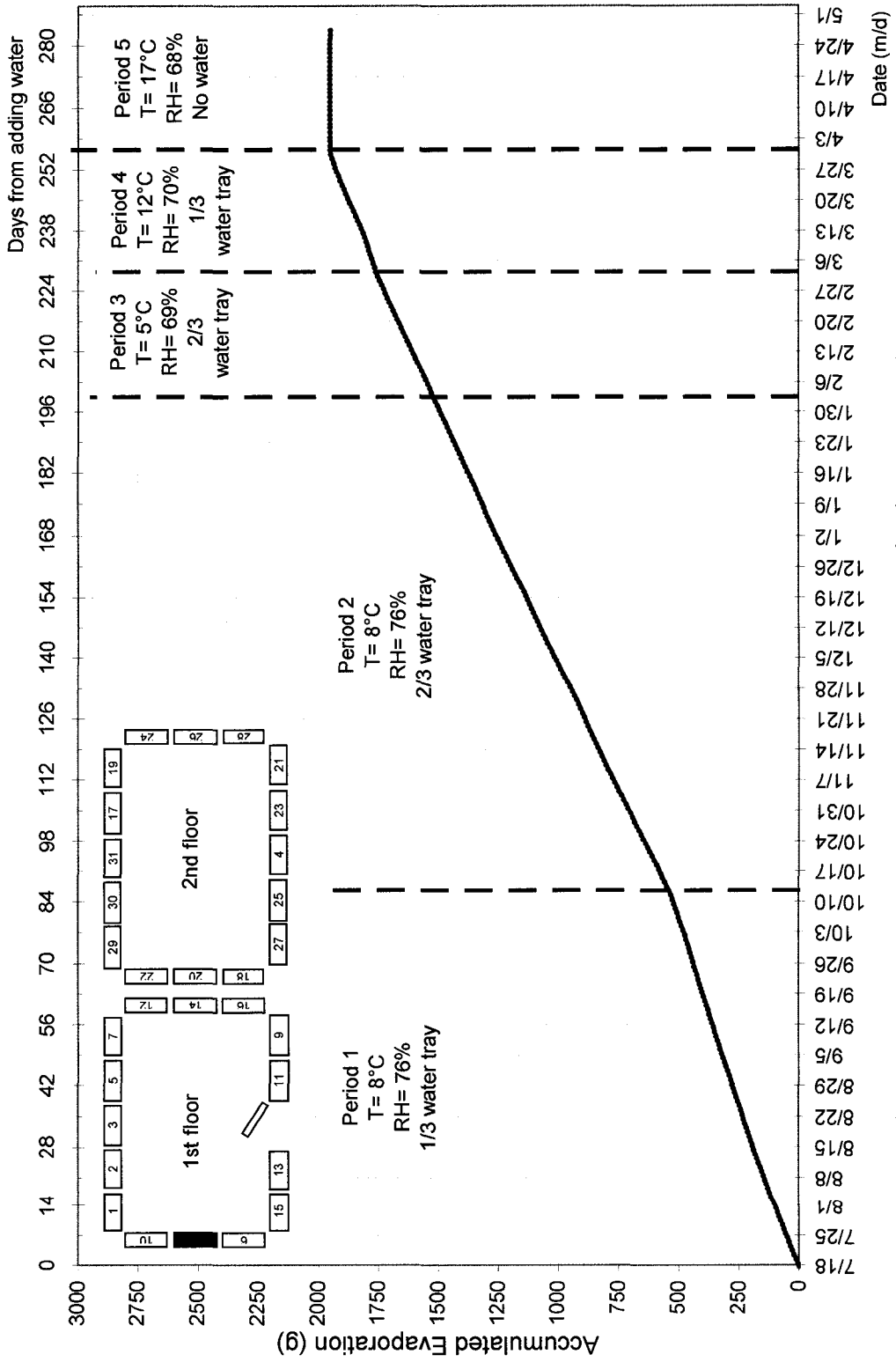


Figure B-8. Accumulated evaporation for wall assembly 08 (plywood, stucco, vb) for the 5 test periods

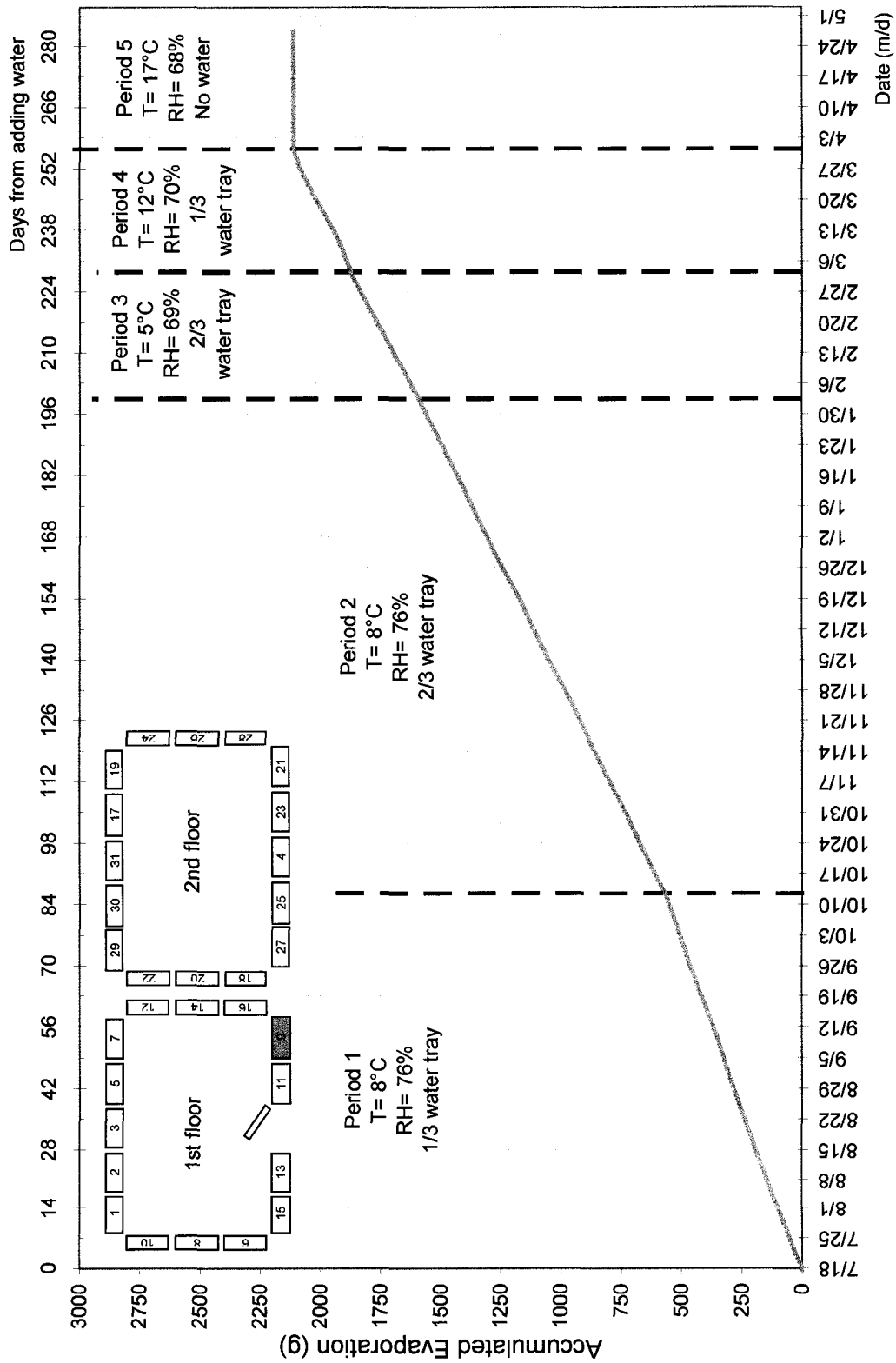


Figure B-9. Accumulated evaporation for wall assembly 09 (fiberboard, wood siding, vb) for the 5 test periods

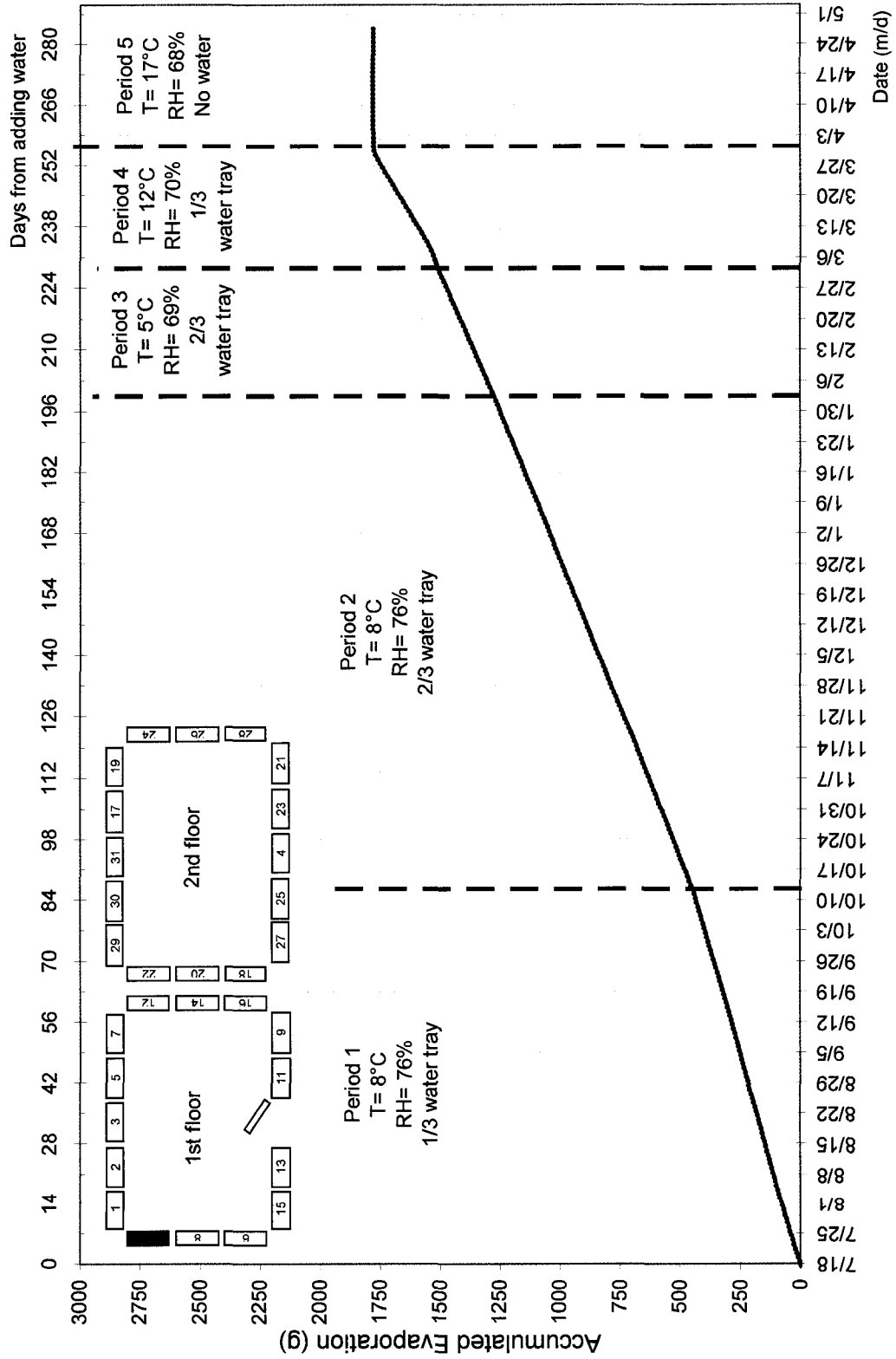


Figure B-10. Accumulated evaporation for wall assembly 10 (fiberboard, stucco, vb) for the 5 test periods

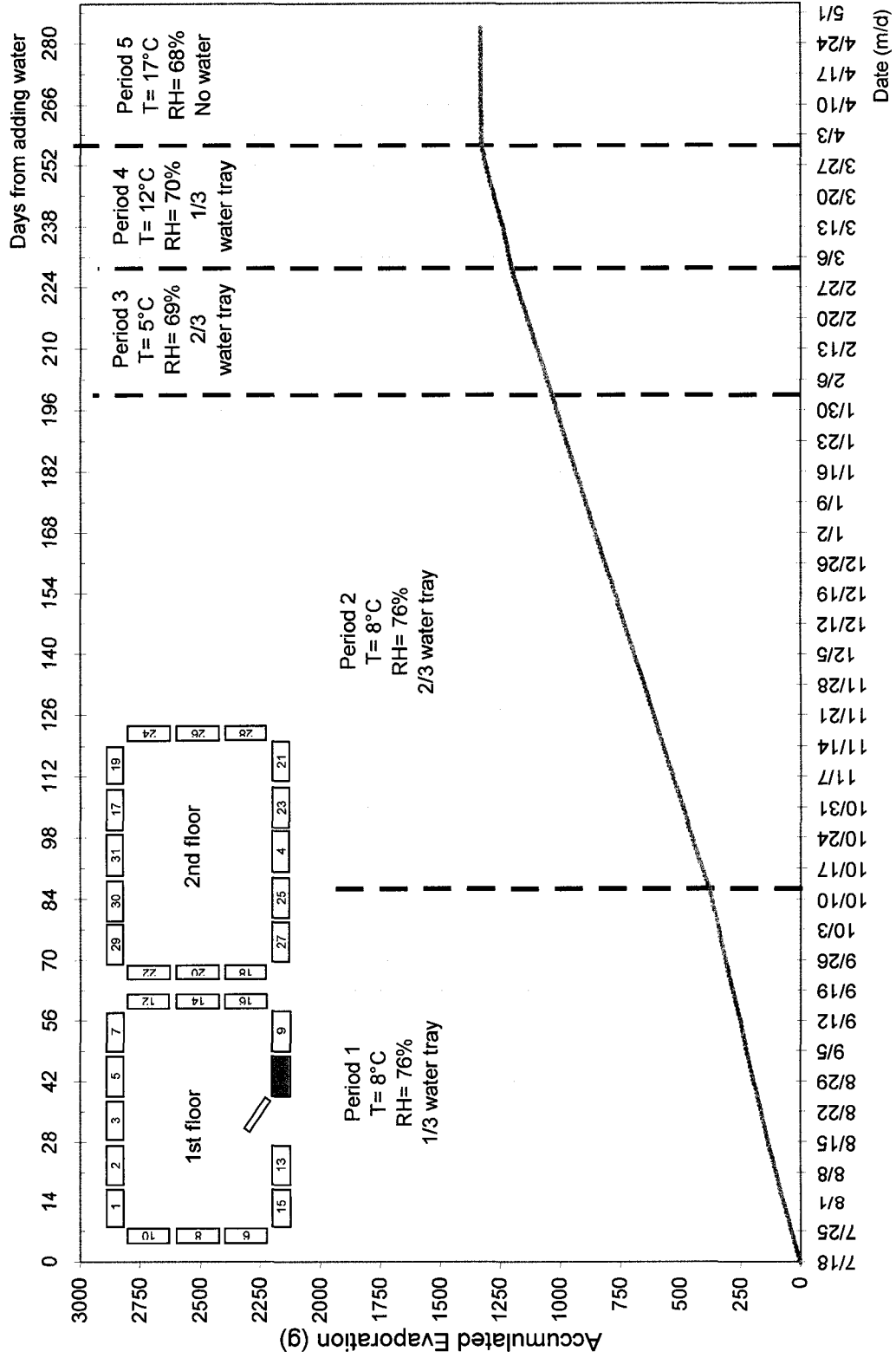


Figure B-11. Accumulated evaporation for wall assembly 11 (OSB, wood siding, no vb) for the 5 test periods



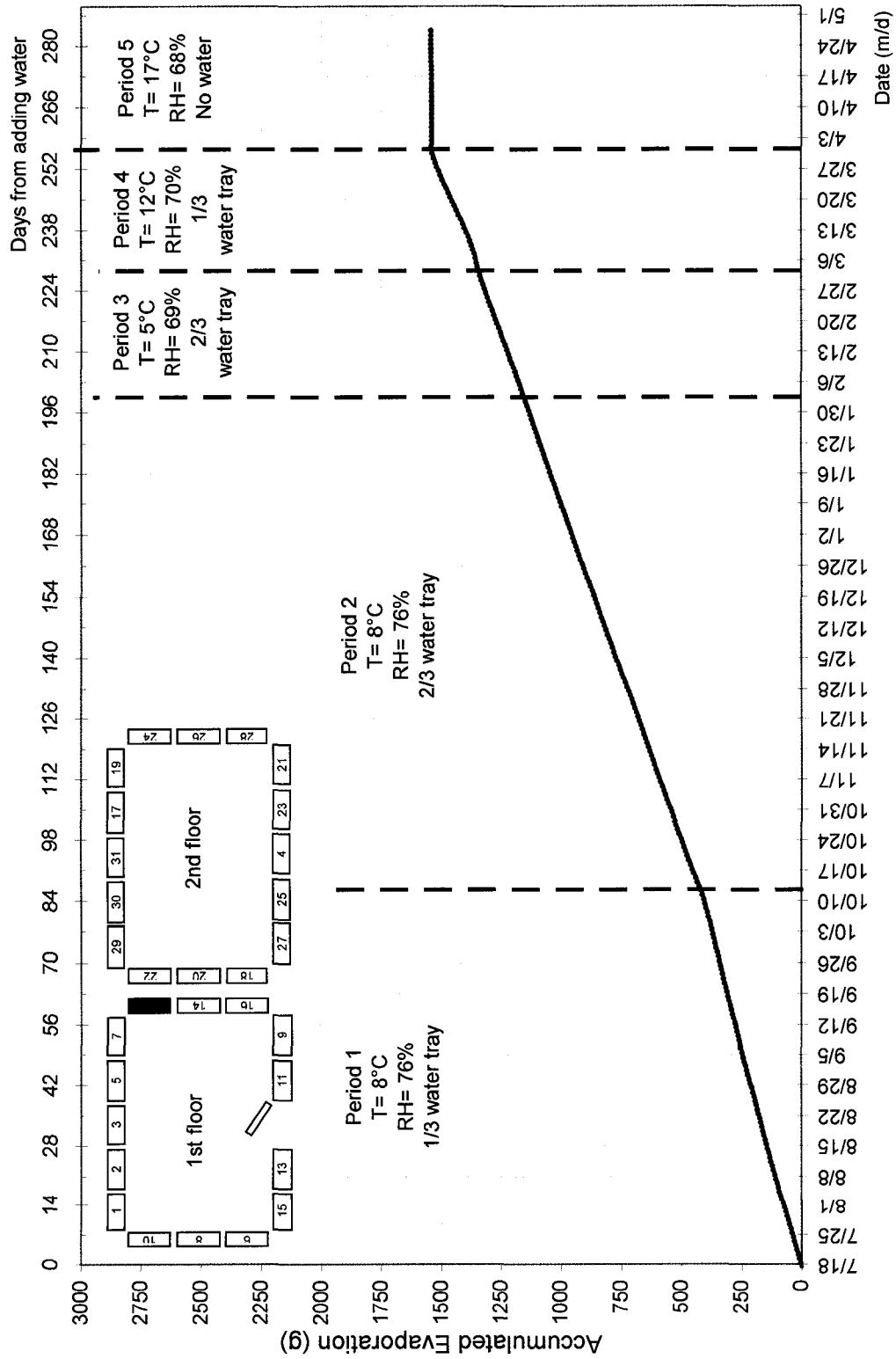


Figure B-12. Accumulated evaporation for wall assembly 12 (OSB, stucco, no vb) for the 5 test periods

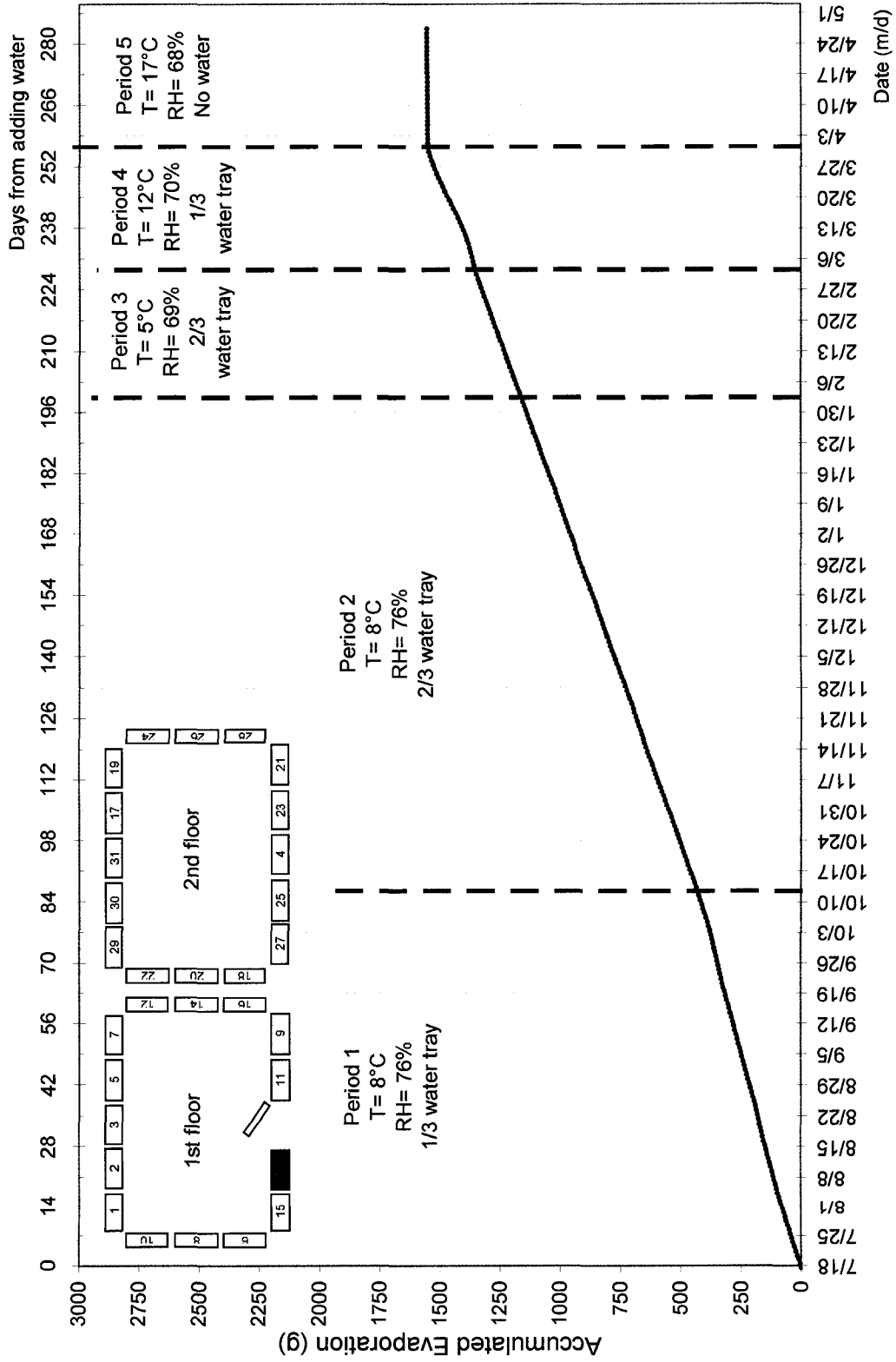


Figure B-13. Accumulated evaporation for wall assembly 13 (plywood, wood siding, no vb) for the 5 periods

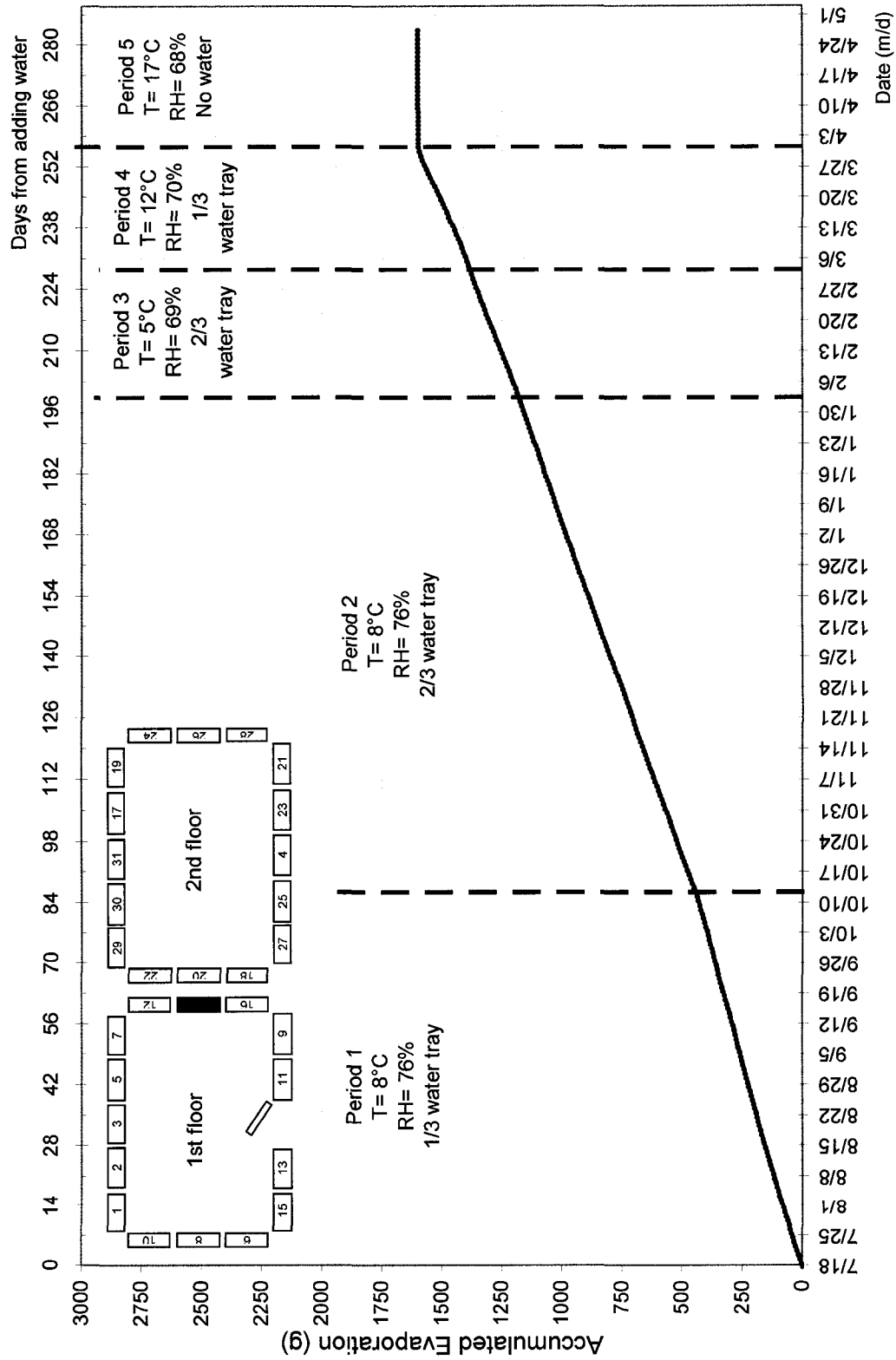


Figure B-14. Accumulated evaporation for wall assembly 14 (plywood, stucco, no vb) for the 5 periods

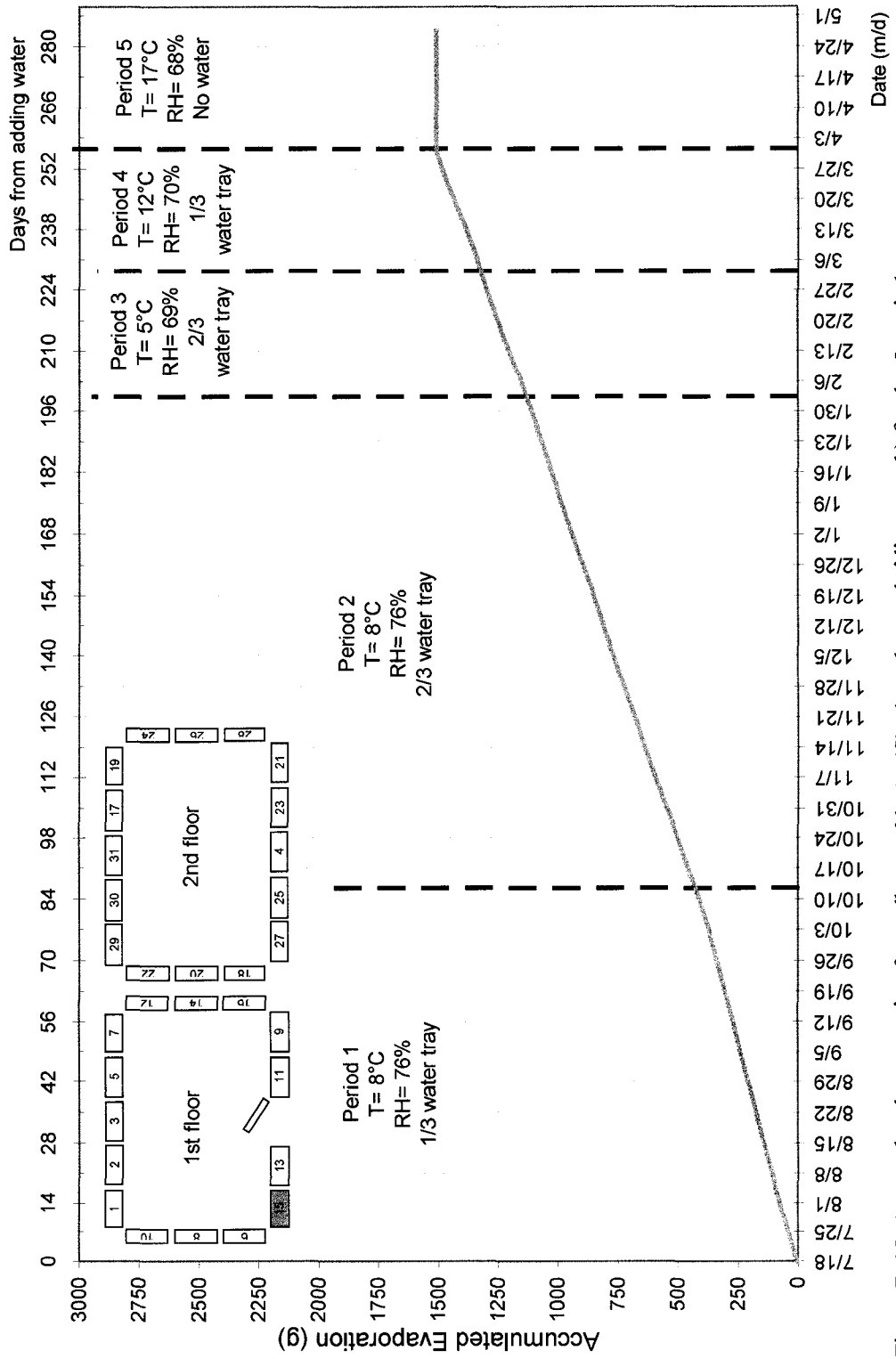


Figure B-15. Accumulated evaporation for wall assembly 15 (fiberboard, wood siding, no vb) for the 5 periods

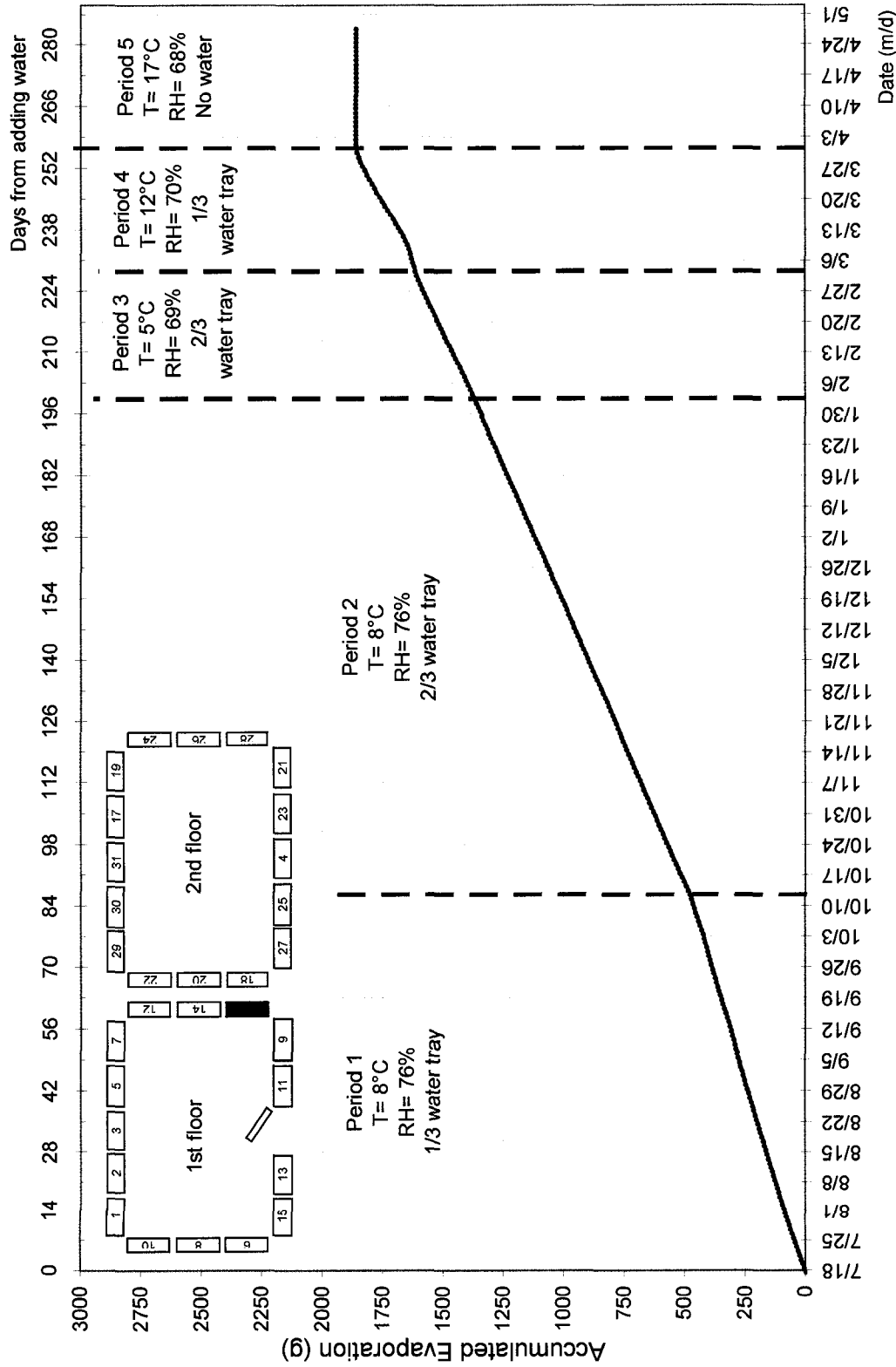


Figure B-16. Accumulated evaporation for wall assembly 16 (fiberboard, stucco, no vb) for the 5 periods

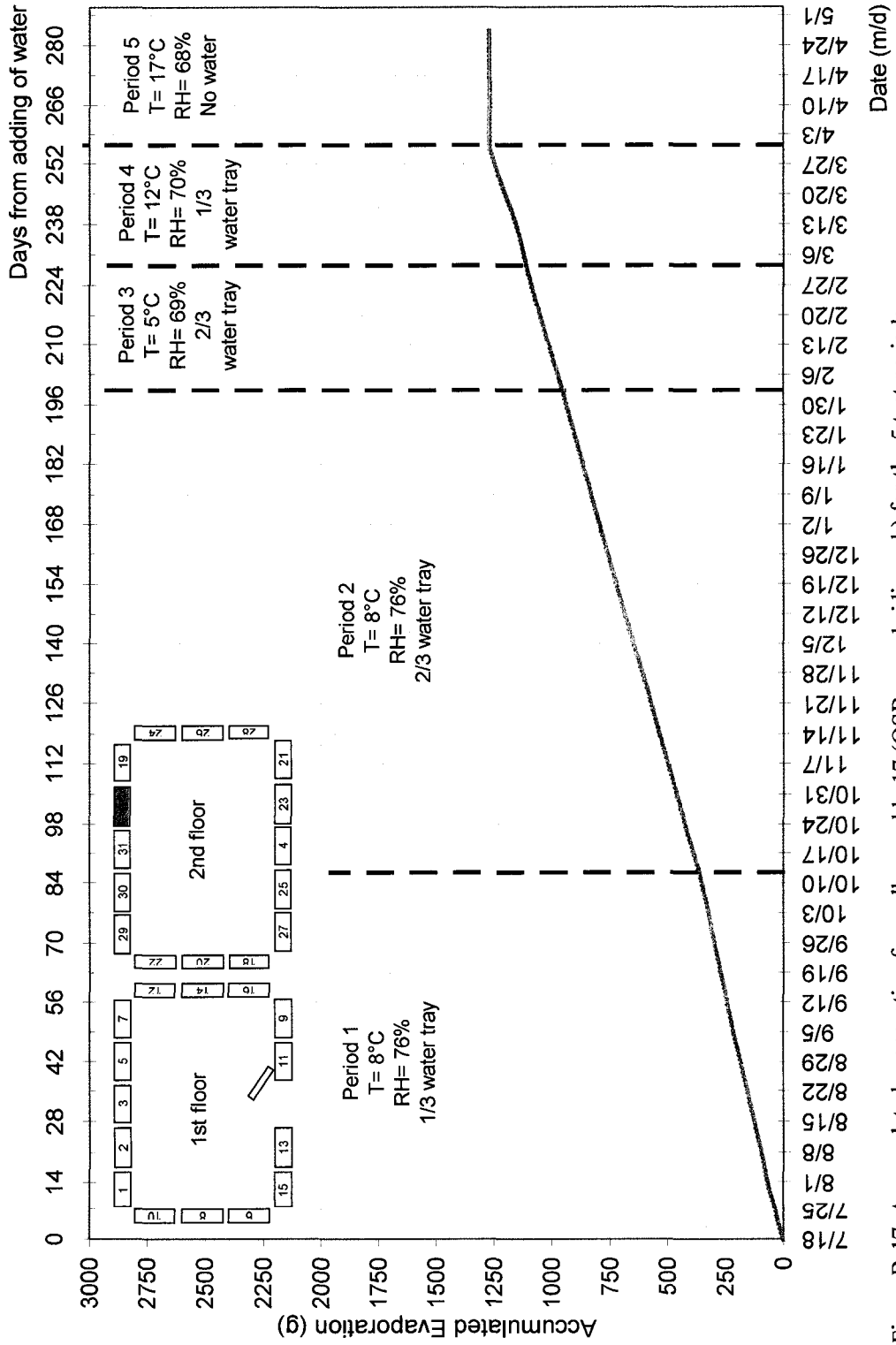


Figure B-17. Accumulated evaporation for wall assembly 17 (OSB, wood siding, vb) for the 5 test periods

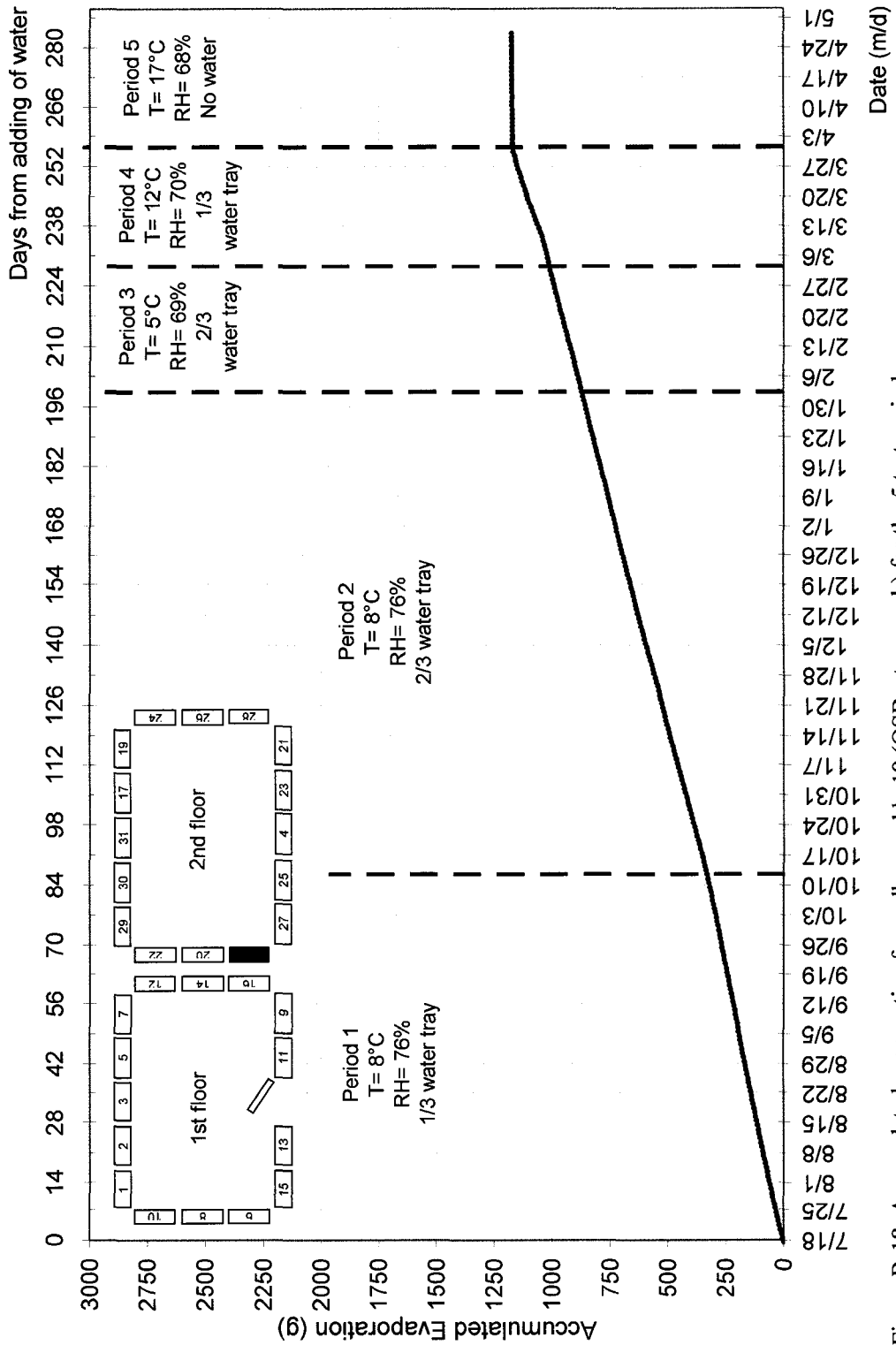


Figure B-18. Accumulated evaporation for wall assembly 18 (OSB, stucco, vb) for the 5 test periods

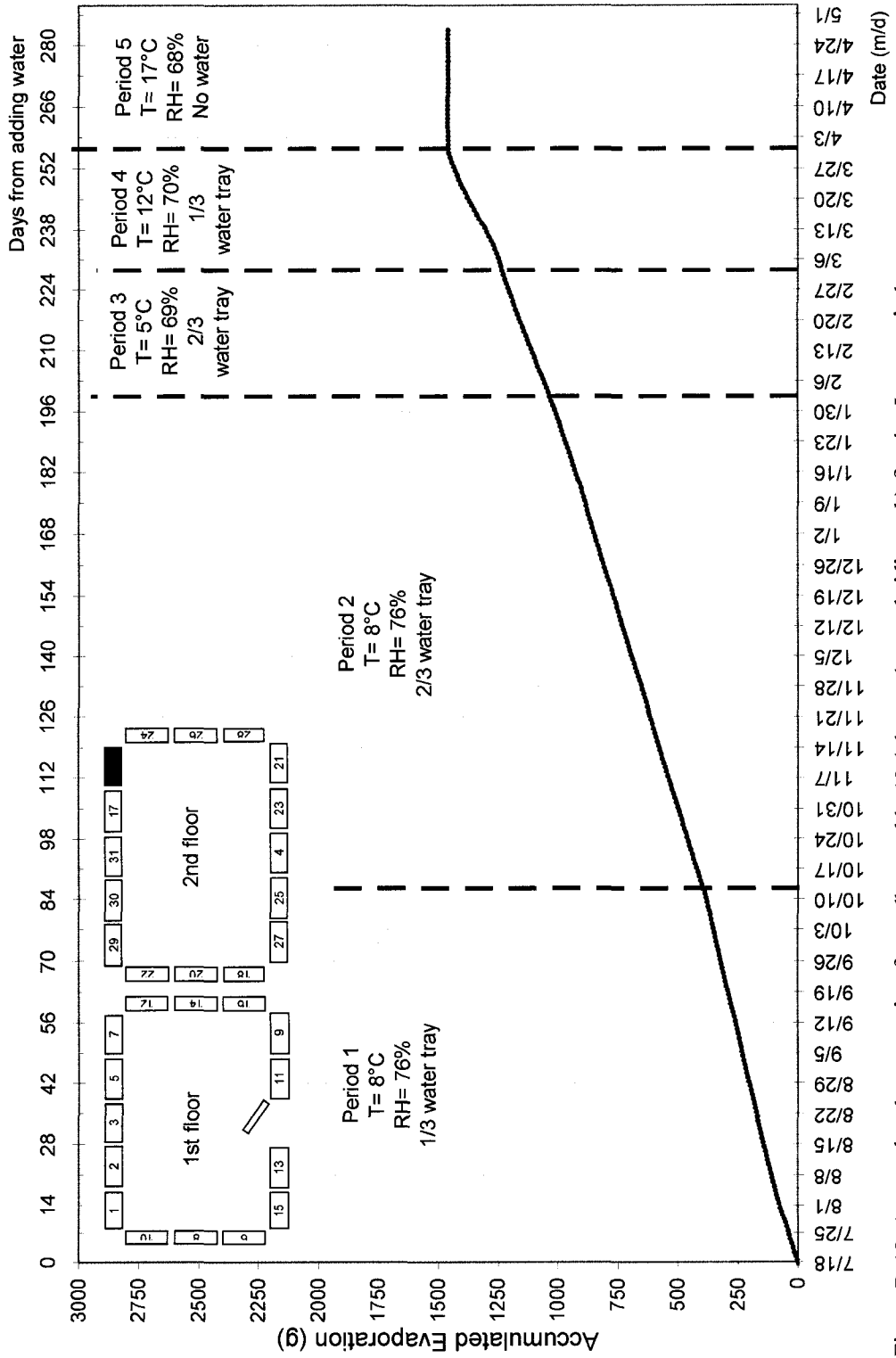


Figure B-19. Accumulated evaporation for wall assembly 19 (plywood, wood siding, vb) for the 5 test periods



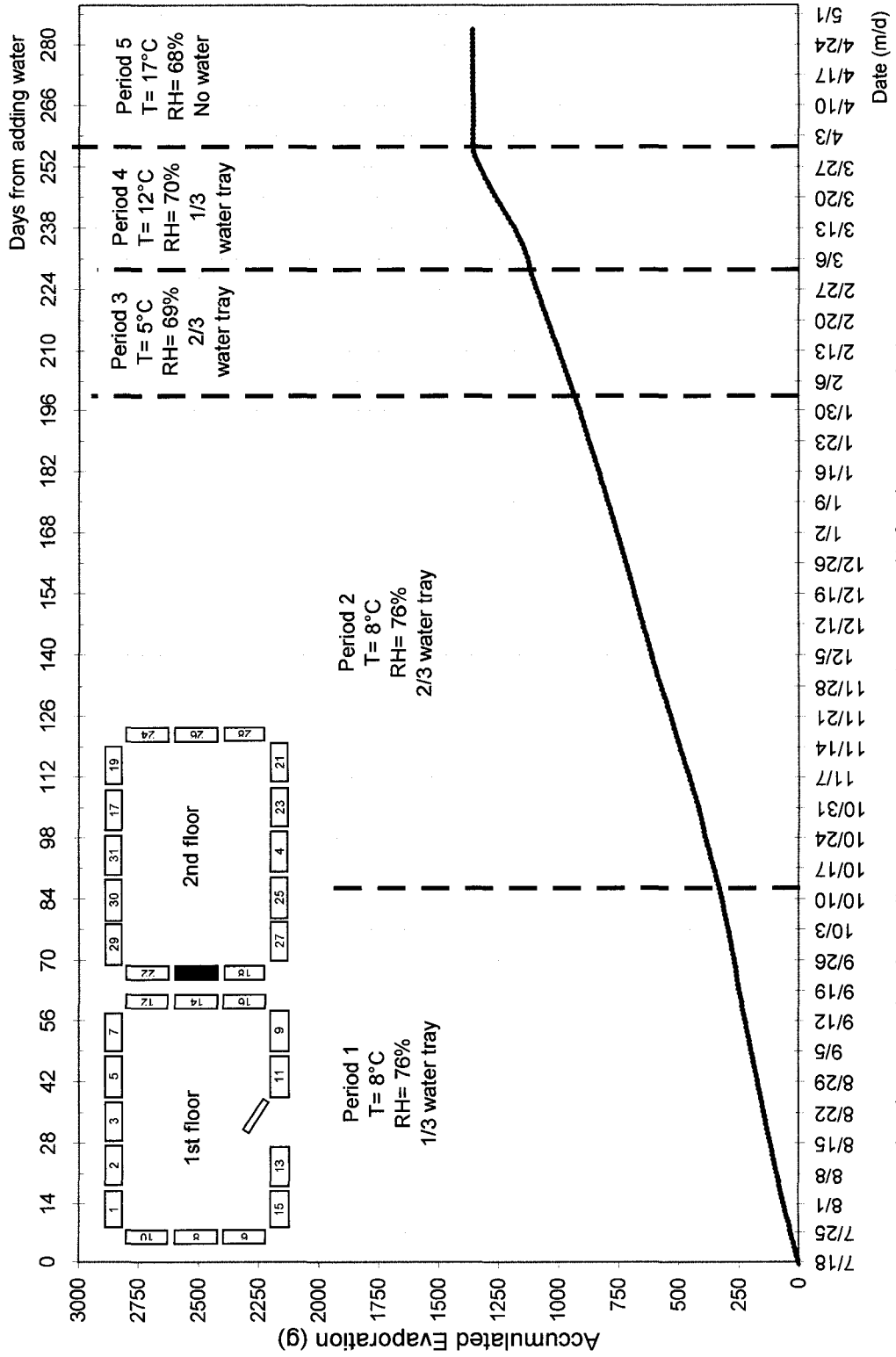


Figure B-20. Accumulated evaporation for wall assembly 20 (plywood, stucco, vb) for the 5 test periods

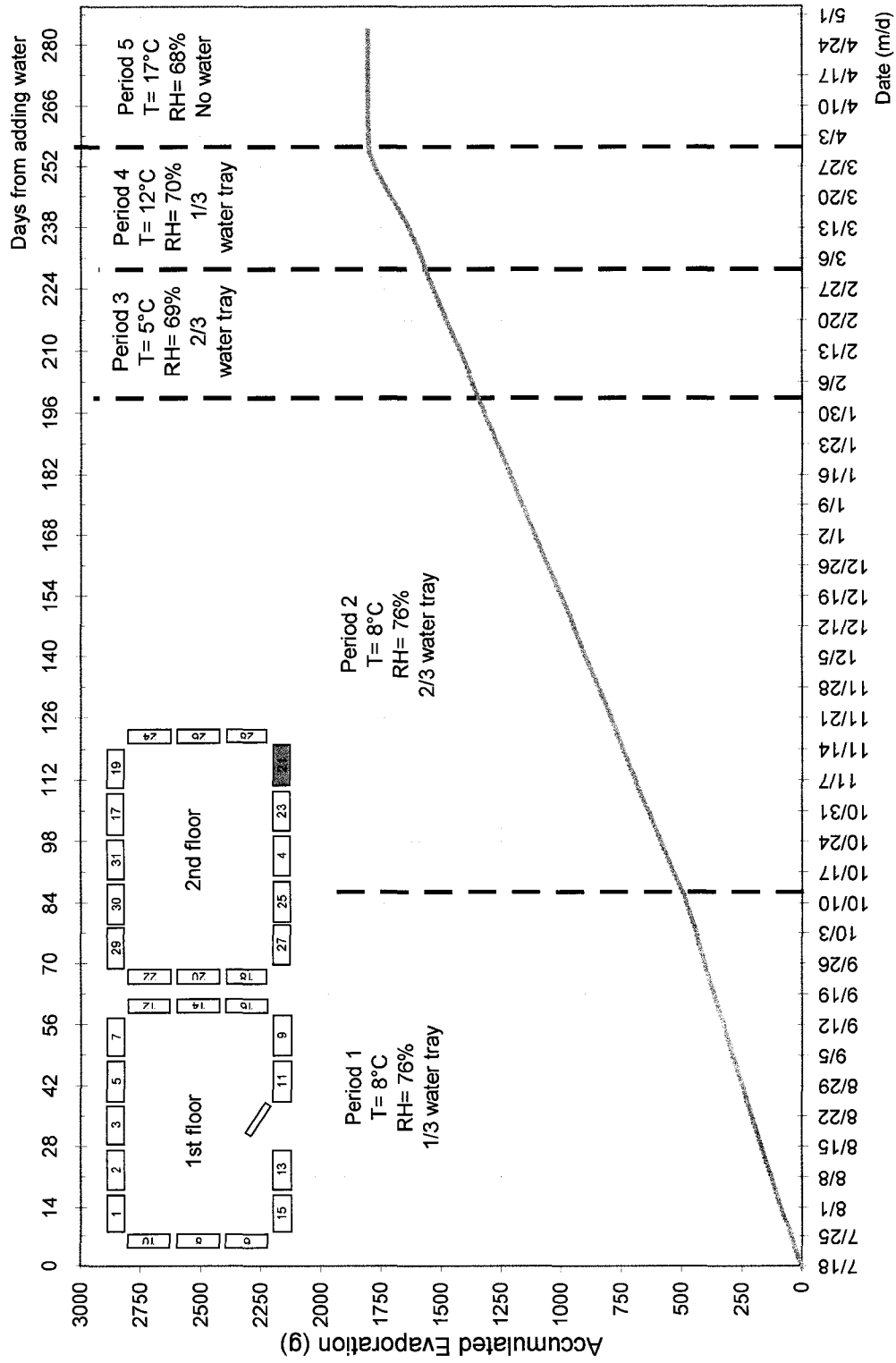


Figure B-21. Accumulated evaporation for wall assembly 21 (fiberboard, wood siding, vb) for the 5 test periods.

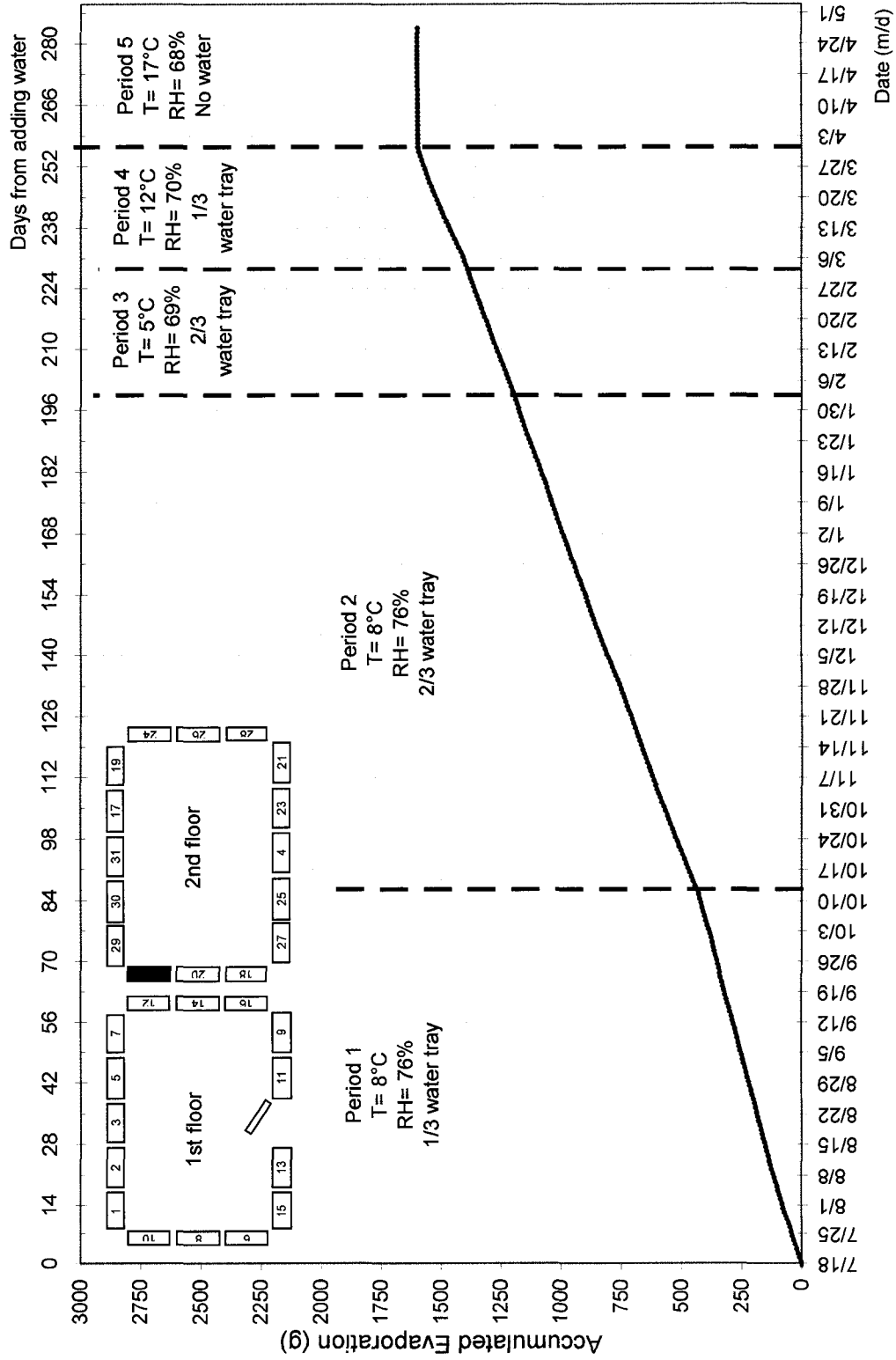


Figure B-22. Accumulated evaporation for wall assembly 22 (fiberboard, stucco, vb) for the 5 test periods

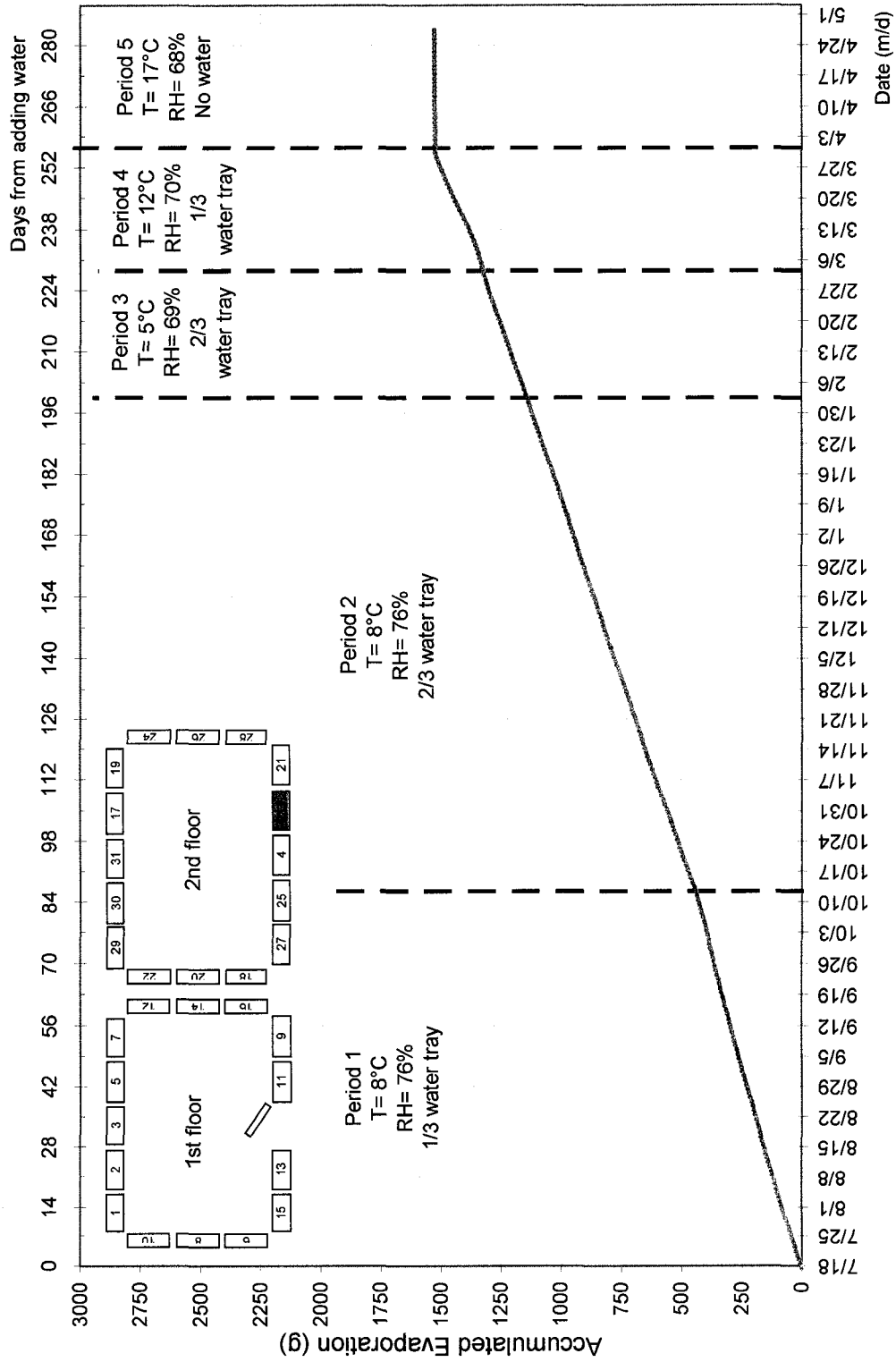


Figure B-23. Accumulated evaporation for wall assembly 23 (OSB, wood siding, no vb) for the 5 test periods

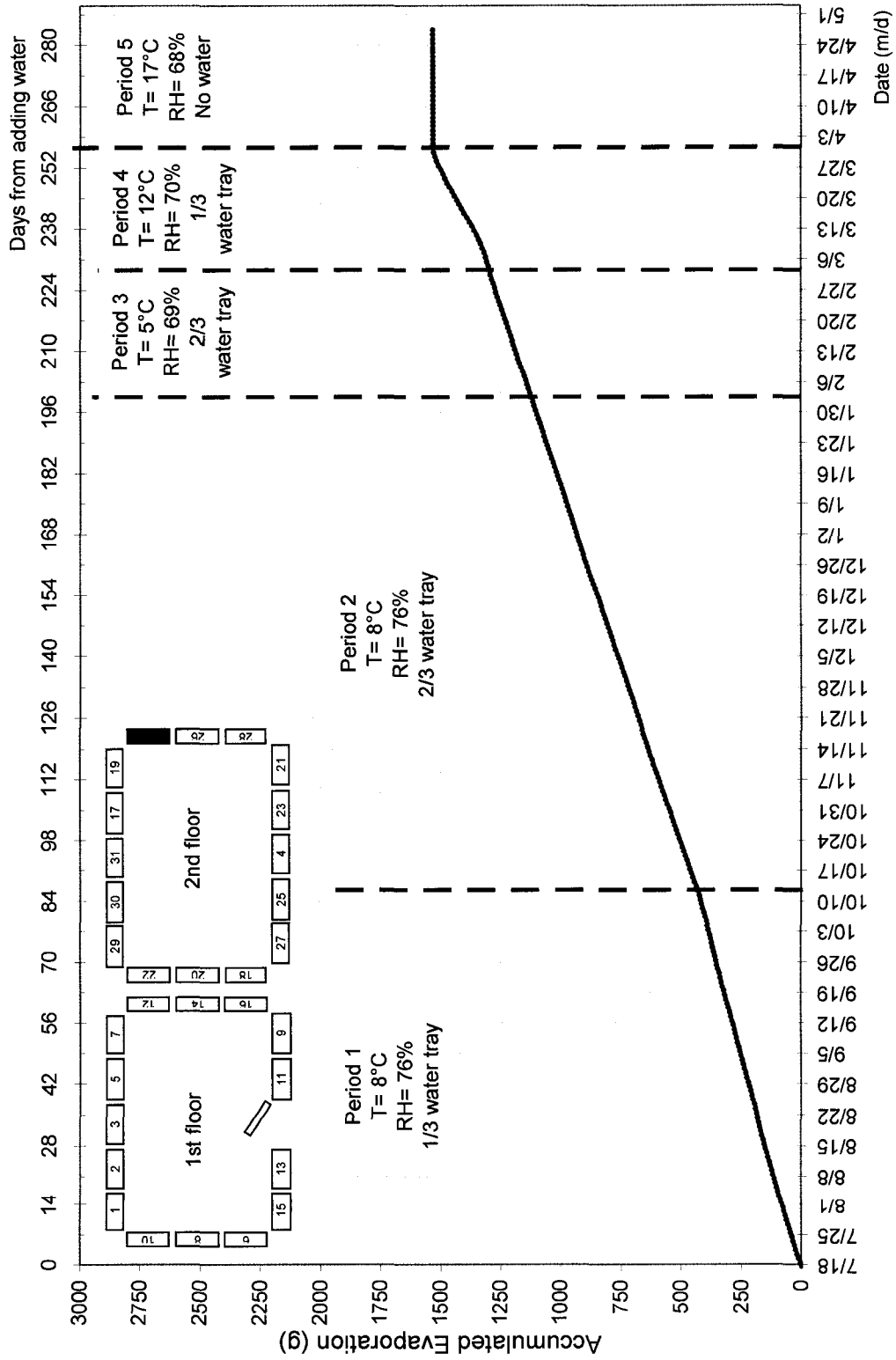


Figure B-24. Accumulated evaporation for wall assembly 24 (OSB, stucco, no vb) for the 5 test periods

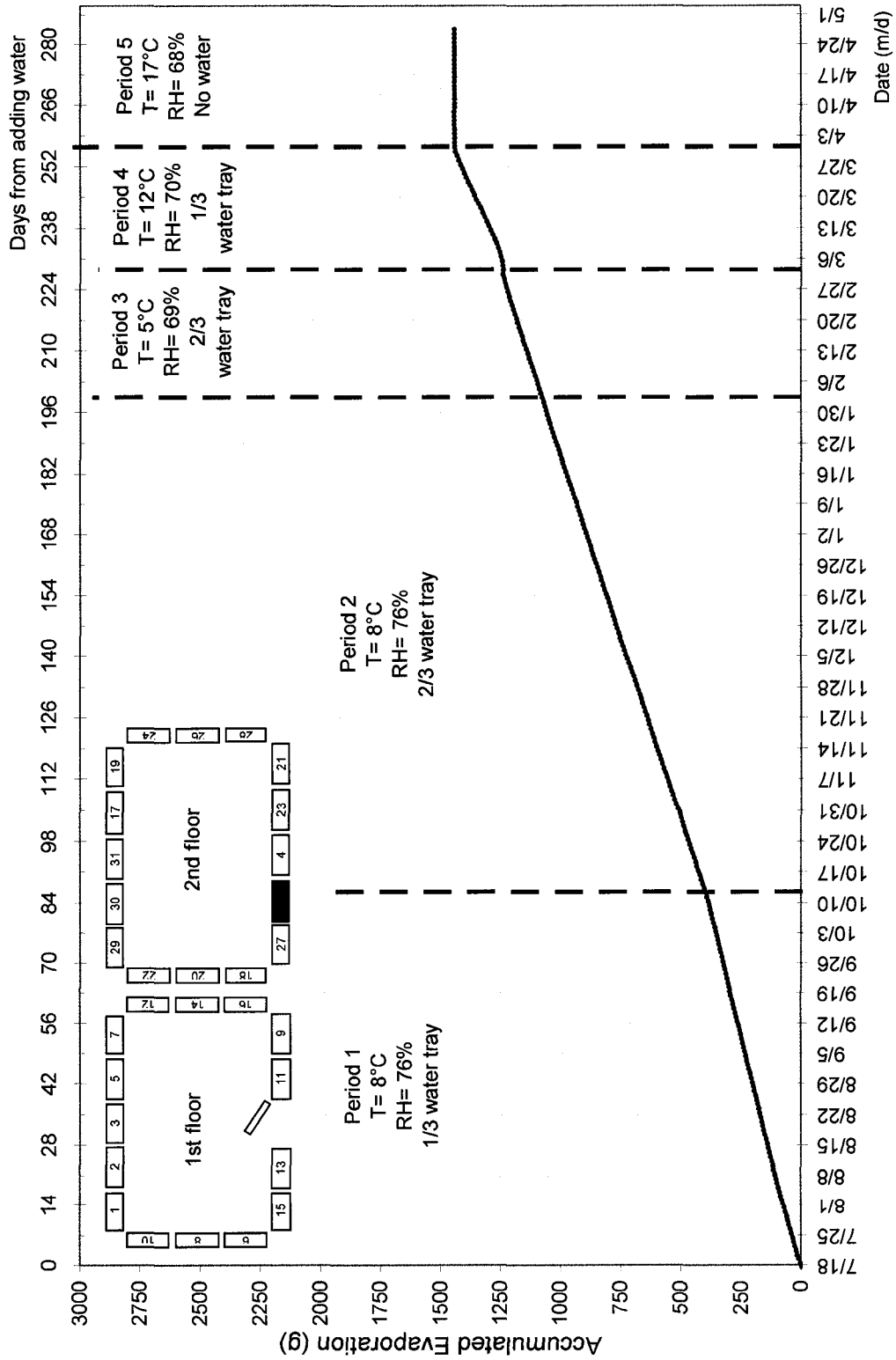


Figure B-25. Accumulated evaporation for wall assembly 2.5 (plywood, wood siding, no vb) for the 5 periods

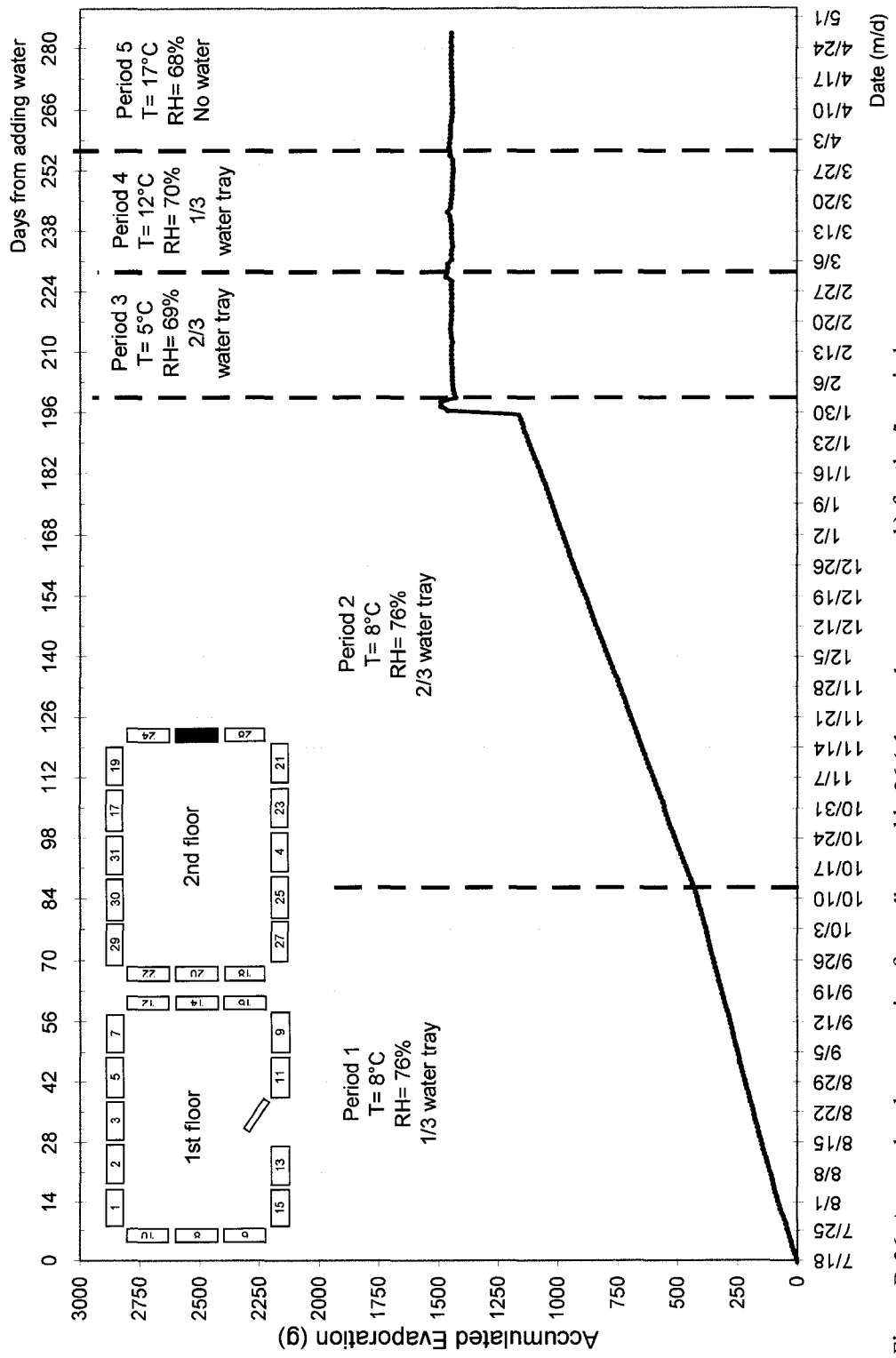


Figure B-26. Accumulated evaporation for wall assembly 26 (plywood, stucco, no vb) for the 5 periods

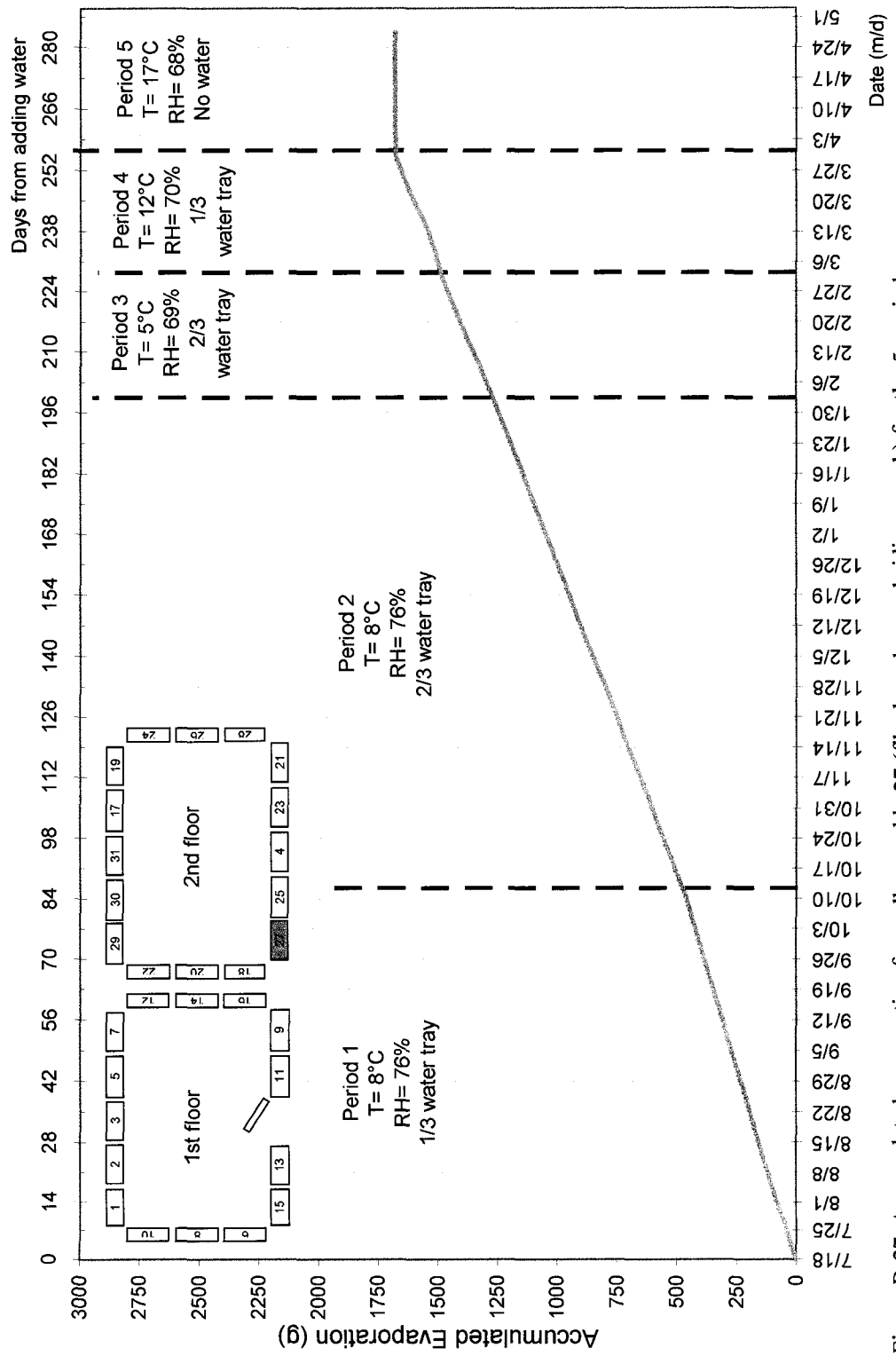


Figure B-27. Accumulated evaporation for wall assembly 27 (fiberboard, wood siding, no vb) for the 5 periods



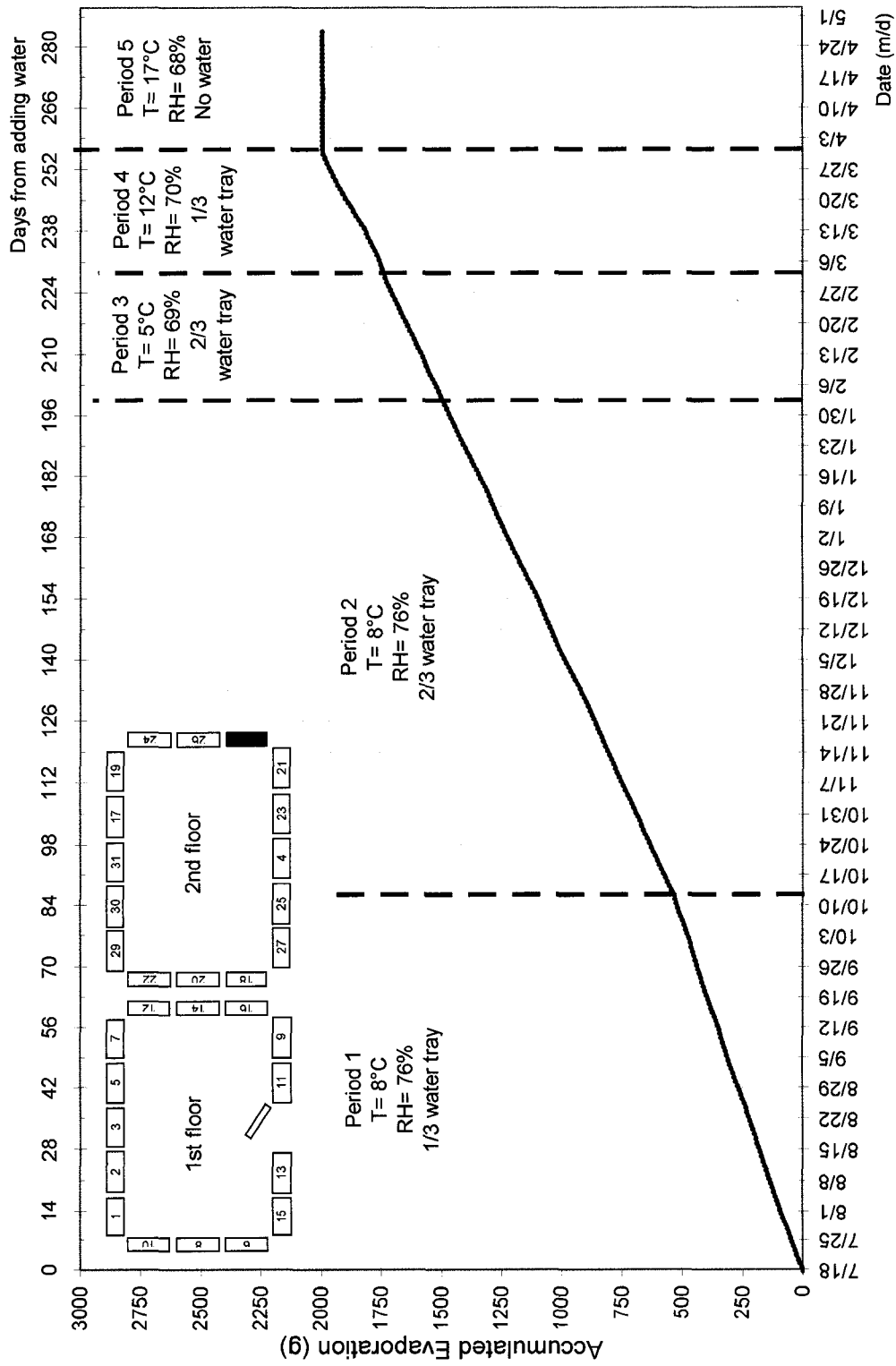


Figure B-28. Accumulated evaporation for wall assembly 28 (fiberboard, stucco, no vb) for the 5 periods

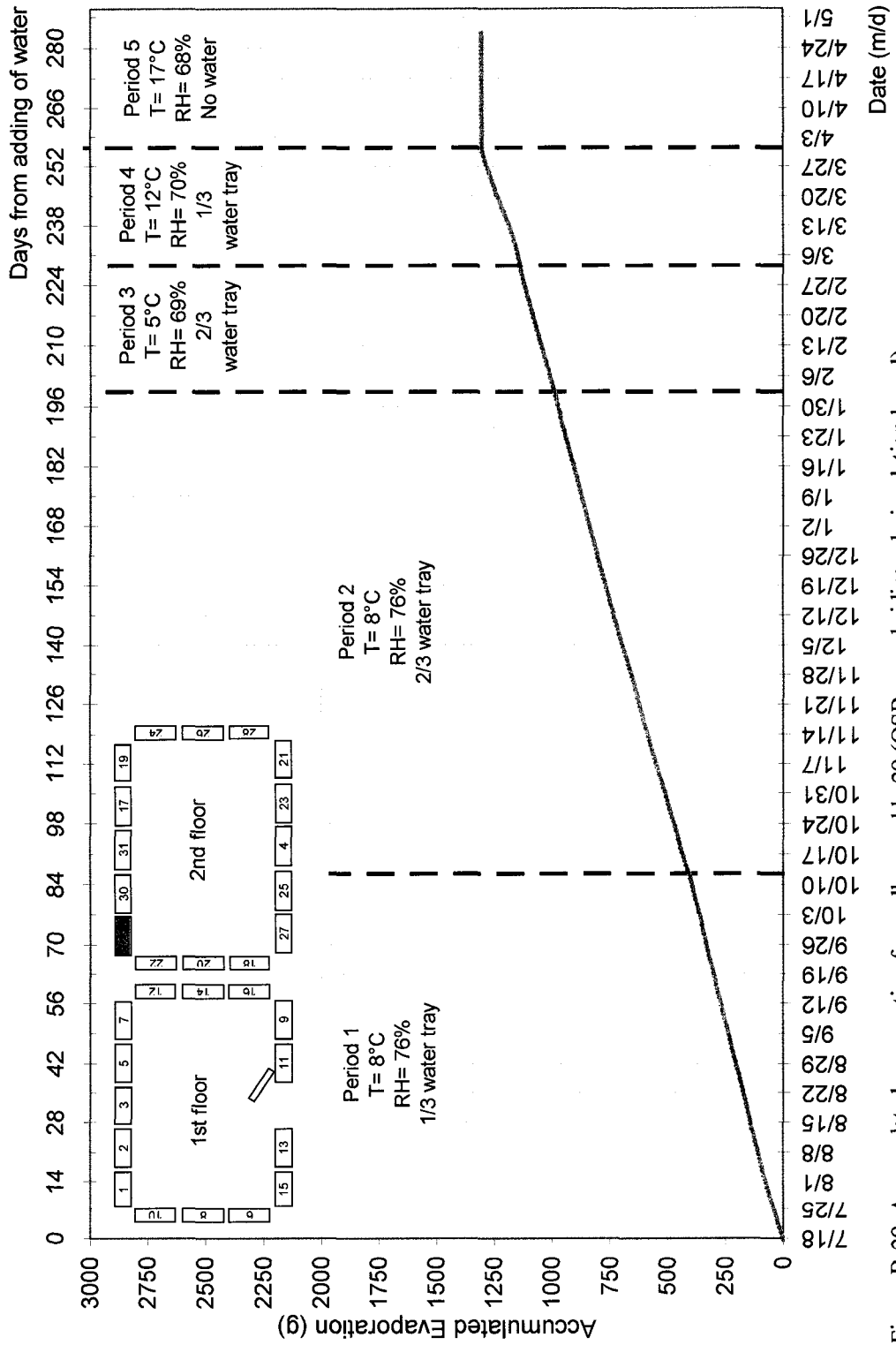


Figure B-29. Accumulated evaporation for wall assembly 29 (OSB, wood siding, vb, insulation board)

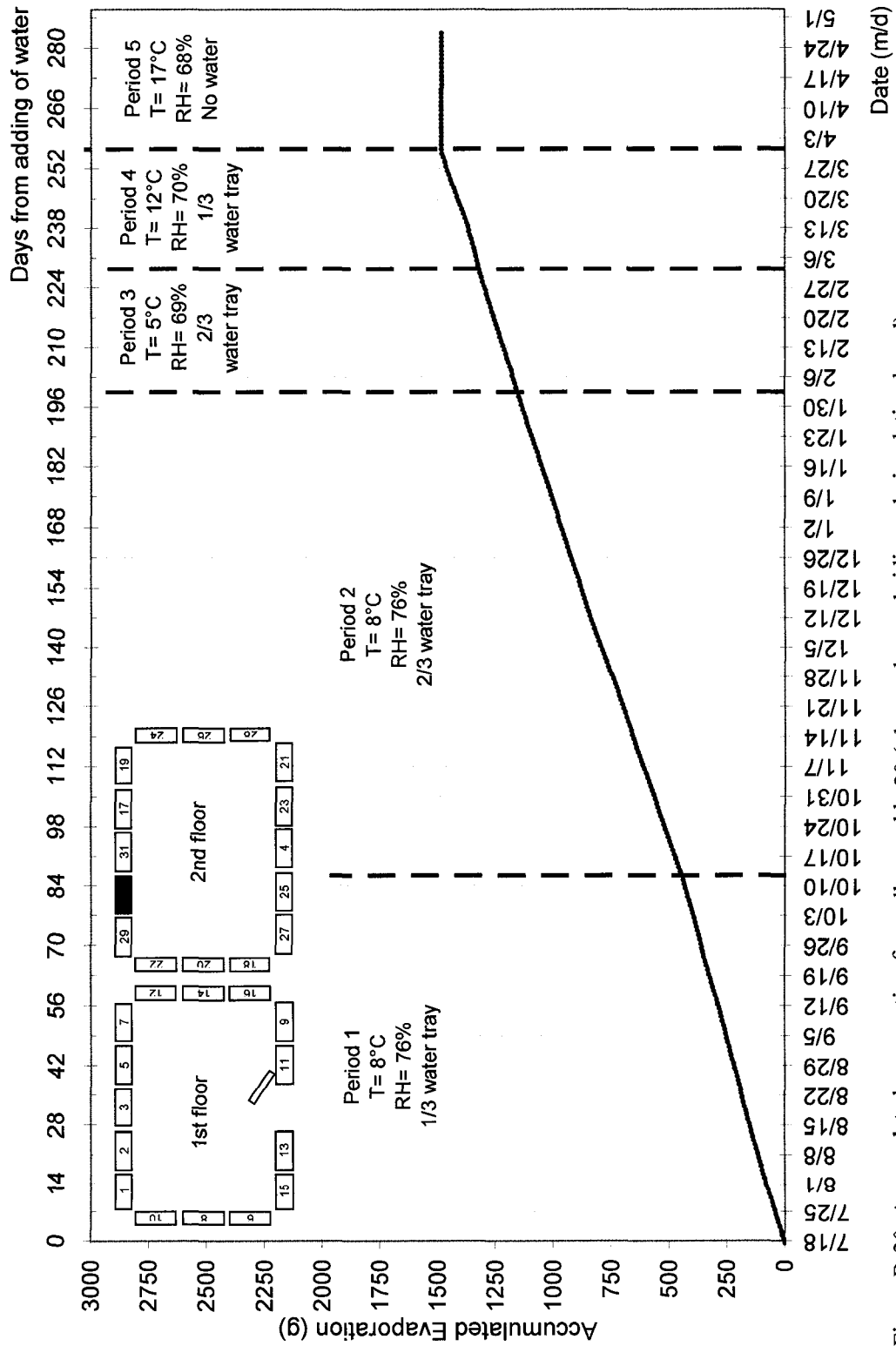


Figure B-30. Accumulated evaporation for wall assembly 30 (plywood, wood siding, vb, insulation board)

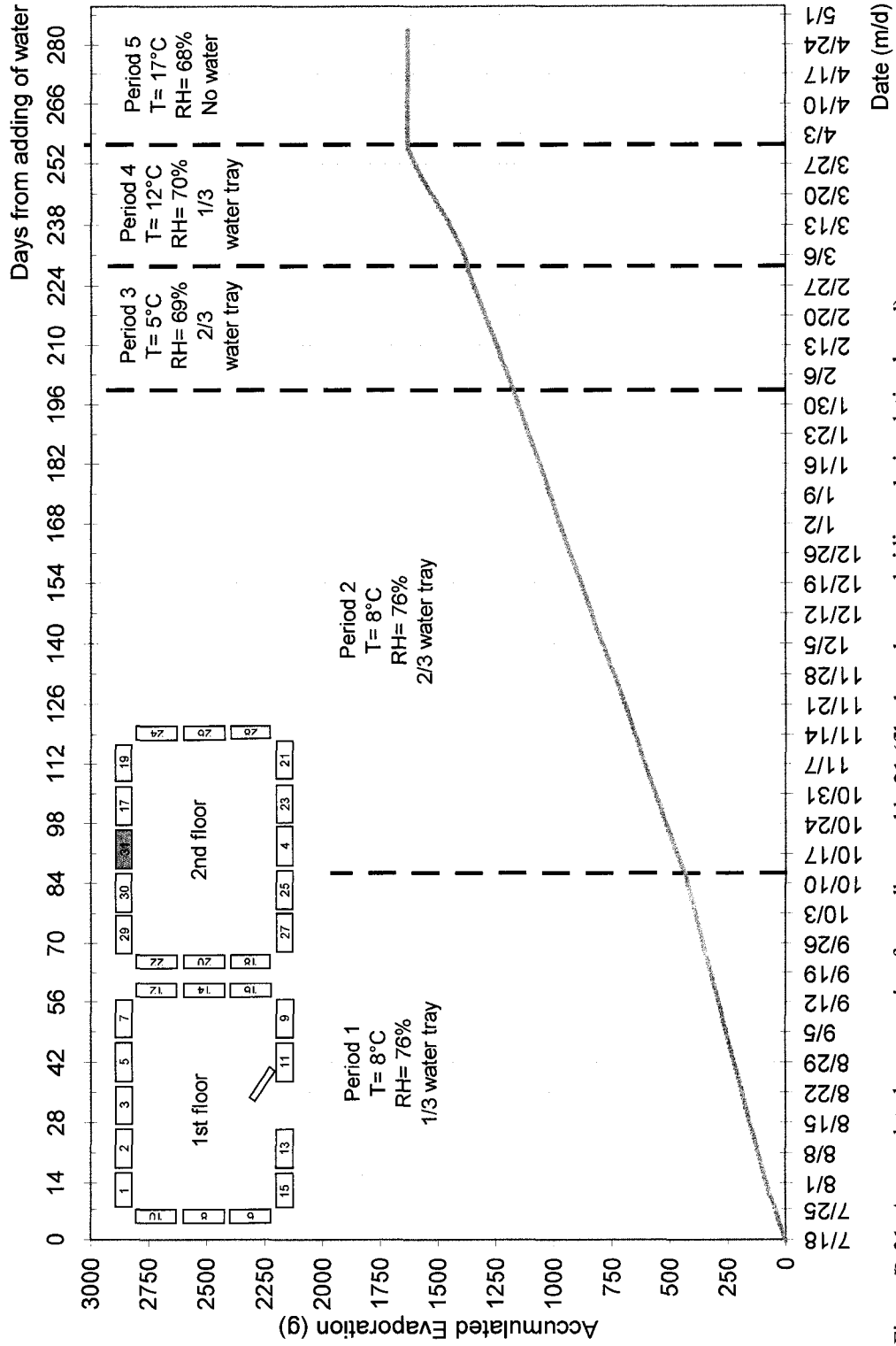


Figure B-31. Accumulated evaporation for wall assembly 31 (fiberboard, wood siding, vb, insulation board)

**Appendix E**  
**MOISTURE CONTENT PROFILES**

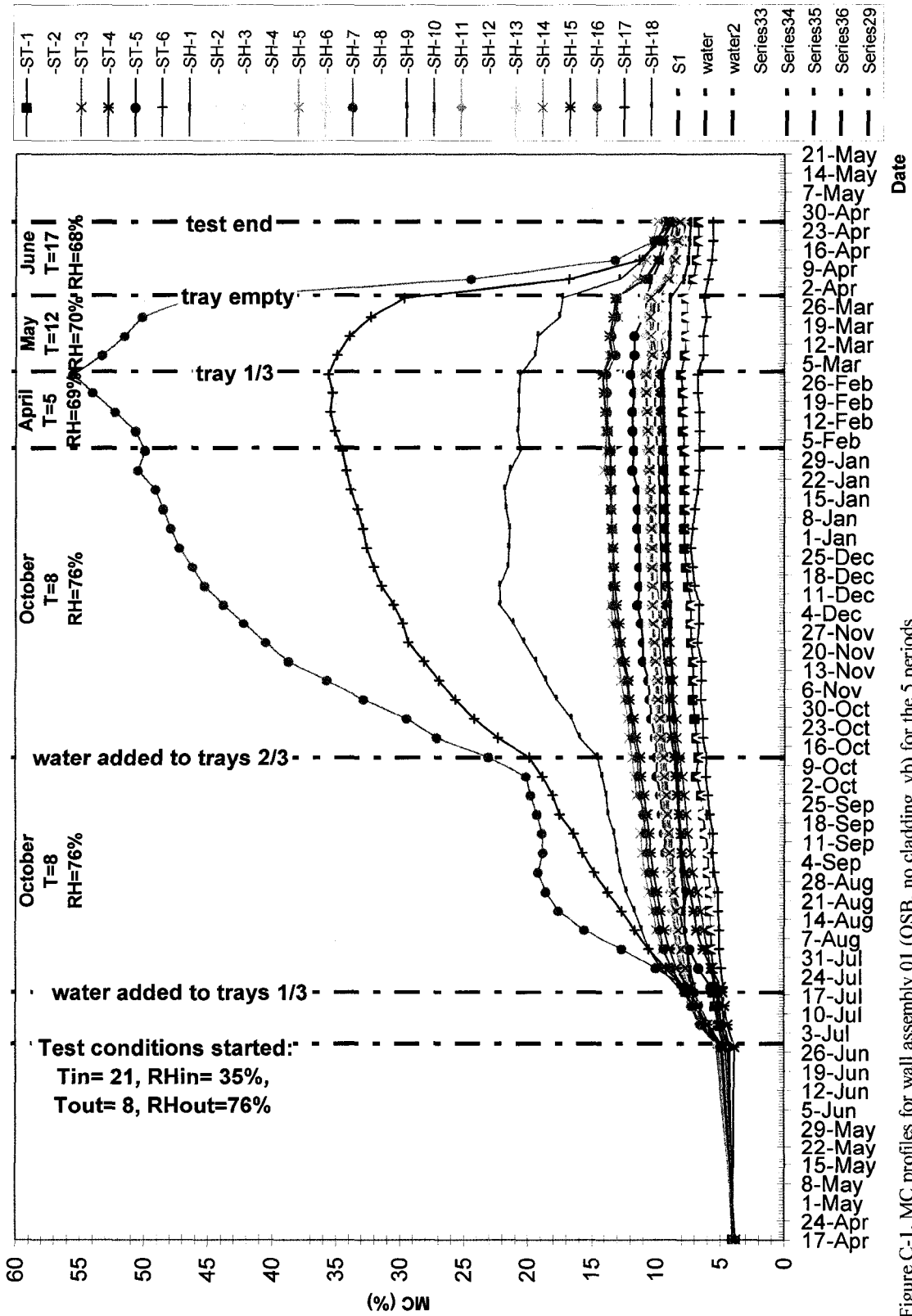


Figure C-1. MC profiles for wall assembly 01 (OSB, no cladding, vb) for the 5 periods

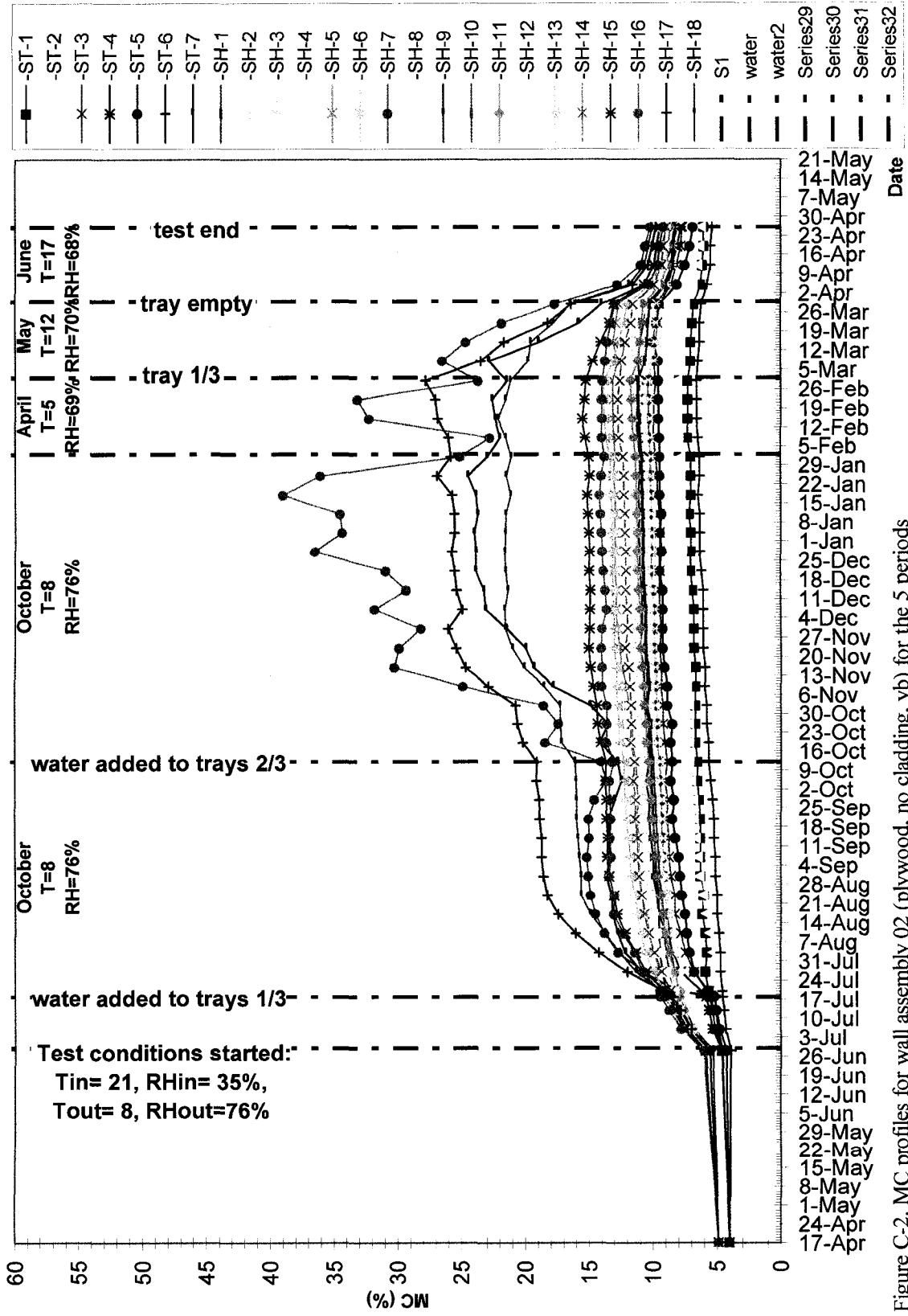


Figure C-2. MC profiles for wall assembly 02 (plywood, no cladding, vb) for the 5 periods

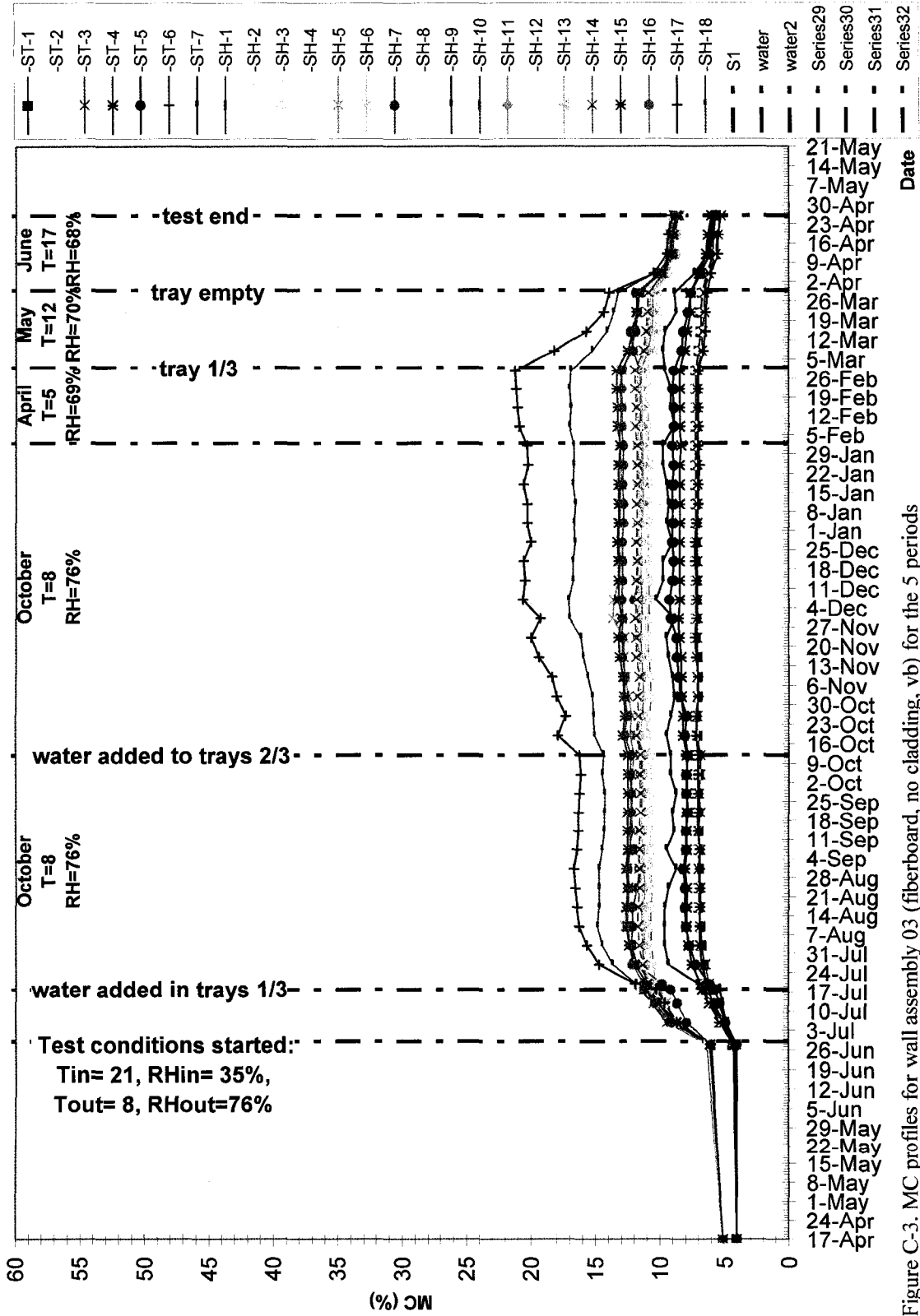


Figure C-3. MC profiles for wall assembly 03 (fiberboard, no cladding, vb) for the 5 periods



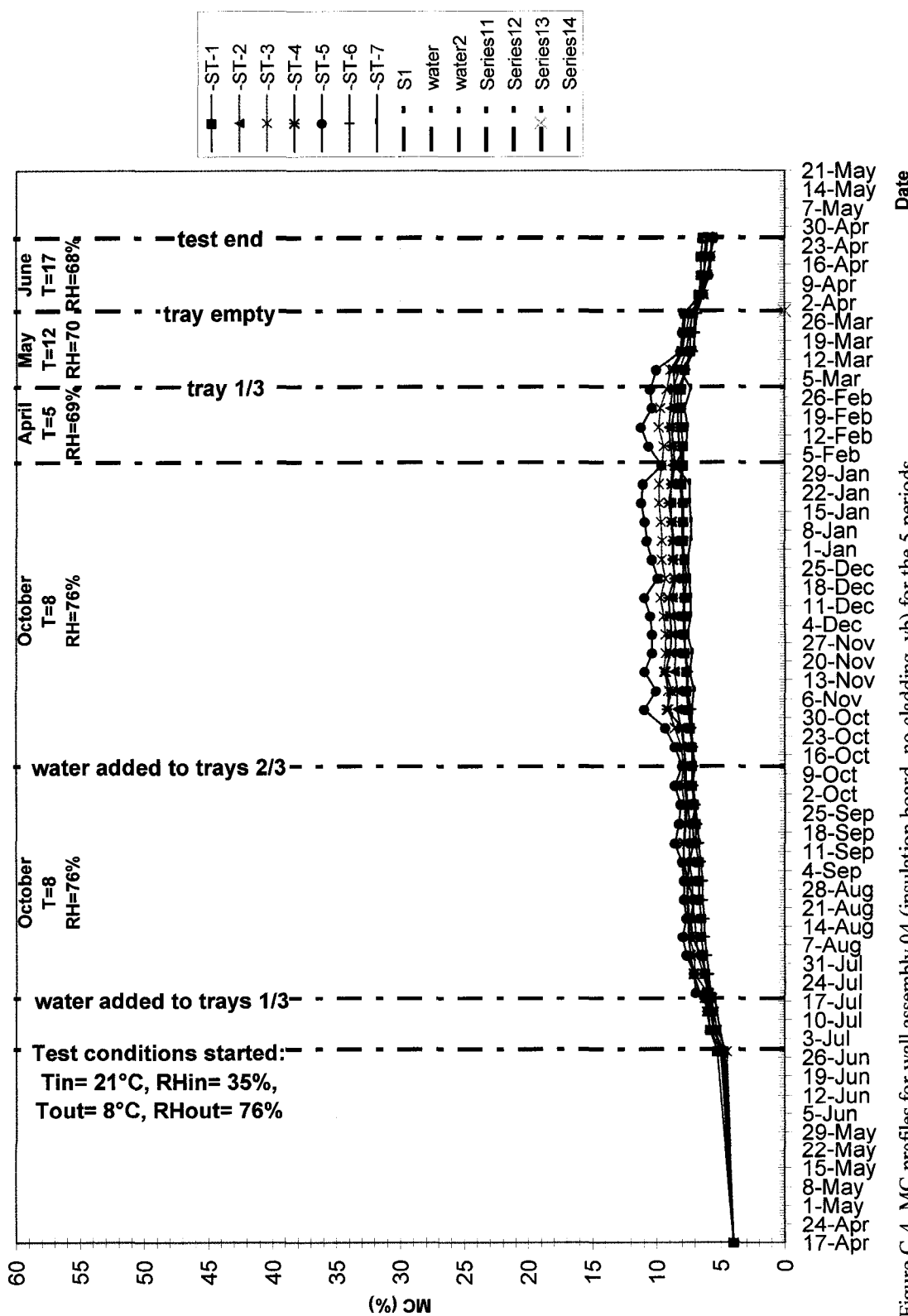


Figure C-4. MC profiles for wall assembly 04 (insulation board, no cladding, vb) for the 5 periods

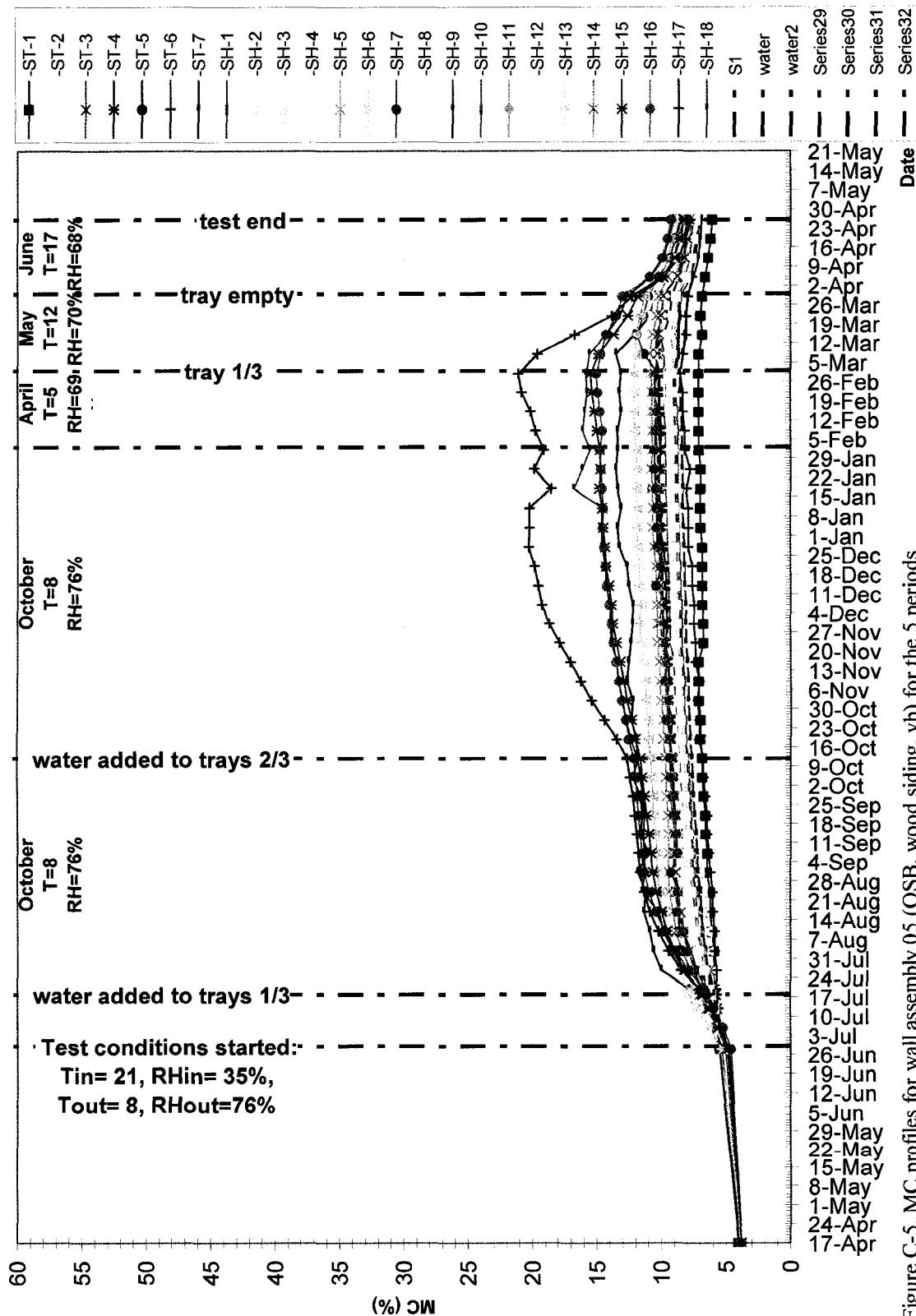


Figure C-5. MC profiles for wall assembly 05 (OSB, wood siding, vb) for the 5 periods

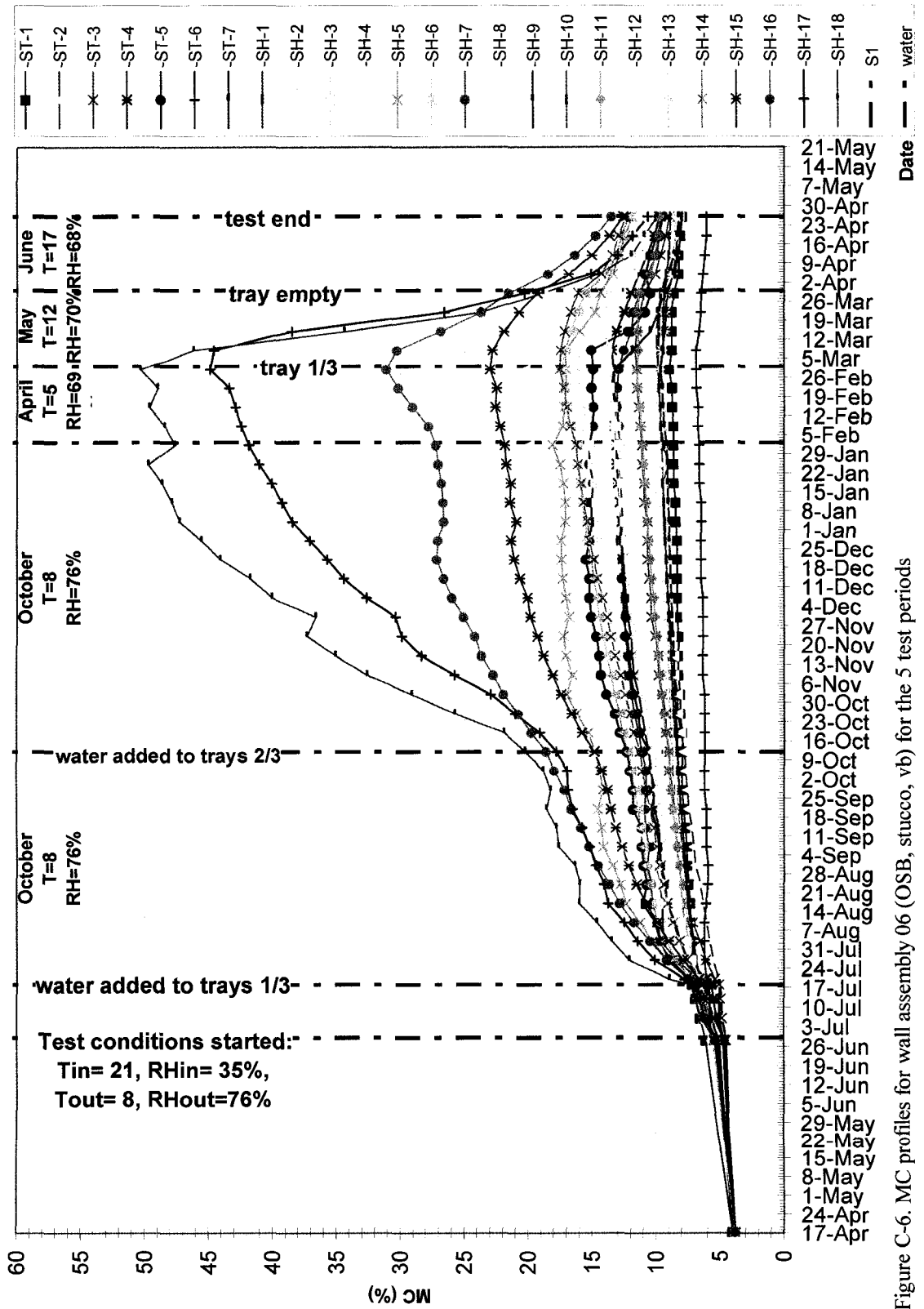


Figure C-6. MC profiles for wall assembly 06 (OSB, stucco, vb) for the 5 test periods

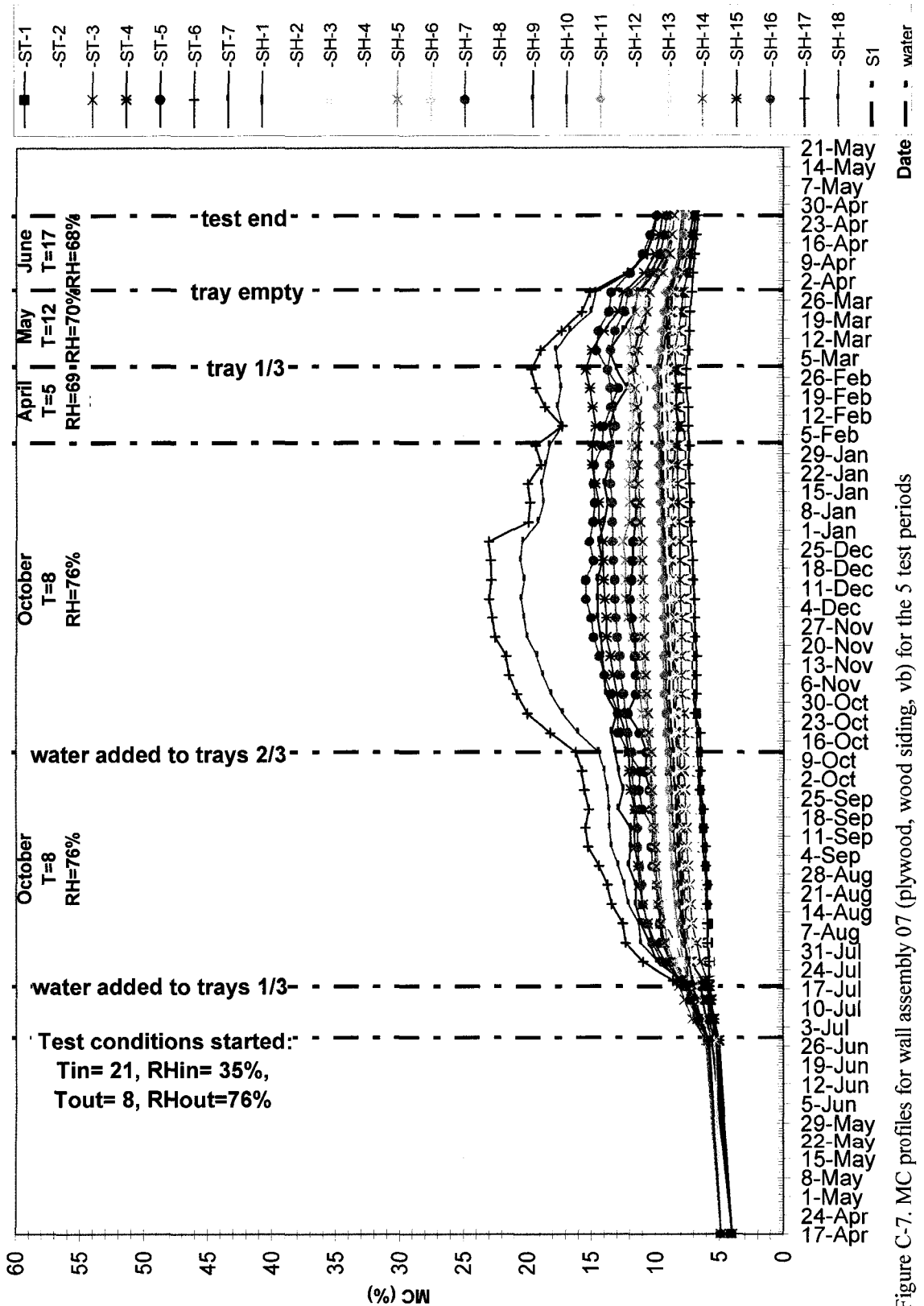


Figure C-7. MC profiles for wall assembly 07 (plywood, wood siding, vb) for the 5 test periods

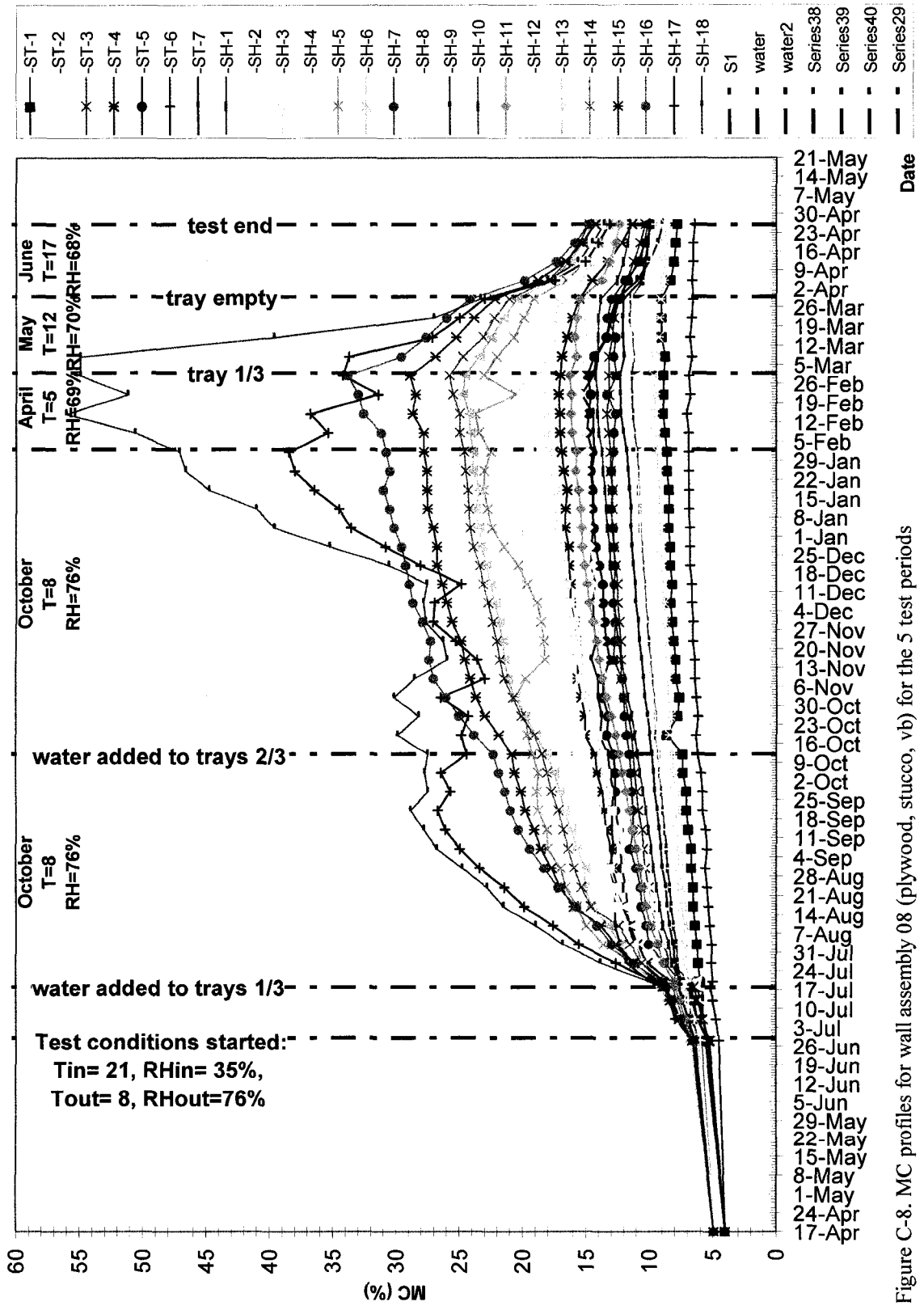


Figure C-8. MC profiles for wall assembly 08 (plywood, stucco, vb) for the 5 test periods

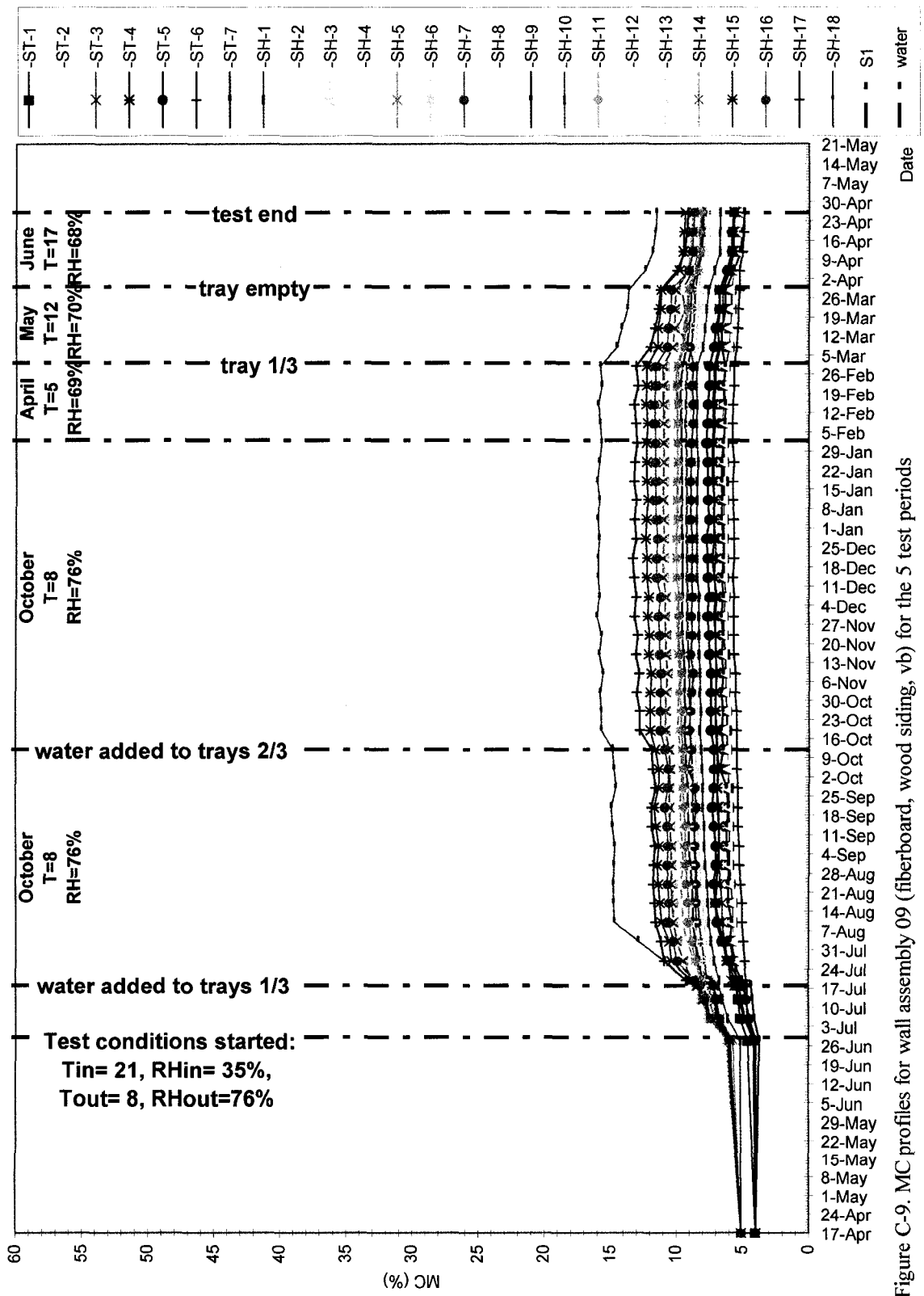


Figure C-9. MC profiles for wall assembly 09 (fiberboard, wood siding, vb) for the 5 test periods

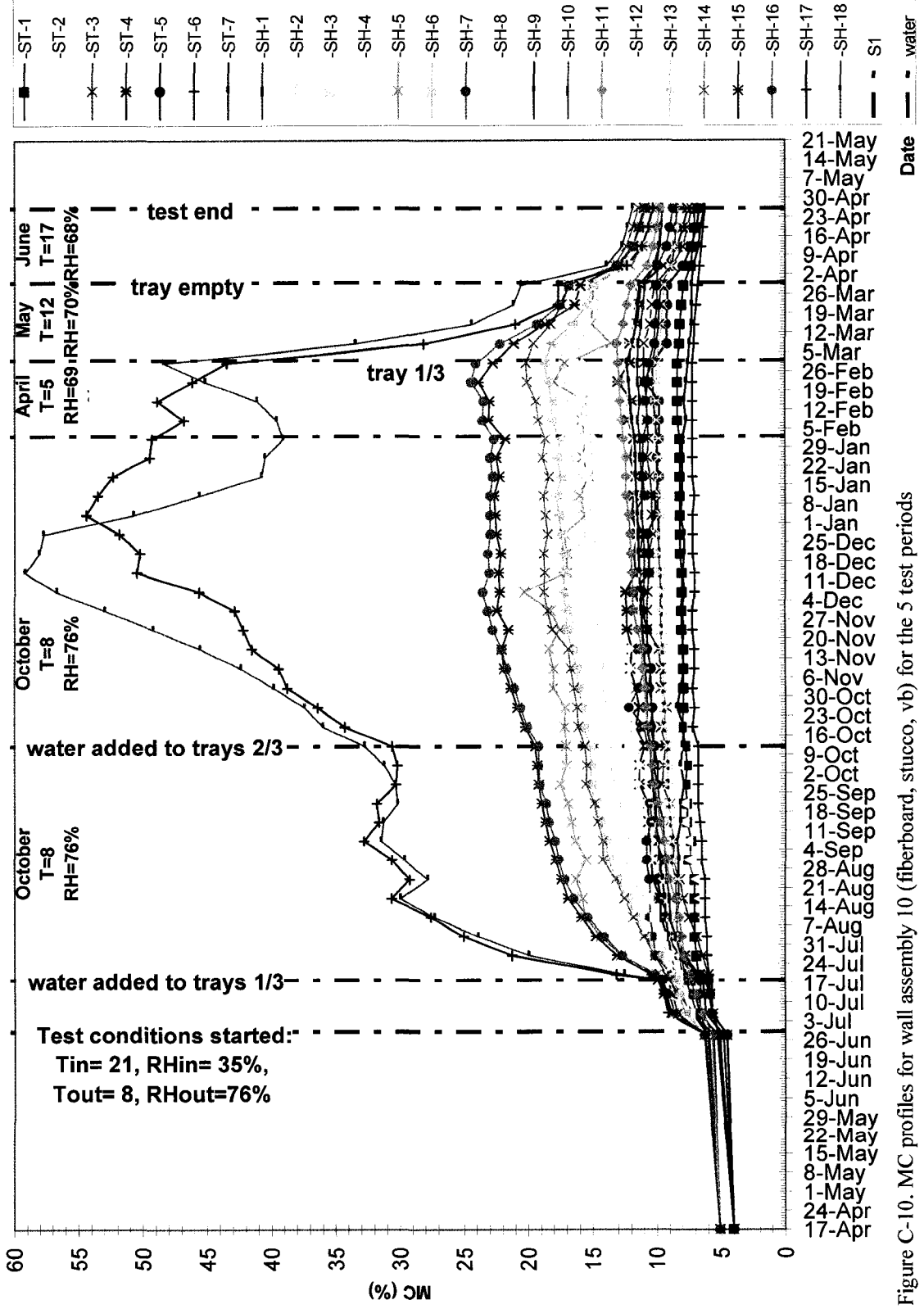


Figure C-10. MC profiles for wall assembly 10 (fiberboard, stucco, vb) for the 5 test periods

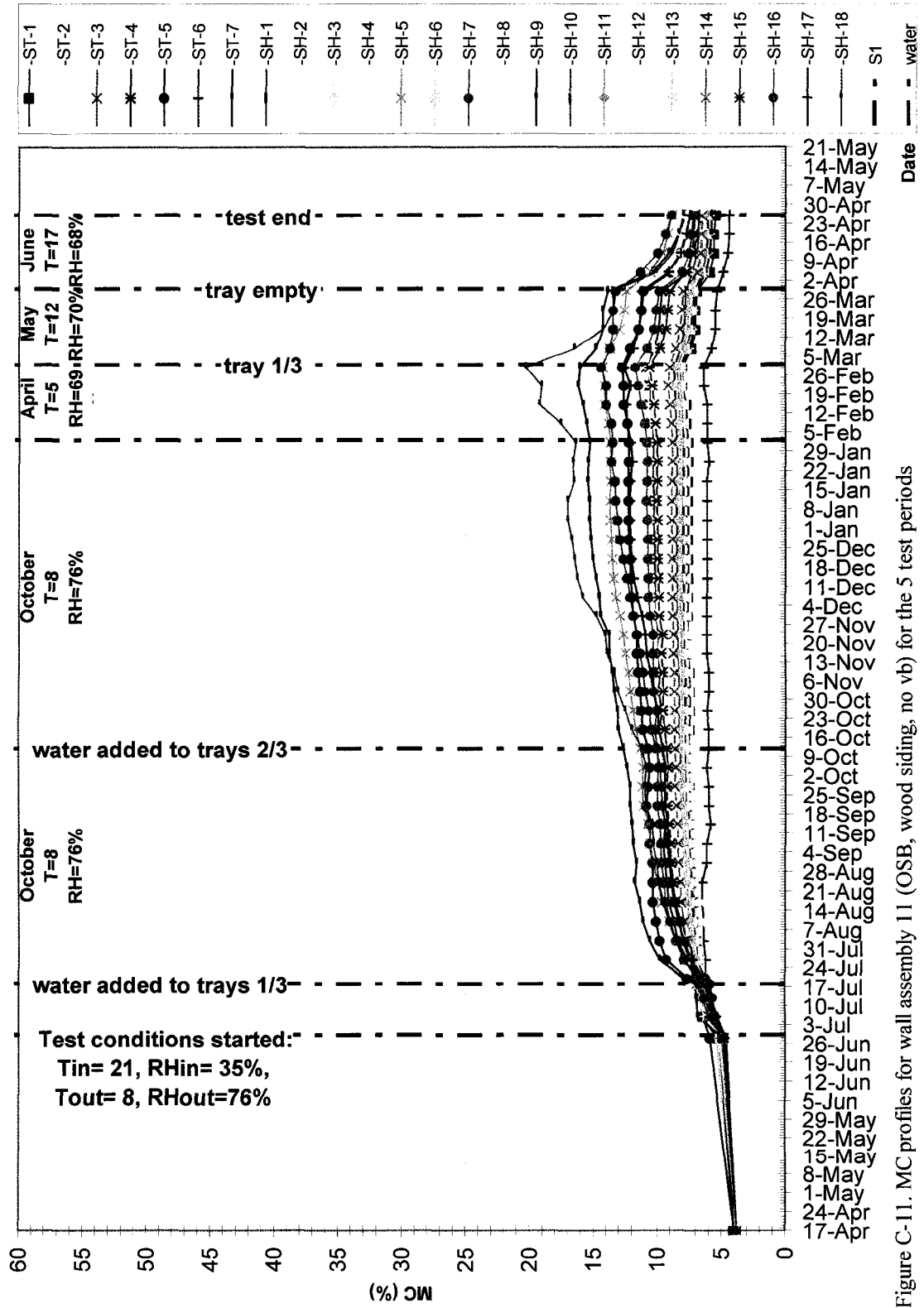


Figure C-11. MC profiles for wall assembly 11 (OSB, wood siding, no vb) for the 5 test periods



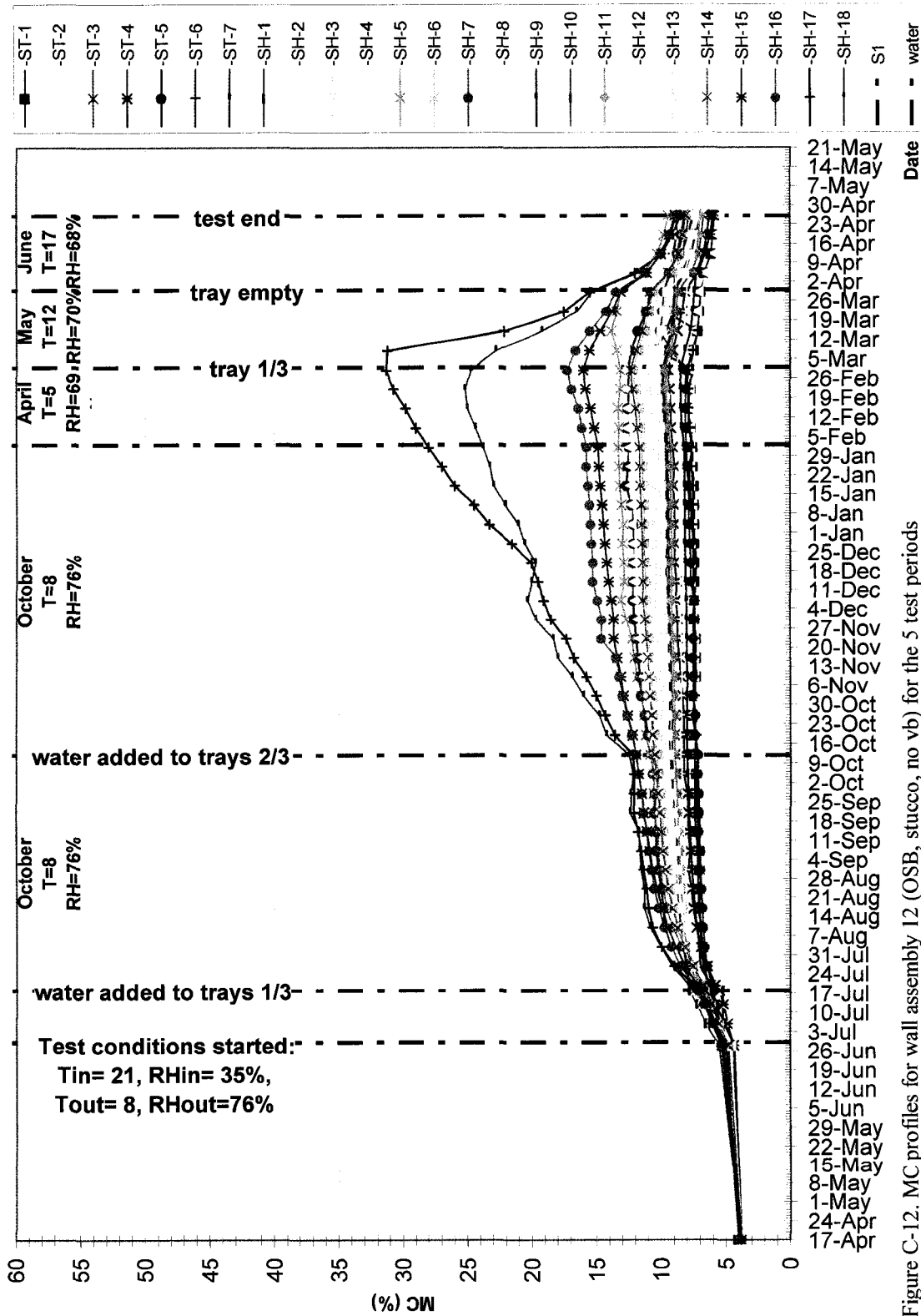


Figure C-12. MC profiles for wall assembly 12 (OSB, stucco, no vb) for the 5 test periods

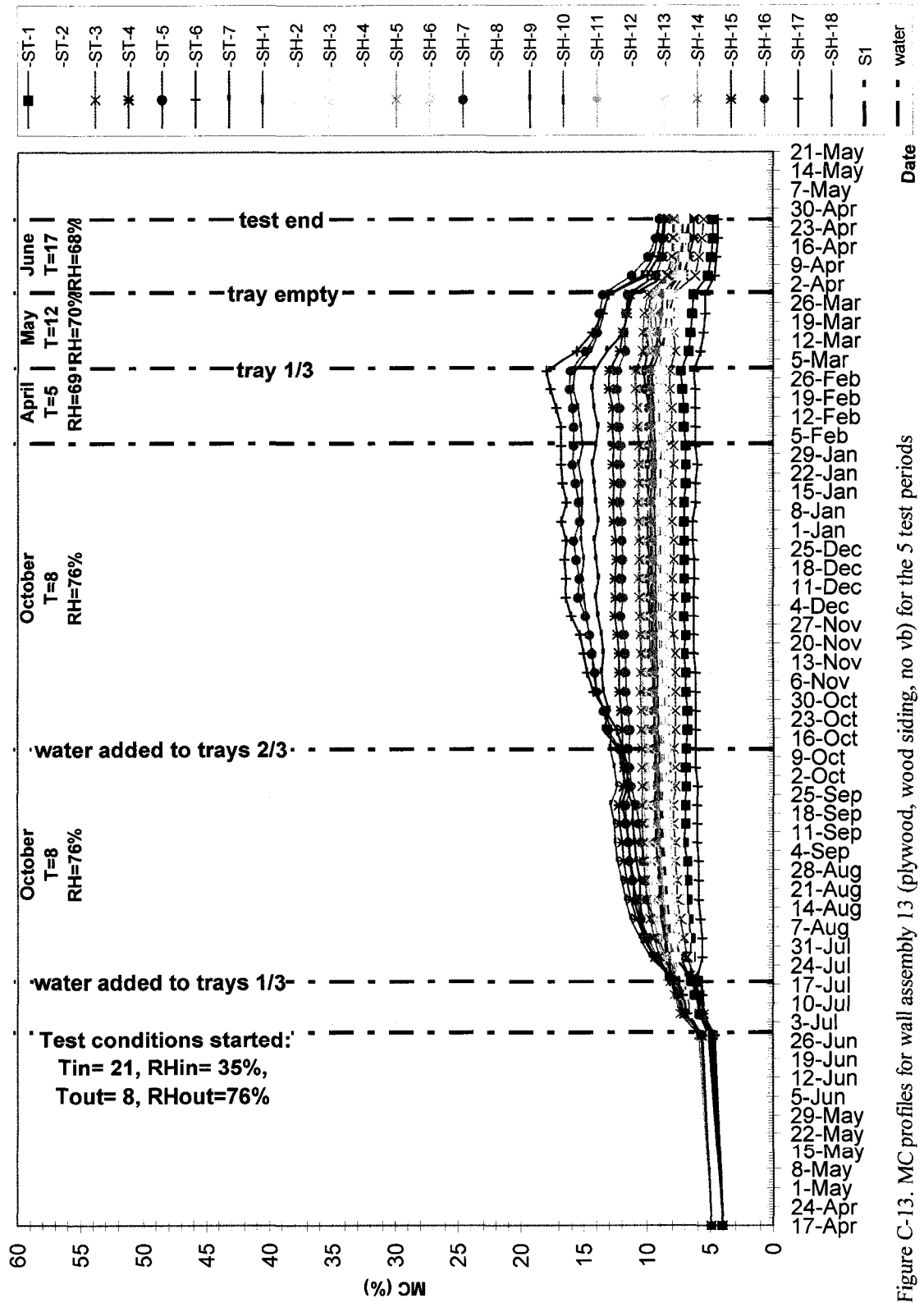


Figure C-13. MC profiles for wall assembly 13 (plywood, wood siding, no vb) for the 5 test periods

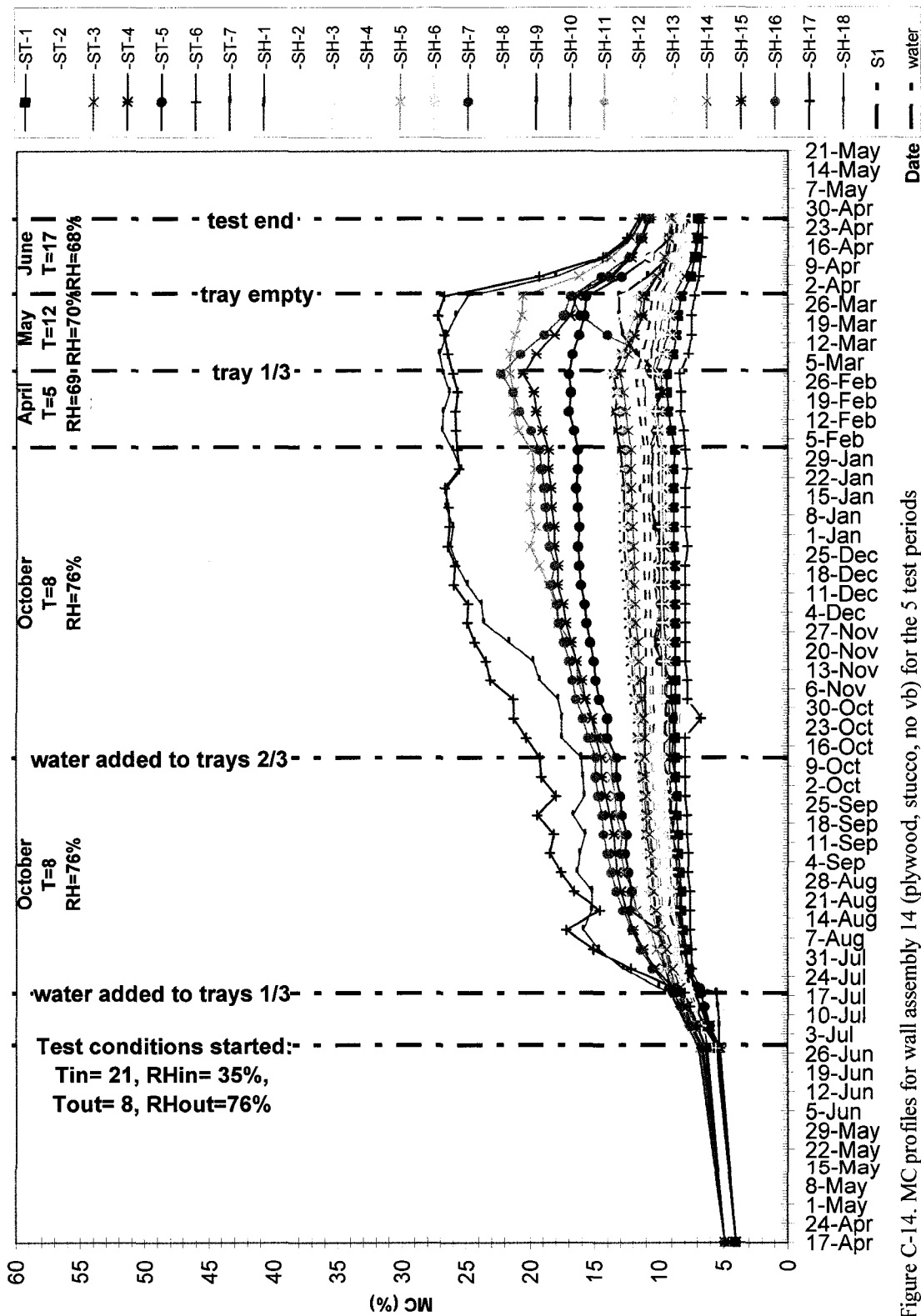


Figure C-14. MC profiles for wall assembly 14 (plywood, stucco, no vb) for the 5 test periods

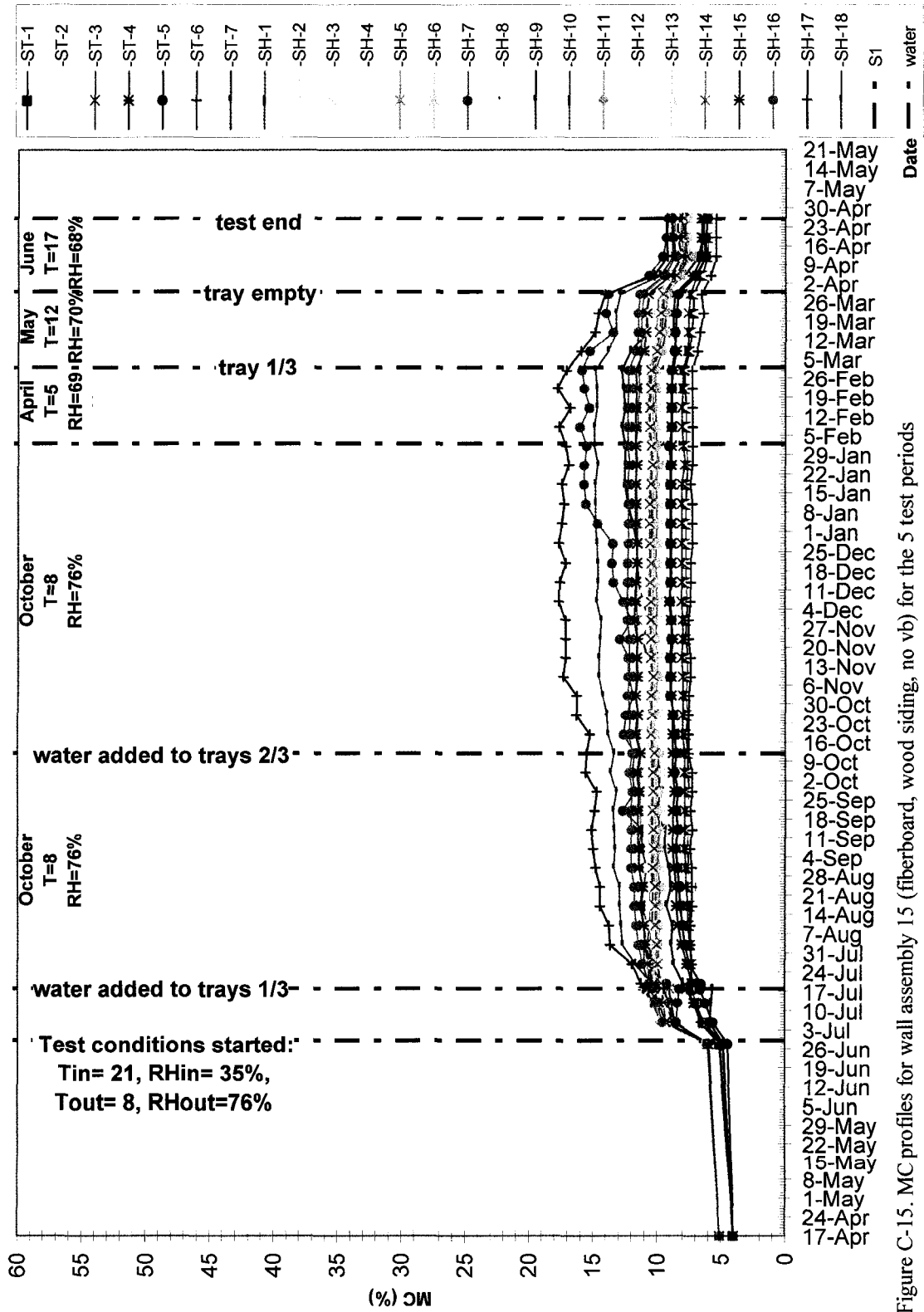


Figure C-15. MC profiles for wall assembly 15 (fiberboard, wood siding, no vb) for the 5 test periods

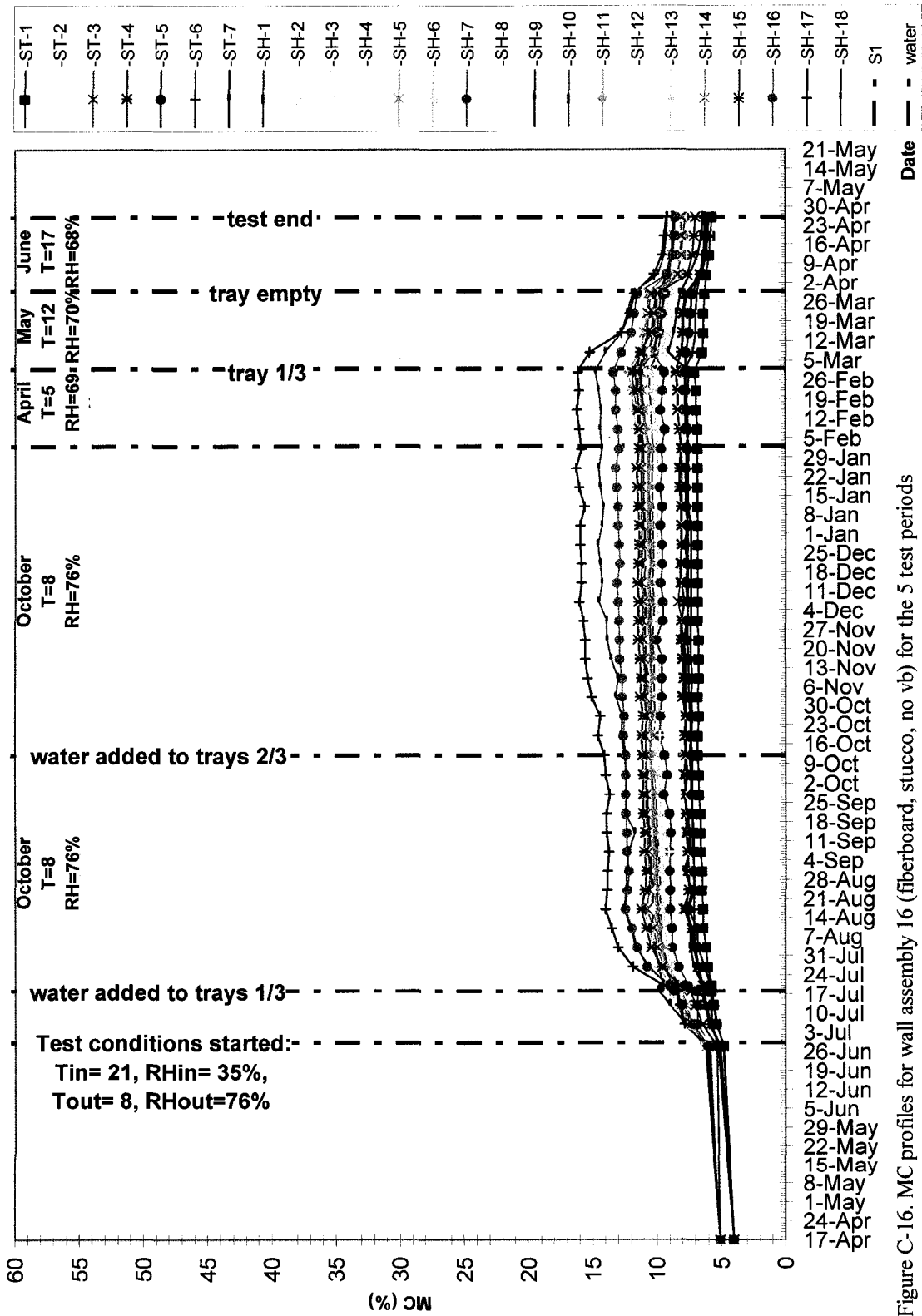


Figure C-16. MC profiles for wall assembly 16 (fiberboard, stucco, no vb) for the 5 test periods

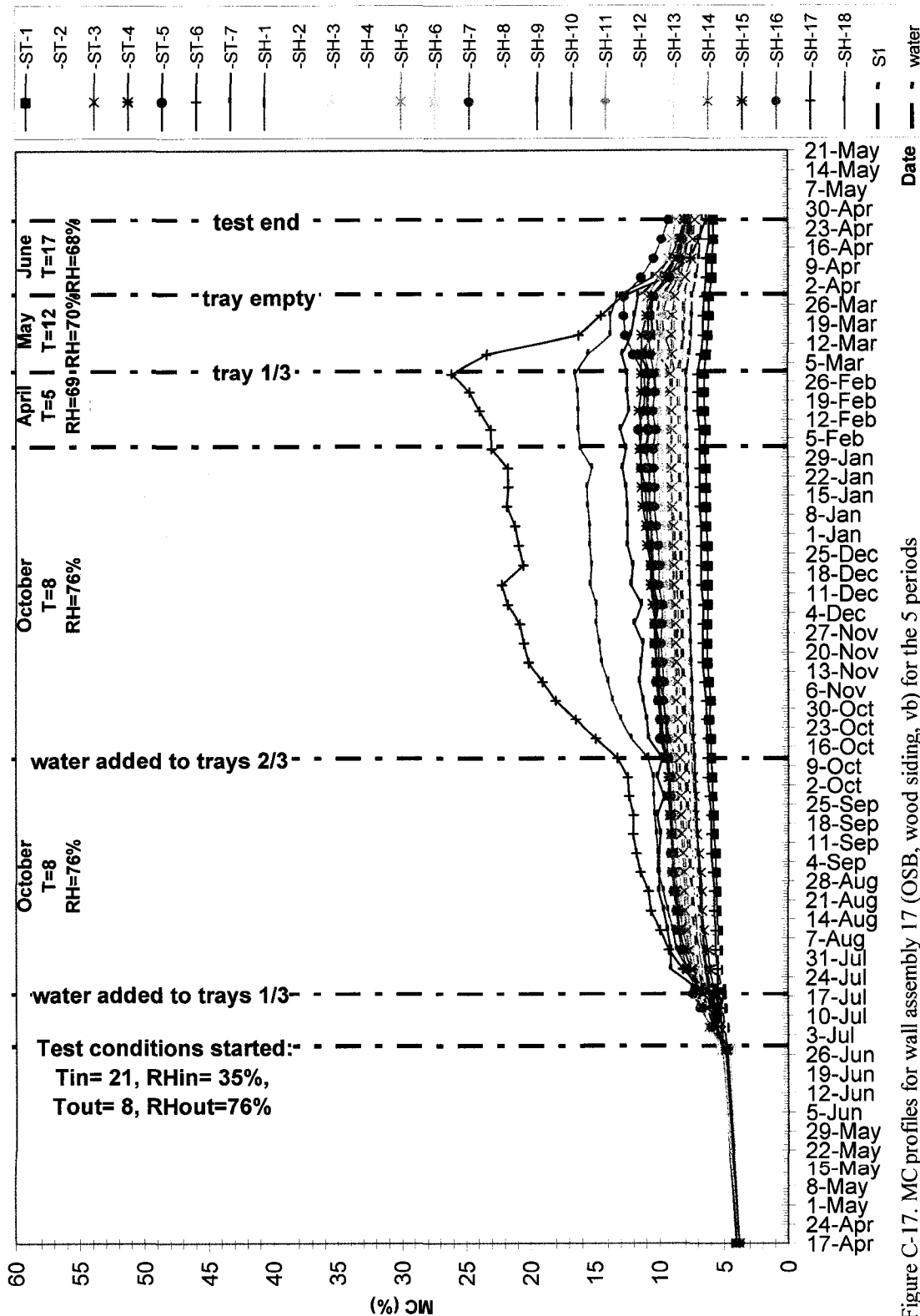


Figure C-17. MC profiles for wall assembly 17 (OSB, wood siding, vb) for the 5 periods

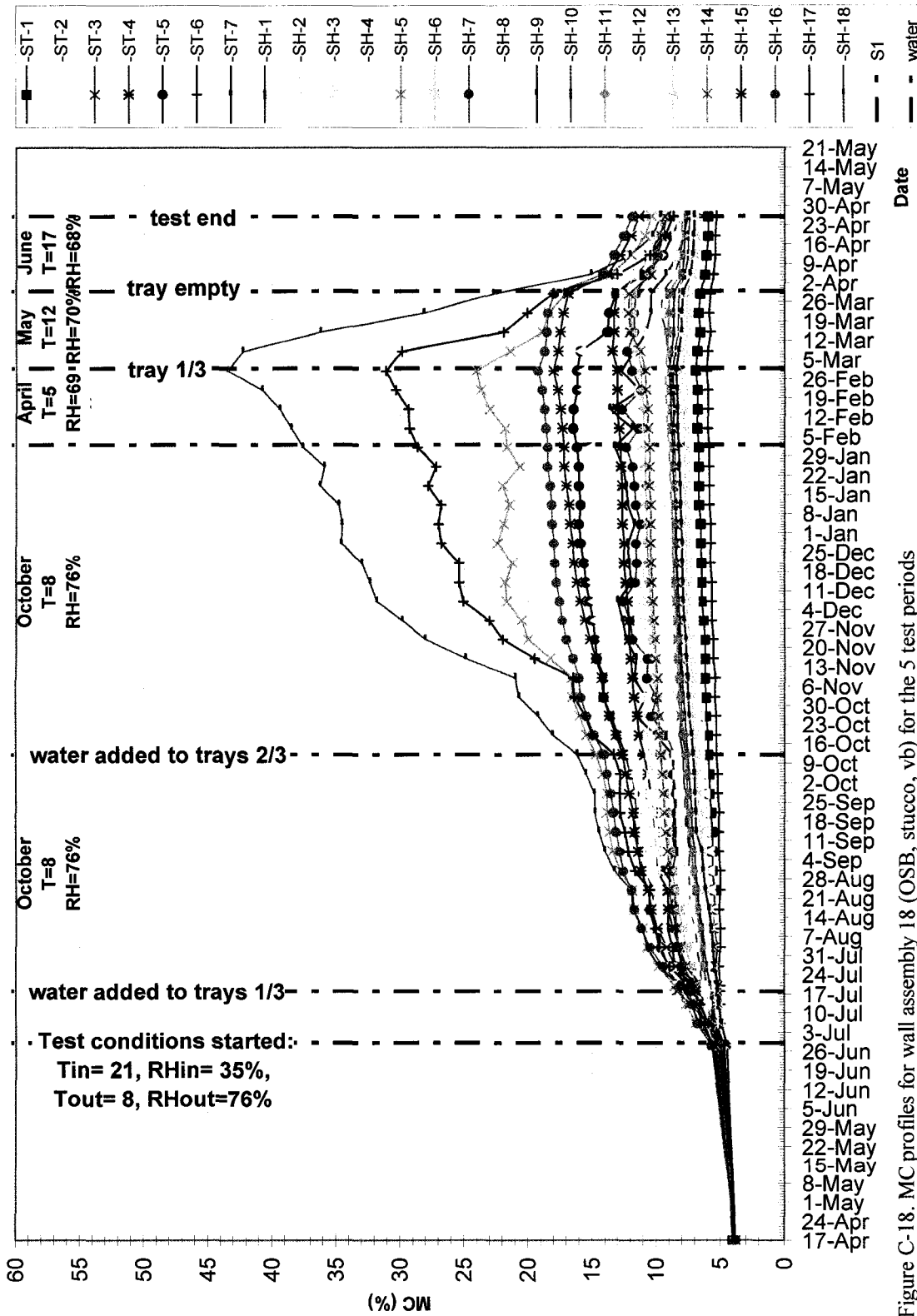


Figure C-18. MC profiles for wall assembly 18 (OSB, stucco, vb) for the 5 test periods

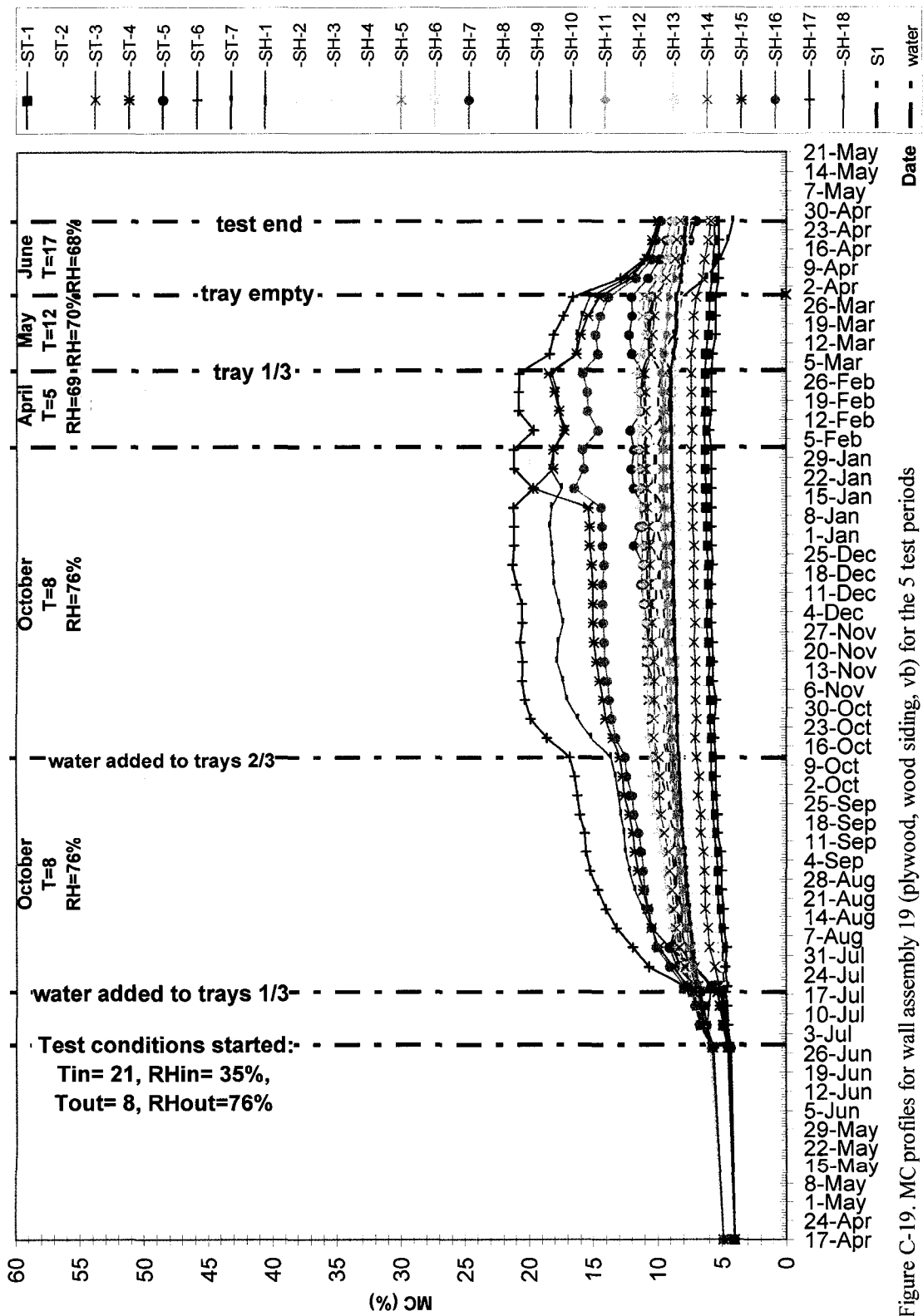


Figure C-19. MC profiles for wall assembly 19 (plywood, wood siding, vb) for the 5 test periods



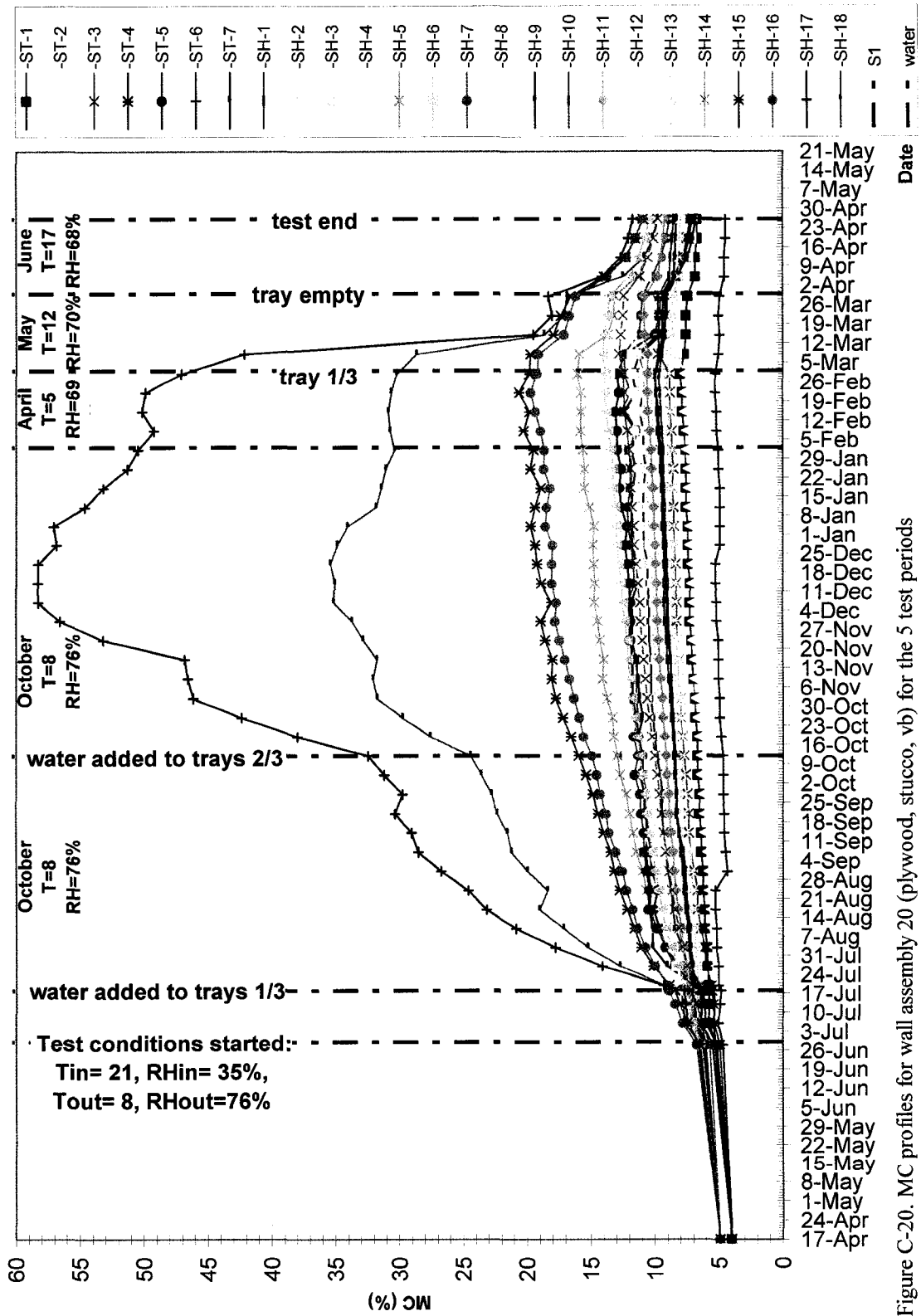


Figure C-20. MC profiles for wall assembly 20 (plywood, stucco, vb) for the 5 test periods

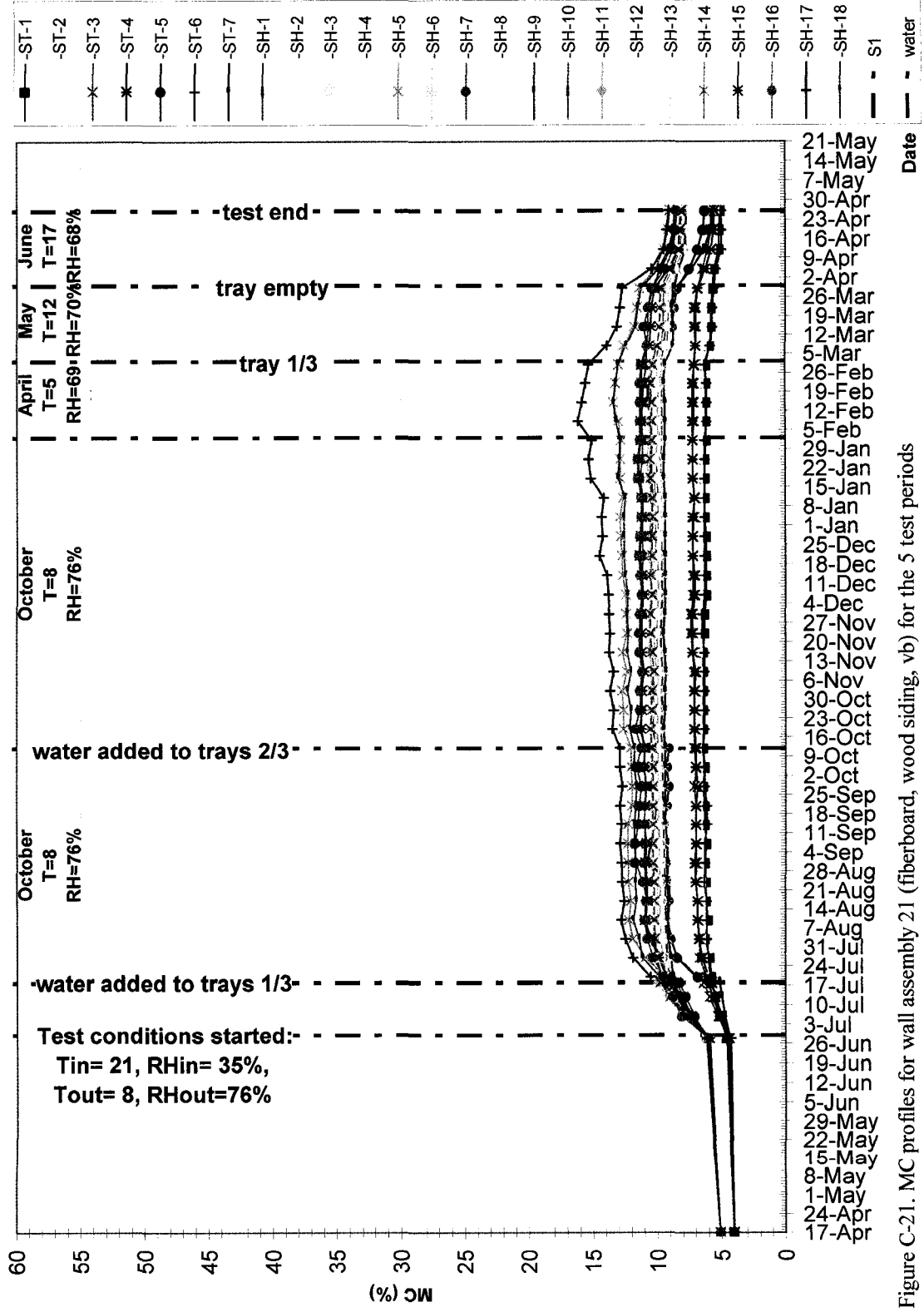


Figure C-21. MC profiles for wall assembly 21 (fiberboard, wood siding, vb) for the 5 test periods

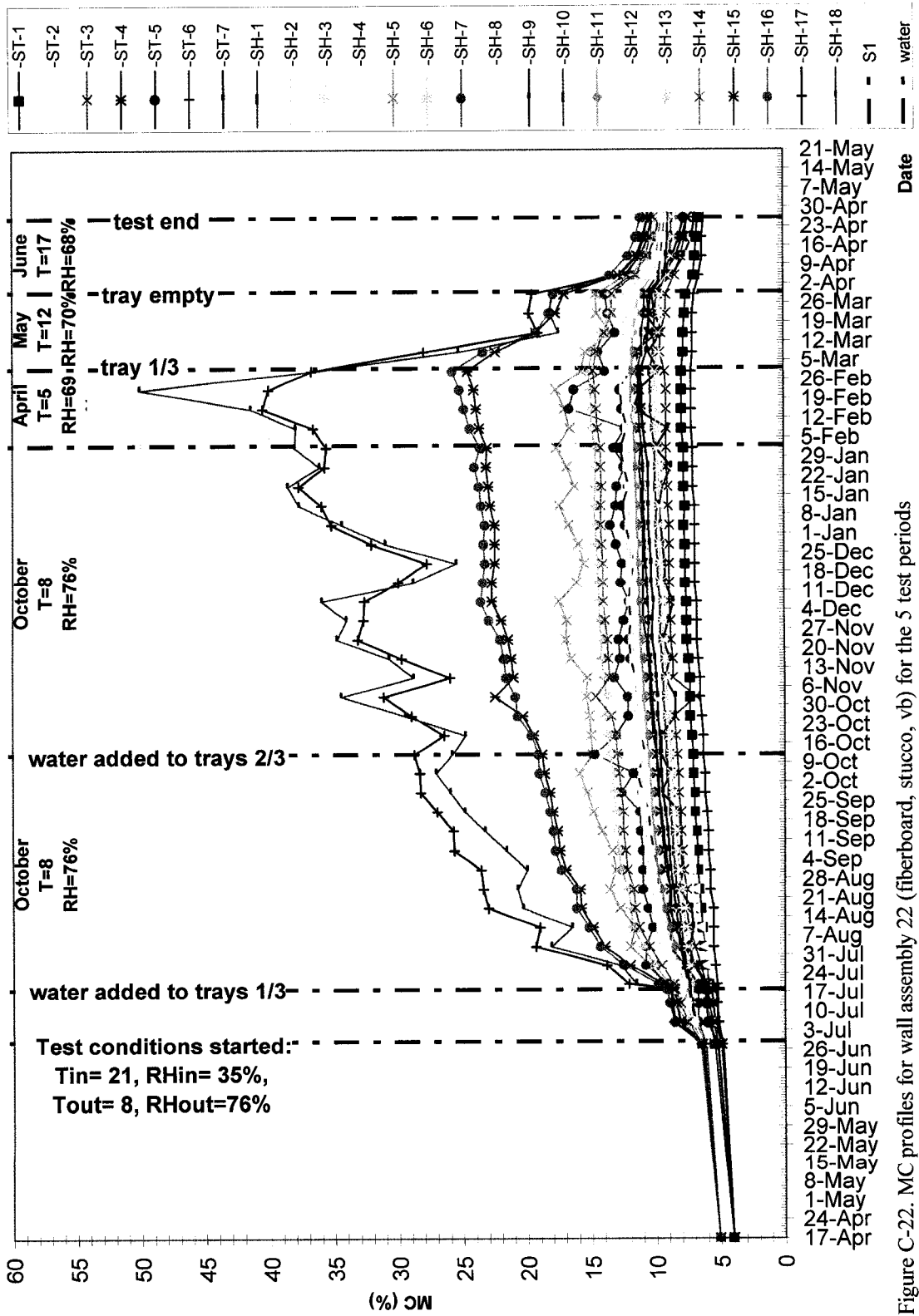


Figure C-22. MC profiles for wall assembly 22 (fiberboard, stucco, vb) for the 5 test periods

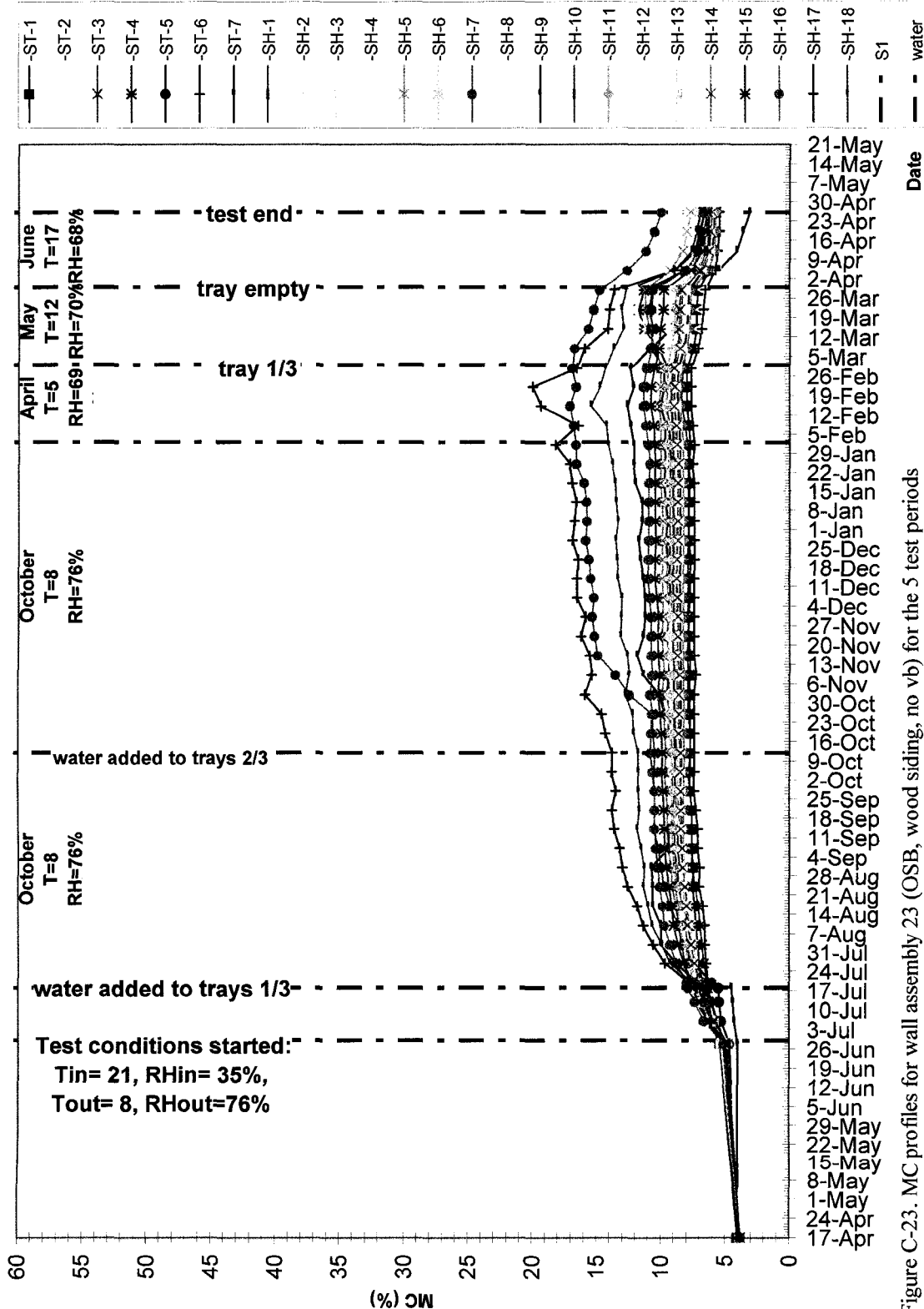


Figure C-23. MC profiles for wall assembly 23 (OSB, wood siding, no vb) for the 5 test periods

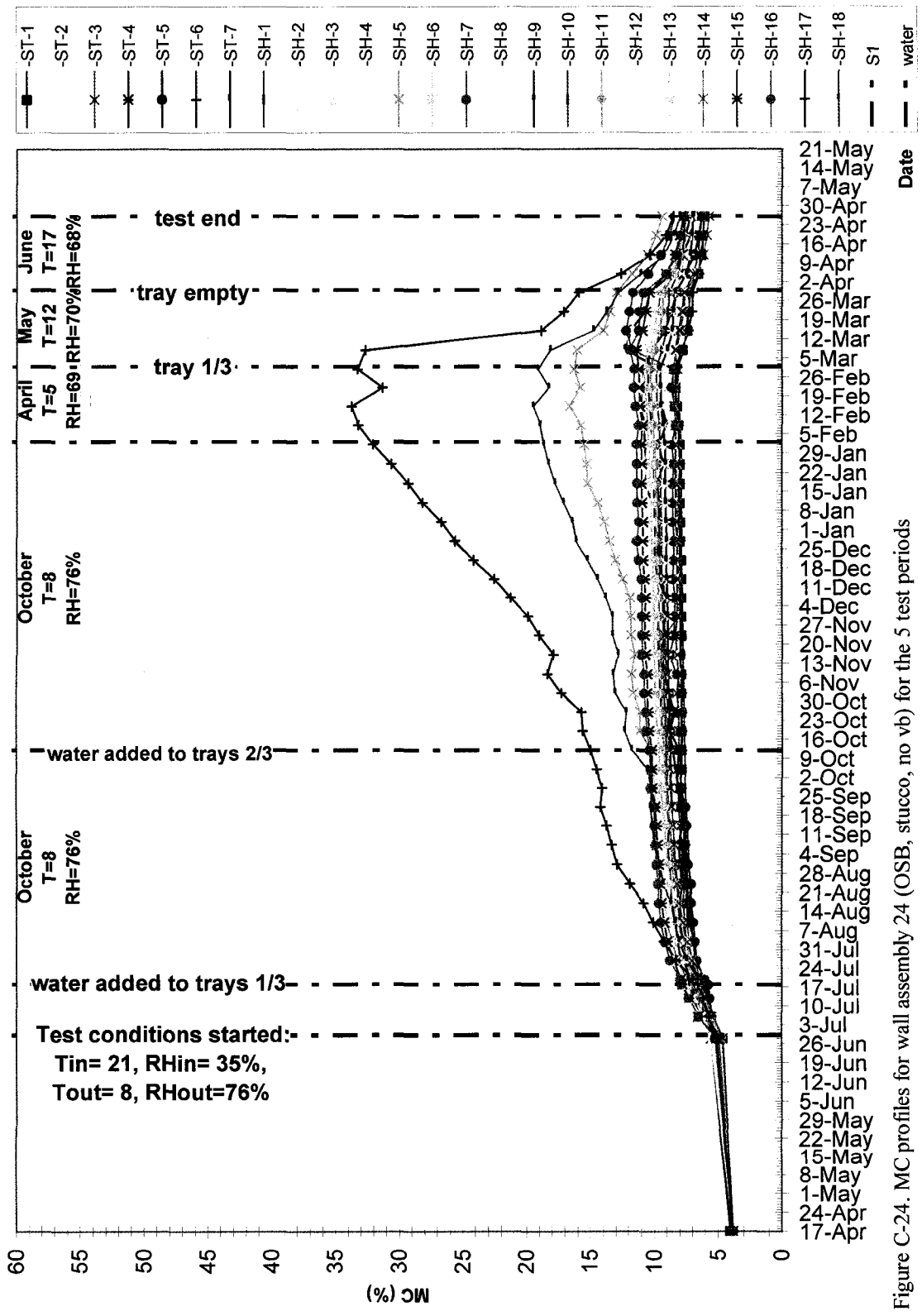


Figure C-24. MC profiles for wall assembly 24 (OSB, stucco, no vb) for the 5 test periods

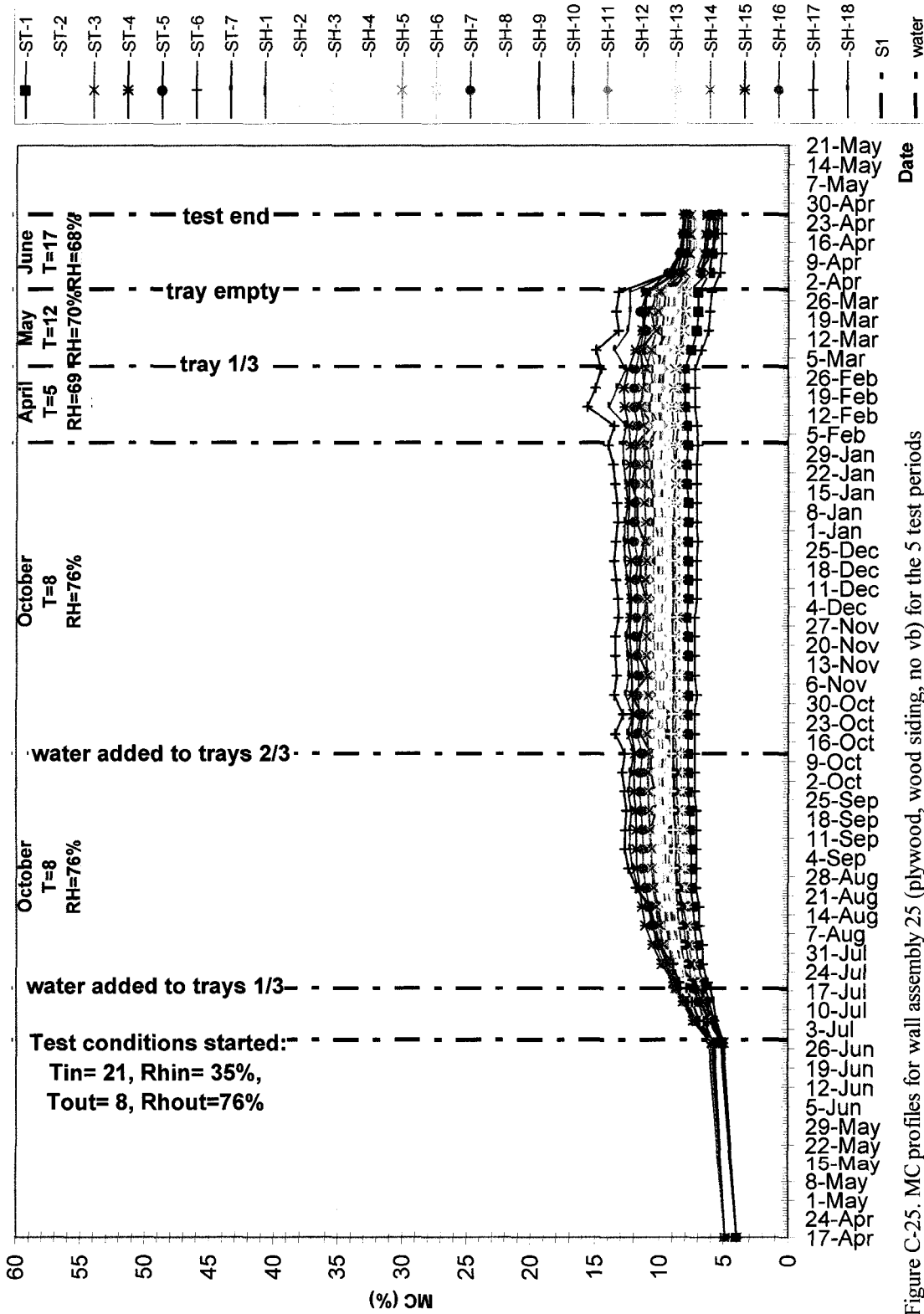


Figure C-25. MC profiles for wall assembly 25 (plywood, wood siding, no vb) for the 5 test periods

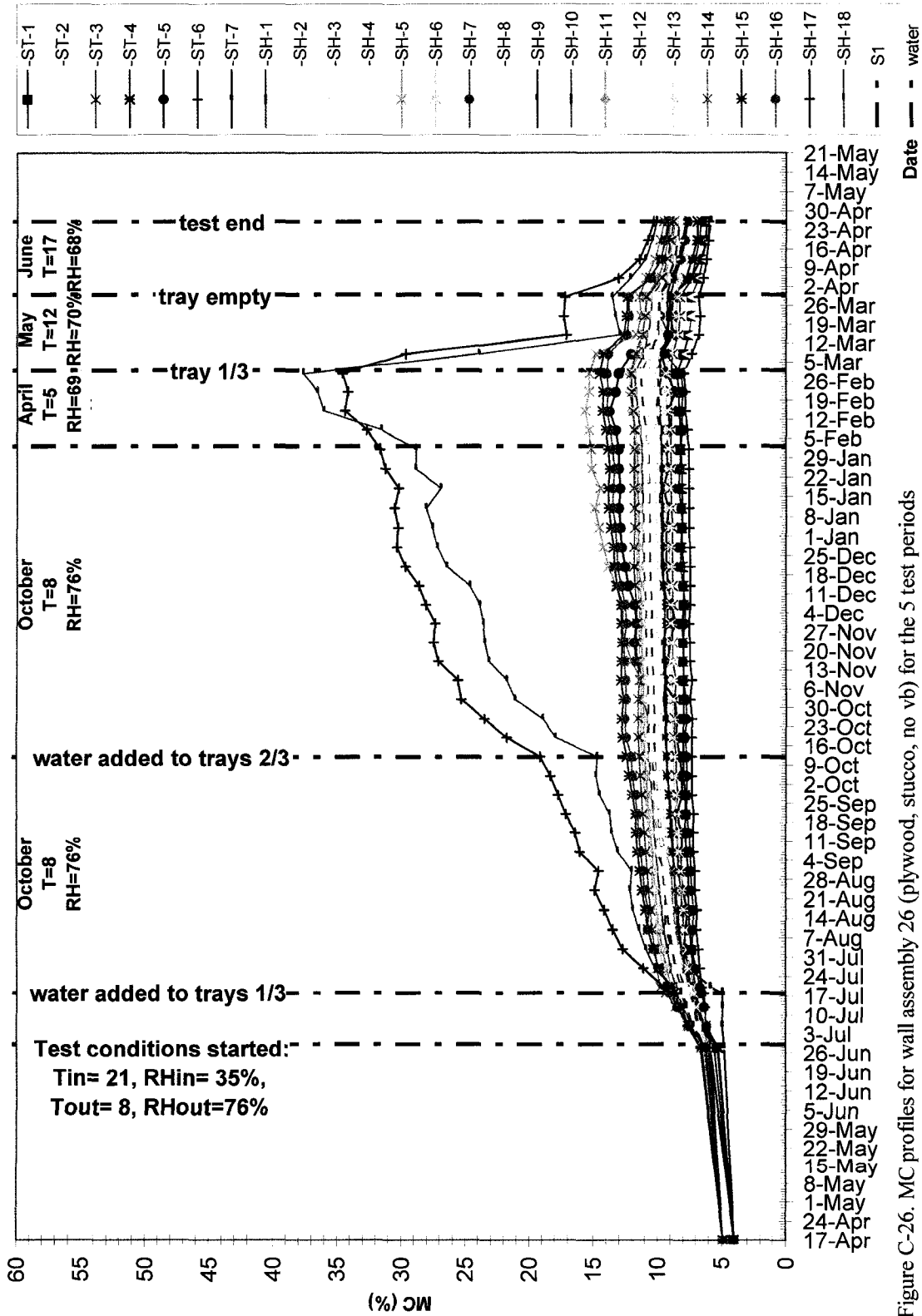


Figure C-26. MC profiles for wall assembly 26 (plywood, stucco, no vb) for the 5 test periods

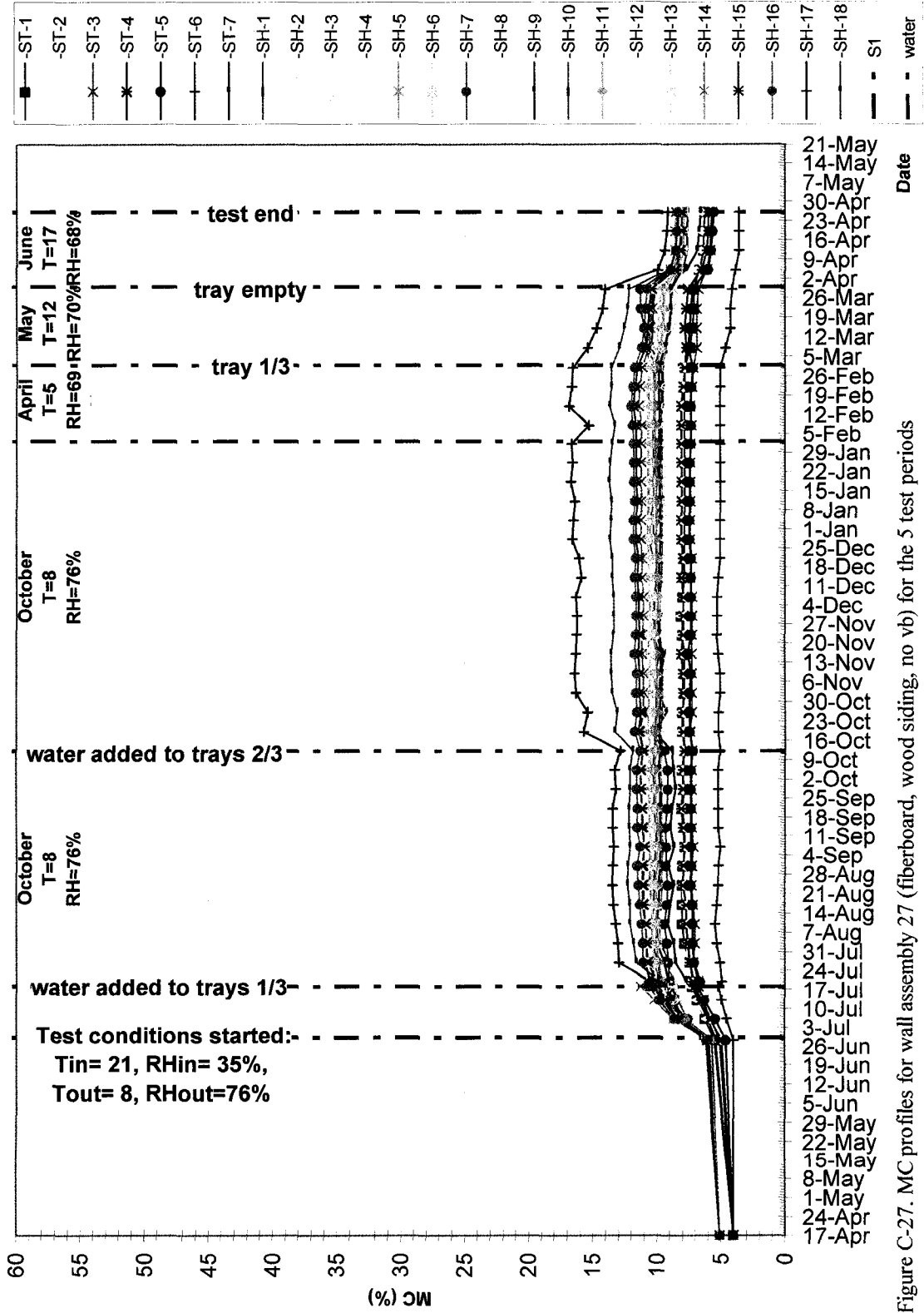


Figure C-27. MC profiles for wall assembly 27 (fiberboard, wood siding, no vb) for the 5 test periods



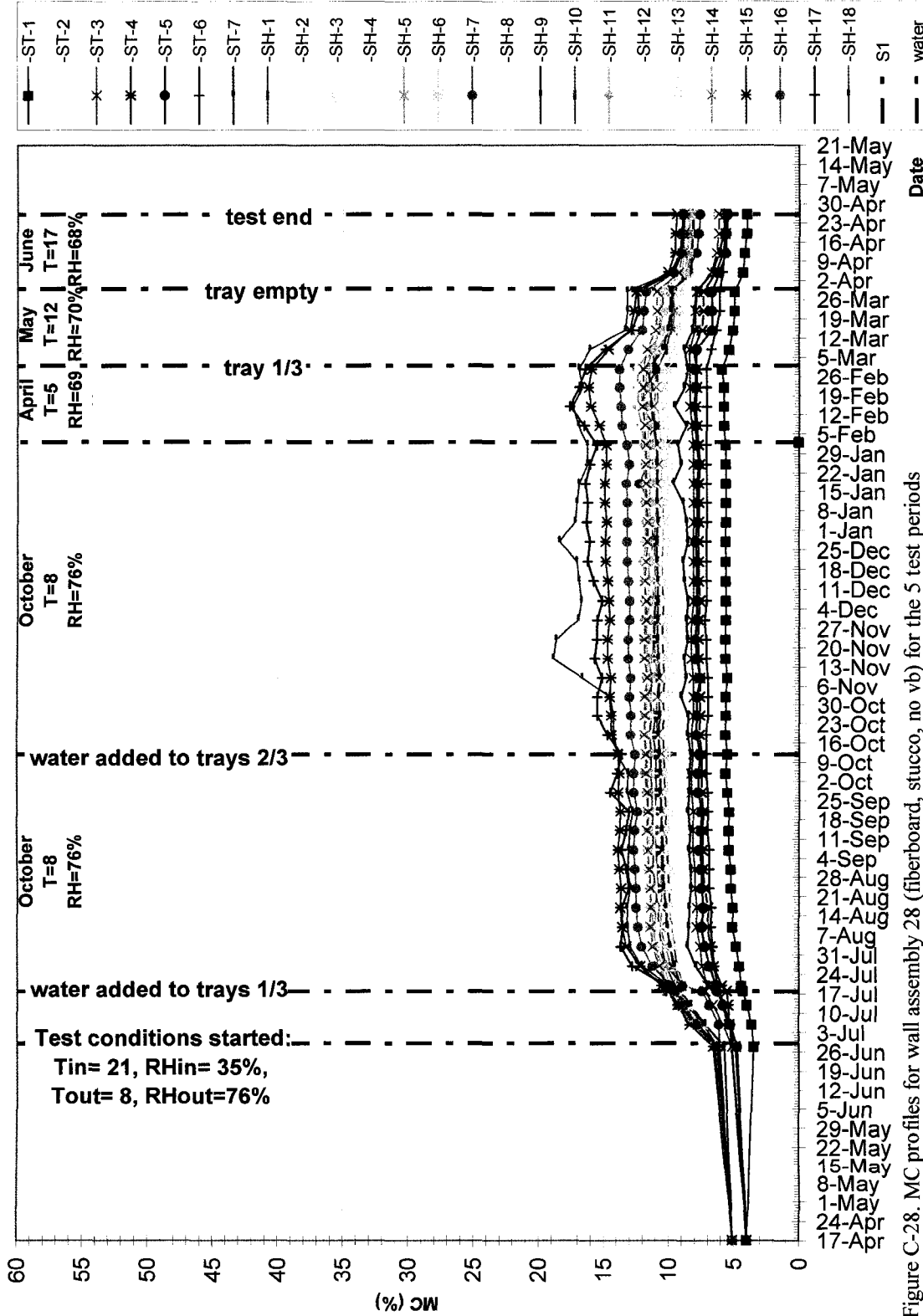


Figure C-28. MC profiles for wall assembly 28 (fiberboard, stucco, no vb) for the 5 test periods

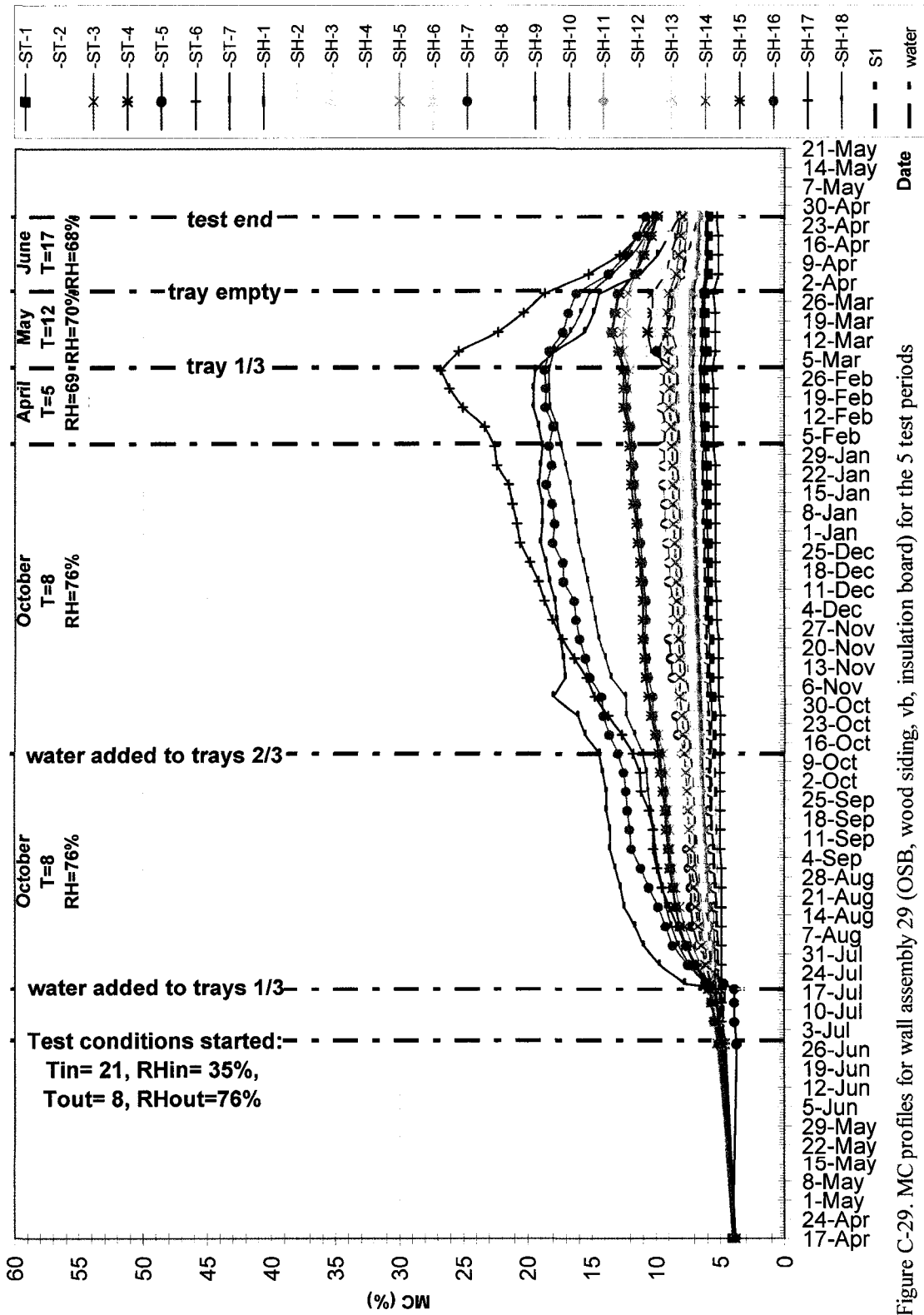


Figure C-29. MC profiles for wall assembly 29 (OSB, wood siding, vb, insulation board) for the 5 test periods

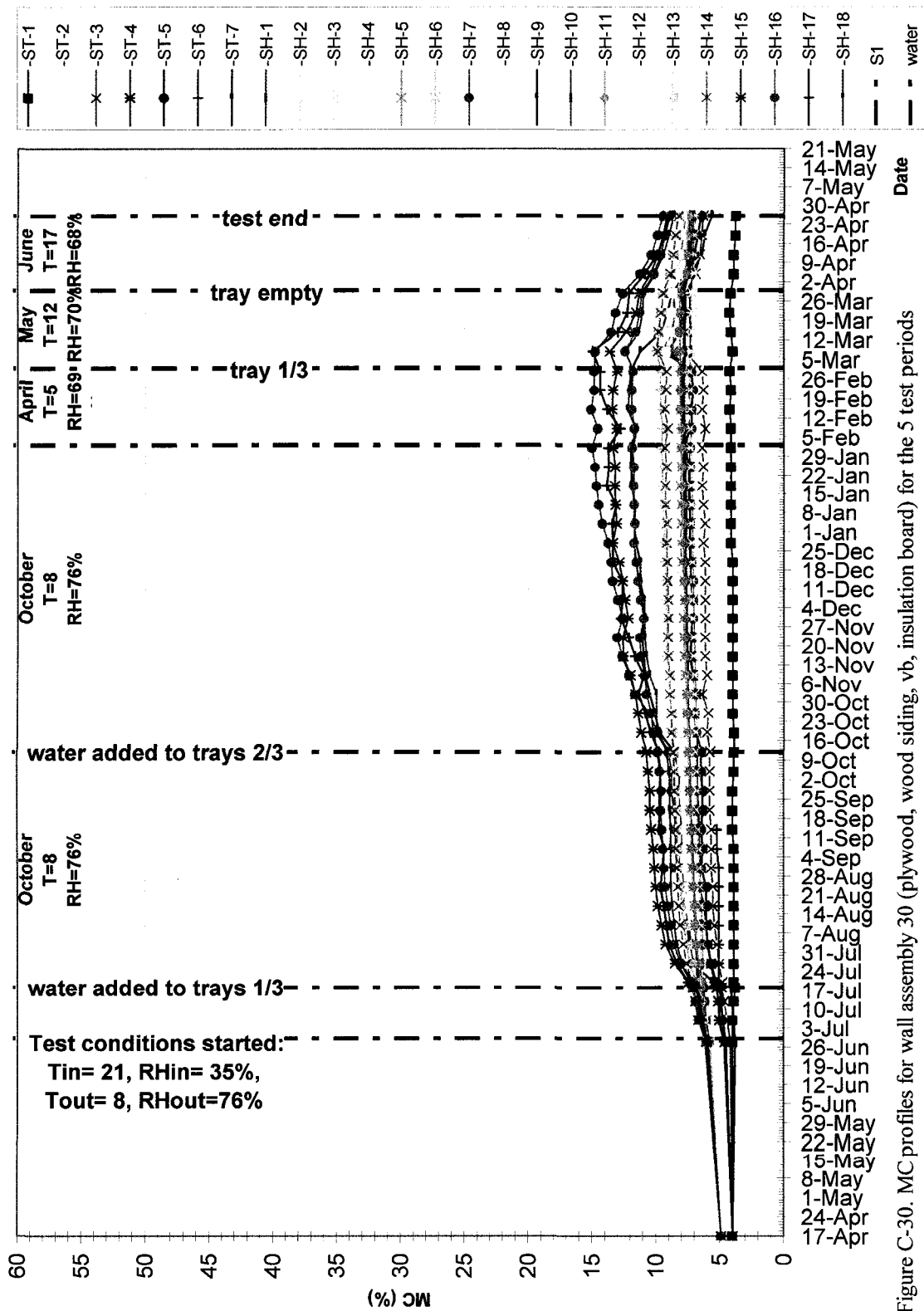


Figure C-30. MC profiles for wall assembly 30 (plywood, wood siding, vb, insulation board) for the 5 test periods

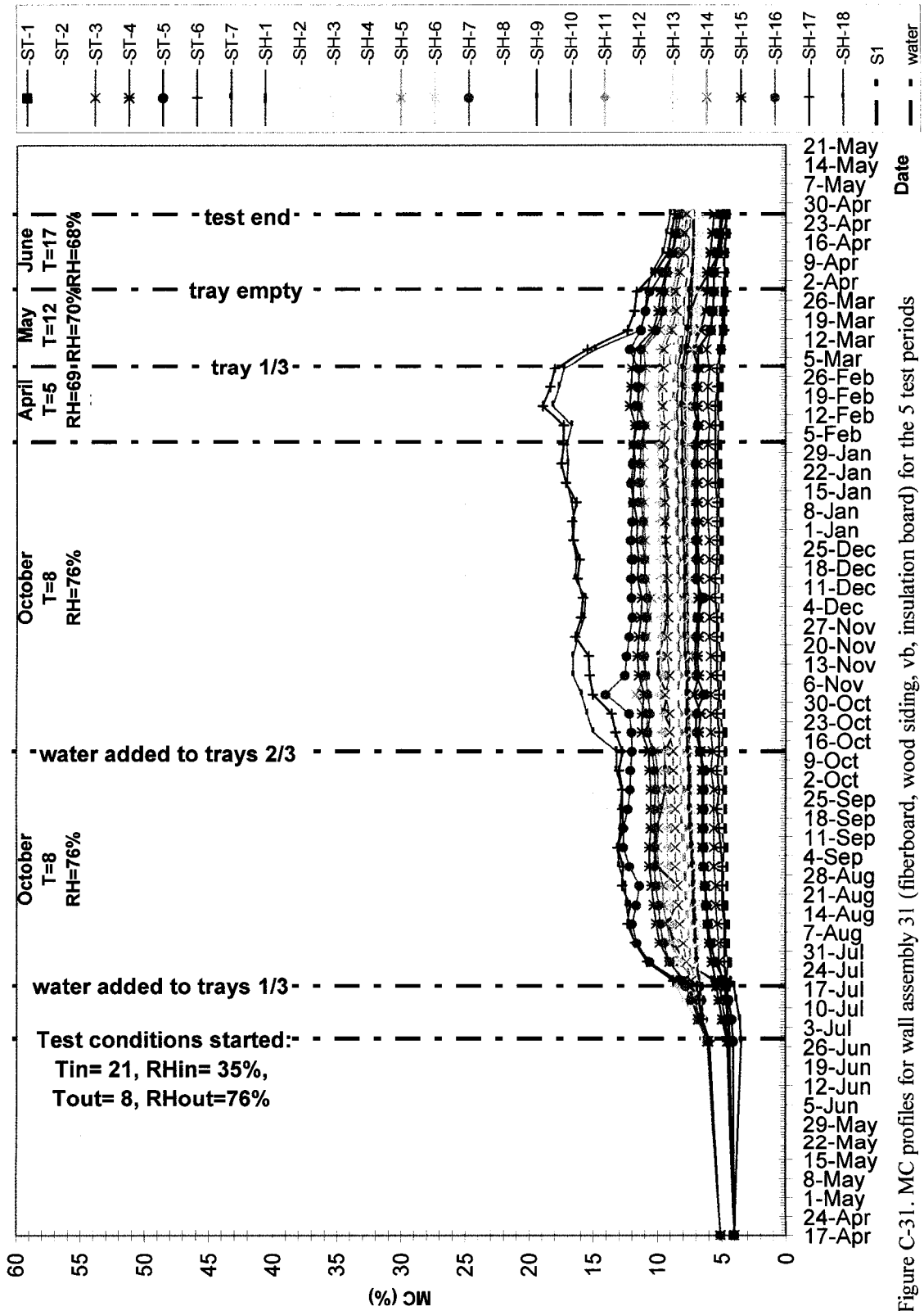


Figure C-31. MC profiles for wall assembly 31 (fiberboard, wood siding, vb, insulation board) for the 5 test periods